Twin Harbors Sediment Dynamics – Final Report

Twin Harbors Sediment Dynamics -
Final Report

January 29, 2021

Prepared for:

Grays Harbor Conservation District

Prepared by:

Stantec Consulting Services and
National Fisheries Conservation Center

Prepared by ______________________________
(signature)
Aaron Chen, PE (Stantec)

Prepared by ______________________________
(signature)
Julia Sanders (National Fisheries Conservation Center)

Prepared by ______________________________
(signature)
Todd Demunda (Stantec)

Prepared by ______________________________
(signature)
Tim Nightengale (Stantec)

Reviewed by ______________________________
(signature)
Wayne Wright (Stantec)

Approved by ______________________________
(signature)
Wayne Wright (Stantec)

Table of Contents

LIST OF TABLES

LIST OF FIGURES

LIST OF APPENDICES

Abbreviations

CDIP	Coastal Data Information Program
CFSR	Climate Forecast System Reanalysis from NCEP
CHL	Coastal Hydraulics Laboratory of the USACE
cm	centimeter
CRLC	Columbia River Littoral Cell
D_{50}	median sediment diameter
DC	Direct Current
EA	ECOncrete Antifers
EM	electromagnetic
ERDC	Engineer Research and Development Center from USACE
ESA	European Space Agency
ft	feet
GHCD	Grays Harbor Conservation District
Hs	significant wave height
InSAR	Interferomic Synthetic Aperture Radar
km	kilometer
m	meter
mg/L	milligrams per liter
MHHW	Mean Higher High Water
MLLW	Mean Lower Low Water
mm	millimeter
MRLC	Multi-Resolution Land Characteristics
NCEI	National Centers for Environment Information from NOAA
NCEP	National Centers for Environment Prediction from NOAA
NDBC	National Data Buoy Center from NOAA
NLCD	National Land Cover Database
NOAA	National Oceanic and Atmospheric Administration
O&M	Operation and Maintenance
PAR	Pendleton Artificial Reef
POC	Proof of Concept
ppt	parts per thousand
SA	Standard Antifers
SLR	Sea Level Rise
SR	Study in the Reference
SSC	Suspended Sediment Concentration
SSUM	Surface Subsidence & Uplift Measurement
The Seattle District	Seattle District, USACE
Tp	peak wave period
UNEP-WCMC	United Nations Environment World Conservation Monitoring Center

U.S.	United States
USACE	U.S. Army Corps of Engineers
USGS	U.S. Geological Survey
WDNR	Washington Department of Natural Resources
WIS	Wave Information Study from USACE
yd^3	cubic yards

1.0 INTRODUCTION

Grays Harbor and Willapa Bay, hereafter referred to as the Twin Harbors, have long been one of the most productive shellfish aquaculture areas in the United States (U.S.), home to 25 percent of domestic oyster cultivation. Shellfish aquaculture and related jobs are key components of the local and regional economy. Shellfish aquaculture also provides ecological benefits to the estuary, including water filtration, juvenile fish and crustacean habitat, and healthy benthic fauna. Shellfish aquaculture has been suffering from excessive sediment movement due to geomorphological changes associated with anthropogenic activities and from biological processes such as overpopulation of the burrowing shrimp. This problem has been reported since 1990 and has been deteriorating, causing continuous degradation in commercial shellfish cultivation. The Grays Harbor Conservation District (GHCD) initiated a three-phase process in 2015 to investigate this problem. Phase I completed a literature review and general analysis to identify Phase II next steps. This study is part of Phase II of the process, with the objectives of:

- obtaining a better understanding of the sedimentation and erosion dynamics in Grays Harbor and Willapa Bay,
- identifying areas of impact and potential new sites for shellfish aquaculture, and
- defining mitigation measures in greater detail to offset impacts to shellfish growing beds in Grays Harbor and Willapa Bay.

This study includes a comprehensive data investigation, data analysis, an extensive numerical modeling effort of the hydro- and morpho-dynamics within the Twin Harbors, evaluation of the sediment fate associated with the dredging activities within Grays Harbor, and development and evaluation of the mitigation measures.

1.1 STUDY AREA

As shown in Figure 1, the Twin Harbors are located 50 miles west of the city of Olympia on the southwest coast of the state of Washington and are approximately 110 miles south of the entrance to the Strait of Juan de Fuca and 45 miles north of the mouth of the Columbia River. The major cities include Aberdeen, Hoquiam, Ocean Shores, and Westport in Grays Harbor, and Raymond and South Bend in Willapa Bay.

Grays Harbor is 15 miles long and 11 miles wide, broadening gradually from the river channel at the city of Aberdeen to a large, pear-shaped, shallow estuary comprised of North and South Bays. The water surface area ranges from approximately 38 square miles at Mean Lower Low Water (MLLW) to approximately 91 square miles at Mean Higher High Water (MHHW). Willapa Bay is 24 miles long and 5 miles wide, aligned in a north-south direction separated by Long Beach Peninsula from the greater expanse of the Pacific Ocean. The water surface area ranges from approximately 78 square miles at MLLW to 150 square miles at MHHW. The geomorphology and dynamics within the Twin Harbors are very complex, being influenced by the Columbia River Littoral Cell (CRLC) along the Pacific Coast and an intricate inland watershed, which are discussed in Section 1.1.1 and Section 1.1.2, respectively.

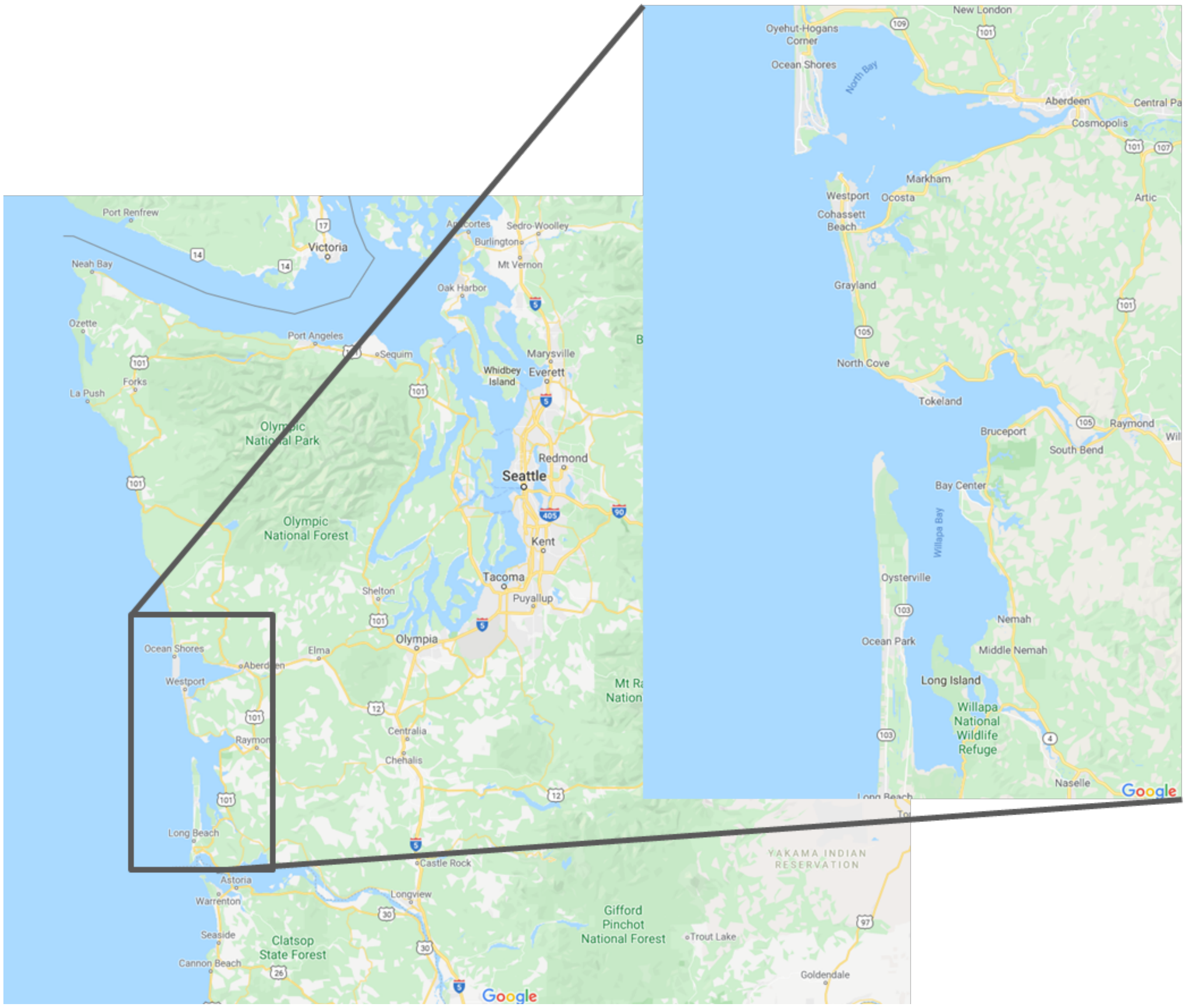

Figure 1: Geographic Overview of the Twin Harbors

1.1.1 Littoral Cell

The Twin Harbors are within the CRLC, which extends approximately 103 miles between Tillamook Head, Oregon, and Point Grenville, Washington (Kaminsky et al. 2010). The CRLC, illustrated in Figure 2, consists of four concave-shaped, prograded barrier plain sub-cells separated by the estuary entrances of the Columbia River, Willapa Bay, and Grays Harbor. Wide, gently sloping beaches characterize the region comprised of sands sourced from the Columbia River, the third largest river in the United States by discharge.

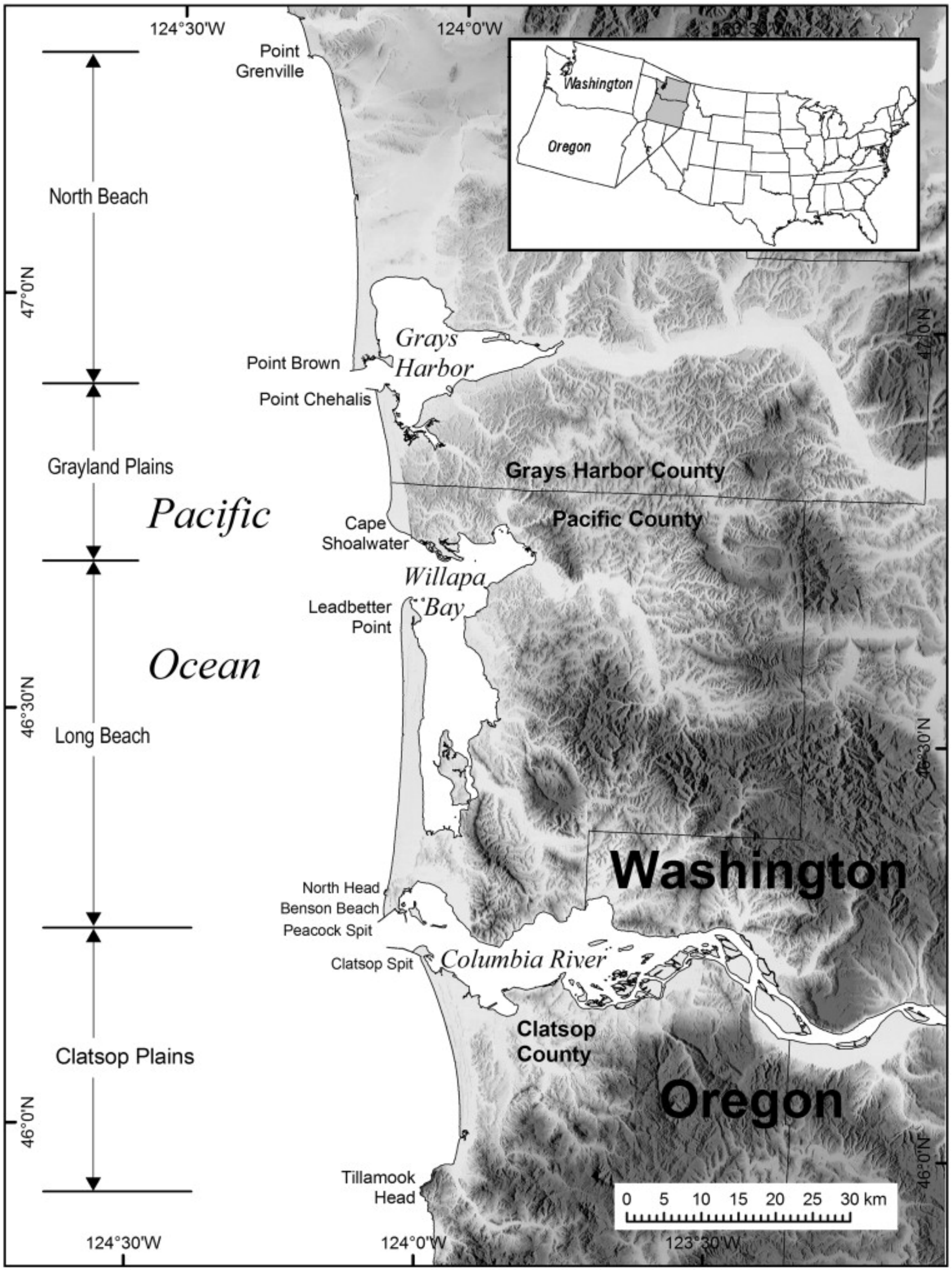

Source: Kaminsky et al. 2010

Figure 2: The Columbia River Littoral Cell (CRLC)

1.1.2 Major Watersheds

The watersheds in Grays Harbor and Pacific County are shown in Figure 3. The primary river discharge into Grays Harbor is the Chehalis River, which is approximately 125 miles long, originating in the Willapa and Doty hills southeast of Aberdeen and flowing northeast and then northwest before emptying into Grays Harbor near the inner harbor at Aberdeen. The drainage basin of Chehalis River is 2,114 square miles with major tributaries consisting of the Satsop River and Wynoochee River, which contributes approximately 80 percent of the freshwater discharge to Grays Harbor. Smaller drainages include Wishkah River (102 square miles drainage area), Hoquiam River (98 square miles drainage area), and Humptulips River.

The main tributaries discharging into Willapa Bay are North River, Willapa River, and Naselle River, which provide most of the freshwater input into Willapa Bay. The smaller streams discharging into Willapa Bay include Bone River, Niawiakum River, Palix River, Cedar River, and Bear River, among others.

Figure 3: Major Watersheds Surrounding Grays Harbor and Willapa Bay and the USGS Stream Stations

1.1.3 Engineering Activities

1.1.3.1 Grays Harbor

The U.S. Army Corps of Engineers (USACE) Seattle District (hereafter referred to as the Seattle District) started to survey the harbor and entrance area to monitor shoreline position and changes in shoal and channel morphology as early as 1894. Subsequently, a series of engineering constructions and rehabilitations were undertaken mainly to improve the navigation within Grays Harbor. USACE compiled a complete list of historical activities (USACE 2003a), which can also be found in Appendix A for completeness. Those engineering activities can be broadly classified into the following four eras:

- Era I (1900 – 1921) encompasses the construction periods of the initial south and north jetties. The South Jetty was constructed first to a height of +8 feet (ft) MLLW for a total length of 13,734 ft between 1898 and 1902, which is followed by the construction of the North Jetty to the same crest height for a total length of 10,000 ft between 1907 and 1916.
- Era II (1936 – 1942) corresponds to the first rehabilitation/extension for the south and north jetties, including a reconstruction of 12,656 ft section of the South Jetty to an elevation of +20 ft MLLW between 1936 and 1939, and a reconstruction of 7,700 ft section of North Jetty seaward of the high-water shoreline to +20 ft MLLW and an additional 528 ft section to +30 ft MLLW.
- Era III (1965 – 1976) is the second rehabilitation for the north and south jetties, including the 1966 rehabilitation of a 4,000 ft section of the South Jetty in 1966, and the 1975 rehabilitation of a 6,000 ft section of the North Jetty seaward of the high-water line to +20 ft MLLW.
- Era IV (1990 – present) represents the third rehabilitation/extension for the north and south jetties, including a rehabilitation of 3,300 ft of the South Jetty between 1999 to 2002, and a rehabilitation of 5,000 ft of the North Jetty to +23 ft MLLW between 2000 and 2001 with a 30 ft rock blanket for scour protection.

According to the Seattle Semiannual Dredging Meetings (the Seattle District 2019), the most recent engineering activities within Grays Harbor include: the Pt. Chehalis revetment repair project that is to place 11,600 tons of armor stone to repair the section of revetment from groins A through D, and the Westhaven beach fill repair project placing 30,000 to 45,000 cubic yards (yd^3) of sand by truck haul. Several other projects planned to begin in the next few years include: the Westhaven breakwater repair project planned for mid-2020 that is to place 1,500 tons of armor stone seaward and 3,000 tons of spalls leeward of the breakwater; the North Jetty repair project planned for 2021 to repair the landward portion of the jetty in smaller sections; and the WRDA 1122 pilot project planned for 2022 placing 250,000 yd^3 of maintenance dredge material on the South Beach shoreline, extending approximately 1.5 miles south of the jetty to mitigate the risk of beach and dune erosion on public and private infrastructure.

The Grays Harbor and Chehalis River navigation system (see Figure 4) is a federally constructed and maintained navigation channel that supports deep-draft shipping through the outer bar, Grays Harbor estuary, and the Chehalis River to Cosmopolis. The authorized depth of the outer harbor navigation channel tapers from 46 ft MLLW at the Bar Reach to 38 ft MLLW at the South and Crossover Reaches.

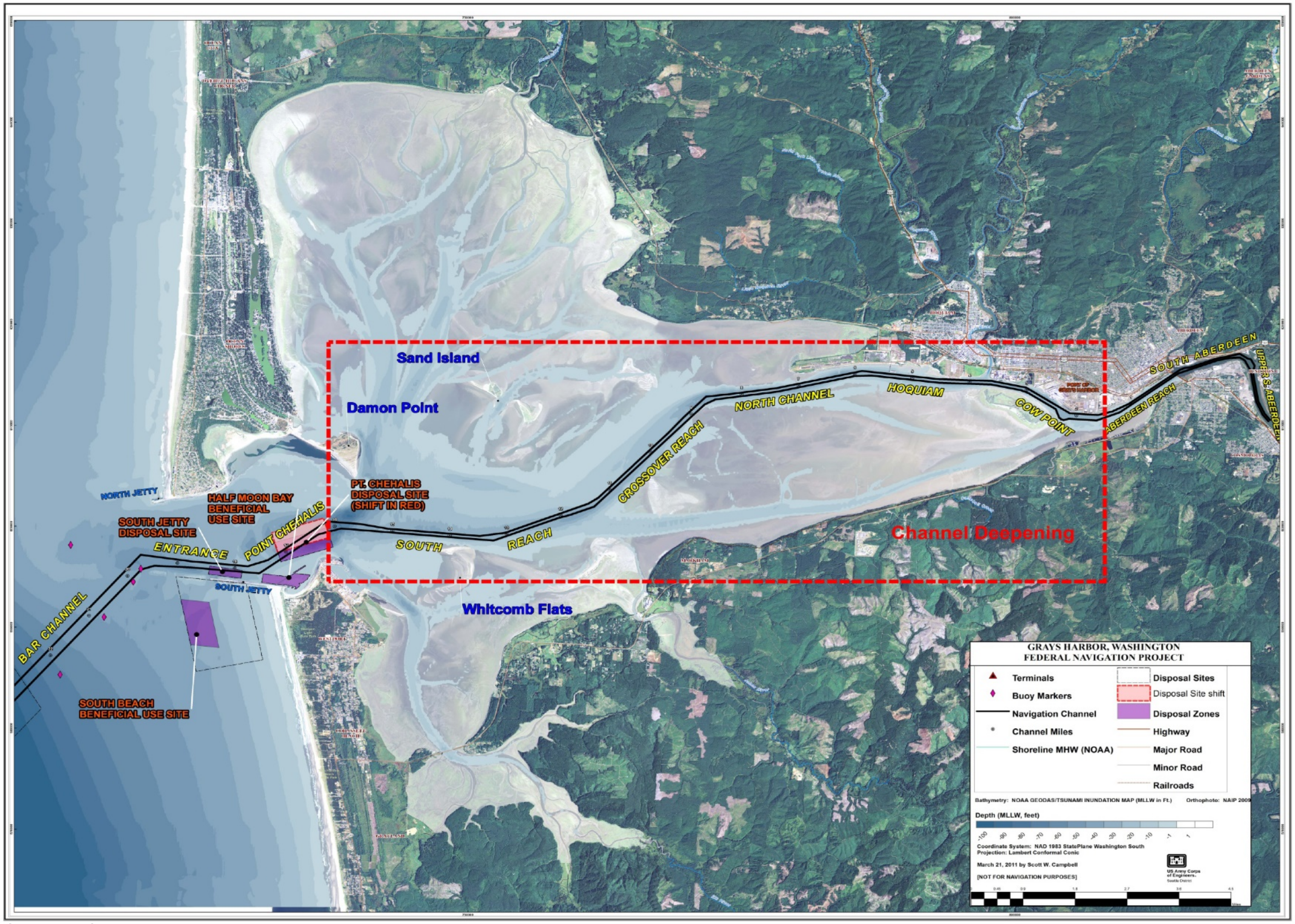

Source: Seattle District 2018

Figure 4: Grays Harbor Navigation Channel Sections

Introduction

The Seattle District performs annual Operation and Maintenance (O&M) dredging of the federal navigation channel within Grays Harbor. The earliest records of federal navigational channel dredging date to 1905, when 12 miles downstream from Cosmopolis was maintained with a 200-foot-wide channel to a depth of 18 ft MLLW (Scheidegger and Phipps 1976). The O&M dredging of the federal navigation channel can be better understood within the following three periods:

- Period I (1916-1940) included a regular O&M dredging of the Bar and Entrance Channels to a depth of 24 ft MLLW prior to 1928 and a depth of 36 ft MLLW since 1928. During this period, the average volume of maintenance dredging at the Outer Bar and Entrance Channel was approximately 850,000 yd^3/ year, all of which was disposed in deep water (below -60 ft MLLW) outside the harbor. Following rehabilitation of the North Jetty in 1942, maintenance dredging in the Entrance and Bar Channels ceased until 1990.

- Period II (1961-1989) included a regular O&M dredging at Crossover and Sand Island Reaches (no data is available between 1940 and 1961). Between 1961 and 1974, an average of 1,040,000 yd^3/year was dredged from Crossover Reach and Sand Island Reach. Following North Jetty rehabilitation in the late 1970s, the annual volumes dredged from Crossover and South Reaches between 1980 and 1989 were 460,000 and 650,000 yd^3/year, respectively.

- Period III (1990-present) includes the most recent channel deepening project completed between 1990 and 1991. Following the completion of the Navigation Improvement Project, O&M dredging resumed at the Outer Bar, Entrance, and Point Chehalis Reaches. Based on the annual O&M dredging volumes from 1991 to 2001 (USACE 2003a) listed in Table 1, approximately 900,000 yd^3/year have been dredged from the combined Bar, Entrance, Point Chehalis, and South Reaches. O&M dredging remained approximately constant at Crossover Reach with approximately 350,000 yd^3/year on average. O&M dredging decreased at South Reach with approximately 275,000 yd^3/year excluding 1994 when 600,000 yd^3 of the sediment were dredged in 1994 to fill the breach between the South Beach and South Jetty.

The Seattle District (2014) provided more details on the O&M dredging by reach for the period from 2000 to 2012, which are listed in Table 2. The outer harbor reaches from the Bar to the Outer Crossover are dredged with a hydraulic hopper dredge, which can operate in harsher conditions. The timing of hopper dredging has historically been in the months of April and May. The load capacity of these dredge events ranges from 1,000 to 6,000 yd^3, with an average daily production ranging from 10,000 to 30,000 yd^3/day. O&M dredged materials from the outer harbor are placed at four different open water placement sites: Point Chehalis Site, South Jetty Site, South Beach Beneficial Use Site, and the Half Moon Bay Beneficial Use Site.

The inner harbor reaches from the Inner Crossover to Cow Point are dredged via clamshell dredge due to mitigation requirements for juvenile crabs. Clamshell dredging has historically been performed within the fish window extending from July 15th to February 14th using a 35 yd^3 clamshell bucket with 2 bottom dump barges, achieving an average daily production of approximately 12,000 yd^3/day. However, due to the timing of clamshell dredging, which typically requires more exposure to adverse weather conditions, hopper dredges are often substituted. Dredged materials are transported by a tug from the dredge area and placed at the Point Chehalis or South Jetty open water placement site by a bottom dump scow barge.

Table 1: 1991-2001 Annual Grays Harbor O&M Dredging Volumes in yd^3 by Reach

Fiscal Year	Bar Channel	Entrance and Point Chehalis Reach	South Reach	Crossover Reach	Total
1991	452,000	453,000	477,000	88,000	1,470,000
1992	636,000	361,000	683,000	521,000	2,201,000
1993	373,000	324,000	158,000	639,000	1,494,000
1994	277,000	163,000	903,600	364,000	1,707,600
1995	0	0	332,000	469,000	801,000
1996	0	308,000	103,600	425,000	836,600
1997	0	136,000	226,400	456,000	818,400
1998	103,000	266,000	293,000	840,000	1,502,000
1999	76,000	382,000	229,000	390,000	1,077,000
2000	209,000	537,000	231,000	463,000	1,440,000
2001	227,000	359,000	169,000	190,000	945,000
Average annual	214,000	299,000	346,000	440,000	-

Table 2: Annual Grays Harbor Navigation Channel Paid Dredge Volumes (FY 2000 - FY 2012)

Dredge Year	Clam Shell Dredging (Inner Harbor) Volume (yd3)						Hopper Dredging (Outer Harbor) Volume (yd3)				Total Volumes (yd3)	
	Elliot Slough Turning Basin	Cow Point / Aberdeen	Cow Point Turning Basin	Hoquiam	North Channel	Inner Crossover	Outer Crossover	South Reach	Entrance / Pt Chehalis	Bar Channel	Inner Harbor	Outer Harbor
2000	-	443,518	-	54,376	200,000	218,163	295,837	198,000	537,000	209,000	916,057	1,239,837
2001	-	271,303	-	42,777	-	-	162,654	191,209	359,000	227,000	314,080	939,863
2002	61,279	705,114	-	115,901	126,780	158,838	22,129	135,706	605,459	144,031	1,167,912	907,325
2003	-	549,026	-	128,874	146,794	301,819	-	135,634	246,792	137,689	1,126,513	520,115
2004	35,619	784,950	-	135,863	113,633	545,896	175,968	177,529	443,470	291,195	1,615,961	1,088,162
2005	-	657,352	-	141,746	143,760	223,542	107,432	-	622,771	217,909	1,166,400	948,112
2006	27,869	638,343	-	37,863	93,825	200,488	163,730	59,931	379,513	55,170	998,388	658,344
2007	-	418,564	-	-	-	-	117,560	94,868	497,795	-	418,564	710,223
2008	-	694,536	208,069	-	-	198,471	-	-	800,258	-	1,101,076	800,258
2009	-	626,247	200,000	-	-	268,179	-	-	684,107	246,873	1,094,426	930,980
2010	-	716,449	171,295	150,000	150,000	198,529	-	67,102	580,218	118,182	1,386,273	765,502
2011	-	521,646	83,853	122,288	104,765	-	-	46,670	459,840	298,163	832,552	804,673
2012	-	451,291	177,185	96,846	103,598	-	-	27,475	1,056,333	141,655	828,920	1,225,463
Sum	124,767	7,478,339	840,402	1,026,534	1,183,155	2,313,925	1,045,310	1,134,124	7,272,556	2,086,867	12,967,122	11,538,857
Average	9,600	575,300	64,600	79,000	91,000	178,000	80,400	87,200	559,400	160,500	997,500	887,600
Max	61,279	784,950	208,069	150,000	200,000	545,896	295,837	198,000	1,056,333	298,163	1,615,961	1,239,837

1.1.3.2 Willapa Bay

The engineering activities within Willapa Bay are mainly associated with the dredging of the navigational channel. According to USACE (2002), the existing project was first adopted in 1916 and last modified through authorization in 1954. The authorization provides for a channel over the bar of the mouth of Willapa Bay to be 26 ft deep at MLLW with a width of at least 500 ft as required for existing shallow-draft commerce. Dredging of the deep-draft river channel of Willapa Harbor was discontinued by the Seattle District in 1976 because of inadequate benefits. Dredging for shallow draft continues at Willapa Harbor for facilities at such locations as Toke Point, Bay Center, and Nahcotta. Since 1976, no O&M dredging has been required along the Federal river channel between Willapa Bay and port facilities located at Raymond, Washington.

1.2 DATA COLLECTION OVERVIEW

High quality data within the system, as well as from Pacific Ocean and the watersheds inland, are required to understand the physics of the complex hydro- and morpho-dynamics within the study areas and to support the development of the numerical models. To ensure the best available data is being used in this study, four data collection efforts were undertaken simultaneously for this study, which are discussed in detail in Section 2.0 and summarized below.

- **Online Data Search**: The online search compiled information including bathymetry, tide attributes, wind/wave data, temperature/salinity, sediment characteristics, and river discharge and sediment load from different agencies including National Oceanic and Atmospheric Administration (NOAA), USACE, U.S. Geological Survey (USGS), etc. The online data search also obtained any available historical field surveys collected by those agencies, which will be used for model calibration/validation. The online data search is a major part of this report, with data sources summarized in Section 2.1 and the subsequent analysis described in Section 3.0.
- **InSAR Data Generation**: Interferomic Synthetic Aperture Radar (InSAR) is a process to detect surface elevation change using satellite imagery. InSAR examines the phase shift of electromagnetic waves travelling at the speed of light to very accurately identify differences in surface elevation over time, which are unaffected by atmospheric conditions such as clouds, fog, smoke, and haze. The ever-growing global archive of InSAR images dates back to 2016 with a temporal resolution of 12 days, which allows for retroactive elevation change detection analysis over tidal flats during low tide going back 5 years at a spatial resolution of 50 ft. This dataset will be used to understand the recent morphological changes and to validate the morphological model. This is an ongoing effort, which will be presented in the final report.
- **Stakeholder Surveys**: The stakeholder survey is to gather the information regarding oyster farms, burrowing shrimp, marsh, sediment, subsidence from the stakeholders, and to incorporate their local knowledge into the study via the development of a WebApp. The outcome of this effort also is to compile the data from the stakeholders and create a unified dataset and/or map product for the stakeholders to use for planning in the future. This is an ongoing effort, which will be presented in the final report.

- **USACE Literature Review**: The USACE literature review is to understand the studies performed by USACE for Grays Harbor and Willapa Bay. The goal is to understand the datasets and/or methodologies (the numerical model in particular) from the relevant literature that this study can benefit from, rather than a thorough review of their objectives, observations and/or conclusions. USACE literature reviews are documented in Appendix A.

1.3 NUMERICAL MODEL OVERVIEW

A comprehensive numerical model also was developed to simulate the hydro- and morpho-dynamic within the Twin Harbors. The numerical model is based on the Delft3D-FM model developed by Deltares. The Delft3D-FM model is a cutting edge, process-based numerical modeling system. It is a flexible, integrated modeling suite capable of simulating two- and three-dimensional hydrodynamics, waves, conservative and non-conservative constituent transport, sediment transport, morphology, and water quality. The model was calibrated against the data obtained from the data investigation for its model skills to reproduce water level, current, waves, which are discussed in Section 4.0. The model also was calibrated for the suspended sediment concentration (SSC), and morphological changes at the inlet as well as over the tidal flats, which are discussed in Section 5.0. The calibrated model was used to understand the hydro- and morpho-dynamics within the Twin Harbors discussed in Sections 4.0 and 5.0, respectively, to investigate the sediment fates associated with the O&M dredging within Grays Harbor documented in Section 6.0, and to evaluate the performance of the mitigation measures presented in Section 7.0.

2.0 DATA COLLECTION

2.1 ONLINE DATA SEARCH

2.1.1 Imagery and Bathymetry

Aerial imagery of Washington State in 2013 is available from the U.S. Department of Agriculture National Agriculture Imagery, which is shown in Figure 5. Based on literature review, USACE has forty bathymetric datasets within Grays Harbor from 1862 to 2002; see Appendix F in USACE 2003a for a complete list. The Seattle District conducted many hydrographic surveys of portions of Willapa Bay on a mostly annual basis between 1927 and 1978, which were curtailed to a portion of the entrance near the navigation channel following the cease of O&M dredging after 1967. More recently hydrographic surveys were made of the bar and entrance channels from 1999 to 2001 (USACE 2006).

However, most of those datasets are not publicly available even though efforts have been made to request the data from the Seattle District. The bathymetric data covering different areas of interest to the project site are mainly available from NOAA's National Center for Environmental Information's (NCEI) Coastal Relief Model, which includes a northwest Pacific bathymetric dataset that combines data collected from 1999 to the present day; bathymetry data for Grays Harbor in 2008, 2014, and 2018; and bathymetry data for Willapa Bay in 1954 and 2018. The USGS published separate Grays Harbor and Willapa Bay bathymetric datasets in 2012.

Figure 5: Imagery of Washington State

2.1.2 Stations/Gauges Data

The established station/buoy locations from different agencies are shown in Figure 6. Specifically, water level data is available from NOAA tide gauges 9440910, 9441102, 9439040, and 9443090. Measurements of wind and/or waves are available from NOAA National Data Buoy Center's (NDBC) buoys 46100, 46211, TOKW1 (9440910), WPTW1 (9441102), and the Coastal Data Information Program (CDIP) station 036 operated by the Ocean Engineering Research Group at UC San Diego. Additional wind data at airports is available from NOAA's NCEI, including Hoquiam Bowerman Airport, Astoria Airport, and Olympia Airport. The Wave Information Studies (WIS) from USACE also provides an hourly hindcast of wind and waves along the Pacific shoreline. The data availability and the corresponding date ranges are summarized in Table 3.

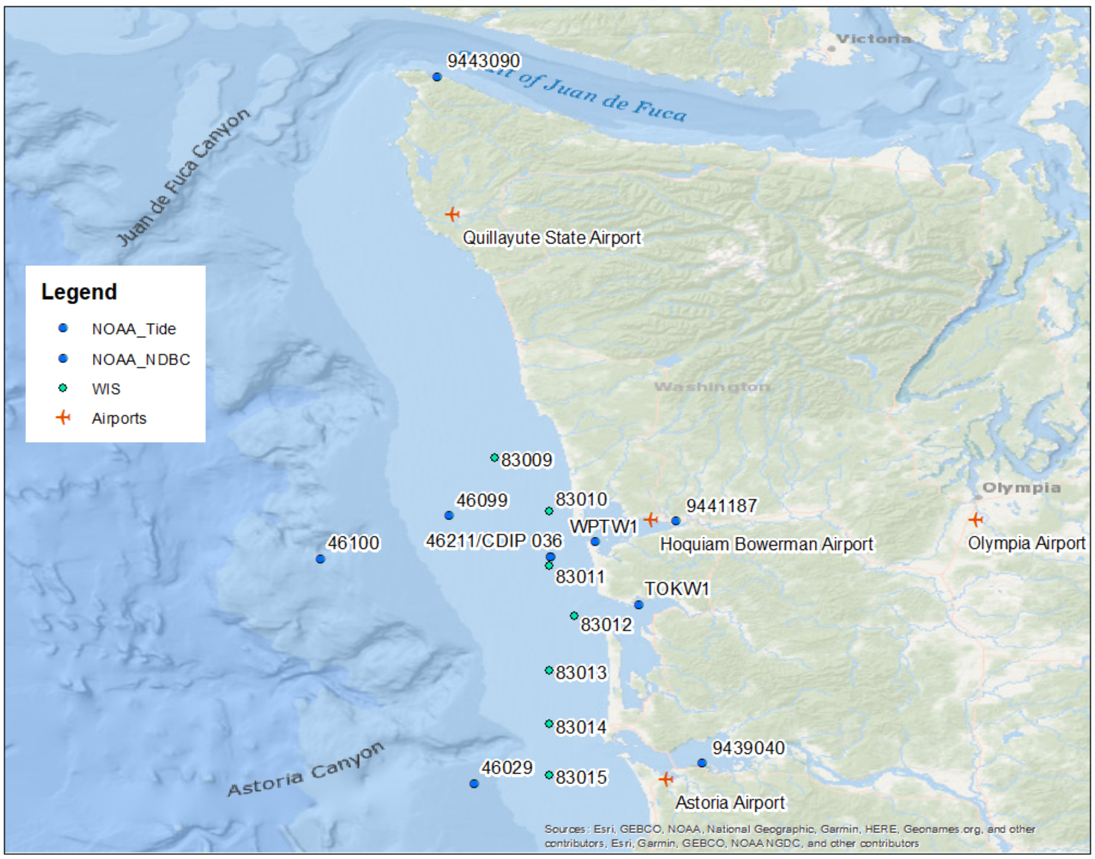

Figure 6: Overview of Station Locations for Water Level, Wind, and Waves

Table 3: Summary of Data Availability for Water Level, Wind, and Waves

Gauge	Source	Date Range	Parameter				
			Water Level	Wind	Wave	Salinity	Sea Surface Temperature
9439040	NOAA Tide Gauge	1925-2020	X				
9443090		1934-2020	X				
9441187		1982-1983	X				
		2004-2005	X				
9441102/WPTW1		2006-2007	X				
		2008-2019	X	X			X
9440910/TOKW1		1972-2004	X				
		2005-2019	X	X			X
46029	NOAA NDBC	1984-2018		X	X		X
46100		2016-2019		X	X	X	X
46099		2016-2017	X	X	X	X	X
		2018		X	X	X	X
		2019		X	X	X	
46211		2004-2019			X		X
CDIP 036	CDIP	1981-1992			X		
		1993-2020			X		X
83009	USACE WIS	1980-2011		X	X		
83010							
83011							
83012							
83013							
83014							
83015							
Hoquiam Bowerman Airport	NOAA NCEI	2001-2020		X			
Astoria Regional Airport		1965-2020					
Olympia Airport							
Quillayute State Airport							

River discharge and SSC data were gathered from USGS stations at the major tributaries within the watersheds of Grays Harbor and Willapa Bay including the Columbia River, which are shown in Figure 3. The available data and the corresponding date range are summarized in Table 4.

Table 4: Summary of Data Availability for Discharge and SSC

Region	Location	Station	Source	Date Range	Parameter	
					Daily Discharge	SSC[1]
Grays Harbor	Chehalis River at Porter	12031000	USGS	1974-2020	X	X[2]
	Chehalis River at Montesano	12035100	USGS	2001-2020	X	
	Satsop River	12035000	USGS	1929-2020	X	
	Wynoochee River	12037400	USGS	1973-2020	X	
	Wishkah River near Nisson	22D110	WA Department of Ecology	2005-2013	X	
	Humptulips River	12039005	USGS	2002-2020	X	
Willapa Bay	North River near Raymond	12017000	USGS	1927-2000	X	
	Naselle River	12010000	USGS	1929-2020	X	
	Willapa River	12013500	USGS	1947-2020	X	X
	Columbia River at Port Westward	14246900	USGS	1986-2020	X	X

[1] SSC data are sparsely available or at shorter time period.
[2] The most recent data is available in turbidity rather than SSC.

2.1.3 Field Surveys

Based on literature review, the most recent comprehensive field surveys of bathymetry, hydrodynamics, waves, and/or sediments within the Twin Harbors includes:

- **1999 and 2001 Surveys by USGS:** As part of the Southwest Washington Coastal Erosion Study to support the multi-year multidisciplinary investigation of the CRLC, USGS performed the Grays Harbor Wave Refraction Experiment in Autumn 1999 (USGS 2000) and subsequently the Grays Harbor Sediment Transport Experiment in Spring 2001 (USGS 2004), during which Acoustic Doppler Velocimeters, Acoustic Doppler Profilers, and Optical Backscatter Sensors were deployed at six locations near the entrance of Grays Harbor (see Figure 7) with wave, current, and turbidity data collected. Along with those data, bottom sediment grab samples also were taken at several locations.

- **1999 and 2003-2004 Survey for Grays Harbor by USACE:** Two major field data sets were collected within Grays Harbor in 1999 (USACE 2003a) and 2003-2004 by USACE's Coastal Hydraulics Laboratory (CHL) and the Seattle District to investigate coastal and inlet physical processes at the entrance and along the entrance channel. Both datasets include water levels, waves, currents, and suspended sediment concentration measurements from multiple stations. Also shown in Figure 7, the 1999 survey covers a large area encompassing the outer channel, the entrance, and inside Grays Harbor from September to December. The 2003-2004 data were collected around Half Moon Bay from December 2003 to February 2004.
- **1998 Survey for Willapa Bay by USACE:** As part of the USACE's Navigation Channel Feasibility Study for Willapa Bay (USACE 2002), a field survey was executed for three short periods in 1998 by Evans-Hamilton, Inc. under task-order contract with the USACE's Engineer Research and Development Center (ERDC), Vicksburg, Mississippi. The field survey includes measurements of waves, currents (point measurements and profiles through the water column), water level, salinity (conductivity and temperature), wind velocity, air temperature, and air pressure at five wave and current stations, four combined water-level and salinity recording stations, and one weather station.

The datasets from USGS surveys are publicly available from the USGS website, which will be used in this study. Measures have been taken to reach out to the USACE for their survey data. At the time of this report, USACE provided the 1999 survey data for Grays Harbor.

2.1.4 Spatial Datasets

Spatial-temporal variations of wind, pressure, temperature, and salinity data are available from the Climate Forecast System Reanalysis (CFSR) by the National Centers for Environment Prediction (NCEP). The CFSR is a third-generation reanalysis product (Saha 2010). It is a global, high resolution, coupled atmosphere-ocean-land surface-sea ice system designed to provide the best estimate of the state of these coupled domains. The CFSR global atmosphere resolution is ~38 km (T382) with 64 levels. The global ocean is 0.25° at the equator, extending to a global 0.5° beyond the tropics, with 40 levels. Sediment grain size information for the Northeast Pacific, including the Twin Harbors, are available from the USGS usSEABED database (USGS 2019), which is an integrated dataset based on sediment characteristics gathered by multiple agencies and stakeholders, including federal, state, and private entities. Wetland maps are available from the National Wetlands Inventory generated by the U.S. Fish and Wildlife Service. The distributions of saltmarsh are available from a web service at the United Nations Environment World Conservation Monitoring Center (UNEP-WCMC), which collated and integrated saltmarsh occurrence datasets from 50 data providers globally with support from Conservation International and The Nature Conservancy (Mcowen et al. 2017). The land covers are available from the National Land Cover Database (NLCD) generated by the Multi-Resolution Land Characteristics (MRLC) consortium (MRLC, 2016) which can be used to determine bottom friction characteristics.

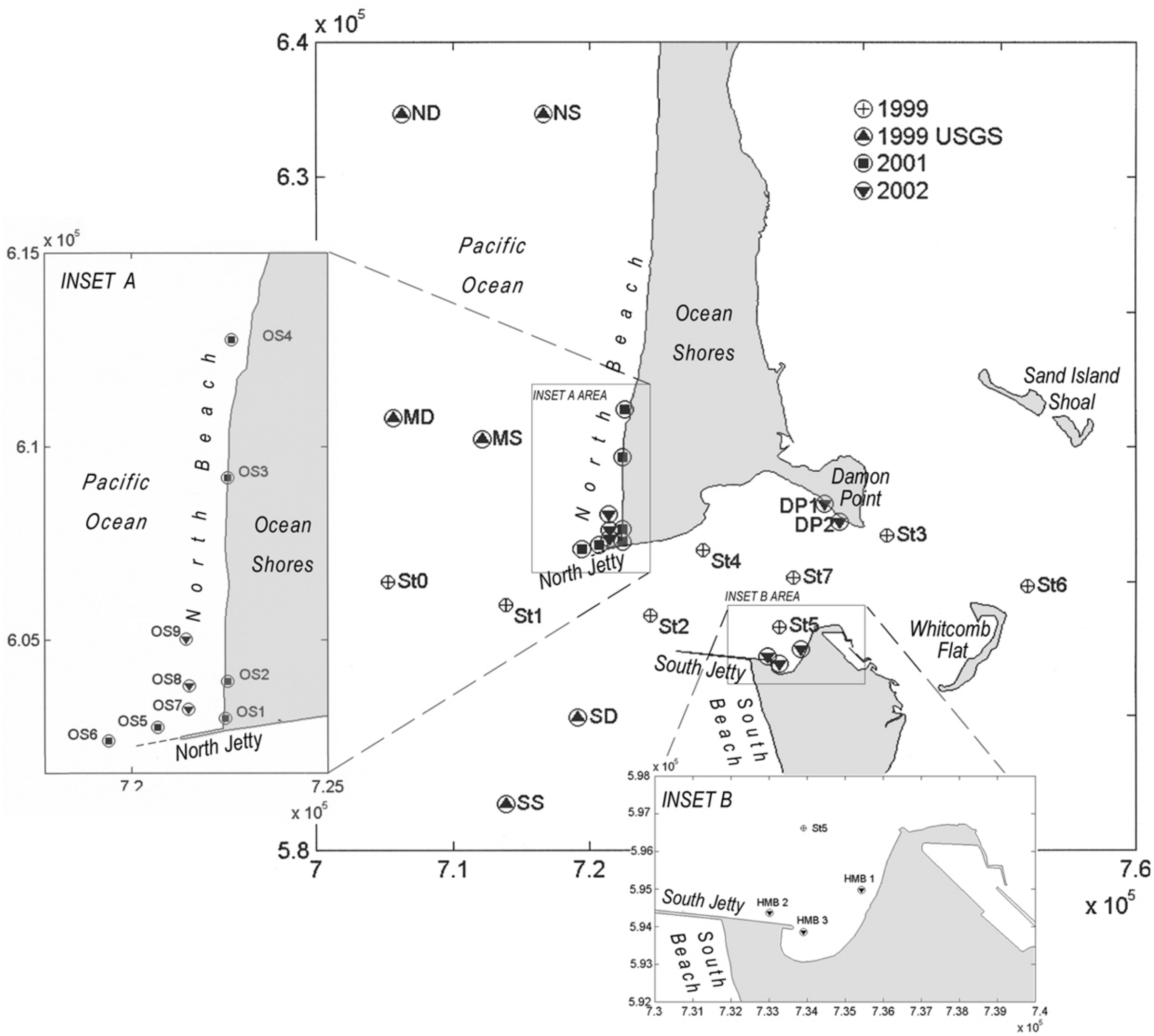

Source: USACE 2003a

Figure 7: Location of Instruments Deployed in Grays Harbor

2.2 INSAR DATA GENERATION

InSAR satellite imagery provides ground deformation monitoring information with millimeter scale precision. Stantec Consulting Services Inc.'s Surface Subsidence & Uplift Measurement (SSUM) remote sensing service ingests InSAR datasets to provide historical and on-going measurements of airport runway infrastructure. SSUM uses a freely available global InSAR dataset from the European Space Agency (ESA) that provides ground deformation velocity measurements with millimeter accuracy. This technology was used in this project to derive the morphological change over tidal flats for model verification and biological assessment that reduced the time and expenses that would otherwise be required for extensive field survey.

2.2.1 Methodology

InSAR satellites transmit pulses of electromagnetic (EM) energy to the Earth's surface and receive the EM waves that are scattered back to the satellite. Satellite sensors record the phase of the EM wave when it leaves and returns to the satellite. This form of data collection is a highly precise method of recording the time it takes an EM wave to travel to and from the Earth's surface. Over time, SSUM compares multiple InSAR images and there can be a slight phase shift between consecutive InSAR images. Two factors remain constant; 1) the speed the EM wave is travelling, which is the speed of light; and 2) the orbital position of the satellite. Therefore, the only factor to account for the phase shift is the elevation of the Earth's surface. SSUM interprets InSAR data phase shifts and calculates ground deformation changes over time ().

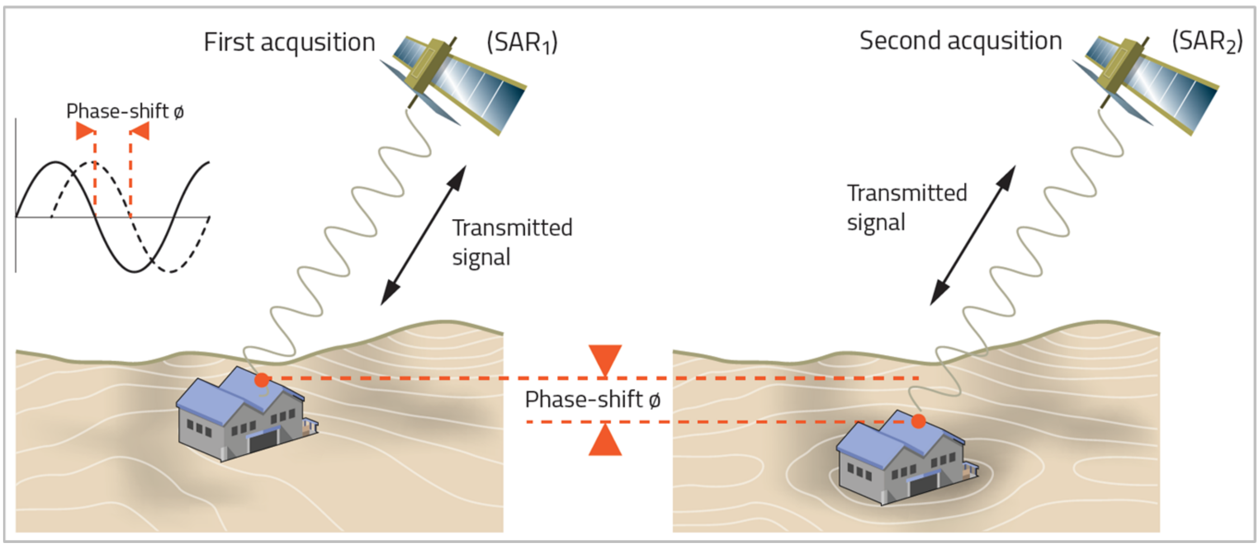

Figure 8: Diagram of an InSAR EM Wave Phase Shift Comparing the First Acquisition to the Second Acquisition. Phase Shifts Represent a Change in Elevation Levels.

A typical InSAR analysis requires between 30 to 60 images to achieve the millimeter accuracy scale required for survey grade studies. The ESA InSAR archive contains imagery that is collected every 12 days from present to 2015. InSAR also is unaffected by clouds, smoke, haze, snow, or vegetation and can acquire imagery both day and night. This allowed SSUM to determine the amount of movement for each individual oyster and burrowing shrimp over several years. SSUM also is able to provide on-going updates on an annual basis.

2.2.2 InSAR Dataset

SSUM used a total of 31 Sentinel-1 InSAR data from the ESA from mid-2015 to late-2019. All InSAR data is not capable of reaching the earth land surface under water; therefore, InSAR data collected at low tide was the only imagery that was useful in this analysis. This resulted in a decrease in images normally used for terrestrial analysis from over 60 dates to 31 dates. However, this did not influence the accuracy or precision of the SSUM results (Table 5).

Table 5: Sentinel-1 InSAR Data Acquisition Dates of Low Tide for the Project Area

Year	Month	Day		Year	Month	Day		Year	Month	Day
2015	06	17		2017	01	25		2018	07	13
2015	08	16		2017	02	24		2019	01	21
2015	10	27		2017	04	25		2019	03	22
2016	03	19		2017	05	07		2019	04	03
2016	05	18		2017	06	24		2019	06	02
2016	07	17		2017	07	06		2019	08	01
2016	09	03		2017	08	23		2019	08	13
2016	10	15		2017	09	04		2019	09	30
2016	12	02		2017	11	03		2019	10	12
2016	12	26		2018	01	02		2019	11	05
				2018	03	15				

2.2.3 Results

SSUM results for Grays Harbor show a subsidence rate of -2.94 millimeters (mm) and an uplift rate of +3.49 mm for the Grays Harbor area (Figure 9) and a subsidence rate of -3.71 mm and an uplift rate of +3.98 mm for the Willapa Bay area (Figure 10) over the span of roughly 4.5 years.

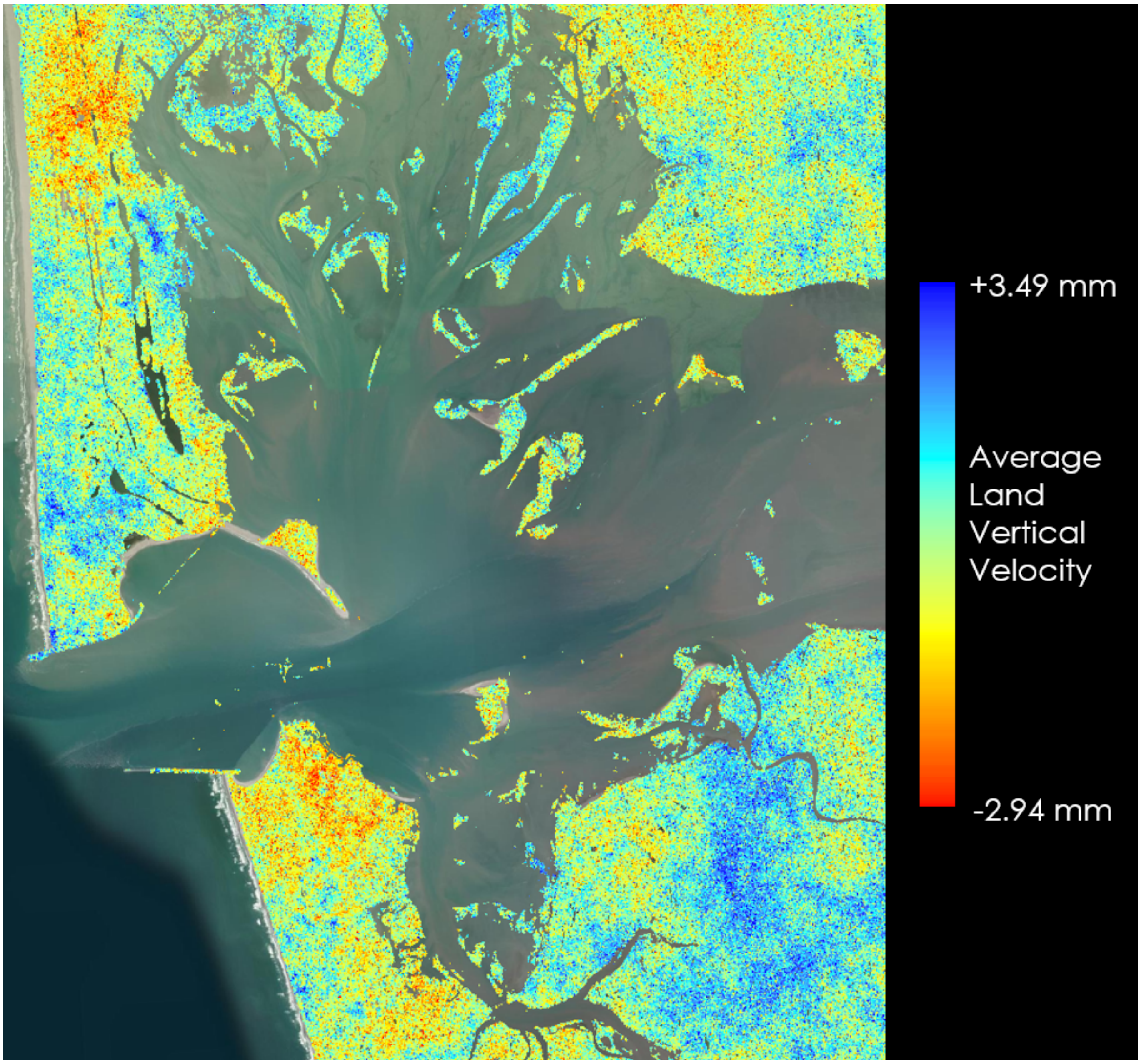

Figure 9: SSUM Results of Average Land Vertical Velocity of Grays Harbor from Mid-2015 to Late-2019

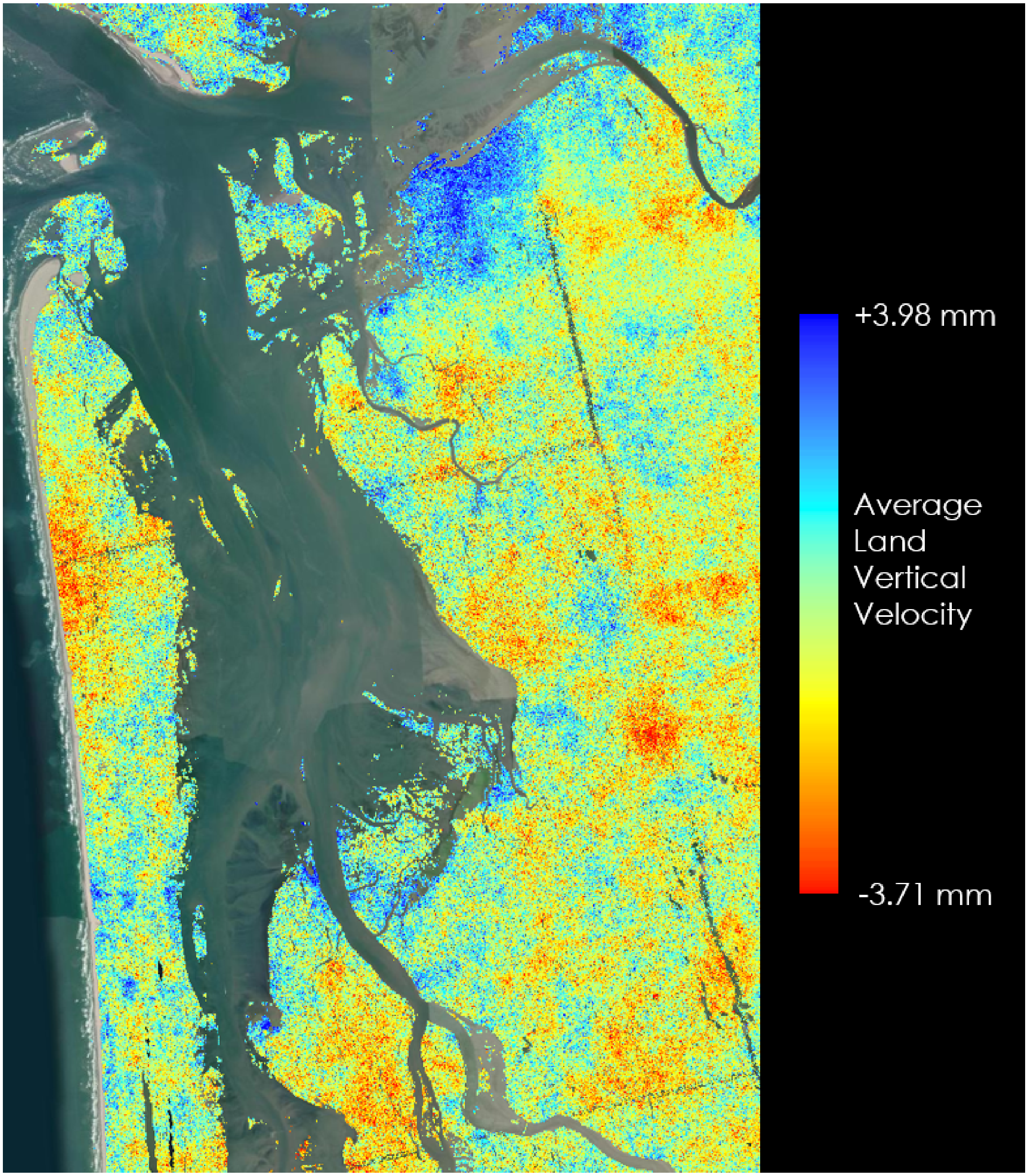

Figure 10: SSUM Results of Average Land Vertical Velocity of Grays Harbor from Mid-2015 to Late-2019

2.3 STAKEHOLDER SURVEYS

An innovative stakeholder app was designed to gather information directly from the local oyster growers who are experiencing a variety of issues in Grays Harbor and Willapa Bay. Many of them come from multi-generational businesses, and the app gave them the opportunity to share information that couldn't have been gathered from any other source. A snapshot of the stakeholder webapp is shown in Figure 11.

Based around Google Earth, the app allowed users to look up an area using coordinates or street address, or hand-draw specific areas using the cursor. The county parcel ID numbers were overlaid on the maps which made identifying specific patches of land extremely user friendly. Once a stakeholder chose an area to provide input, they had the option to use a color-coded system to indicate whether they were referring to an area of oyster production, sediment, subsidence, burrowing shrimp, marsh, water quality, or other relevant project activities. Specific locations on the map also could be addressed with a direct comment. Commentor identity and comments explaining their reason for highlighting that section, anecdotes about the area, or information about the type of sediment, growing conditions, or instances of shrimp infestation or other mortality, as well as supporting documentation could be uploaded. Many stakeholders enthusiastically participated in building this source of information promoting an intrinsic value with this database.

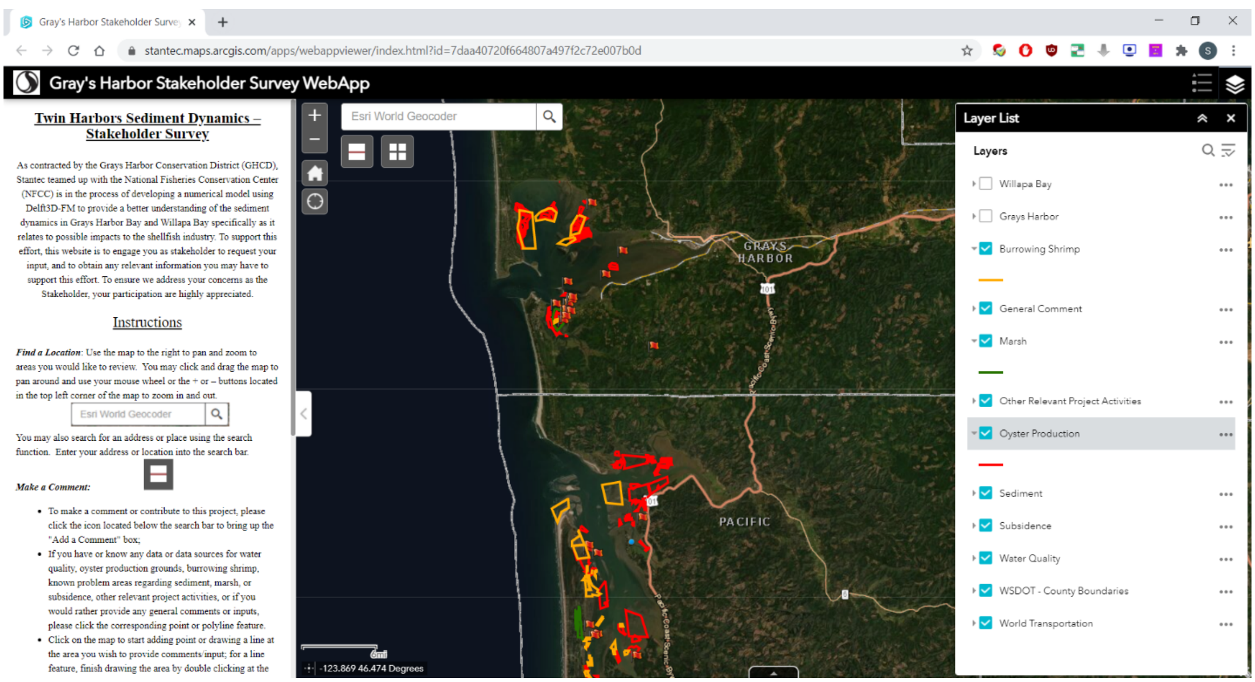

Figure 11: A Snap of the Stakeholder Webapp and the Data Collected

In addition to the stakeholder's contributions, GIS data from a map of all the active oyster production areas in Grays Harbor was added to allow emphasis of the analysis to focus on oyster production areas. The final result gave the project team a unique source of information "from the ground" -- discovering attributes of the harbors and its conditions that could only come directly from oyster producers in those estuaries. The data collected through this effort (as shown in Figure 11) are included in the deliverable as the ERSI Geodatabase.

2.4 USACE LITERATURE REVIEW

The Twin Harbors, particularly in Grays Harbor, were heavily studied by the ERDC and CHL from the USACE. The following reports were found, which are summarized in Appendix A.

USACE. 2000. Study of Navigation Channel Feasibility, Willapa Bay, WA. USACE ERDC/CHL-TR-00-6. Vicksburg, MS.

----------. 2002. Study of Navigation Channel Feasibility, Willapa Bay, WA – Report 2: Entrance Channel Monitoring and Study of Bay Center Entrance Channel, WA. USACE ERDC/CHL-TR-00-6.

----------. 2003a. North Jetty Performance and Entrance Navigation Channel Maintenance, Grays Harbor, Washington. USACE, ERDC/CHL TR-03-12. Vicksburg, MS.

----------. 2003b. South Jetty Sediment Processes Study, Grays Harbor, WA: Evaluation of Engineering Structures and Maintenance Measures. USACE, ERDC/CHL TR-03-4. Vicksburg, MS.

----------. 2006. Breach History and Susceptibility Study, South Jetty and Navigation Project, Grays Harbor, WA. USACE ERDC/CHL TR-06-22. Vicksburg, MS.

----------. 2010. Waves, Hydrodynamics and Sediment Transport Modeling at Grays Harbor, WA. USACE, ERDC/CHL TR-10-13. Vicksburg, MS.

----------. 2012. Dredged Material Placement Site Capacity Analysis for Navigation Improvement Project at Grays Harbor, WA. USACE, ERDC/CHL TR-12-18.

3.0 DATA ANALYSIS AND OBSERVATIONS

3.1 BATHYMETRY

The offshore bathymetry for the northwest Pacific and 2018 bathymetry for the Twin Harbors are obtained from NOAA's Coastal Relief Model and the 2018 NOS study, respectively, which is shown in Figure 12. Generally, the continental shelf within the CRLC has a very smooth bathymetry variation with contour lines trending approximately 15 degrees west of north. The continental shelf varies in width from about 20 to 45 miles with a general nearshore slope of 0.4 percent. The nearshore slope just seaward off Grays Harbor, Willapa Bay, and the Columbia River is slightly different due to the ebb-shoal deposits. Within Grays Harbor, a federal navigation deep-draft channel is maintained by the Seattle District. The channel is aligned generally in a northeasterly direction, from the Pacific Ocean into the mouth of the Harbor at Point Chehalis. From 2016 to 2018, the channel was deepened from a depth of 36 ft MLLW to a depth of 38 ft MLLW. The areas surrounding the channel are comparatively shallow, with a depth of around 0-meter (m) MLLW. There are small, naturally occurring channels intermittently around the bay. Willapa Bay does not have a dredged channel but does have naturally occurring channels up to a depth of 80 ft MLLW at the mouth of the bay, which extend into the rest of the bay. The majority of Willapa Bay consists of tidal flats that are exposed at low tide, making navigation difficult for commercial ships. Similar to Grays Harbor, the tidal flat elevations are generally 0 ft MLLW.

3.2 TIDES AND WATER LEVELS

Tides in the Twin Harbors are typical of the Pacific Coast of North America, which are mixed tide and exhibit diurnal inequality with two unequal high and low elevations each lunar day. Tide prediction and water level records are available from NOAA tide gauges 9441102 at Westport, 9441187 at Aberdeen in Grays Harbor, and 99441101 at Toke Point in Willapa Bay, where the corresponding tidal datums are summarized in Table 6.

For Grays Harbor, the diurnal range is 9.14 ft at the harbor entrance, increasing to 10.11 ft at Aberdeen with a 1-hour phase lag because of the amplification of the tidal wave through the pear shape of the harbor. The diurnal range is similar in Willapa, which is 8.92 ft at Toke Point. Observed water levels are primarily a function of astronomic tide influences, with deviations from the predicted astronomic tide due to factors including changes in atmospheric pressure, wind setup, wave setup, and river discharge. The relatively large tidal range along with the broad bay area leads to a significant volume of tidal exchange within the Twin Harbors. Diurnal tidal prism volumes are approximately 1.7 x 10^{10} ft^3 within Grays Harbor (The Seattle District 1989) and more than 1.0 x 10^{10} ft^3 within Willapa Bay (Jarrett 1976).

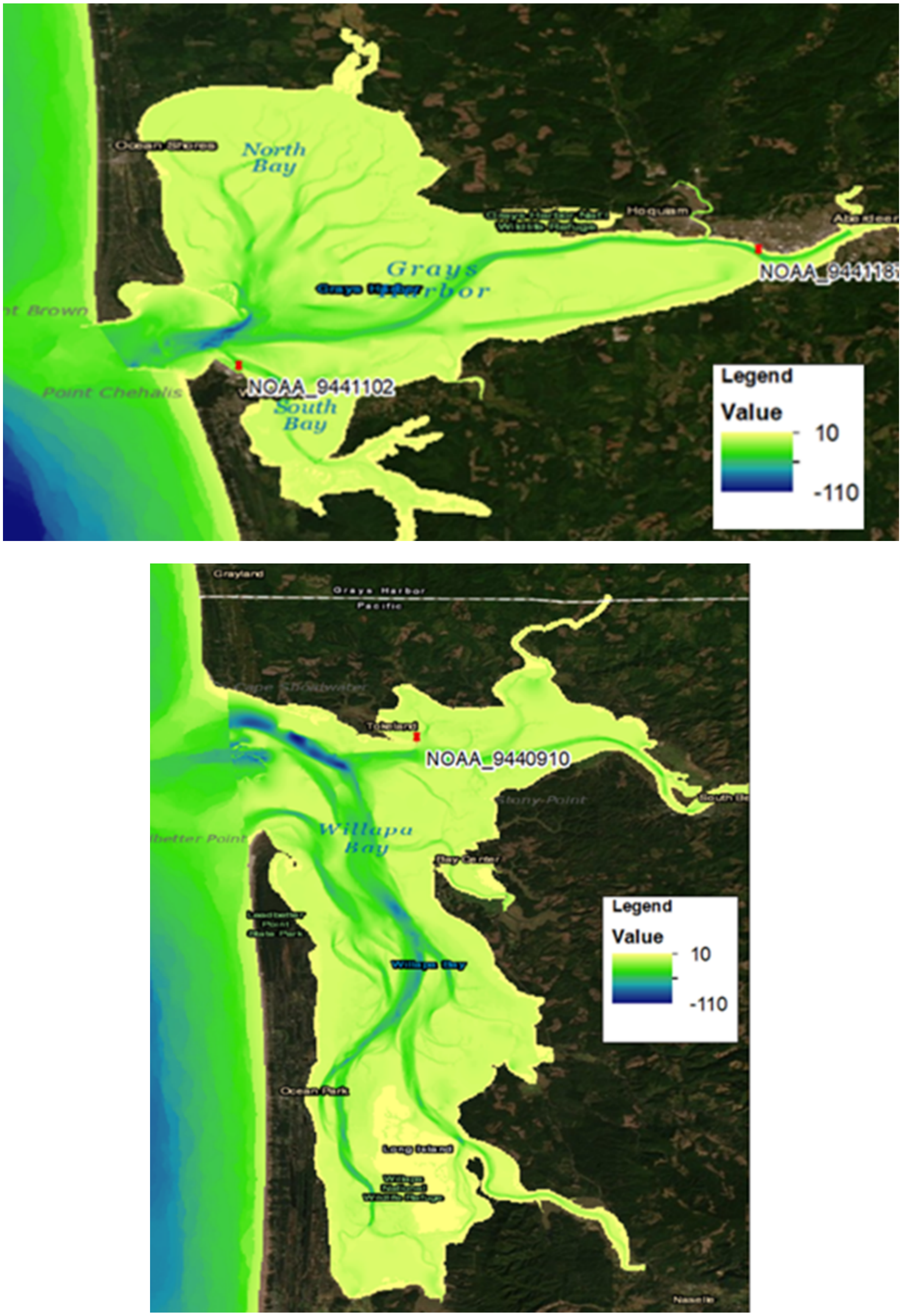

Figure 12: Bathymetry in ft MLLW of Grays Harbor (Top) and Willapa Bay (Bottom)

Table 6: Summary of tidal datums (relative to MLLW).

Datum	NOAA 9441102 at Westport (ft)	NOAA 9441187 at Aberdeen (ft)	NOAA 9440910 at Toke Point (ft)
Highest Observed Water Level	12.65	13.86	14.41
Mean Higher High Water (MHHW)	9.14	10.11	8.92
Mean High Water (MHW)	8.40	9.41	8.18
Mean Tide Level	4.90	5.44	4.77
North American Vertical Datum of 1988 (NAVD88)	1.77	1.64	0.82
Mean Low Water	1.39	1.47	1.37
Mean Lower Low Water (MLLW)	0	0	0
Lowest Observed Water Level	-3.61	-3.35	-3.81
Mean Range	7.01	7.94	6.81
Diurnal Range	9.14	10.11	8.92

3.3 SEA LEVEL RISE

Sea Level Rise (SLR) was calculated using the USACE Sea Level Change Calculator for NOAA tide at Toke Point, Washington, which is based on a USACE 2013 study (USACE 2019). Curves for low, intermediate, and high sea level rise scenarios are shown below in Figure 13, and the predicted values every 10 years between 1990 to 2100 are shown in Table 7. Based on the USACE estimations, by 2100 the estimations of Mean Tide Level for low, intermediate, and high sea level rise scenarios are 5.19 ft, 6.15 ft, and 9.22 ft NAVD88, respectively. The initial 1990 mean sea level at Toke Point is 3.96 ft NAVD88.

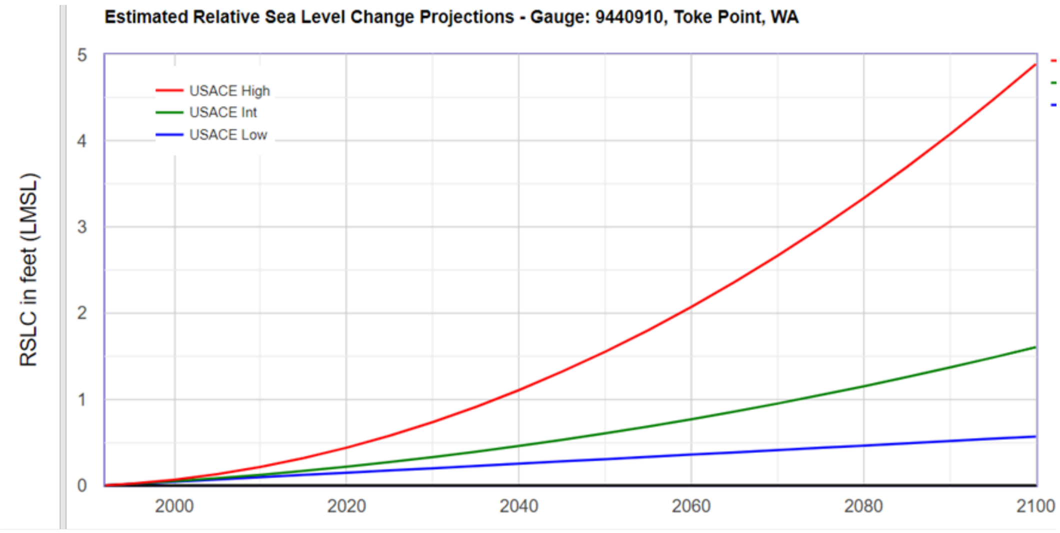

Figure 13: SLR Projection at NOAA Tide Gauge 9440910 (Toke Point) from USACE

Table 7: Decadal SLR Projection in ft Mean Sea Level at Toke Point from USACE

Year	USACE Low	USACE Int	USACE High
1992	0	0	0
2000	0.04	0.05	0.07
2010	0.09	0.12	0.22
2020	0.15	0.22	0.44
2030	0.2	0.33	0.74
2040	0.25	0.46	1.11
2050	0.3	0.6	1.55
2060	0.36	0.77	2.07
2070	0.41	0.95	2.67
2080	0.46	1.15	3.33
2090	0.51	1.37	4.08
2100	0.57	1.6	4.89

3.4 DISCHARGE

River discharge data from major tributaries are available from USGS stream gauges including, from east to west, Chehalis River at Porter, Satsop River, Wynoochee River and Humptulips River for Grays

Harbor, and from north to south, North River near Raymond, Willapa River, and Nasselle River for Willapa Bay.

The seasonal variations of the discharge from those rivers are shown as violin plots in Figure 14 and Figure 15 for Grays Harbor and Willapa Bay, respectively. It's clear that the seasonal variations of the discharge are very similar between the watersheds. River discharge is very small with confined distribution from May through October, and river discharge generally increases with large variations from November to March. The rainy seasons begin early in October and the annual spring snowmelt from the mountainous areas that feed into the rivers commonly occurs in February and March. The Chehalis River contributes more than 50 percent of total freshwater discharge into Grays Harbor while North River contributes the largest freshwater inflow into Willapa Bay, with Willapa River being slightly less. Willapa Bay receives a few times less freshwater from the watersheds than Grays Harbor.

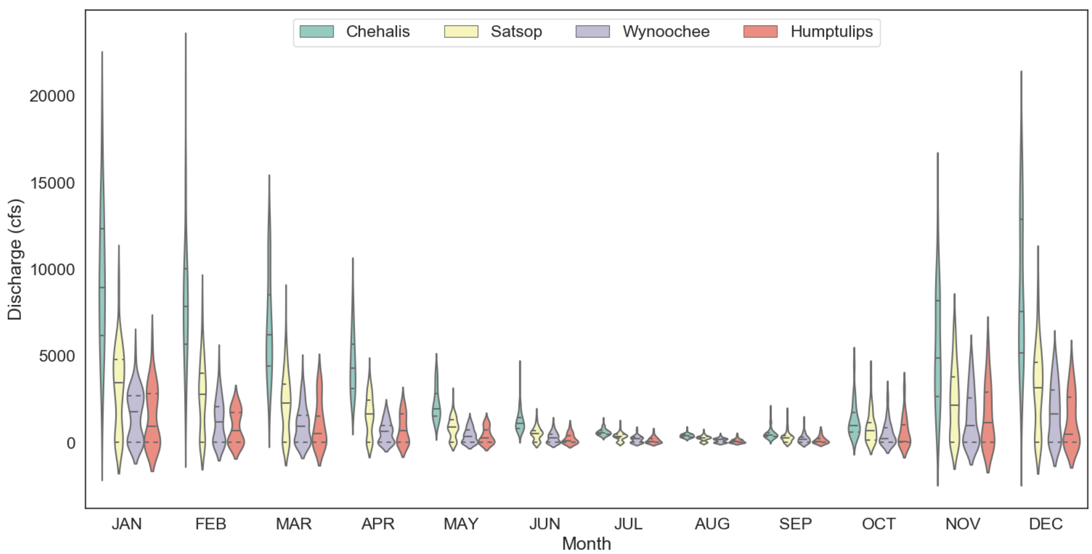

Figure 14: Violin Plots of Discharges for Major Tributaries of Grays Harbor

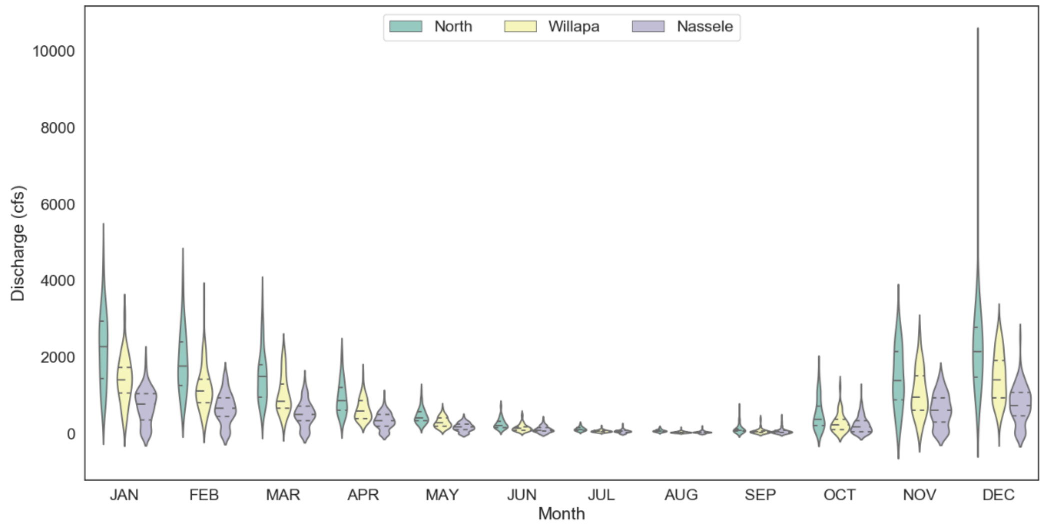

Figure 15: Violin Plots of Discharges for Major Tributaries of Willapa Bay

3.5 WIND

Winds over the Northeast Pacific Ocean generally correspond to the seasonal atmospheric cycles, which is largely determined by pressure distribution from the movement of the North Pacific high-pressure system and the Aleutian low-pressure system in the Bering Sea that drive the jet stream over the North Pacific (Anderson and Foster 1979).

During the summer months, the East Pacific high-pressure system migrates northward from the equatorial region and becomes seasonally stationary off the coasts of California and Oregon. It reaches its greatest development in July while the Aleutian low is almost nonexistent; this weather system generates clockwise winds with predominantly northwest and north winds over the coastal and near-offshore areas of Oregon and Washington. During the winter months, the East Pacific high-pressure system retreats to the equatorial region and low-pressure systems over the Gulf of Alaska (Aleutian Low) strengthen and migrate west to east across the coast and dominate the Washington coast; this weather system causes considerable day-to-day variations in wind speed and direction. Particularly, when the low-pressure systems make landfall on the coast, they produce hurricane-like conditions with sustained wind speeds greater than 40 knots for fetches greater than 125 miles. The counterclockwise winds associated with cyclonic activity predominantly originate from the south and southeast near the Washington coast. Compared to winds in summer from the north, wind speeds in the winter months are generally of greater magnitude, with 5 to 8 percent of the wind speeds between gale-force and storm-force levels. More specifically, monthly wind roses at NDBC buoy 46009 offshore, buoy WPTW1 at Westport in Grays Harbor, and buoy TOKW1 at Toke Point in Willapa Bay are shown in Figure 16 through Figure 18. The winds at Toke Point and Westport are greatly affected by the geometry of Grays Harbor and Willapa Bay respectively. Winds at Toke Point are predominantly from the northwest in summer months and from the east in winter months while winds at Westport are predominantly from the east and south in winter months.

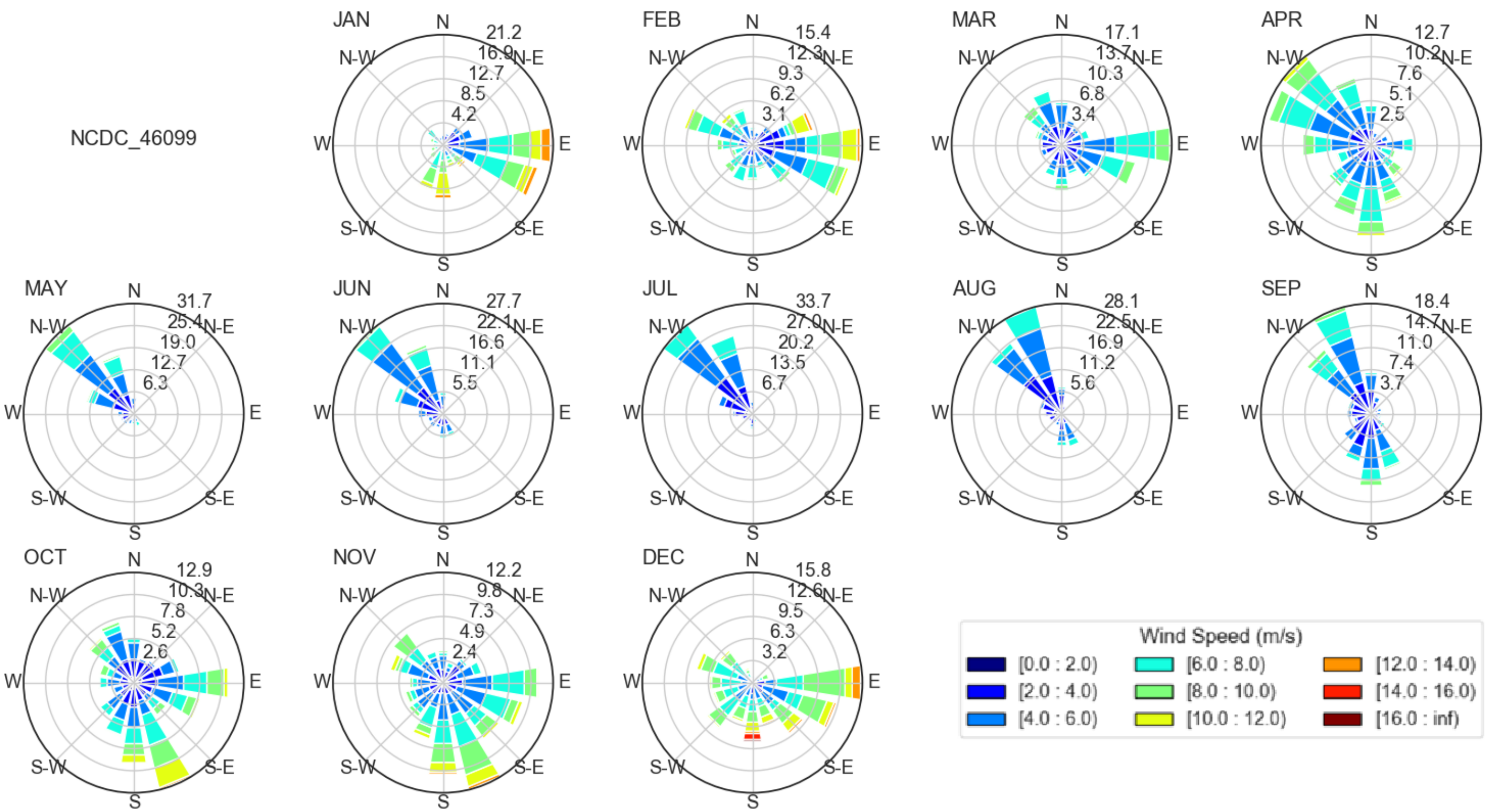

Figure 16: Monthly Wind Roses Offshore of the Twin Harbors at NDBC Buoy 46009

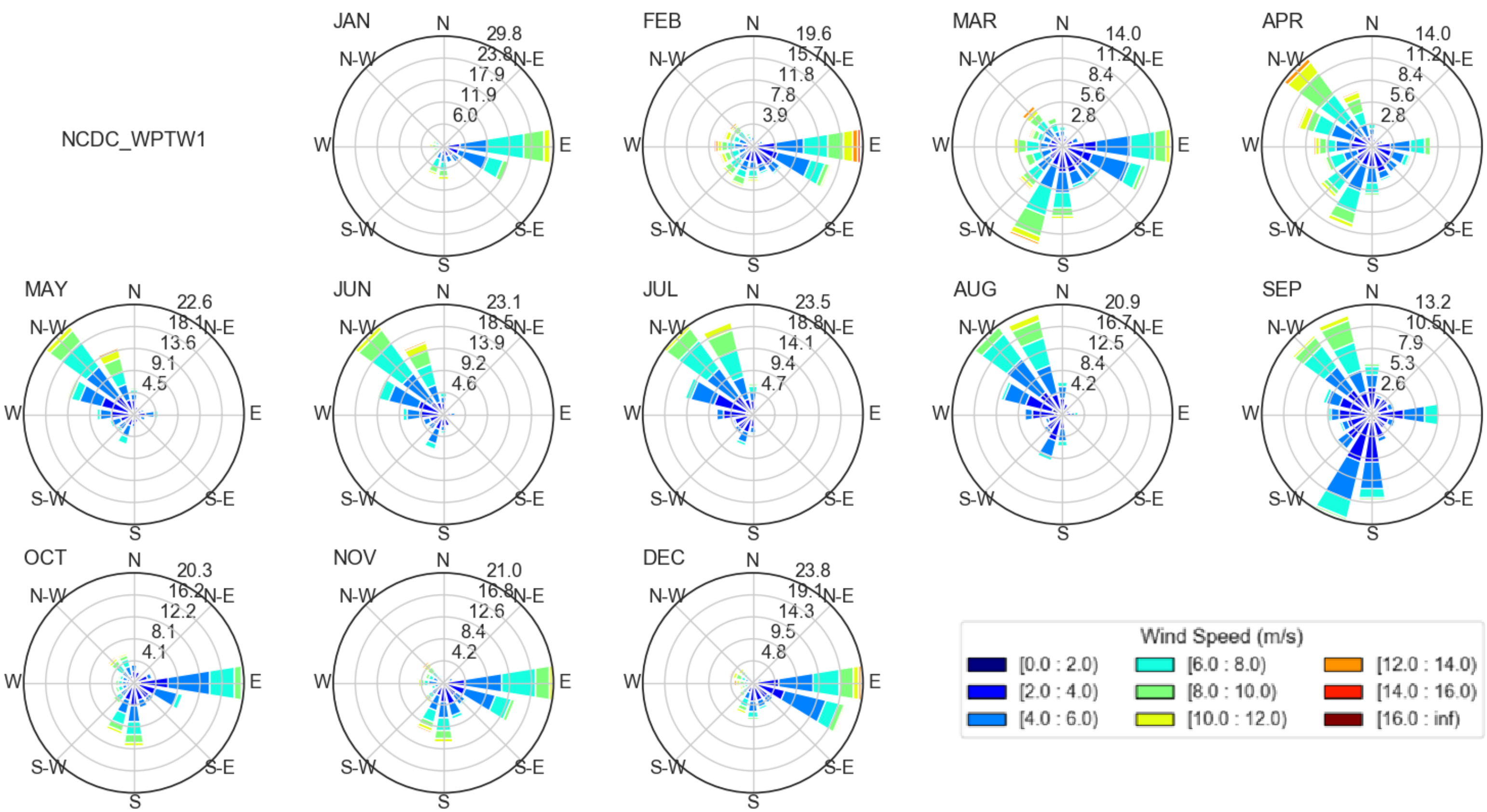

Figure 17: Monthly Wind Roses at NDBC Buoy WPTW1 in Grays Harbor

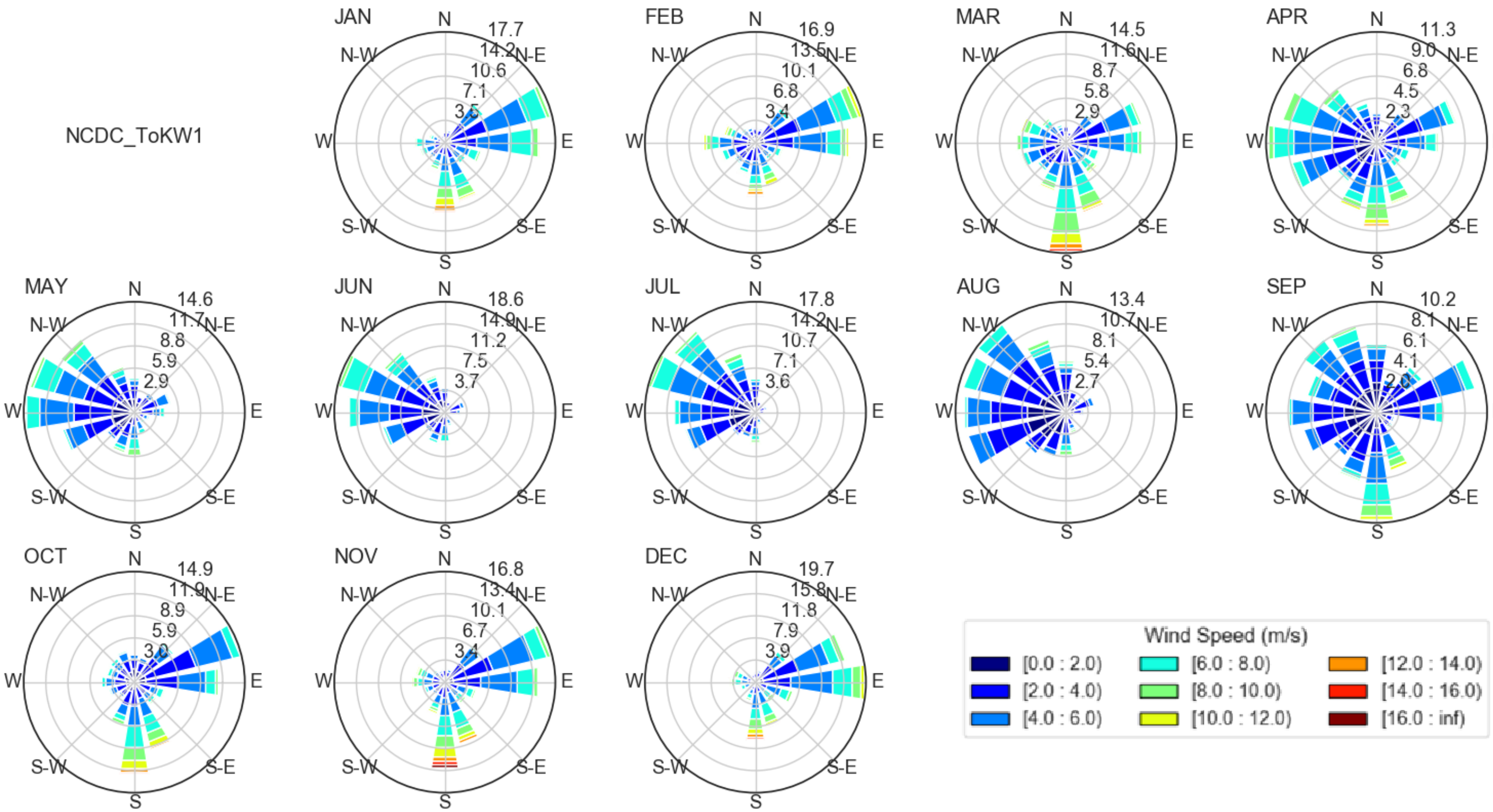

Figure 18: Monthly Wind Roses at NDBC Buoy TOKW1 in Willapa Bay

3.6 WAVES

Waves can mobilize bed sediments into the water column and cause nearshore currents and water level changes at the shoreline, which are a primary mechanism controlling sediment transport in the nearshore and ebb-shoal regions of tidal inlets for the Twin Harbors. This may result in episodes of erosion and accretion. The wave climate offshore of the Pacific Coast is different from that within the Twin Harbors because of wave dissipation and the relatively narrow entrances with respect to the wave lengths associated with longer period waves offshore. Offshore waves and local wind waves are discussed separately in Sections 3.6.1 and 3.6.2, respectively.

3.6.1 Pacific Ocean Waves

The CDIP buoy 036, located near the entrance of Grays Harbor in 130 ft of water, has the longest continuous wave record in the area, with recorded wave heights since 1981 and wave directions since 1994. Figure 19 shows the corresponding wave rose and the joint plots between significant wave height (Hs) and peak wave period (Tp), which indicate that the predominant wave direction is from west to northwest. The strongest waves are generally from the west. The joint plots between Hs and Tp indicate that most wave energy is concentrated around 2 m heights with 10 sec periods. It is important to understand in the numerical model how much wave energy associated with such conditions can reach into the harbors, given the moderate wave periods. The extremely long wave periods above 18 sec rarely coincide with very large wave heights.

Offshore waves also exhibit seasonal variations, which can be seen from the violin plots of Hs for each month in Figure 20. Summer months are calm with smaller and tighter distribution of Hs, while winter months have stronger waves with a wide distribution of Hs due to large winter storms. Seasonal variations of wave direction at CDIP buoy 036 can be understood via the monthly wave roses in Figure 21. The prevailing waves in the milder summer months are from the northwest, while large storms in the winter months generate waves from the west (deviating slightly towards the south from 270°). Such seasonality of waves determines the direction of net alongshore sediment transport, which is discussed in Section 3.9.3.

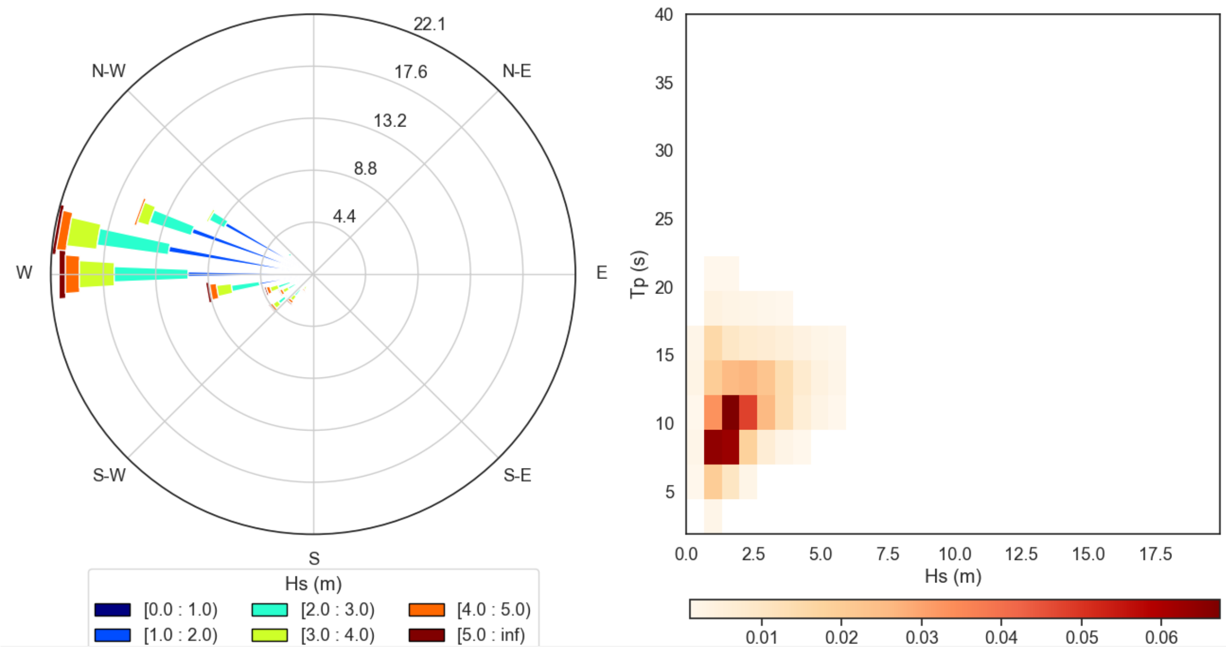

Figure 19: Wave Rose and the Joint Plot between Hs and Tp at CDIP Buoy 036

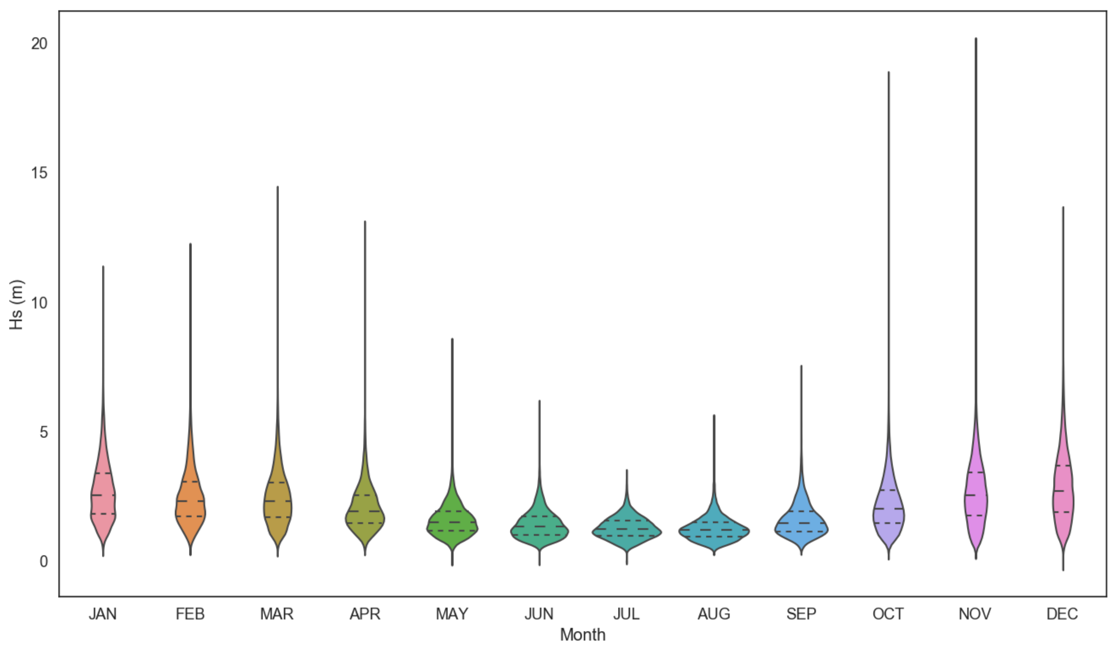

Figure 20: Violin Plots of Wave Height at CDIP Buoy 036 by Month

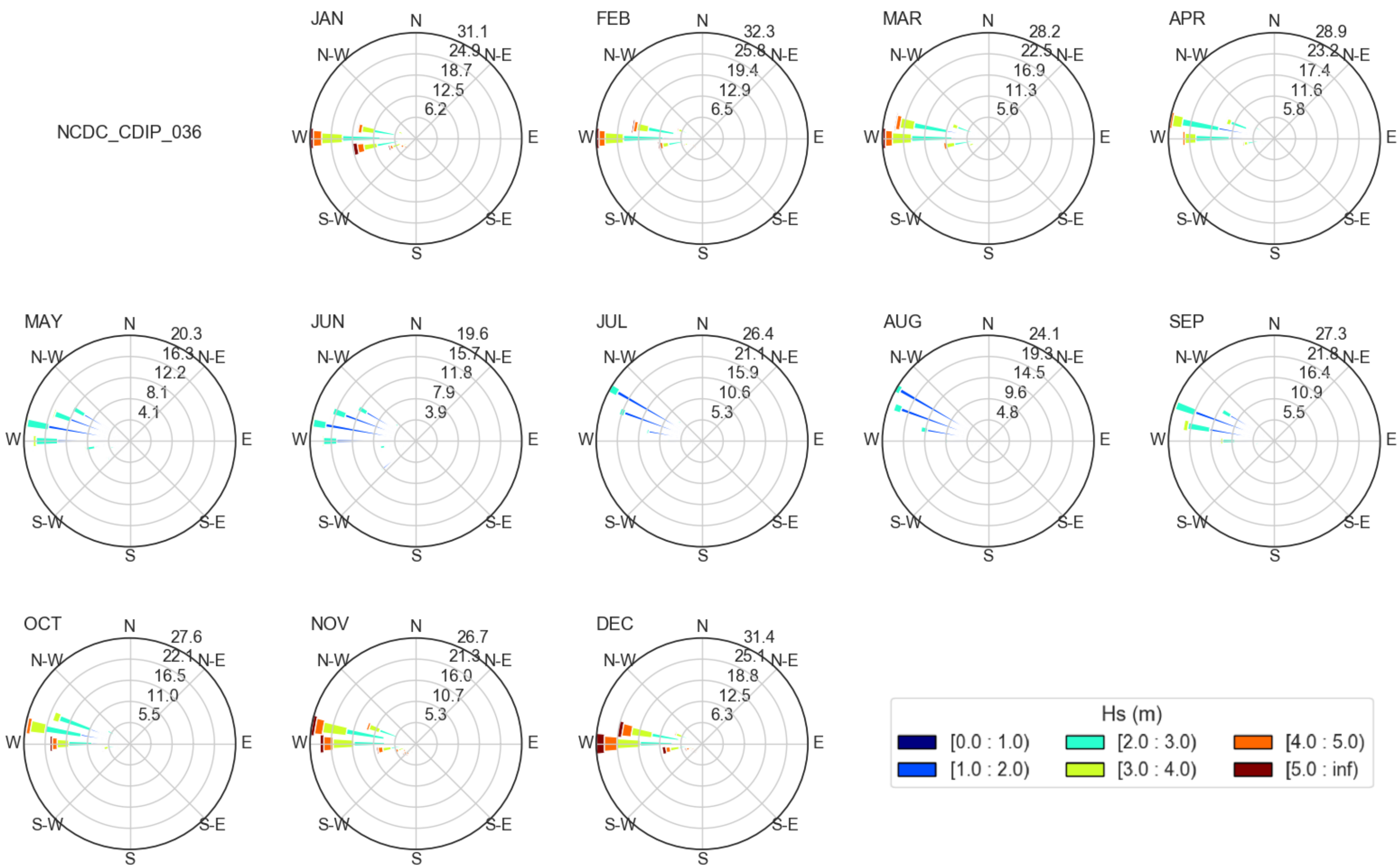

Figure 21: Monthly Wave Roses at CDIP Buoy 036

3.6.2 Local Wind Waves

Ocean swell is dissipated in the outer cross-over reach and becomes negligible within the harbors due to the restriction of the narrow inlets. The inner harbor reaches are exposed to locally generated wind waves. The direct measurement of waves within the Twin Harbors are not available to this study; however, based on the literature review of the analysis of the field survey data, fetch lengths are largest during high tide and can produce wave heights on the order of 1 to 3 ft. Wind-generated waves have shorter periods than ocean swell, typically ranging from 2 to 4 seconds. These waves transport fine-grained materials within the harbors.

3.7 CURRENT

The offshore currents along the shoreline of the Twin Harbors are generally weak large-scale currents with speed of 0.16 to 1 ft/s and are influenced by seasonal variations in the discharge of coastal rivers, particularly the Columbia River. Coastal currents also respond rapidly to local winds, and therefore are strongly affected by the yearly cyclical changes of the North Pacific high-pressure system and the Aleutian low-pressure system as discussed in Section 3.5. During the summer months, the Pacific Northwest high-pressure systems drive clockwise winds blowing from the north along the Washington coast causing surface currents to flow toward the southwest, which is referred to as the California Current (Hickey 1979). The California Current has a typical velocity of 0.3 ft/s. Near the bottom, the combination of wind stress, ocean density gradients, and Coriolis force creates upwelling of colder, denser bottom water, which causes easterly moving bottom water upwelling at the coast. During the winter months, the Aleutian low-pressure system interrupts the summer density gradient, creating dominant northward surface flow with an onshore component, which is called the Davidson Current, and offshore bottom flow (nearshore downwelling). Coastal currents off Washington State also are heavily influenced by freshwater discharge from the Columbia River. The freshwater dilution extends seaward some 31 to 62 miles and northward to the Strait of Juan de Fuca (Barnes et al. 1972). Currents within Grays Harbor and Willapa Bay are only available from the field surveys, which are mostly within the channels. The currents are strongest at the entrance and diminish inland.

3.8 TEMPERATURE AND SALINITY

The temperature and salinity are strongly influenced by the Columbia River Plume and the upstream freshwater discharge. Surface salinity nearshore close to the entrance of the harbors is generally between 29 to 30 parts per thousand (ppt) during winter and spring when the Columbia River Plume moves northward along the coast with winds from the south and are between 30 to 32 ppt during the remainder of the year, peaking in June when the Columbia River Plume is minimally present due to north winds (Landry et al. 1989). Salinity less than 20 ppt is observed within Grays Harbor during periods of peak river discharge. For Willapa Bay, long-term (1961-1987) monitoring data collected by the Washington State Department of Fish and Wildlife in the southern part of the bay indicate that the average monthly surface layer salinity varies from 15 ppt in February to 29 ppt during August and September. In general, the bay is vertically well-mixed during low tributary flows (May to October) and alternates between vertically well-mixed and partly mixed during strong tributary flows from November through April (The Seattle District 1971).

3.9 SEDIMENT

3.9.1 Bed Sediments

The modern bed sediments for the southwest Washington continental shelf are comprised of fluvial sediments from the Columbia River during the Holocene, with an estimated annual sediment discharge rate of 0.55 to 2.3 x 10^7 tons/year (Karlin 1980). The most comprehensive bed sediment data are available from the usSEABED database described earlier, which mainly compiles the historical sediment samples of Roberts (1974), Nittrouer (1978), and Twitchell et al. (2000). Twitchell et al. (2000) also collected sidescan sonar imagery and bottom photographs within the CRLC and described the surficial geology of the inner continental shelf with those datasets. The spatial distribution of the median sediment diameter (D_{50}) and the percentage of mud derived from the usSEABED (PAC_EXT) database are shown in Figure 22 and Figure 23, respectively. The distribution of the surface sediments largely corresponds to the level of wave energy acting upon on the seabed, which can be broadly classified in the following zones:

- Lower Beach Face: this region represents the shoreward zone extending seaward to about the 60-ft depth contour where wave energy can mobilize the sediment into the water column and plays a significant role in longshore sediment transport. Therefore, sandy sediment dominates this region, with mean grain size ranging from about 0.25 mm in the nearshore (<30 ft) to 0.12 mm near the offshore boundary.

- Nearshore Zone: this region extends beyond the lower beach face region to a depth contour of 165 ft, where typical wave energy level is still strong enough to prevent significant deposition of silt; very fine sand (greater than 90 percent) dominates surface sediments to a distance offshore where silt and clay become more than 25 percent of the sample distribution.

- Inner Continental Shelf: this region extends from the 165-ft depth contour out to the edge of the continental shelf, where the presence of clay and silt characteristic of a Columbia River source increases to 40 to 70 percent of the bottom composition.

- Outer Continental Shelf: this region is relict deposits in depths greater than 425 ft, which largely consists of sand.

- Gravel Patch: an area of gravel exists west-northwest of the Grays Harbor entrance, which is a patchwork of relict gravel deposits, as the sediment samples indicate the same sediment characteristics of lower beach face region.

- Ebb Shoal Patch: ebb shoals exist at the entrance of Grays Harbor, Willapa Bay, and the Columbia River, where the sediments available for bypassing the entrance are close to 100 percent sand with a median grain size of 0.21 mm.

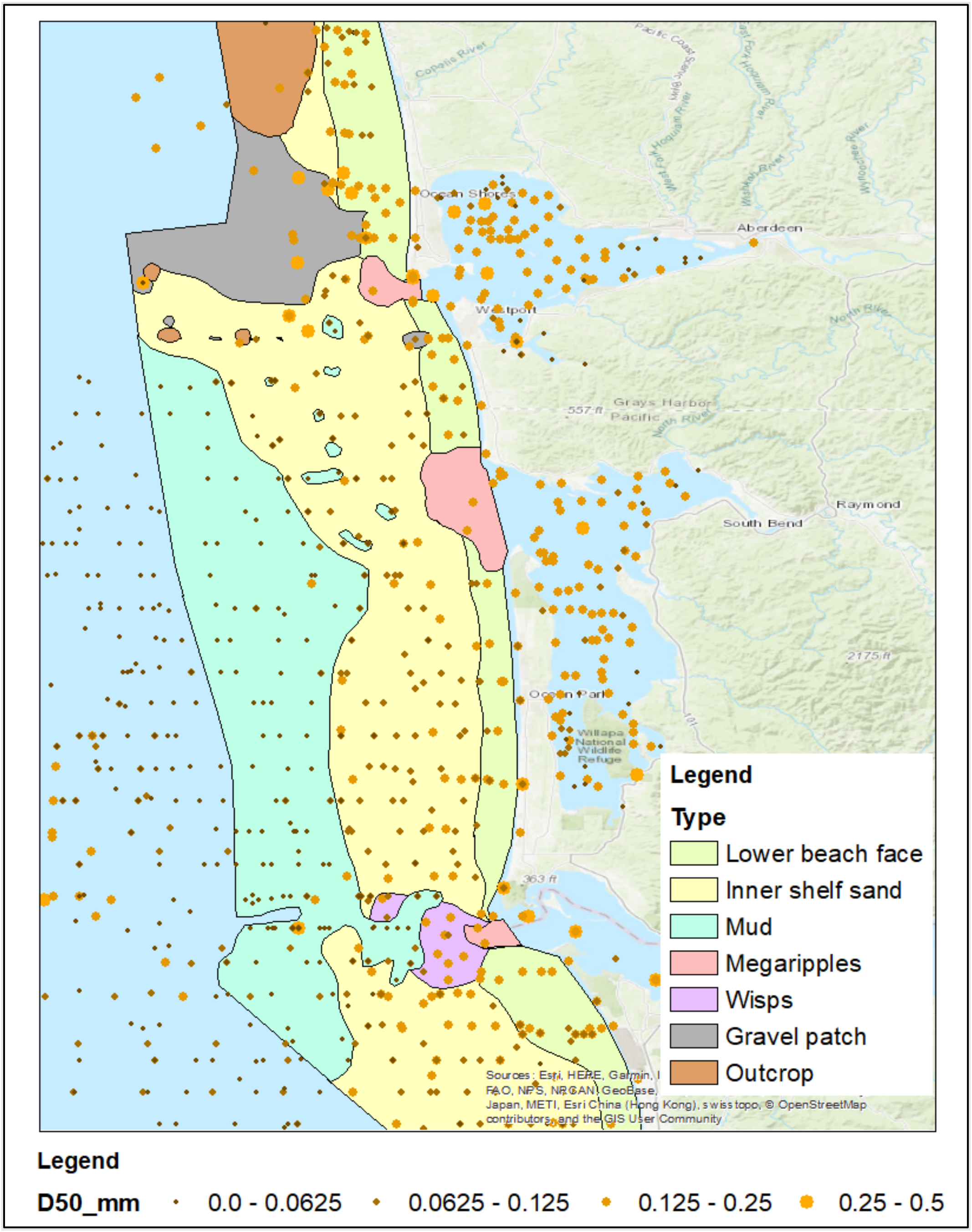

Figure 22: Spatial Distribution of D50 from usSEABED – PAC_EXT Database

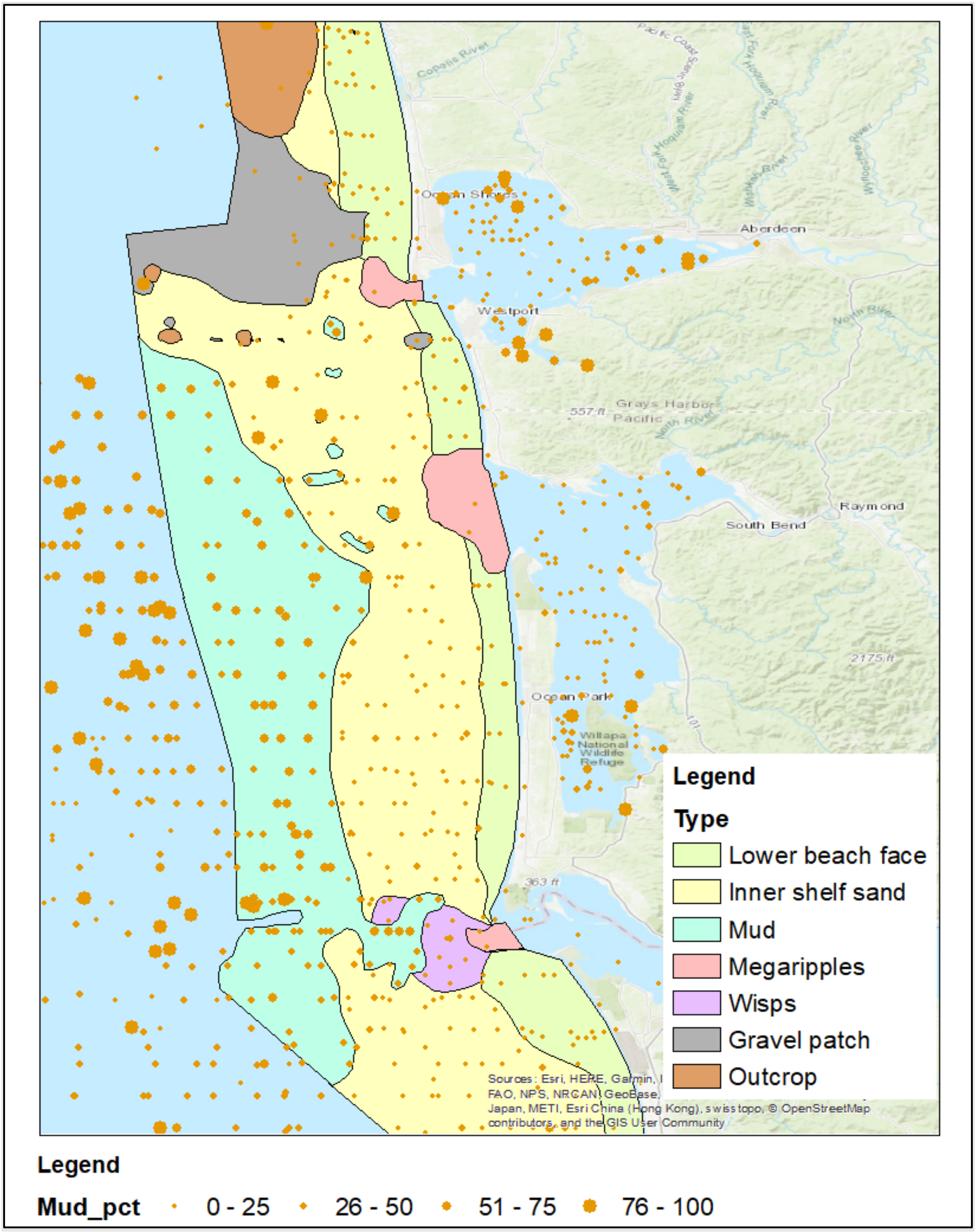

Figure 23: Spatial Distribution of Mud Percentage from usSEABED – PAC_EXT Database

Sediment from the Columbia River enters Grays Harbor and Willapa Bay as a marine source from the beaches and nearshore zone adjacent to the bay entrance. Sediment with distinctive heavy mineral components are found within Grays Harbor and Willapa, which originates from the respective inland watersheds as fluvial discharge (Scheidegger and Komar 1984). The depositional pattern in both Grays Harbor and Willapa Bay is dynamic, associated with seasonal variations in estuarine hydrography. Sand and gravel from local rivers are transported down the estuary with high fluvial discharge during winter months, while beach and nearshore sand is transported into the estuary by flood-tidal currents during summer months. Figure 24 and Figure 25, respectively, show the sediment distribution within Grays Harbor and Willapa Bay. Despite the seasonal migration of different sediment materials, sandy sediments from the Pacific Ocean dominate the outer bay while mud-rich deposits (greater than 50 percent silt and clay) dominate the inner bay and upper estuary.

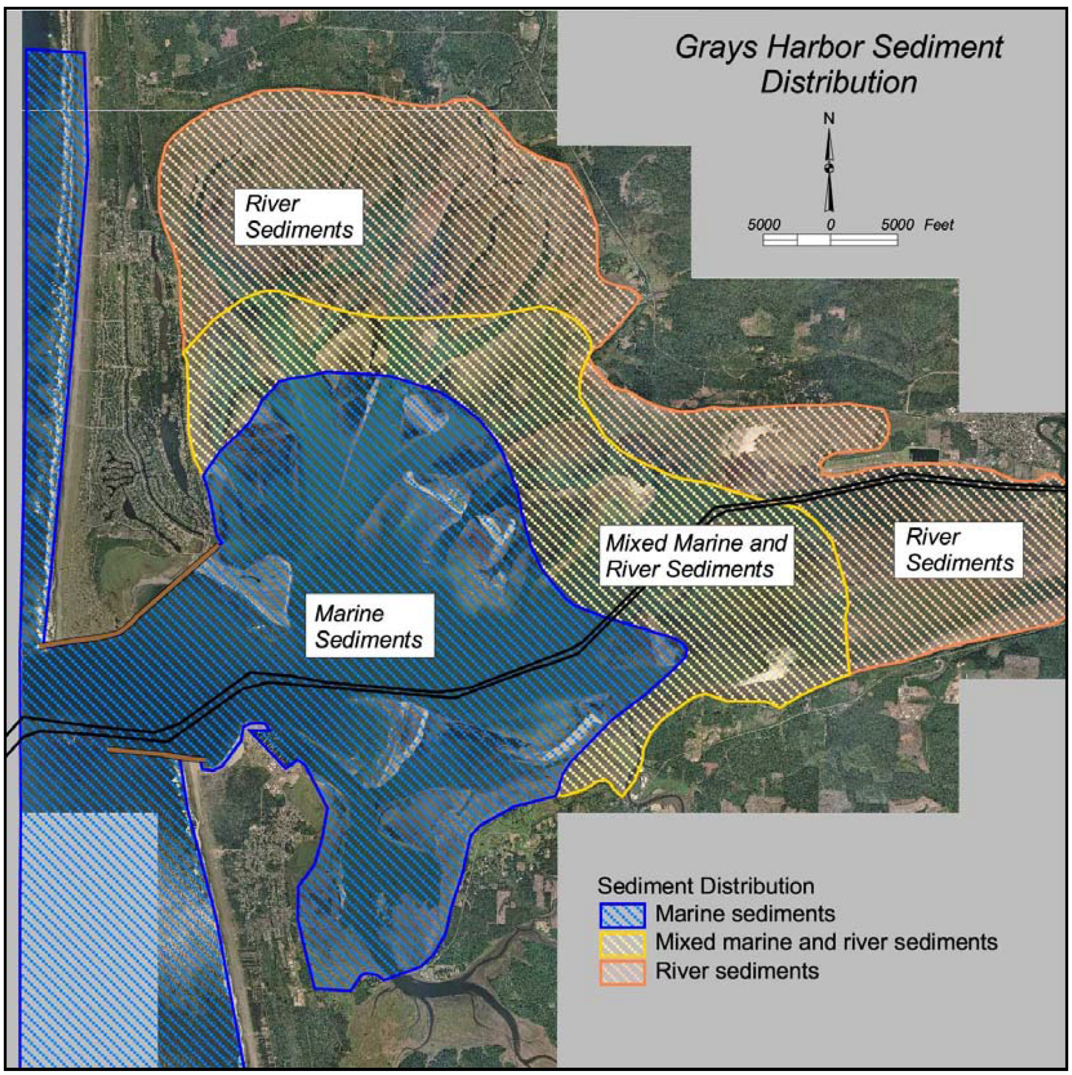

Source: Scheidegger and Phipps 1976

Figure 24: Provinces of Sand Deposition in Grays Harbor

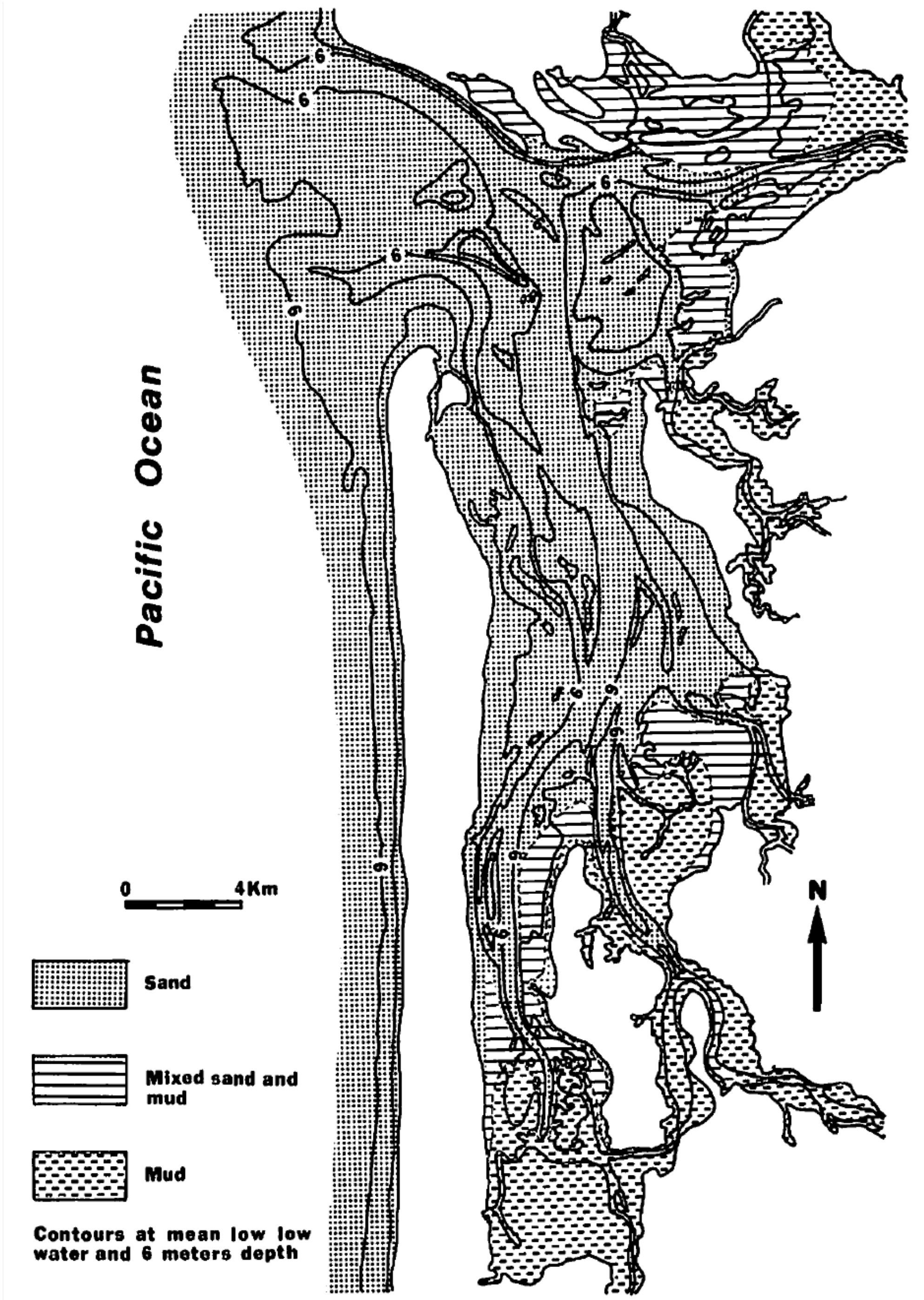

Source: Clifton and Philips 1980

Figure 25: Sediment texture in Willapa Bay, WA

3.9.2 Littoral Sediment Transport

As discussed in Section 3.6, waves dominate the offshore within the CRLC, and show distinctive seasonal characteristics. During summer months, waves approaching from northwest generate longshore currents that transport sand to the south, while high energy winter waves approach from west to southwest and produce faster longshore currents that transport sand to the north. The dominant source of sand for beach and offshore environments in the CRLC is from the Columbia River, which is moved northward in a net sense by seasonally reversing longshore currents due to higher energy winter waves.

3.9.3 Watershed Sediment Load

Upstream sediment load, as measured by SSC, are only available at two USGS stream gauges: one for Grays Harbor from the Chehalis River at USGS gauge 12035000 at Porter, and one for Willapa Bay from the Willapa River at USGS gauge 12013500. The datasets are only available from 1973 to 1995 for the Chehalis River and from 1979 to 1986 for the Willapa River, which are relatively sparse. Bed sediments near the Twin Harbors entrances originate from the Columbia River; suspended sediment data from the Columbia River also was analyzed, which is available from 1991 to 1995 at USGS gauge 14246900 near Port Westward.

Time series of SSC against the discharge for the Willapa, Chehalis, and Columbia Rivers are shown in Figure 26 through Figure 28, which indicate that SSC generally increases as water discharge increases, i.e., a very minor sediment discharge occurs during the period from May to October, when runoff is small, while runoff and surficial flushing associated with the rainy season beginning in early October increases sediment discharge. SSC peaks often occur around the runoff peaks. The suspended sediment data are sparsely available or cover short periods of time. Figure 26 through Figure 28 also show the regressions between SSC and discharge, percentage mud and discharge, and, for the Chehalis River, the regression between SSC and turbidity, which can be used to derive the corresponding concentration of mud and sand for the discharge time series. These figures also show that the majority of the sediments are mud with a small portion of sand, the percentage of which also increases with the discharge.

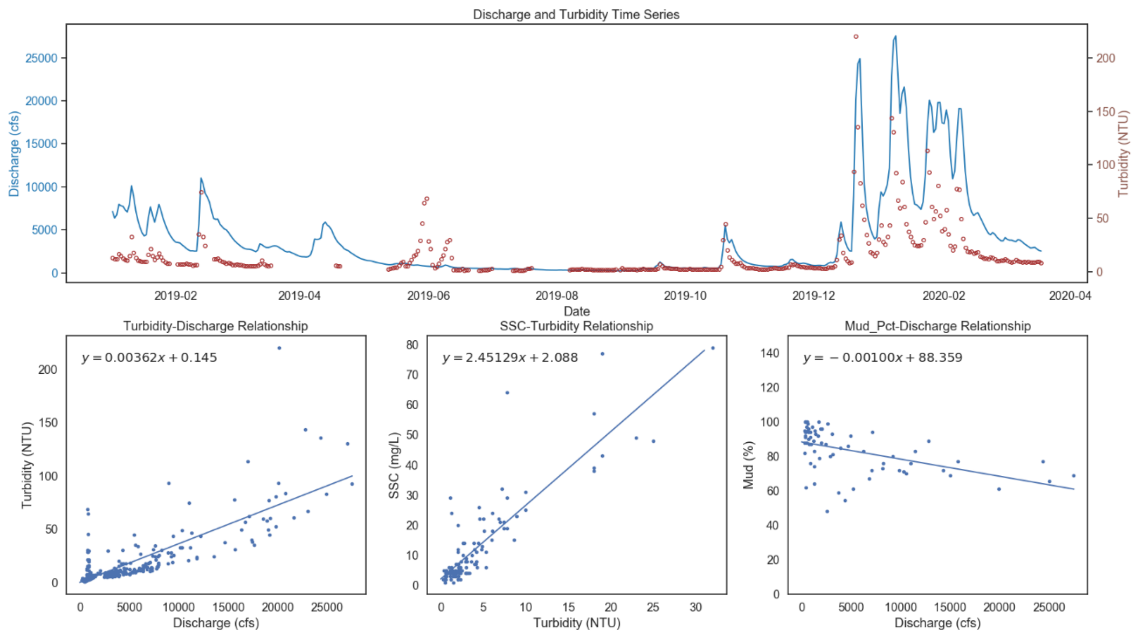

Figure 26: Time Series of Turbidity and Discharge and the Corresponding Regressions for Chehalis River at Porter

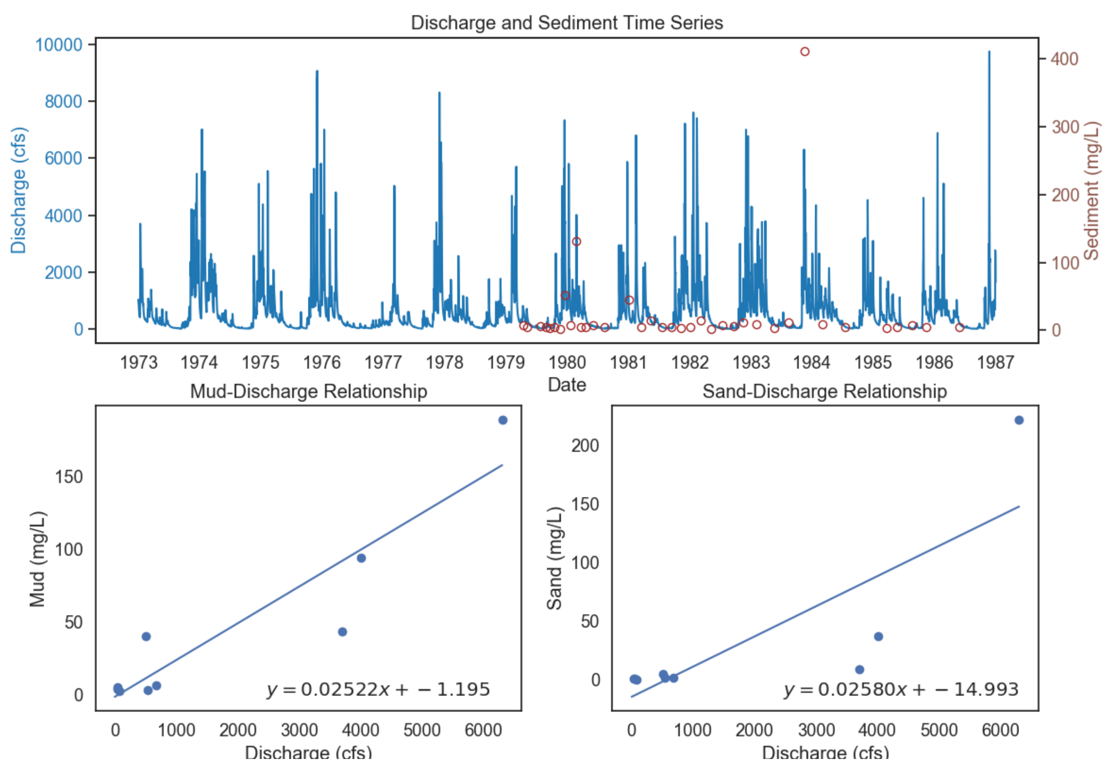

Figure 27: Time Series of SSC and Discharge and the Corresponding Regressions for Willapa River

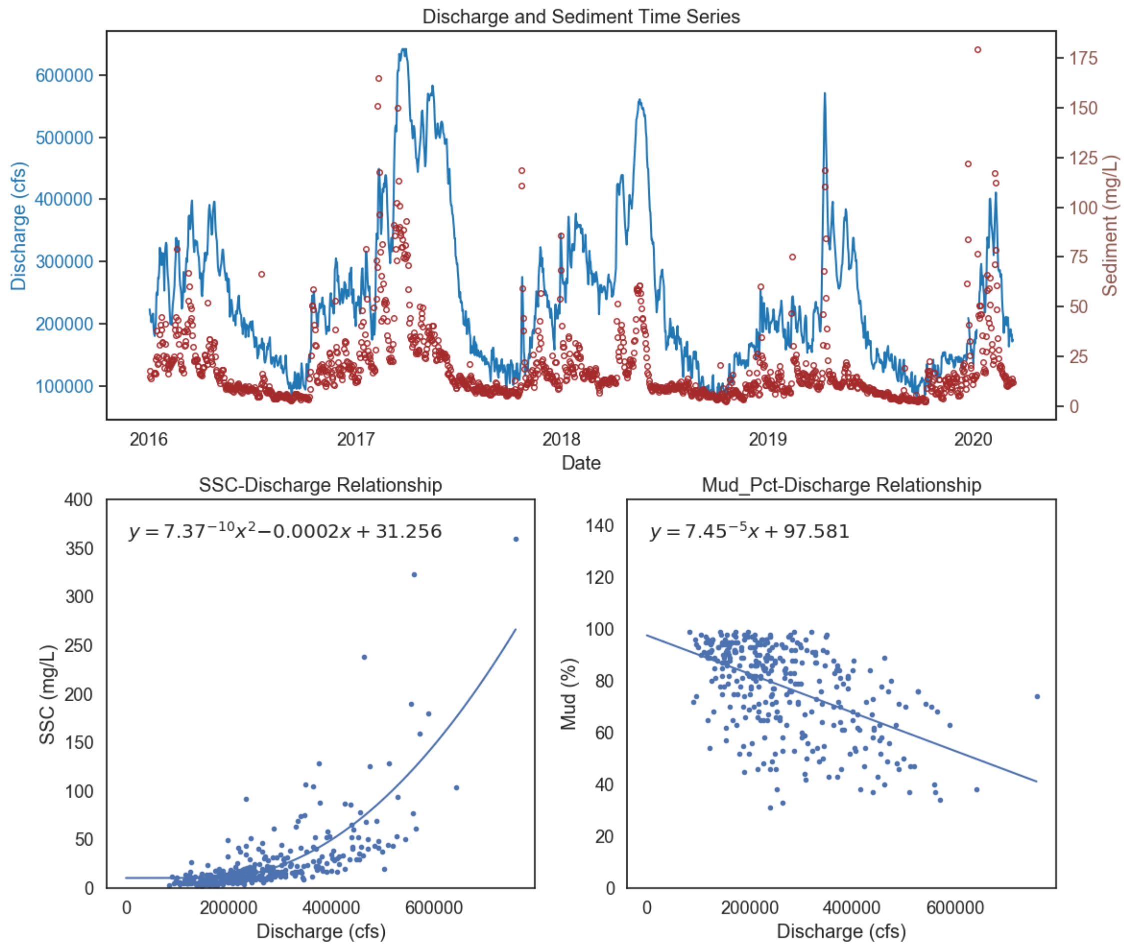

Figure 28: Time Series of SSC and Discharge and the Corresponding Regressions for Columbia River at Port Westward

3.10 MORPHOLOGICAL CHANGES

3.10.1 Grays Harbor

The morphological changes within Grays Harbor largely correspond to the major engineering construction eras identified in Section 1.1.3 and discussed below, including the discussion of Whitcomb Flats and Sand Island.

As shown in Figure 29, prior to any engineering activities before 1900, the geomorphology of Grays Harbor was a typical ebb shoal-inlet system characterized by a tidal inlet with extensive shallow shoals. The morphological evolution of this ebb shoal-inlet system was controlled by tidal currents and wave processes. Specifically, the primary inlet channel was almost perpendicular to the shoreline with a maximum depth of 90 ft in 1862, which was controlled by Point Brown to the north and Point Hansen to the south. The ebb shoal south of Point Brown (North Spit) extended 2 miles into the entrance. With a dominant direction of net sediment transport from south to north, the ebb shoal northwest of Point Hansen

(South Spit) extended northwest, causing the primary inlet to bend towards the northwest. Compared to the bathymetry data in 1984, the shoreline at Point Hansen was advancing north and west filling in South Spit, while North Spit was receding, which caused the inlet to migrate towards the north with an east-west orientation.

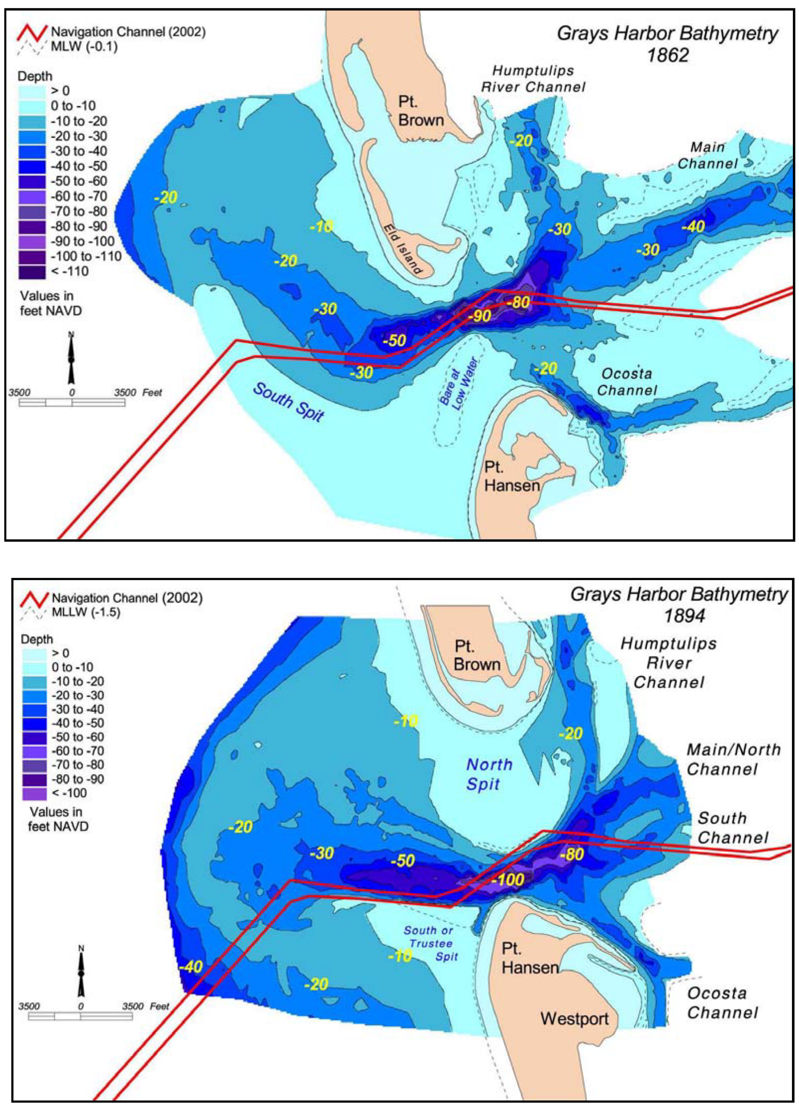

Source: USACE 2003a

Figure 29: Bathymetric Surface Morphology for Grays Harbor Entrance Prior to Jetty Construction in 1862 (Top) and 1894 (Bottom)

As shown in Figure 30, immediately after the construction of the South Jetty, the channel was scoured to a maximum depth of about 110 ft due to rapid hydrodynamic response. The South Jetty also blocked longshore sediment transport to the north, which caused the accretion of the beach to the south, a diminishing of South Spit, and erosion of the shoreface seaward of Point Hansen. The North Jetty was then constructed to alleviate channel navigation hazards by reducing localized sediment transport from beaches seaward of Point Brown into the entrance channel. This created a self-scouring of the adjacent ebb shoals between the inlet and North Jetty to a depth of 40 to 50 ft. The sediments were transported by strong ebb tidal currents to the west and north of the entrance, which caused the accretion of the beach to the north creating what is now known as Ocean Shores. The increase in tidal currents caused the north and south jetties to subside rapidly to the extent that the foundation was destabilized, and rocks were displaced by wave forces.

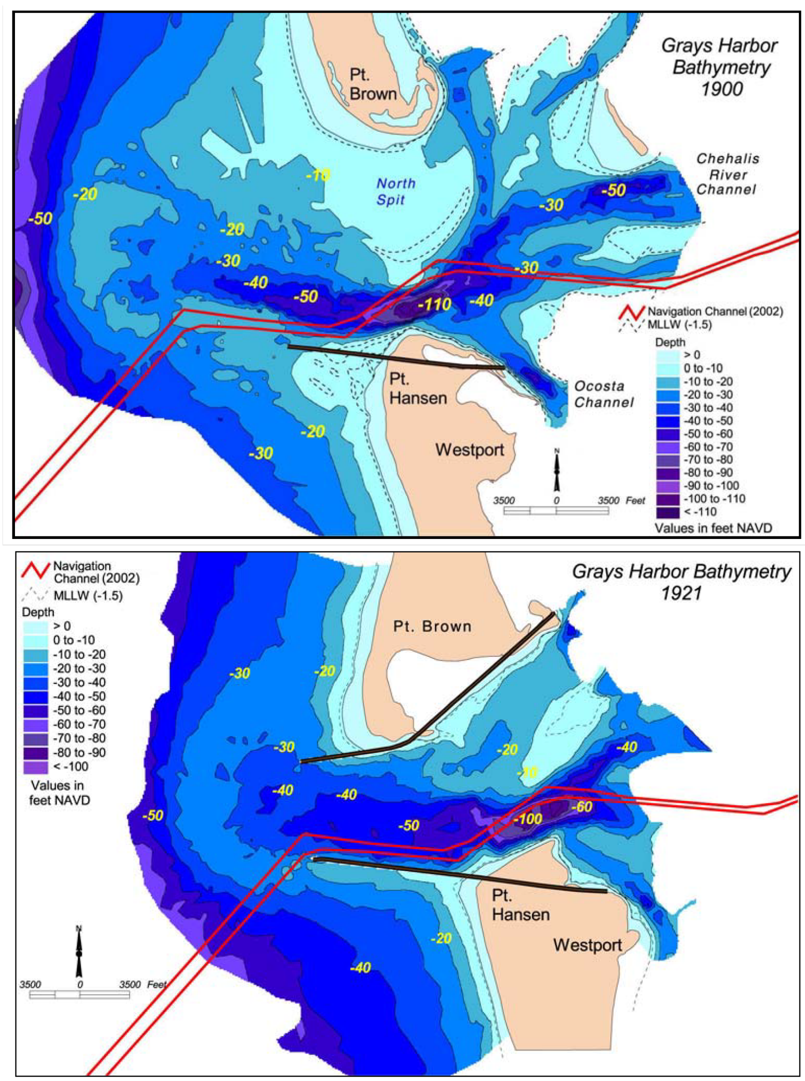

Source: USACE 2003a

Figure 30: Bathymetric Surface Morphology for Grays Harbor Entrance During Construction of North and South Jetties in 1900 (Left) and 1921 (Right)

As shown in Figure 31, a sediment pathway was created over and through the North Jetty as the deterioration of the north and south jetties continued, which created a large sand spit to the east of the

North Jetty by 1940. The deterioration of the South Jetty resulted in transport of sands over and through the jetty, which fed the growth of the spit at Point Chehalis to the north. Following the rehabilitation of the north and south jetties in 1939 and 1942, respectively, sediment transport into the bay was blocked, which resulted in further accretion of the beaches north and south of the entrance. In addition, the impoundment of littoral transport from the south caused erosion of the Point Chehalis shoreline north of the jetty, creating an offset between beaches on either side of the jetty which led to an erosional cove landward between 1944 and 1946. The erosion along the landward end of the jetty continued and reached to a maximum in 1965, creating an erosional cove known as Half Moon Bay. Further, the extensive sand spit eastward of the North Jetty was deteriorating due to strong ebb tidal currents that transported sand associated with this feature southwest along the north margin of the channel.

The second rehabilitation of the south and north jetties in 1966 and 1976, respectively, was not completed for the entire length of either jetty. This allowed sand transported by north-to-south-directed longshore currents to freely move around the North Jetty into the estuary via flood current and created large subaerial and subaqueous spit forming, now known as Damon Point. As shown in Figure 32, the ebb shoal continued to deflate, as indicated by the recession of the 30-ft-depth contour seaward of the beaches fronting Point Brown following the rehabilitation, and later the recession of the 40-ft-depth contour between 1987 and 2002, where the sediments were transported to the nearshore and beach fronting Ocean Shores. At some point, the seaward advancement of the north beach shoreline had advanced seaward enough to begin bypassing sediment around the terminus of the North Jetty during flood tides, further supplementing the sediment source to Damon Point. This led to the progressive advancement of Damon Point to the southeast and resulted in increased shoaling in the Bar, Entrance, and Sand Island reaches of the channel, which is discussed in Section 3.10.1.1. Encroachment of the sand spit on the channel scoured the channel and forced the thalweg to migrate from its historic position adjacent to Sand Island to the south near Whitcomb Flats, posing a significant impact on the morphological evolution of Whitcomb Flats, as discussed in Section 3.10.1.2.

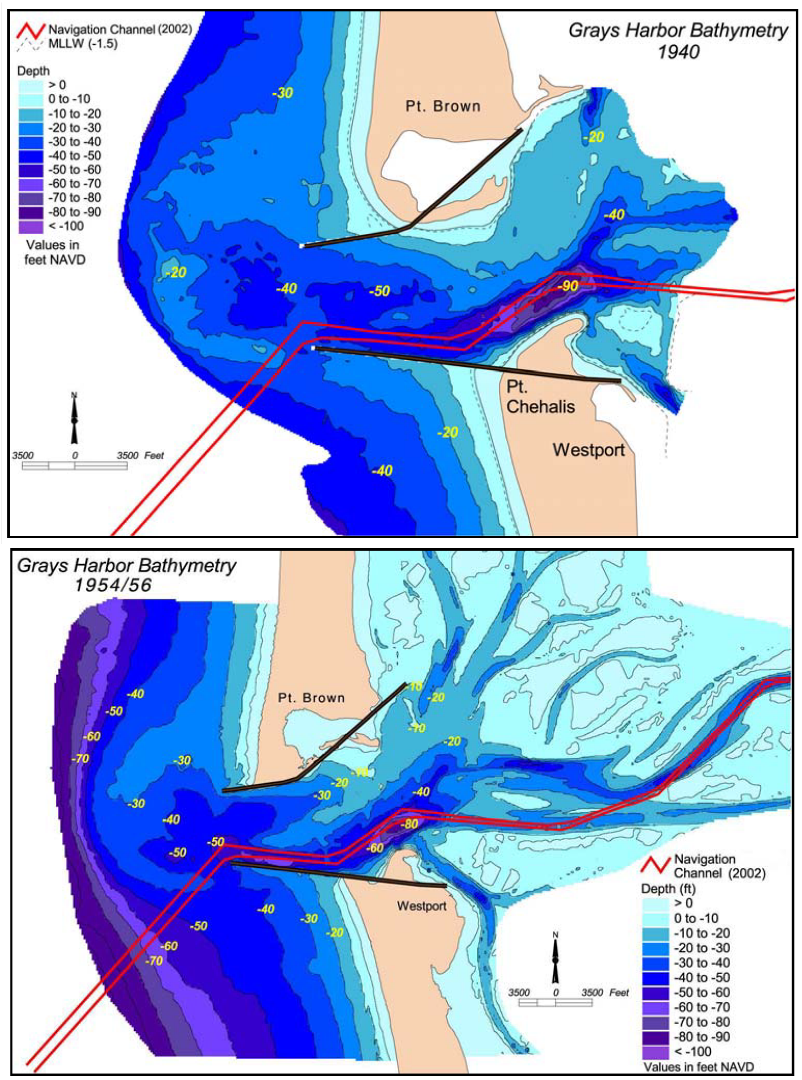

Source: USACE 2003a

Figure 31: Bathymetric Surface Morphology for Grays Harbor Entrance Before (1940 Left) and After (1956 Right) the First Rehabilitation of North and South Jetties

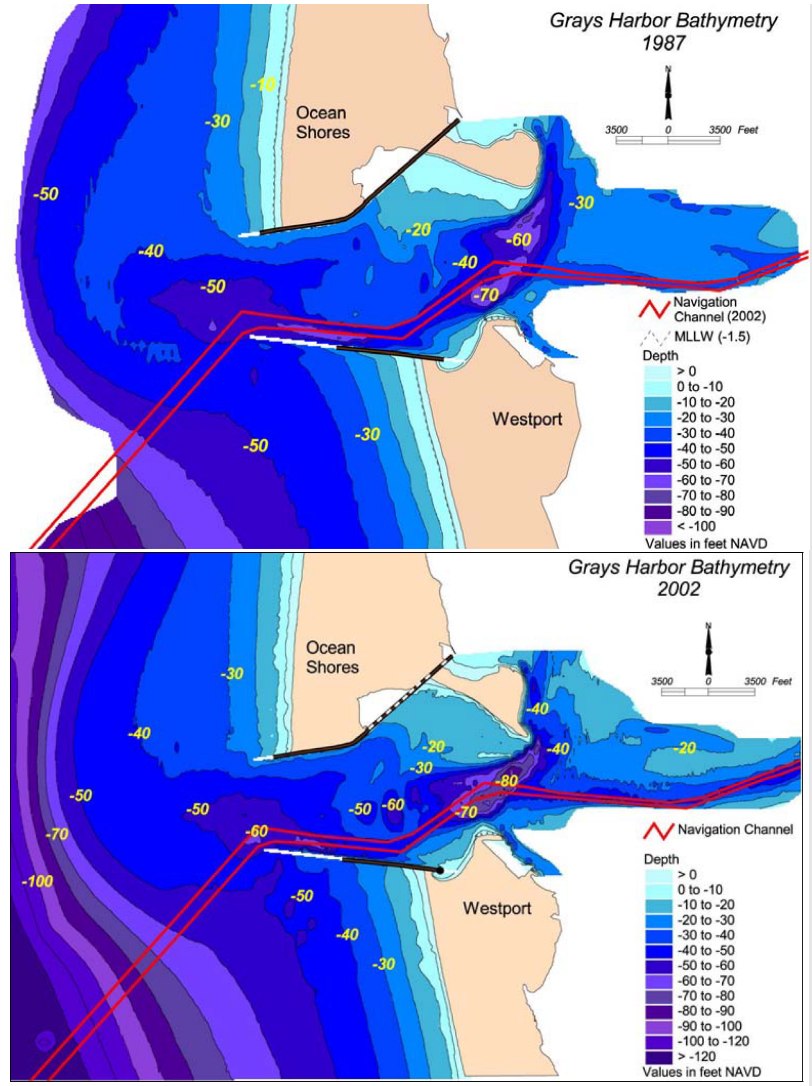

Note: White areas seaward of jetties represent sections of original jetties that were not rehabilitated.
Source: USACE 2003a

Figure 32: Bathymetric Surface Morphology for Grays Harbor Entrance After Partial Rehabilitation of North and South Jetties in 1965 and 1976, respectively, in 1987 (Left) and 2002 (Right)

3.10.1.1 Sand Island

Sand Island is a flood tidal shoal complex located approximately 5 miles east of Point Brown, which has been a long-standing land feature within Grays Harbor predating any engineering activities. As discussed in the previous section, the deterioration of the North Jetty, together with the advancement of the north beach, resulted in a significant amount of sediment bypassing over and through the North Jetty, which caused the distal end of Damon Point to grow toward the southeast. This is a trend that has continued up until the present time. The growth of Damon Point sheltered Sand Island from offshore wave energy. Therefore, the subaqueous shoal fronting Sand Island has been accreting sediment, with a net deposition of 6.6 million yd^3 between 1987 and 2002 (Kraus and Arden 2003).

3.10.1.2 Whitcomb Flats

Whitcomb Flats also is a flood tidal shoal complex predating any engineering activities. It is located approximately 1 mile east of Point Chehalis. The sediments are composed of sand from marine sources due to tidal flood currents and wave-induced transport. The continuous growth of Damon Point towards the southeast constricted the throat of the inlet between Damon Point and Point Chehalis, which resulted in a net erosion of 40 million yd^3 of sediment from the seabed since 1954. The eroded sediment has been primarily directed offshore due to the strength of the ebb currents on the outgoing tide, resulting in a diminished sediment supply to Whitcomb Flats over time. The continuous growth of Damon Point also forced the southward migration of the channel thalweg towards Whitcomb Flats, which altered the wave transmission into the inner harbor. The west or northwesterly offshore wave energy is able to propagate into the harbor through the inlet throat and eventually refract into the shallows near Whitcomb Flats. The geomorphology analysis by Osborne (2003) suggests these waves likely cause the eastward migration of Whitcomb Flats.

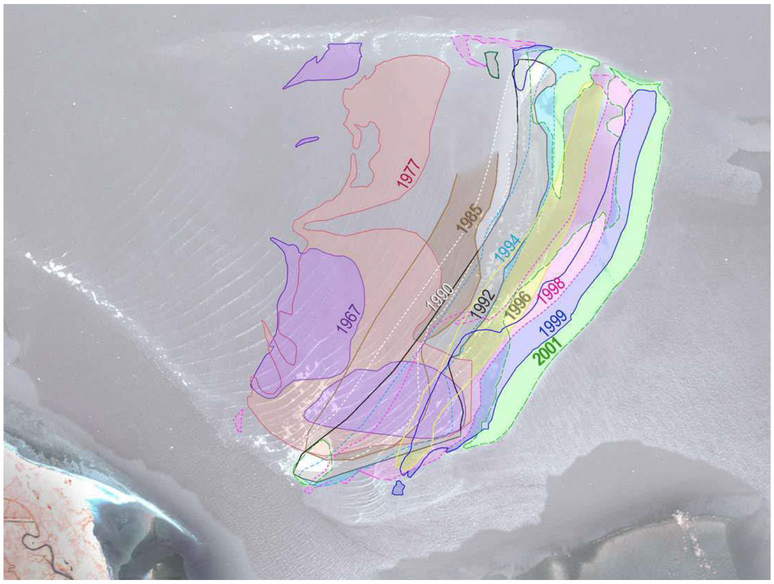

Source: USACE 2003a

Figure 33: Eastward Migration of Whitcomb Flat from 1967 to 2001

3.10.2 Willapa Bay

Willapa Bay has existed as a relatively stable tidal inlet ebb shoal system for more than a century by maintaining a strong tidal exchange of water entering and exiting the inlet. Three channels exist at the inlet, which are the North Channel, the Middle Channel, and the South Channel. The North Channel is the dominant one, which appears to be a continuation of the Willapa River and directs river discharge and water from tidal flats along the Willapa River into the Pacific Ocean. Waters within the bay are directed by the ebb tidal currents along the southern arm (the arm extending toward Oceanside) to Cape Shoalwater, which also exits via the North Channel. The other two channels through the bar exist ephemerally. As illustrated in Figure 34, the entrance channel exhibits a periodic migration with following stages:

- The North Channel typically migrates southward across the ebb shoal, deflected by the shore-tied submerged spit growing from Cape Shoalwater.
- The south migration of the North Channel is interrupted by spit dissection, which allows ebb currents to flow directly seaward out of the North Channel. Dissection always starts with erosion of a notch on the landward side of the submerged spit. At such times, multiple incipient outlets often form. Typically, the notch or notches will widen and extend oceanward for several years until the depth across the entire spit reaches 18 ft, at which point the distal end of the spit (which is now an isolated shoal) begins to migrate to the southeast. The shoal migration rate is relatively rapid compared to extension of the spit. The new outlet captures the majority of the North Channel discharge and the other outlets gradually fill.
- The shoal eventually merges with others in the middle portion of the bay entrance.

This periodical migration of the entrance channel has occurred seven times between 1933 and 1998, approximately 9 years per cycle, based on a recent inspection of the longer bathymetry record at roughly annual intervals (USACE 2000). Repeated cycles of spit growth influence not only the position of the bar channel, but its depth and alignment, the size and location of entrance shoals, and the erosion rates along the North Cove shoreline.

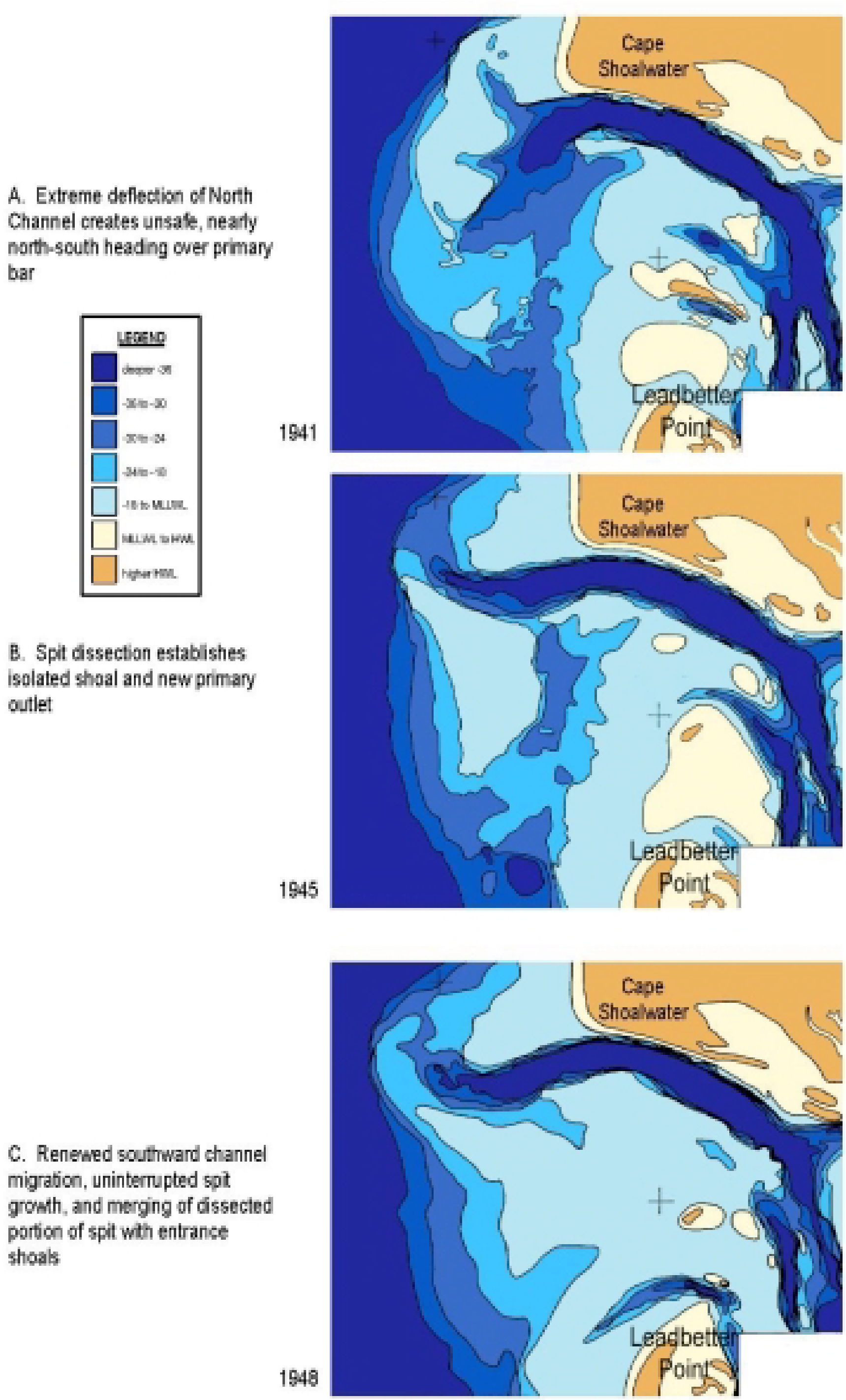

Source: USACE 2000

Figure 34: Second Half of One Channel Migration Cycle in Willapa Bay

3.11 VEGETATION

Wetlands maps from the National Wetlands Inventory and the saltmarsh maps from the UNEP-WCMC are presented in Figure 35, which shows that the tidal flat areas are covered by estuarine and marine wetlands. However, the information is not detailed enough for the model parameterization of bottom friction due to vegetation. Instead, the MRLC NLCD dataset will be used to determine the appropriate bed friction factor for use in the hydrodynamic modeling effort. Figure 36 illustrates the estimated Manning's *n* friction factor for the region based on land cover; it ranges from a value of 0.02 for open water (blue) to 0.15 for high-intensity development (red). These values may be modified during model calibration and validation to maximize model accuracy relative to benchmark data.

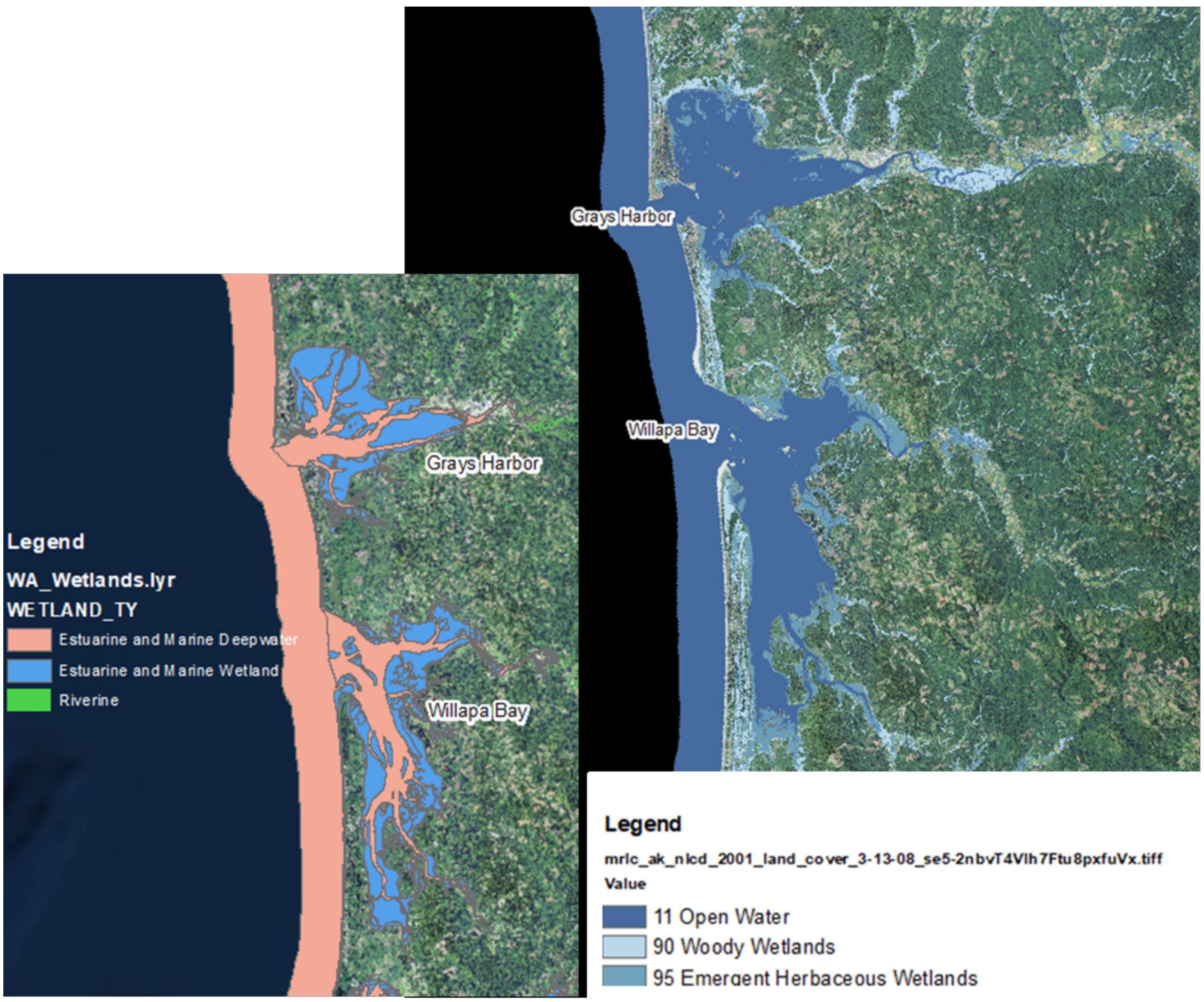

Figure 35: Wetlands Maps from the National Wetlands Inventory and the Distribution of Saltmarshes from the UNEP-WCMC within the Twin Harbors

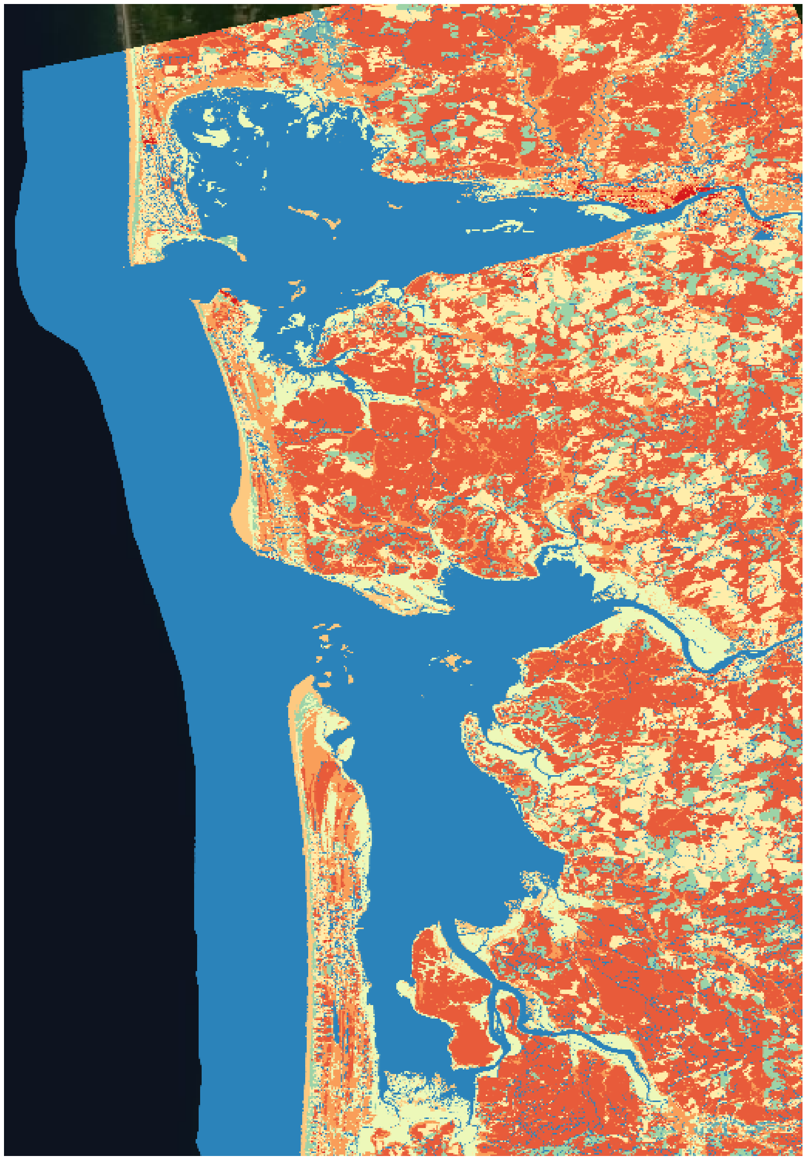

Figure 36: Preliminary Bed Friction Factors (Manning's n) Based on the 2016 NLCD Dataset (0.02 for Open Water [Blue] to 0.15 for High-intensity Development [Red])

3.12 DATA GAPS AND UNCERTAINTY

A comprehensive online data search and literature review particularly on the studies from USACE for both Grays Harbor and Willapa Bay were performed in this study. The available data and the corresponding sources are summarized in this report, which will be used for the subsequent numerical modeling efforts to understand the hydro- and morpho-dynamics within the Twin Harbors. Through a detailed analysis of the best available datasets, the following uncertainties or data gaps were identified, and corresponding assumptions were made:

- Wind data are sparsely available at adjacent airports, and temporally and spatially varying hindcast wind data from NOAA NCEP will be applied in this study.
- Sediment load from inland watersheds that discharge into both water bodies are only available for the Chehalis River in Grays Harbor and the Willapa River in Willapa Bay where sediment discharge will be applied in the model; however, those rivers contribute most of the discharge into the harbors. Specifically, for each river:
    - Daily sediment load data for the Chehalis River is available for a short period of time compared to the discharge data, and the most recent sediment load from Chehalis River is available as turbidity. Continuous sediment loads will be developed from the three regressions of discharge and turbidity, SSC and turbidity, and discharge and percentage of mud derived from the corresponding historical datasets.
    - Daily sediment load data for the Willapa River is available for a short period of time compared to the discharge data, and the most recent sediment load are from the 1990s. Continuous sediment loads will be developed from the regressions of discharge and SSC, and discharge and percentage of mud derived from the corresponding historical datasets.
- Bed sediment data along the Pacific Coast and within the Twin Harbors are a composite of the historical datasets from 1974 to date, which will be used to inform the spatially varying sediment characteristics.
- Sediment parameterization such as settling velocity, critical erosion shear stress, erosion parameters, etc., are generally of high uncertainty, which will be informed based on the recommendations in the USACE's models and adjusted as necessary through the model calibration.
- Marsh or vegetation data are not specific enough to be meaningfully included in the model; therefore, the bottom friction will be inferred from the landcover dataset only.
- At the time of this report, USACE have only provided the 1999 survey within Grays Harbor, which will be used for model calibration/validation; this will be supplemented by the 1998 survey within Willapa Bay digitized from figures in the USACE report.
- Any other uncertainties and/or assumptions through the model calibration, if any, will be communicated and documented in the final report.

4.0 HYDRODYNAMIC MODELING

4.1 OVERVIEW

A dynamically coupled hydrodynamic, wave, and sediment transport model was developed using Delft3D-FM to understand the hydro- and morpho-dynamics within the Twin Harbors as well as to determine the effects of dredging and disposal activities in Grays Harbor on the fate of the dredged sediments. Delft3D-FM is a flexible, integrated modeling suite capable of simulating two- and three-dimensional hydrodynamics, waves, conservative and non-conservative constituent transport, sediment transport, morphology, and water quality. Delft3D is a cutting edge, process-based numerical modeling system developed by Deltares (Deltares 2020).

4.1.1 Hydrodynamics

For hydrodynamics and sediment transport, the Delft3D-FM framework was used, which allows for easier transitions in spatial resolution. This is extremely helpful when a large domain and areas of fine detail are both required for accurate reproduction of the important hydrodynamic attributes. The model domain, illustrated in Figure 37 and Figure 38, for the full domain and the Twin Harbors, respectively, extends roughly 450 kilometers (km) offshore and 200 km north and south of Grays Harbor and Willapa Bay. Spatial resolution ranges from 50 km offshore to 90-120 m in the tidal flats and 30-60 m in the channels. Hydrodynamics are driven by tidal constituents at the offshore boundaries from the ADCIRC tidal database, discharge into the domain from major rivers in the Twin Harbors, and temporally and spatially varying wind and pressure fields from the NCEP CFSR dataset. Table 8 summarizes the major tidal constituents at the offshore boundary.

Table 8: Major Tidal Constituents Used in the Model

Constituents	Amplitude	Phases
K1	0.45	247.85
O1	0.29	232.37
M2	1.02	249.02
N2	0.21	224.50
S2	0.31	279.55
K2	0.08	272.47
P1	0.14	244.32
Q1	0.05	224.40

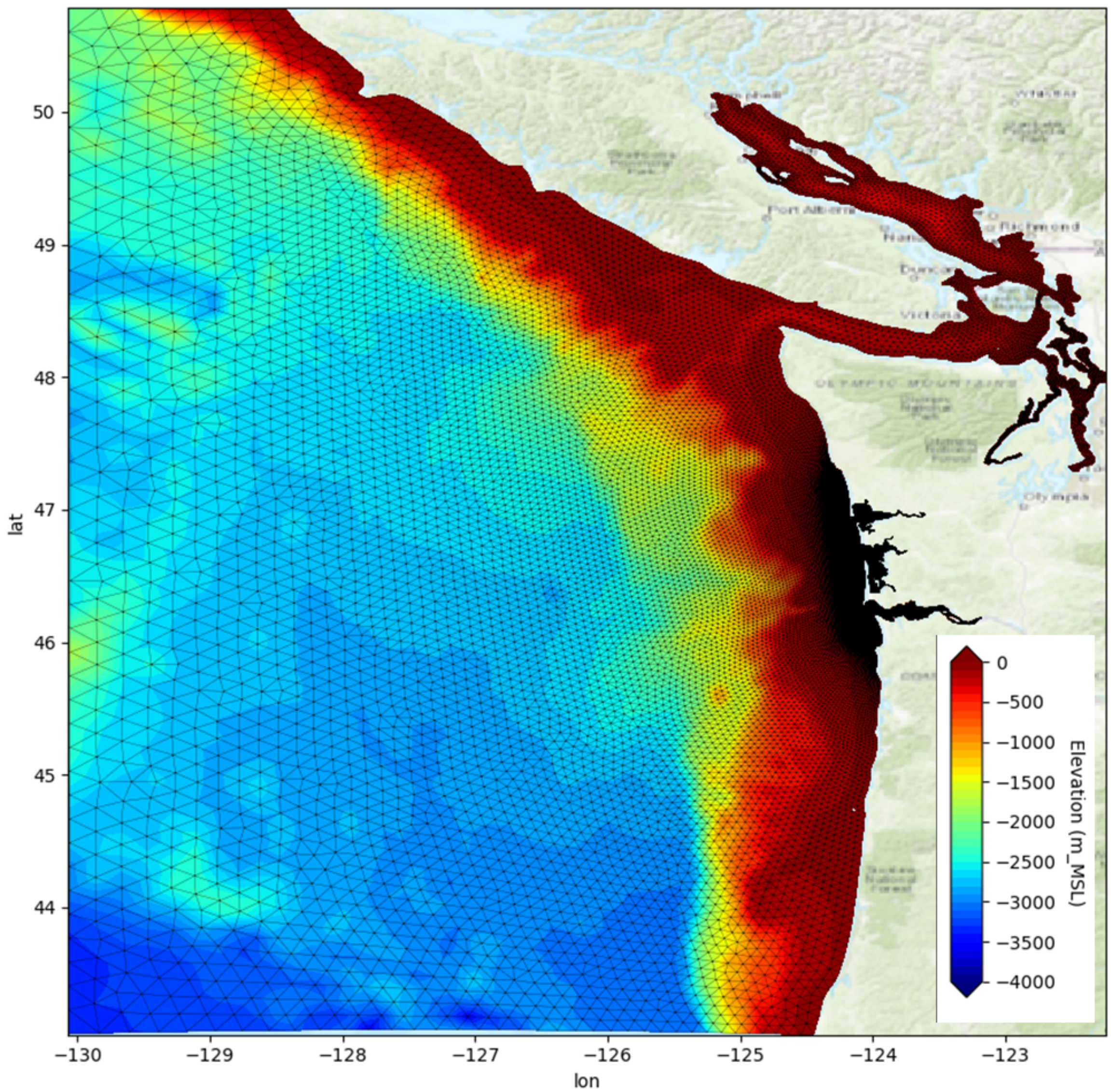

Figure 37: Unstructured Mesh of the Delft3D-FM Hydrodynamic Model, Full Domain

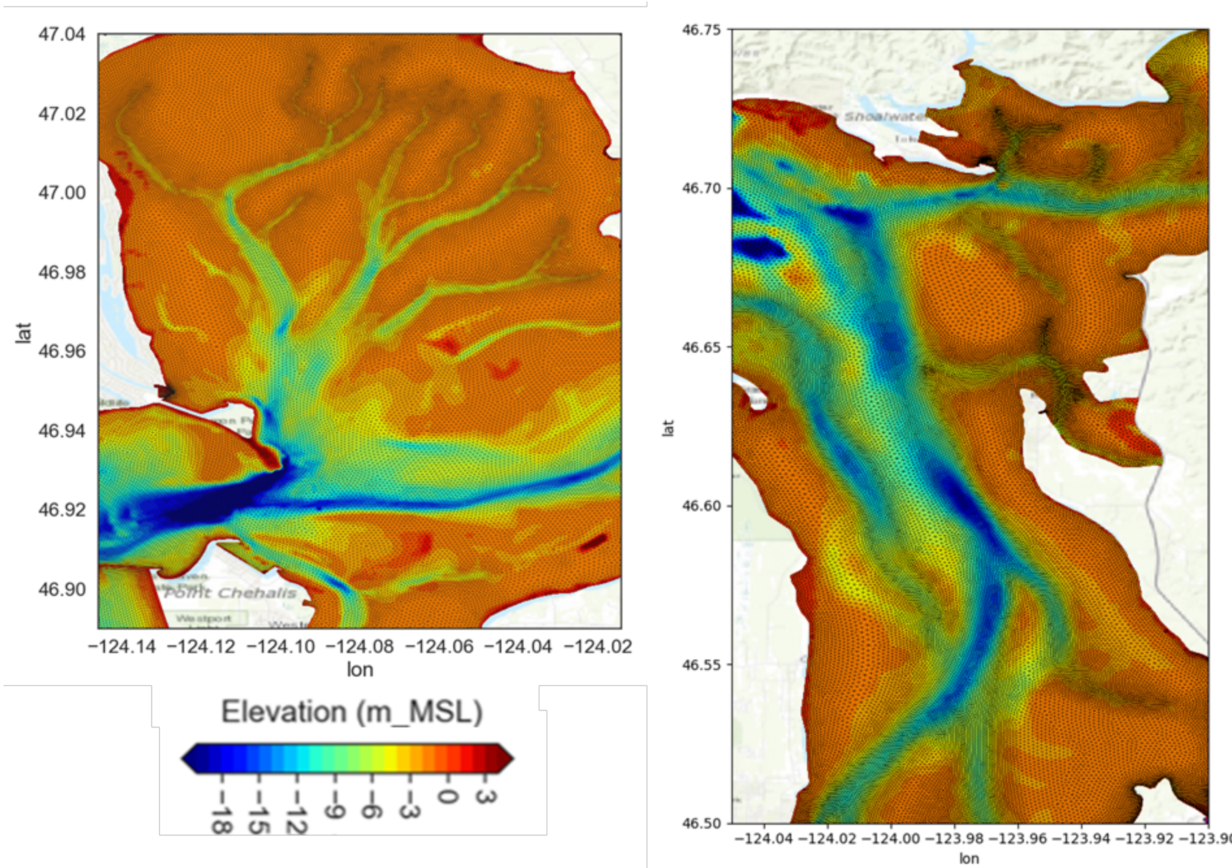

Figure 38: Unstructured Mesh of the Delft3D-FM Hydrodynamic Model near Grays Harbor (Left) and Willapa Bay (Right)

4.1.2 Waves

Wave propagation and generation was computed by the Delft3D-WAVE module, which requires a structured grid separate from the hydrodynamic model. The wave domain, shown in Figure 39, is limited to the Twin Harbors and the immediately adjacent Pacific Ocean, south to the Columbia River and offshore to wave buoy CDIP 036. The curvilinear grid is roughly uniform throughout the domain, with a spatial resolution of 100-120 m. The offshore wave boundary is driven by a time series of measured wave data from CDIP 036. The wave model and hydrodynamic model are dynamically coupled; the wave model receives wind fields and water levels from the hydrodynamic model, and in turn passes back wave radiation stresses, on a continually updating basis.

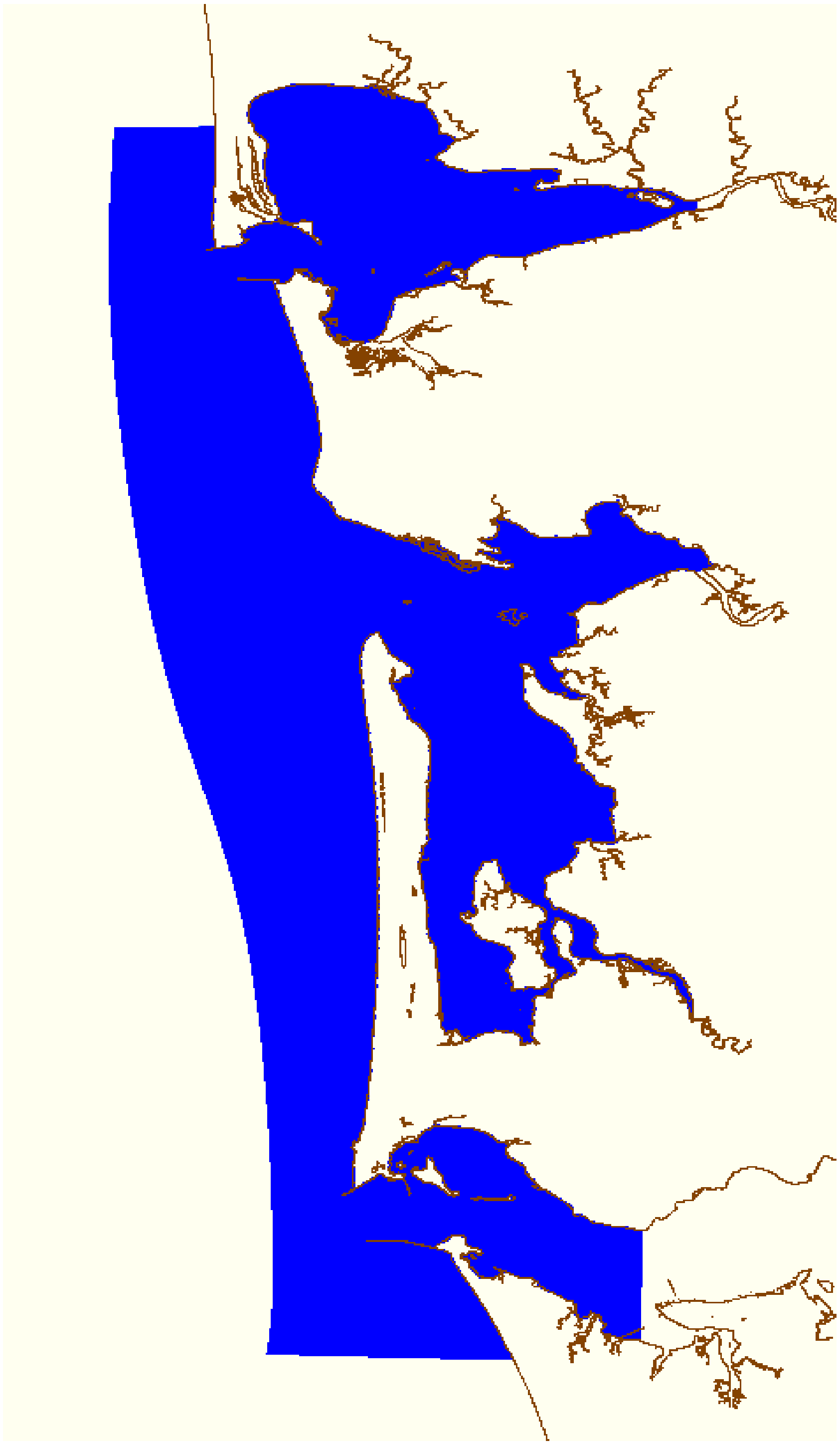

Figure 39: Structured Grid of the Delft3D-WAVE Model

4.2 HYDRODYNAMICS

4.2.1 Calibration/Validation

Parameters within the model, such as bottom friction and eddy viscosity and diffusivity, were calibrated and validated using measured data from three different time periods: June 2010, a time of low wind and low river discharge; March 2010, which exhibited high winds and high river discharge; and September 1999, during a time in which the USACE conducted a field study and deployed instruments to collect the water level, current velocity, and SSC. Water levels were examined during all three time periods, but current velocities and wave heights were only evaluated for September 1999 when data are available.

The water level gauge locations and comparisons between measured and modeled water levels for the June 2010 time period as an example at NOAA gauges WPTW1 and TOKW1 are shown in Figure 40. Aside from slight underestimation of spring low tides, the modeled water levels largely match the measured data in both magnitude and phase.

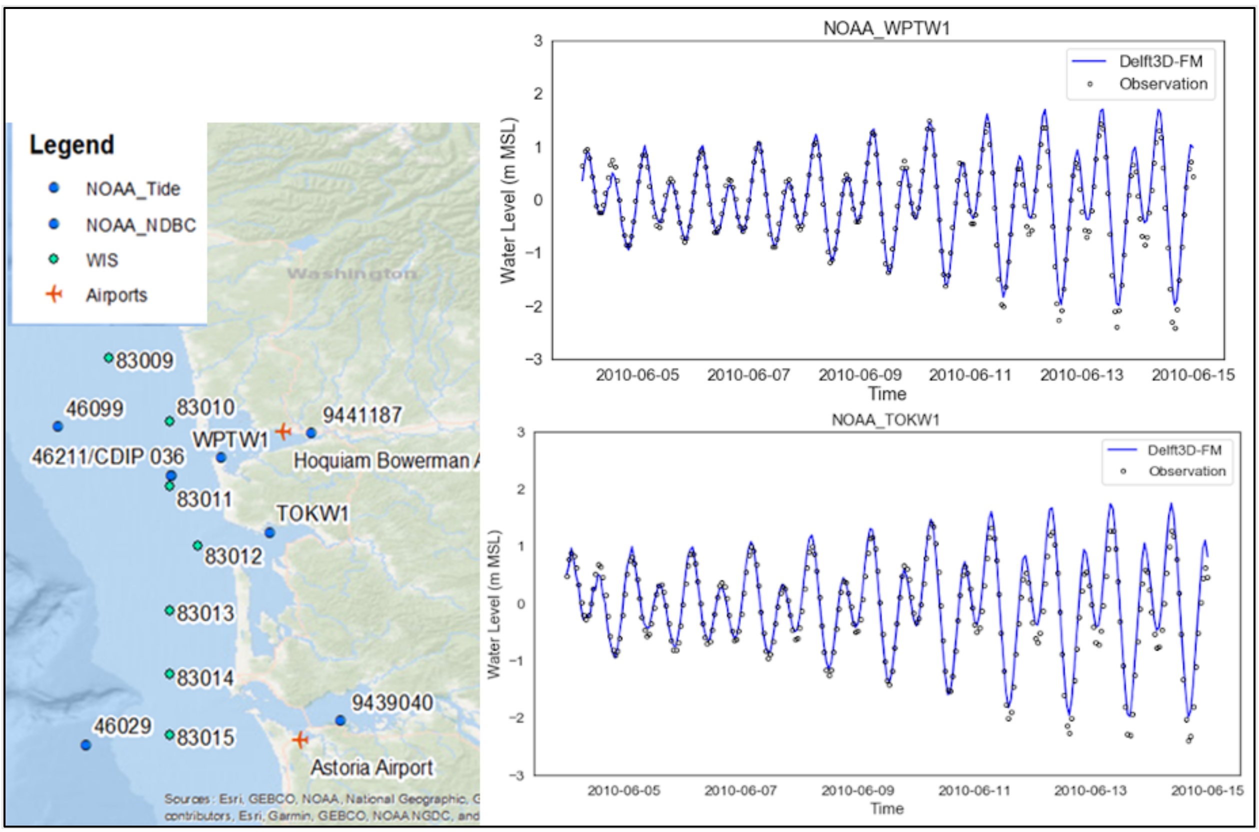

Figure 40: Water Level Time Series at WPTW1 and TOKW1, Measured vs. Modeled

Quantitatively, Figure 41 presents a Taylor Diagram (Taylor 2001), which summarizes the statistical comparison between measured and modeled water levels and includes the standard deviation, correlation coefficient, bias, and model skill. To read a Taylor Diagram, first take note of the location of the observed, or true value, shown as a star along the x-axis where normalized standard deviation, correlation coefficient, and model skill are all equal to 1.0 (a perfect match). Model skill decreases radially away from this point, standard deviation is worse with distance from the 1.0 curve, and the correlation coefficient is read from the green lines radiating from the origin. Bias, or over/underestimation, is read from the model point's color. From this diagram, all the modeled points are clustered close to the observed point, with a skill greater than 0.90, correlation greater than 0.95, normalized standard deviation close to 1.0, and balanced biases not exceeding 0.3 m in either direction, which all indicate an accurate model with regard to water levels.

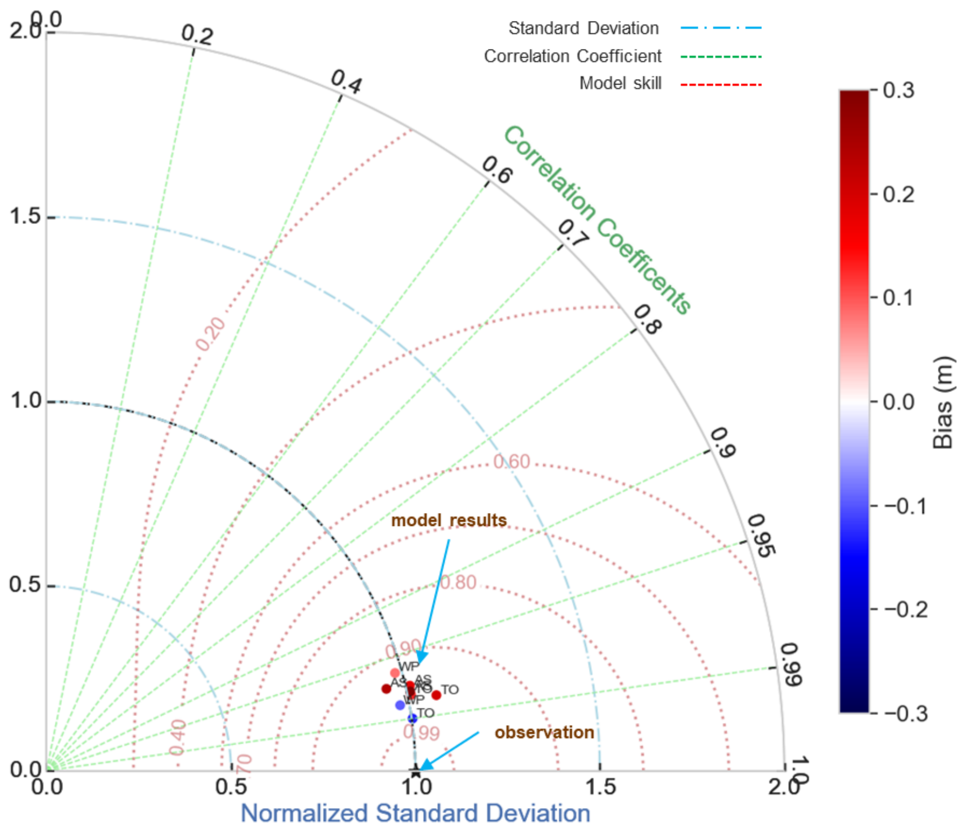

Figure 41: Taylor Diagram Demonstrating Model Skill with Respect to Water Levels

The comparisons between measured and modeled current velocities for the September 1999 time period at USACE gauges (where data are available) are shown in Figure 42. Aside from slight underestimation of peak ebb current magnitudes at GH_1, the modeled currents largely match the measured data in both magnitude and phase.

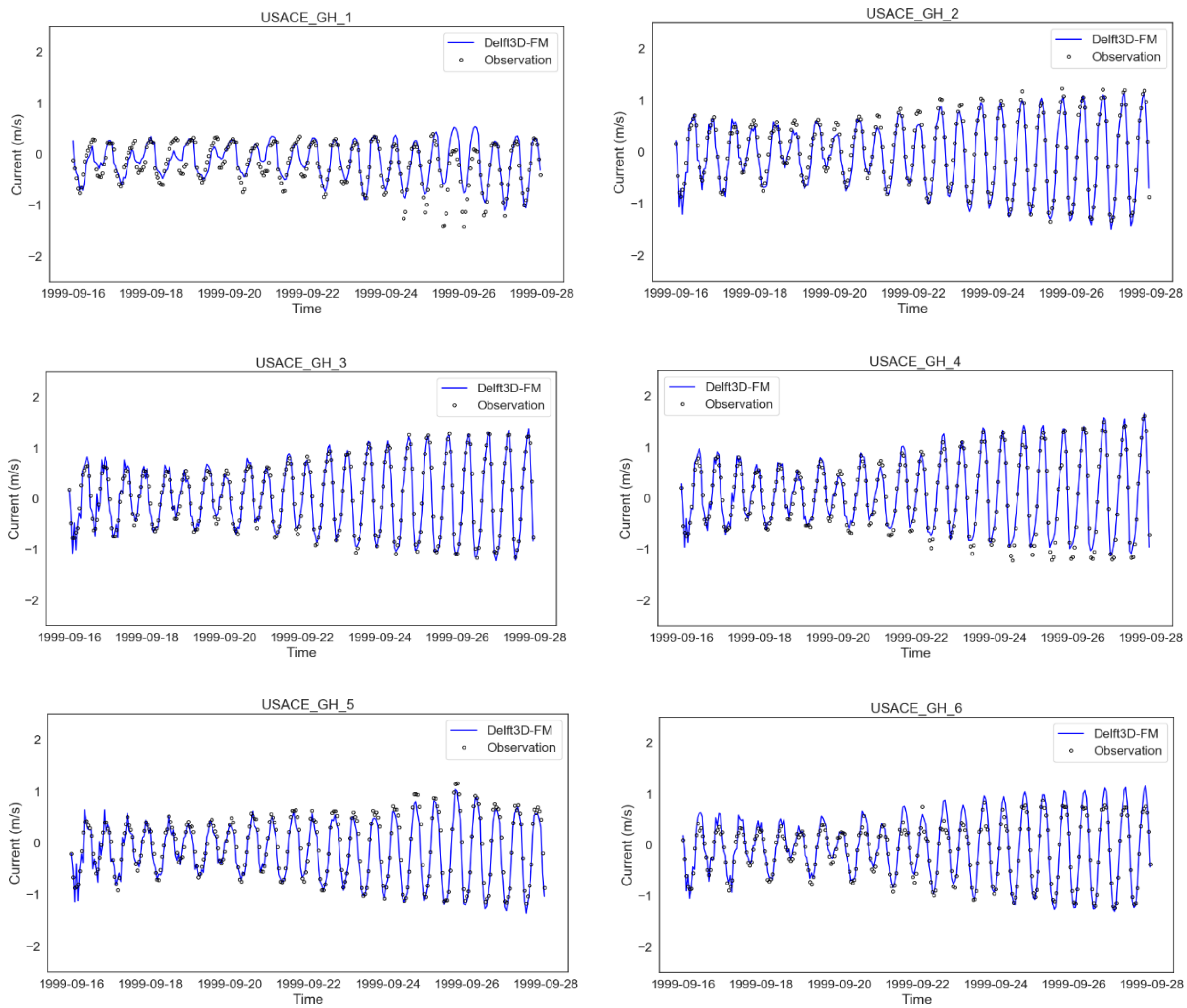

Figure 42: Current Velocity Time Series at All Stations from USACE 1999 Survey, Measured vs. Modeled

Quantitatively, Figure 43 illustrates the Taylor Diagram summarizing the statistical comparison between measured and modeled current velocities. From this diagram, with the exception of a one outlier, all the modeled points are clustered close to the observed point, with a skill greater than 0.90, correlation greater than 0.95, normalized standard deviation close to 1.0, and balanced biases not exceeding 0.3 m/s in either direction, which all indicate an accurate model with regard to current velocities.

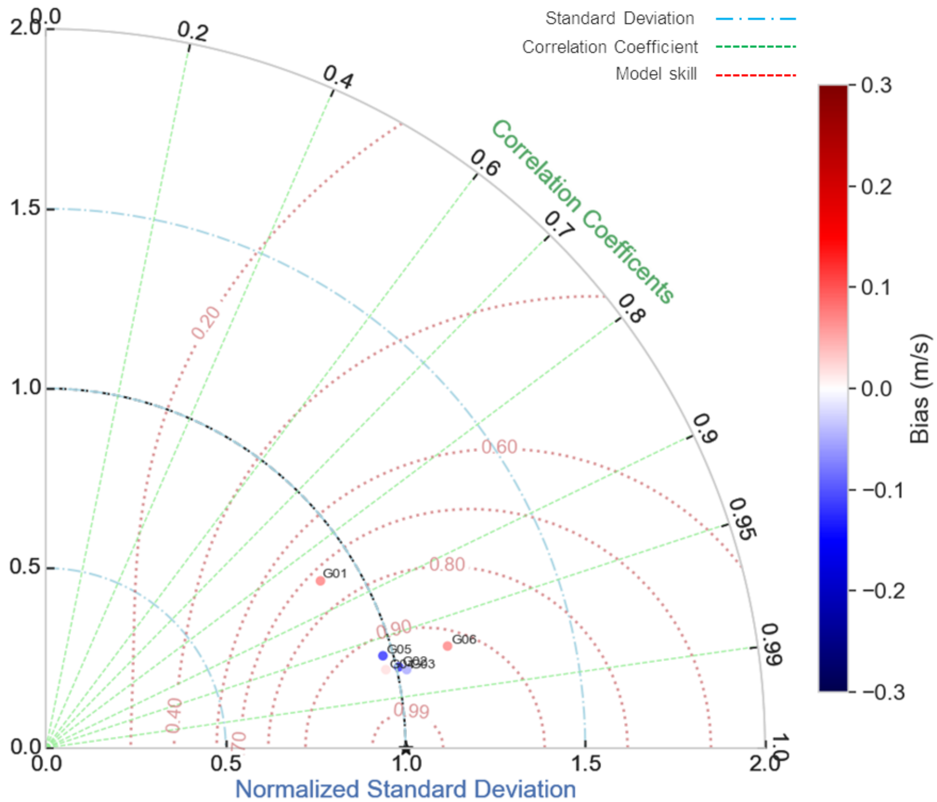

Figure 43: Taylor Diagram Demonstrating Model Skill with Respect to Current Velocities

Finally, comparisons between measured and modeled wave height for the September 1999 time period at USACE gauges (where data is available) are shown in Figure 44. Aside from some underestimation of peak wave heights at sometimes, the modeled wave heights largely match the measured data in both magnitude and timing.

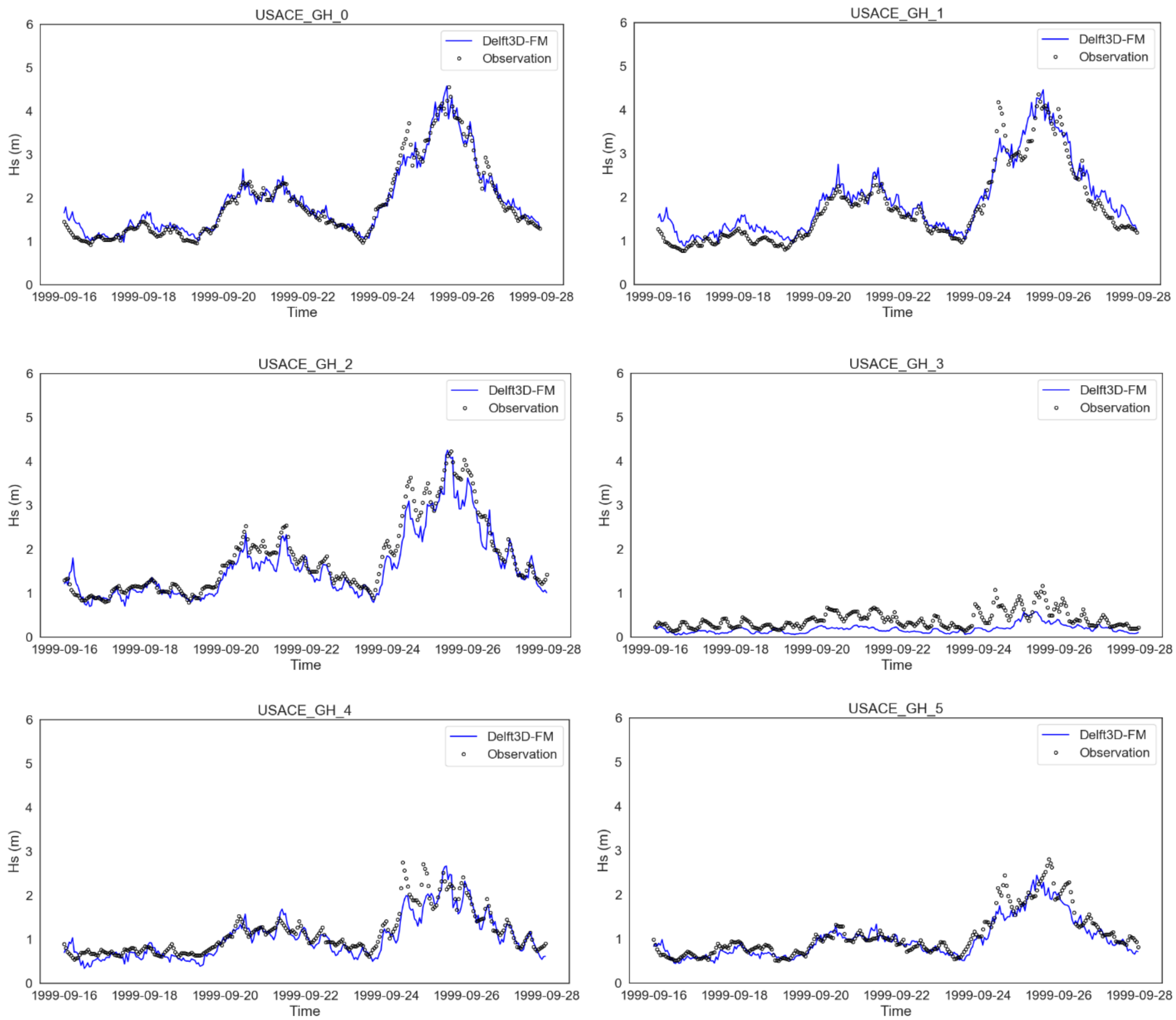

Figure 44: Wave Height Time Series at All Stations from USACE 1999 Survey, Measured vs. Modeled

Quantitatively, Figure 45 illustrates the Taylor Diagram summarizing the statistical comparison between measured and modeled wave heights. From this diagram, except for one outlier, all the modeled points are clustered close to the observed point, with a skill greater than 0.80, correlation greater than 0.90, normalized standard deviation close to 1.0, and overall, slightly negative biases not exceeding 0.3 m in either direction, which all indicate an accurate model regarding wave heights. The outlier station is located near Damon Point, a location known to be highly dynamic in terms of morphological changes. This indicates that the bathymetry data and shape of the Damon Point used for the 1999 condition may not be accurate.

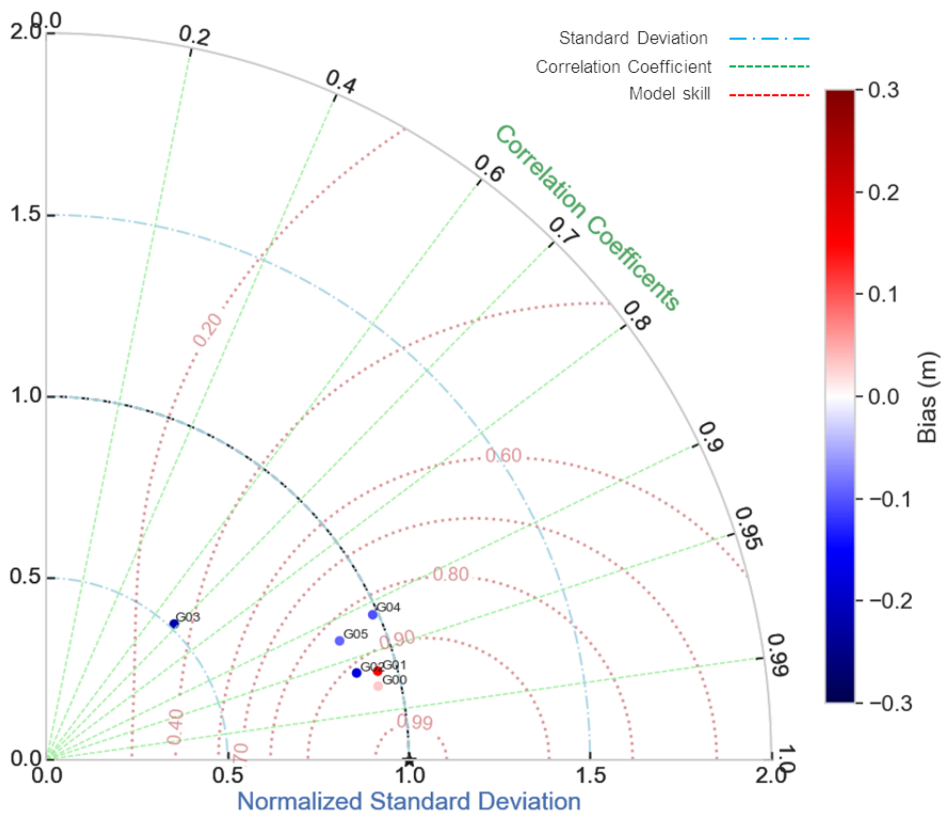

Figure 45: Taylor Diagram Demonstrating Model Skill with Respect to Wave Heights

4.2.2 Grays Harbor

The hydrodynamics are evaluated using the residual current over a 1-month period. The residual current patterns and magnitudes in the entrance to Grays Harbor for summer and winter conditions are shown in Figure 46. In general, a net outward flow through the channel causes localized circulation patterns at the entrance and within the inlet, which feed the water to the deeper part of the channel. Circulation patterns north of the inlet entrance potentially send sediments exiting the harbor back towards Ocean Shores due to the presence of a stronger ebb current. Additionally, the circulation pattern within the inlet indicates a potential sediment pathway from North Jetty to Damon Point, and an eastward sediment pathway within Half Moon Bay. Comparing summer versus winter conditions, the northerly-directed longshore current in winter is stronger than the southerly-directed longshore current in summer; this is consistent with the observed net northerly sediment transport along the coast.

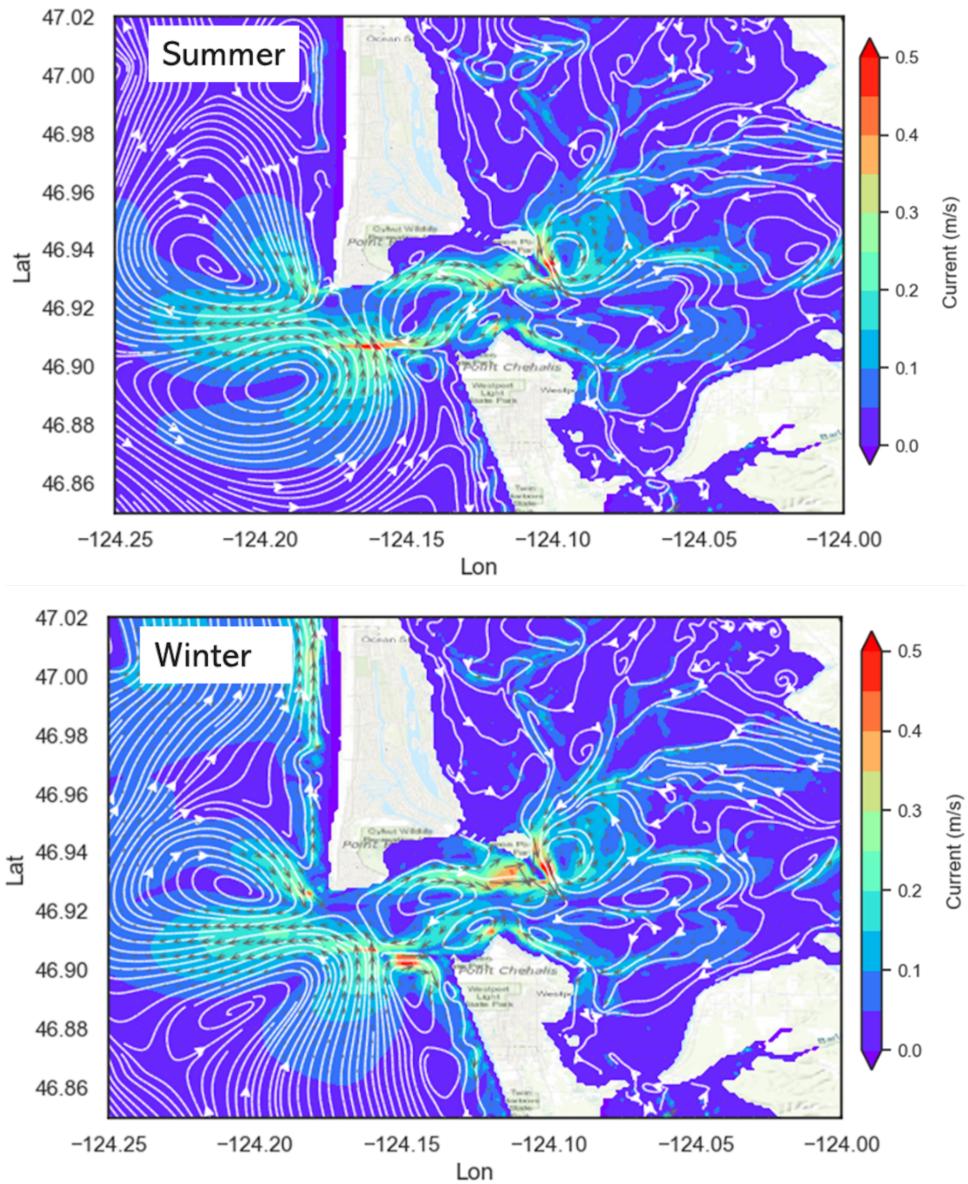

Figure 46: Residual Currents for Summer (Top) and Winter (Bottom) in Grays Harbor

4.2.3 Willapa Bay

Figure 47 illustrates the summer and winter conditions residual current patterns and magnitudes in the entrance to Willapa Bay. In general, a net inward flow over the entrance shoals and outward water through the channel suggests that water tends to flood in over shoals and ebb through channels. Breaking waves also drive localized circulation patterns, where water is directed inwards over shallower areas and then returns out through the deeper channels. Further, these waves drive significant residual currents from the outer (western) tip of the ebb-tidal delta in towards the coastline. Comparing summer versus winter conditions, the situation is similar to Grays Harbor, where the northerly-directed longshore current in winter is stronger than the southerly-directed longshore current in summer, consistent with observed net sediment transport patterns.

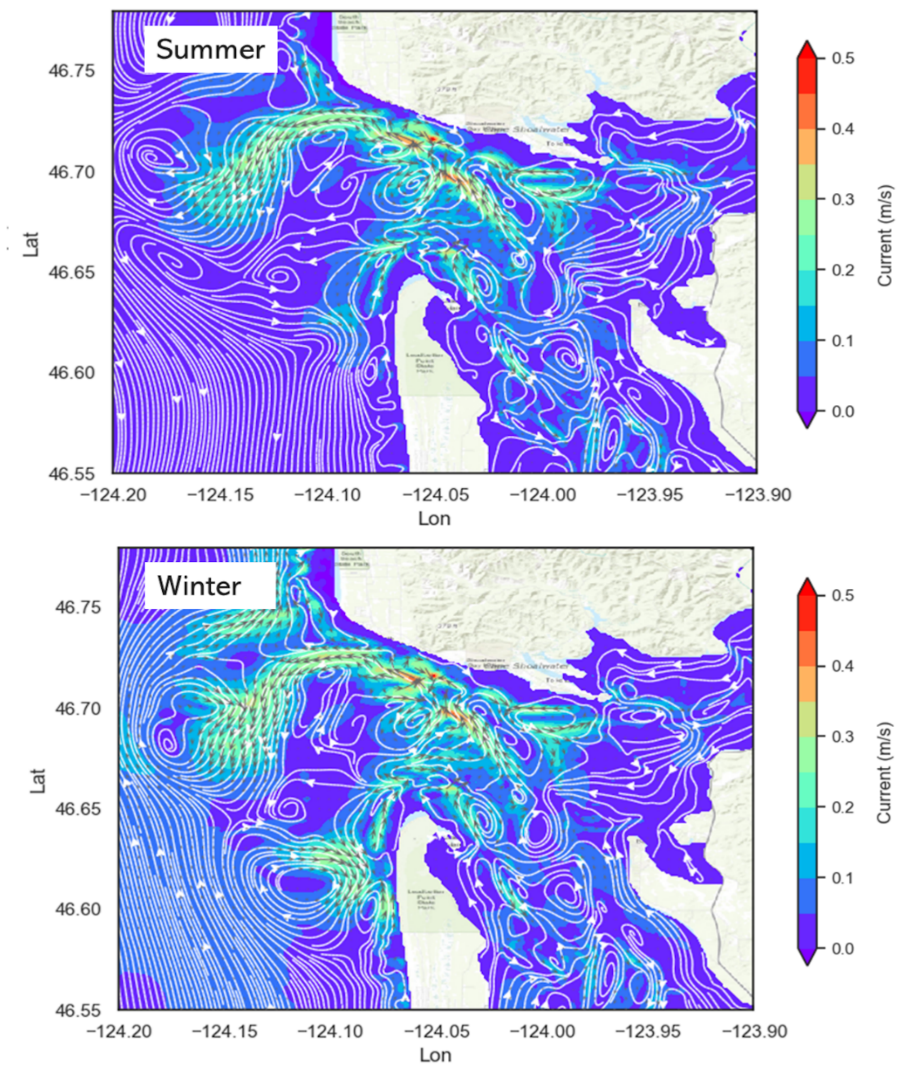

Figure 47: Residual Currents for Summer (Top) and Winter (Bottom) in Willapa Bay

5.0 MORPHODYNAMIC MODELING

5.1 OVERVIEW

The processes for sediment transport and morphological changes were incorporated and activated in the calibrated hydrodynamic model. Sediments in the model were parameterized using the sediment data from the usSEABED and substrate data collected from the stakeholder survey. Three sediment classes were developed to represent mud, marine sand, and riverine sand with a spatially varying mass fraction. The critical shear stress for erosion and sedimentation for mud is spatially varying based on the mass fraction as well. In addition, sediment load from the Chehalis River, Willapa River, and Columbia River were included based on regression equations developed.

A technique called morphological acceleration was applied to simulate long-term morphological evolution in a reasonable amount of computational time and without an overwhelming amount of output to process. This involves binning the wave and wind conditions into representative groups to define a reduced set of conditions characteristic of overall conditions. Similarly, a morphological tide was developed, representative of overall tidal characteristics but evenly applied and with the spring/neap cycle eliminated. The morphological acceleration, a multiplier of the sedimentation magnitude, was applied to each wave condition according to its annual frequency. Finally, the river discharge hydrographs were scaled to correlate with the reduced simulation time. This is discussed in detail in Section 5.3.1.

SSC from the model were compared to those during the 1999 USACE study, as that was the only time where data are available. Based on data availability, three different periods were used to compare measured and modeled morphological changes: June 2009 to February 2010 for Grays Harbor inlet, January 1998 to December 2003 for Willapa Bay inlet (qualitative comparison only), and 10-year average morphological changes for the tidal flats (for qualitative comparison to the InSAR data).

5.2 SSC CALIBRATION

Data collected during the 1999 USACE field survey was used to assess model performance with respect to SSC. The comparison is qualitative and relative for a number of reasons as listed below:

- The data are derived from backscatter data rather than direct measurement.
- The data have high uncertainty, with standard error over 100 percent and are poorly correlated with wave energy.
- The data are measured near the bed, whereas the model produces depth-averaged values, which are adjusted assuming a Rouse profile.
- The model does not include USACE sediment characteristics at the disposal site. The disposed sediments have a high concentration of mud, which is prone to erosion and increases the overall SSC in the water column.

Figure 48 illustrates the comparison between measured and modeled SSCs during the USACE field survey at several locations within Grays Harbor inlet. Due to the aforementioned factors, close correlation is not expected. However, there are events and spikes, such as 9/17 at GH_6, where the model and measurements match. Unfortunately, due to the limitations of these data and the lack of alternative sources of verification, no other validation of modeled SSC can be performed.

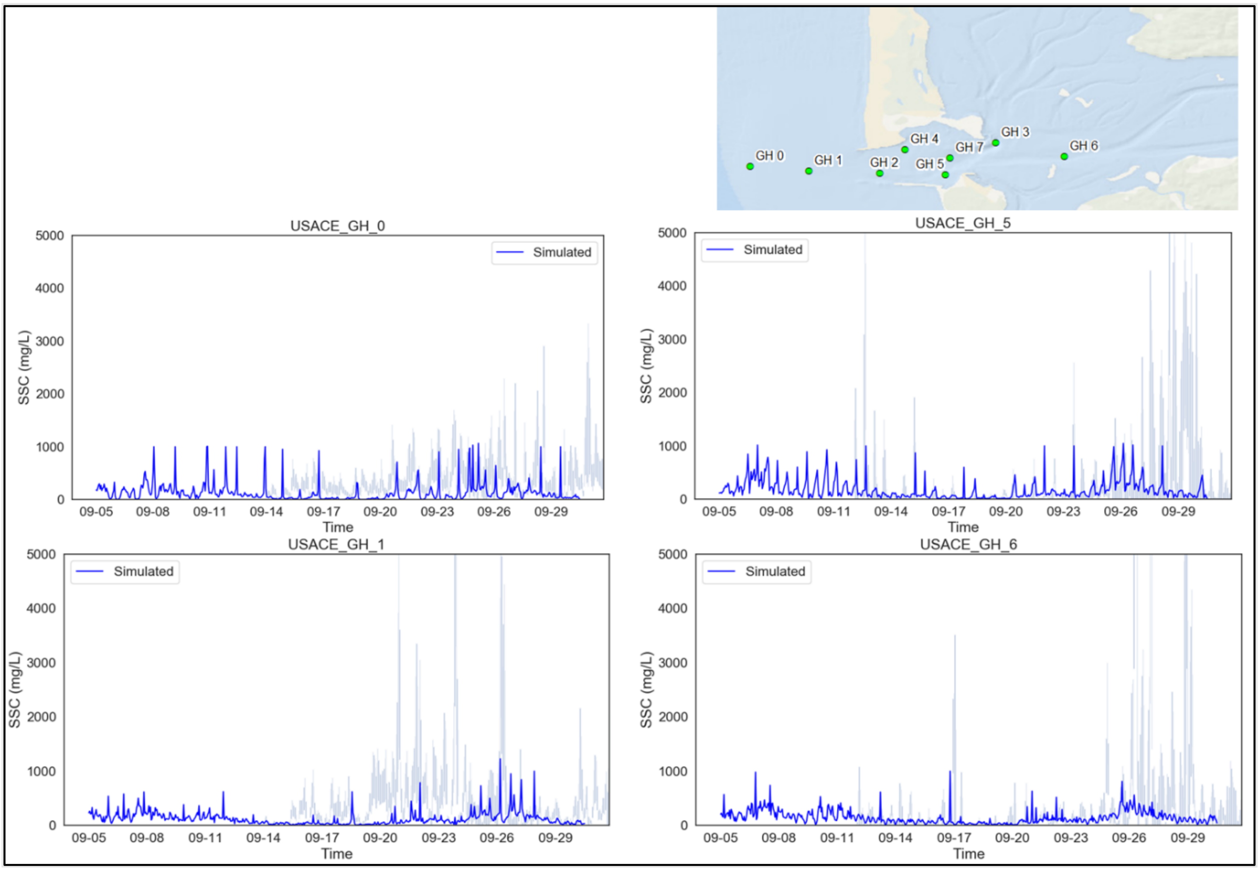

Figure 48: Suspended Sediment Concentration: Measured vs. Modeled

5.3 MORPHOLOGY CALIBRATION

5.3.1 Inlet

For the inlets of both Grays Harbor and Willapa Bay, a period from June 2009 to February 2010 was modeled. This is a direct comparison to measured morphological change at Grays Harbor, but a qualitative comparison for Willapa Bay, and both are primarily focused on overall patterns and magnitudes.

5.3.1.1 Model Setup

As discussed earlier, the morphological acceleration was applied to reduce the set of conditions to be modeled but achieve the effect of the equivalent morphological responses in long term. Firstly, the time series of wave heights at CDIP 036 (shown in Figure 49) was divided into two periods, calm summer conditions and active winter conditions. For the summer conditions, waves were grouped into 4 bins by 3 wave directions and 3 wave heights. For the winter conditions, waves were grouped into 9 bins by 4 wave directions and 4 wave heights. Figure 50 demonstrates the bins used for summer and winter wave distributions. The criteria for binning the waves ensures wave energy within each bin is approximately the same. The wave height that generates the average wave energy within each bin is used as the representative condition, along with the average wave period and wave direction and the corresponding average wind speed and most frequent wind direction.

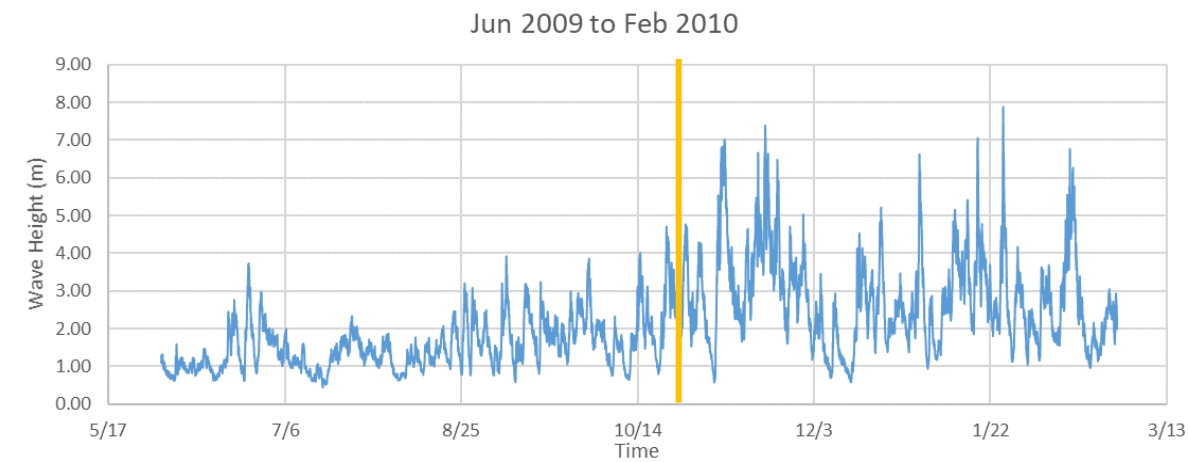

Figure 49: Wave Height Time Series During Period of Representative Long-term Conditions

To simplify the tide for each wave condition, a morphological tide was constructed based on actual tides in the region. On the U.S. west coast, residual sediment transport is controlled by the interaction of the M2, O1, and K1 harmonic components. The morphological tide consists of two components: M2 and C1. The morphological M2 constituent has the same amplitude and phase as the real M2, but with its period adjusted to be exactly 745 minutes. The C1 component is a hypothetical tide, with an amplitude equal to $\sqrt{2O_1K_1}$, and the average phase between those of O1 and K1, and a period of 1490 minutes. A comparison between the full astronomic tide and the morphological tide is shown in Figure 51.

The morphological tide is repeated throughout the simulation, and each wave condition is run for one tidal cycle. The bed change during each wave condition is accelerated by the frequency of that condition in the actual record, multiplied by the ratio of the total simulation period to the morphological tide period. This achieves the equivalent morphological response as the underlying dynamics but accelerates the morphological evolution in the numerical model. The time series of the morphological acceleration factor is presented in Figure 52.

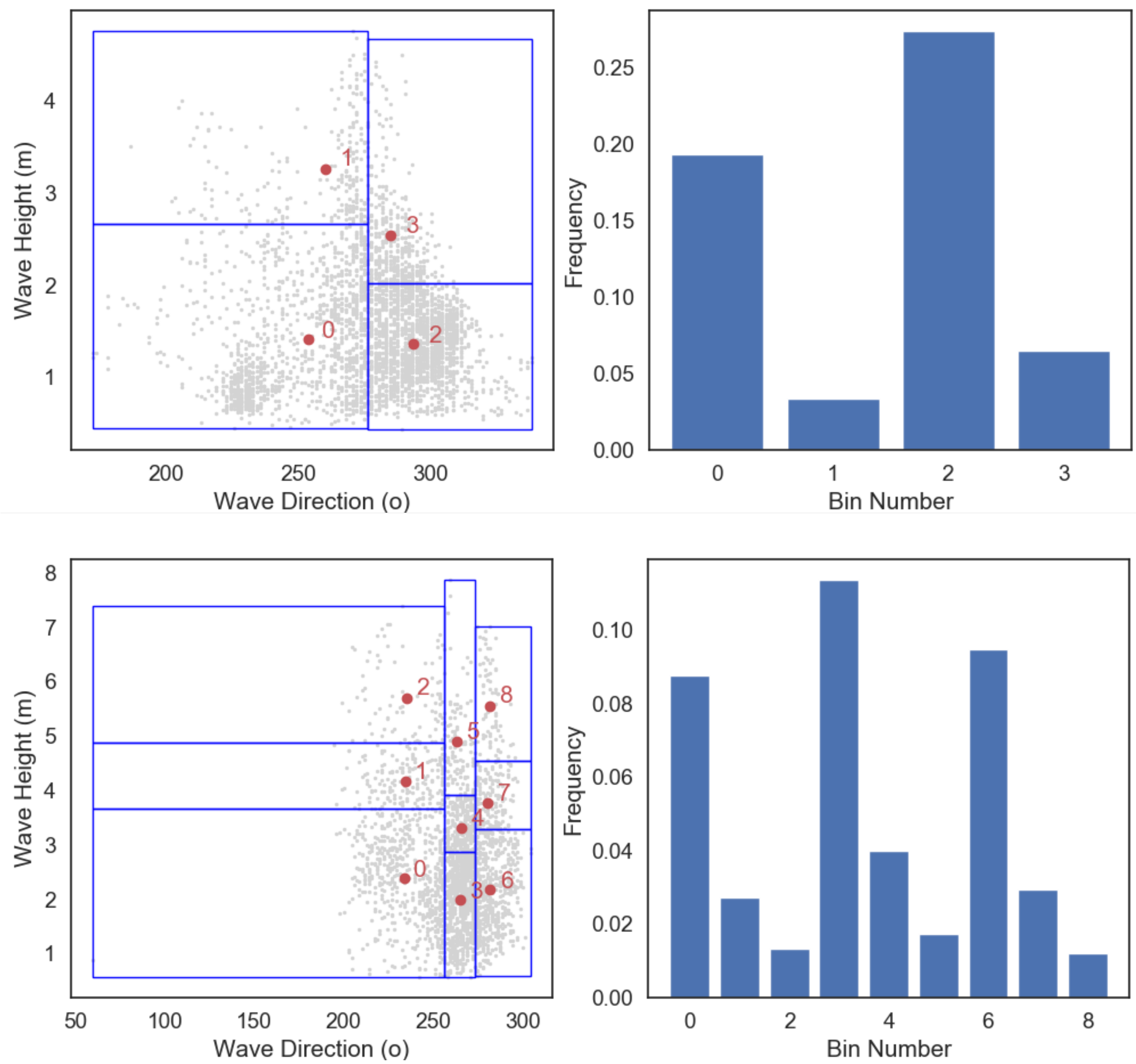

Figure 50: Wave Energy Bins for Summer Conditions (Top) and Winter Conditions (Bottom)

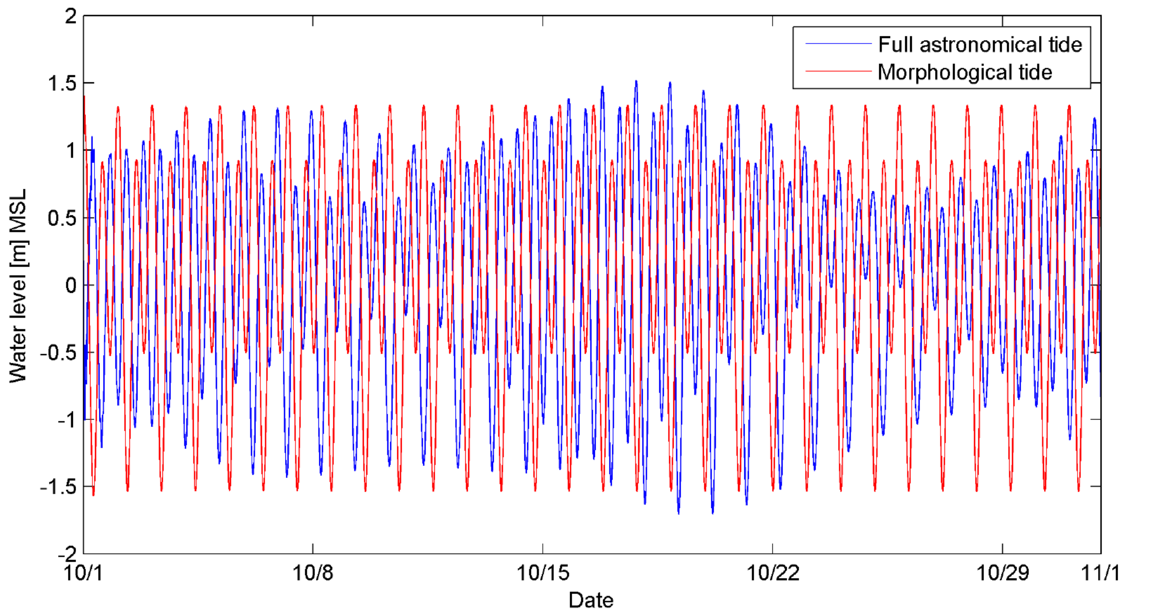

Figure 51: Comparison Between the Morphological Tide and Astronomical Tide

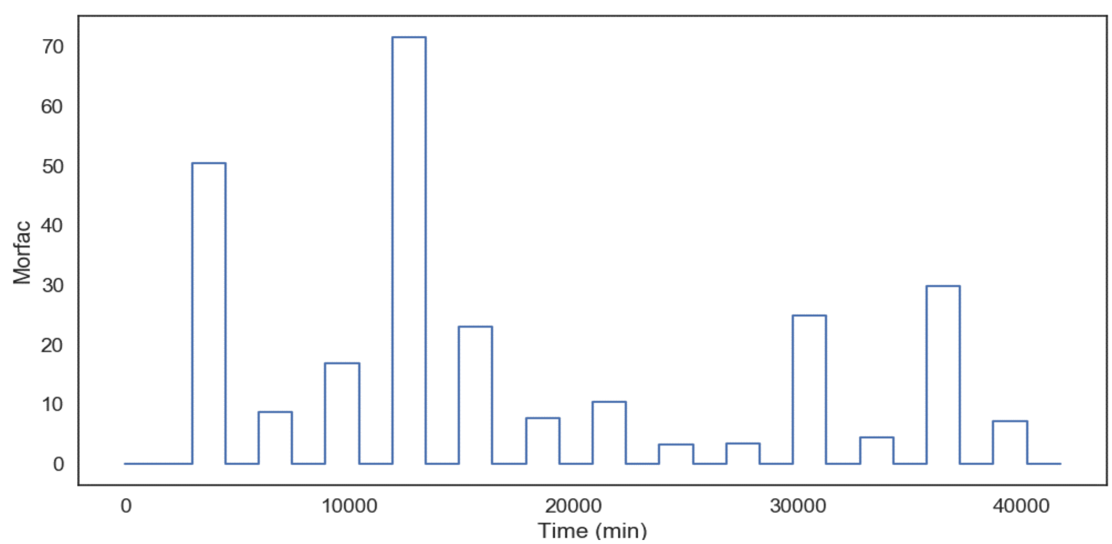

Figure 52: Time Series Illustrating the Variation of Morfac for Each of the Binned Wave Conditions

Finally, the river discharge hydrographs are condensed to fit within the shortened model timeframe based on the time series of the morphological acceleration factor. Figure 53 shows an example for the Chehalis River.

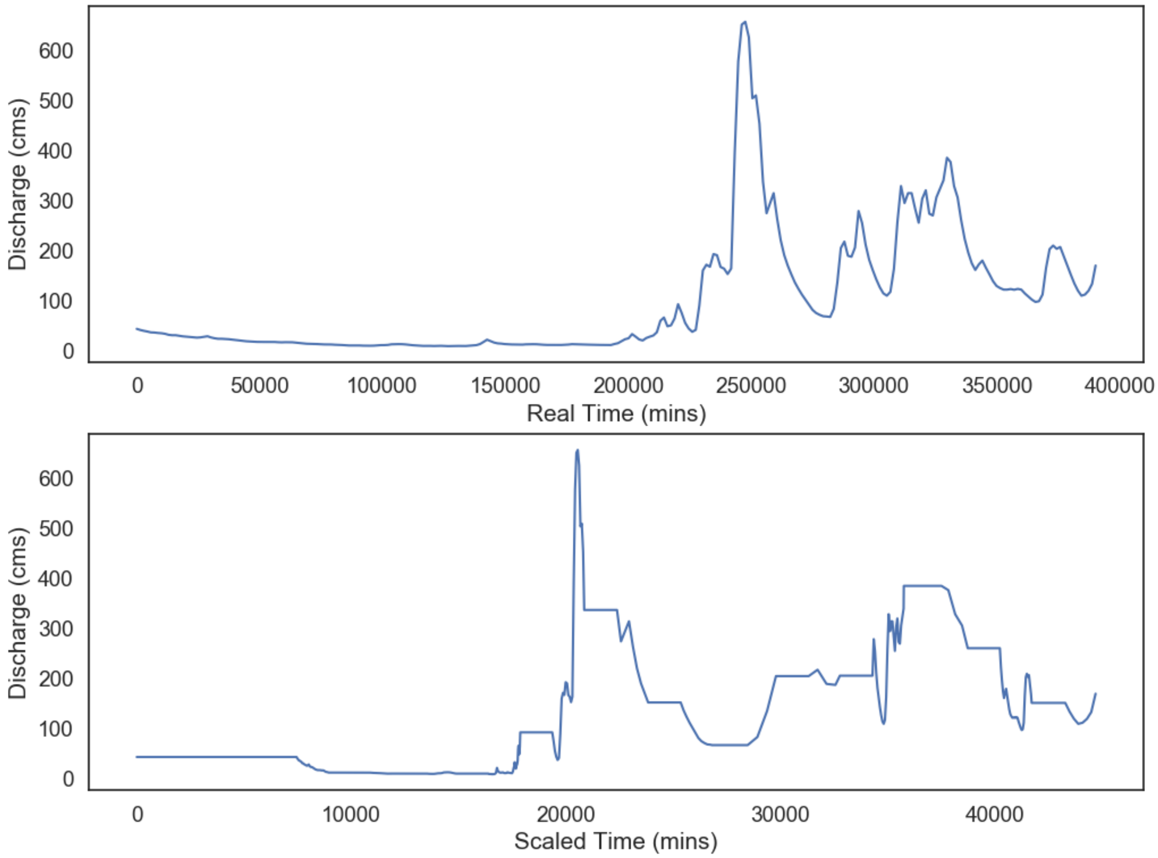

Figure 53: Scaled Chehalis River Hydrograph for the Morphological Model

5.3.1.2 Model Results

The measured versus modeled morphological change at Grays Harbor inlet is first presented, which is shown in Figure 54. The model captures most of the major changes and patterns; for example, the large accretion and erosion areas adjacent to one another just southeast of Damon Point, as well as the accretion in the navigation channel bend north of South Jetty and the erosion adjacent to North Jetty.

Figure 55 compares the measured versus modeled erosion at the entrance to Willapa Bay. Although this is not the same time period, the general patterns are replicated, including the erosion in the main channel and accretion to the north immediately outside of the inlet. The North Channel exits are migrating southward across the ebb shoal deflected by the accretion of the shore-tied submerged spit growing from Cape Shoalwater, which matches the channel migration period (see Section 3.10.2) of the present time.

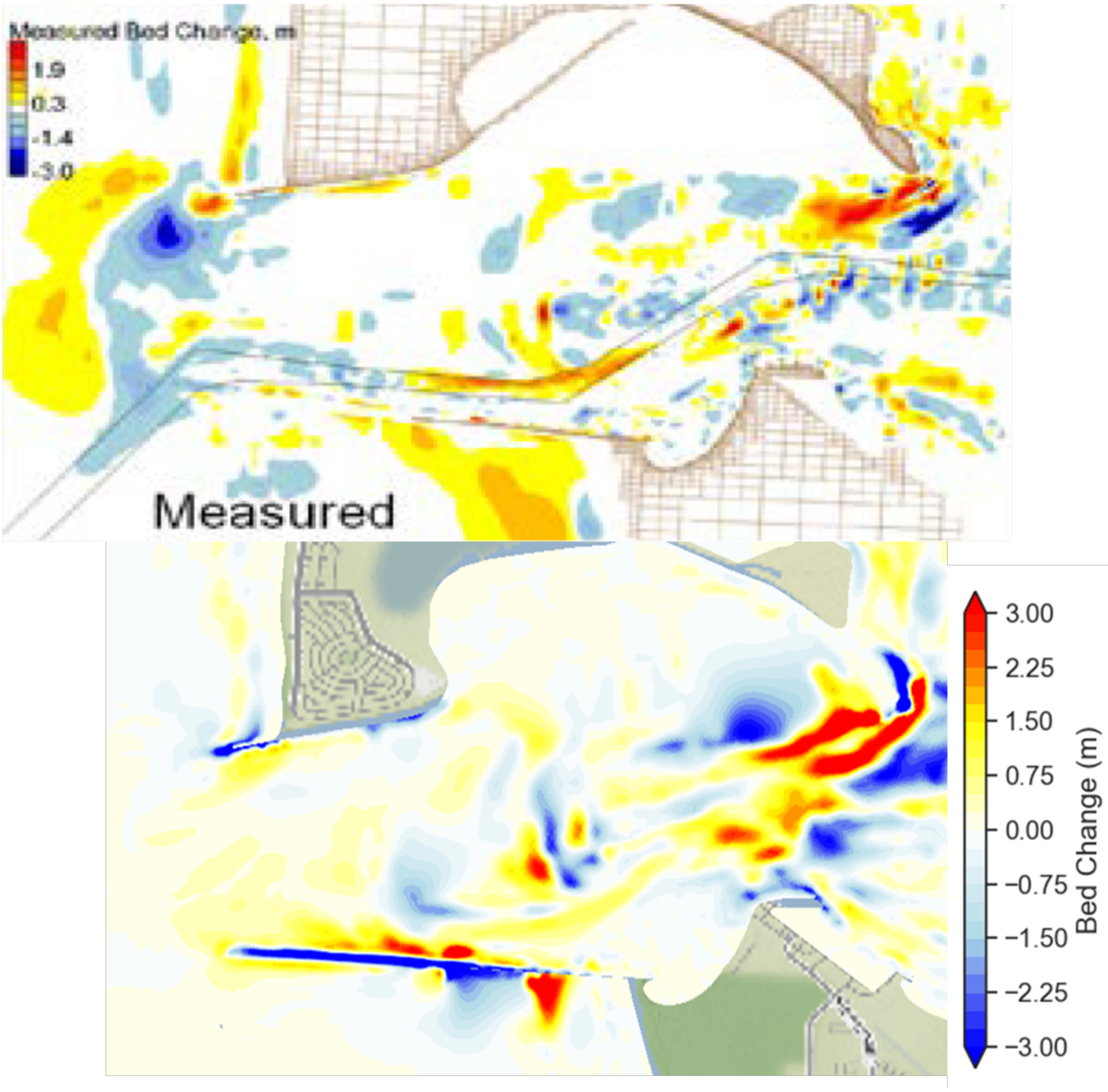

Figure 54: Measured vs. Modeled Erosion and Sedimentation, Grays Harbor

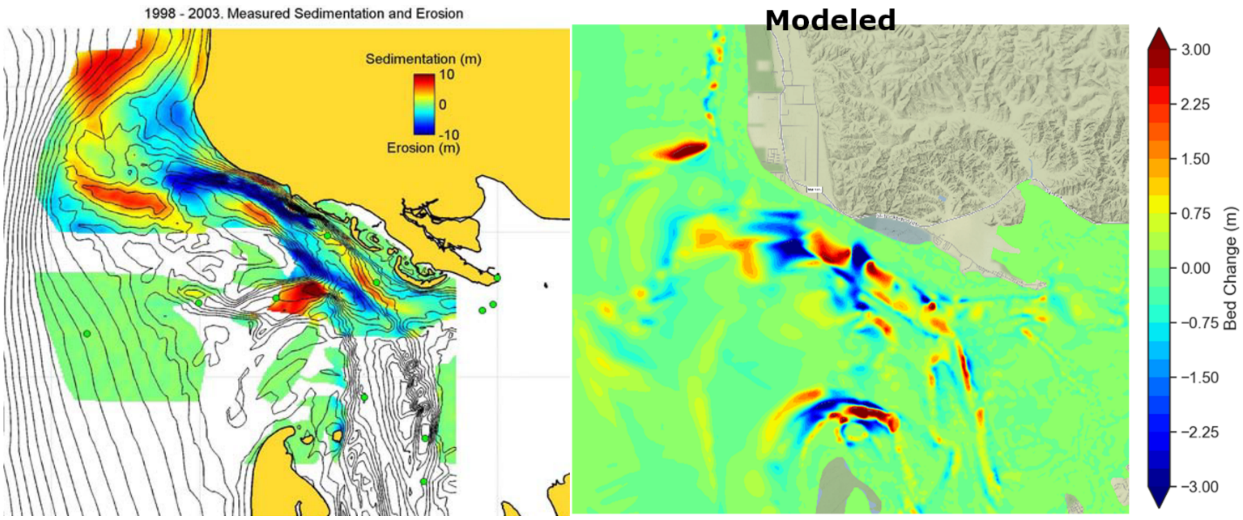

Figure 55: Measured vs. Modeled Erosion and Sedimentation, Willapa Bay

5.3.2 Tidal Flats

5.3.2.1 Model Setup

The model performance in replicating the morphological changes in tidal flats was evaluated using the InSAR data. Since the InSAR data is more accurate when a longer period of record is examined, yielding the corresponding average annual rate of morphological changes, a morphologically accelerated model run was developed for a 10-year period. The 10-year period was selected based on data availability where both wind and wave data are more than 95 percent complete for the year. Figure 56 and Figure 57 show, respectively, the time series of wind speed and wave height from 1999 to 2019. In combination, only 8 years meet such criteria including 2001, 2003, 2004, 2010, 2011, 2013, 2014, 2018. Additional 2 years were randomly selected from the 8 years. The long-term variations of the waves, shown as annual violin plot of wave height in Figure 58, indicate that the wave conditions are similar from year to year. The primary differences are the extreme wave height depending on winter storms. Although the data are limited to those 8 years, they represent well any sequential 10-year conditions.

With the selected datasets, a hydraulic year is defined from May to May such that the time series within a year can be divided by two periods, a calm period in summer and active conditions for the rest of the year. The morphological acceleration procedure as discussed in Section 5.3.1 was performed for each year to generate the corresponding conditions for the 10-year morphological modeling. This includes using 4 wave bins for summer conditions and 9 wave bins for the rest of the year, yielding a total of (4+9)*10=130 conditions. These conditions are summarized in Appendix C.

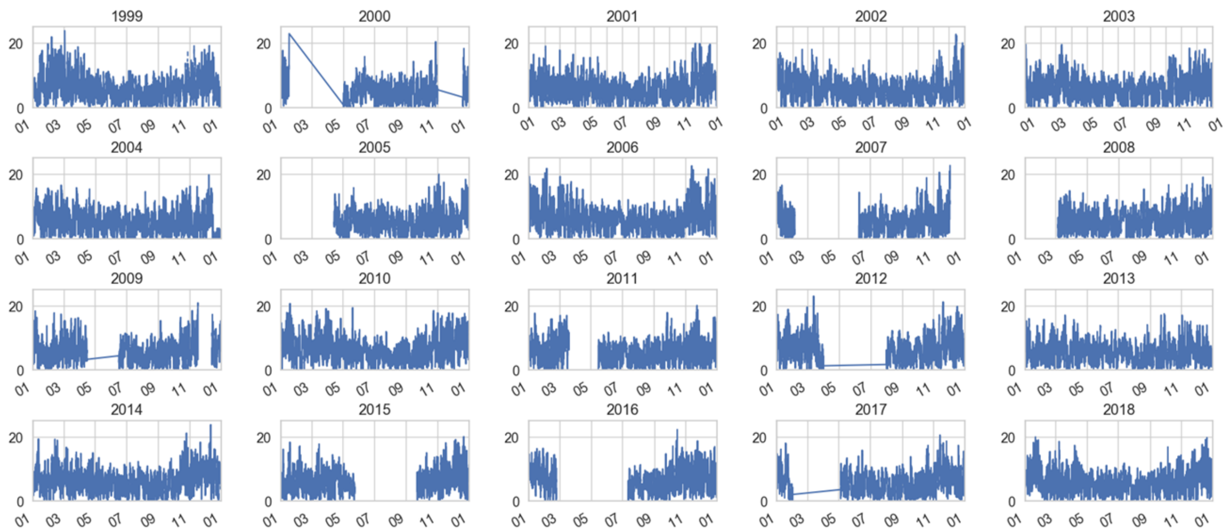

Figure 56: Time Series of Wind Speed from 1999 to 2019

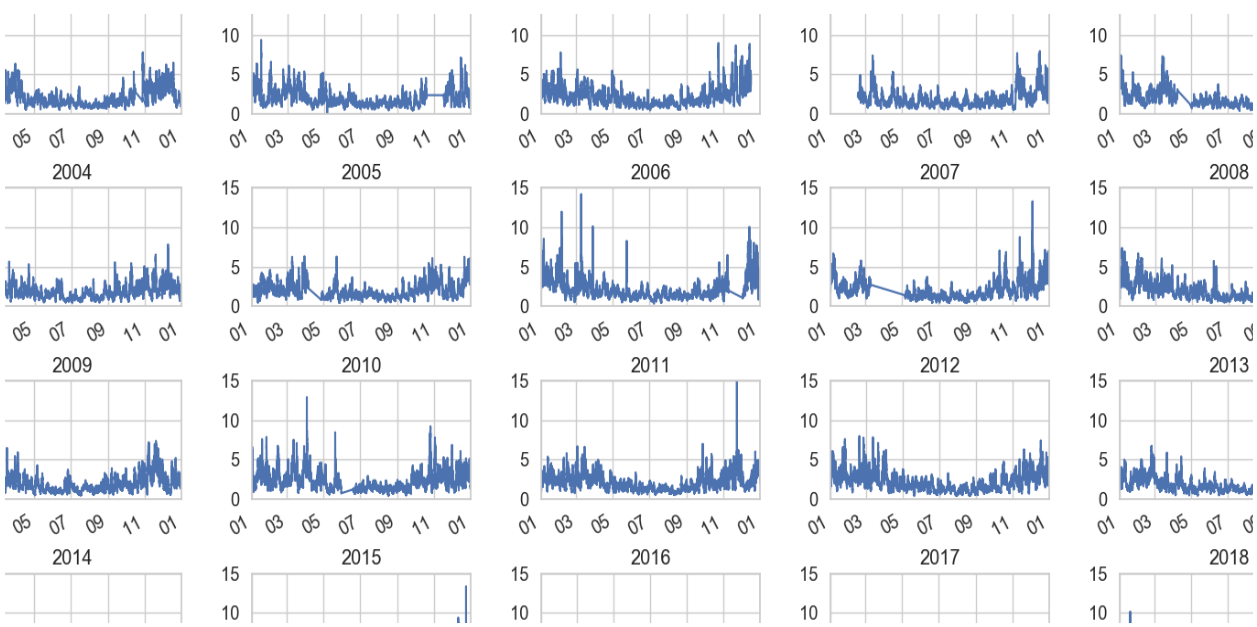

Figure 57: Time Series of Wave Height from 1999 to 2019

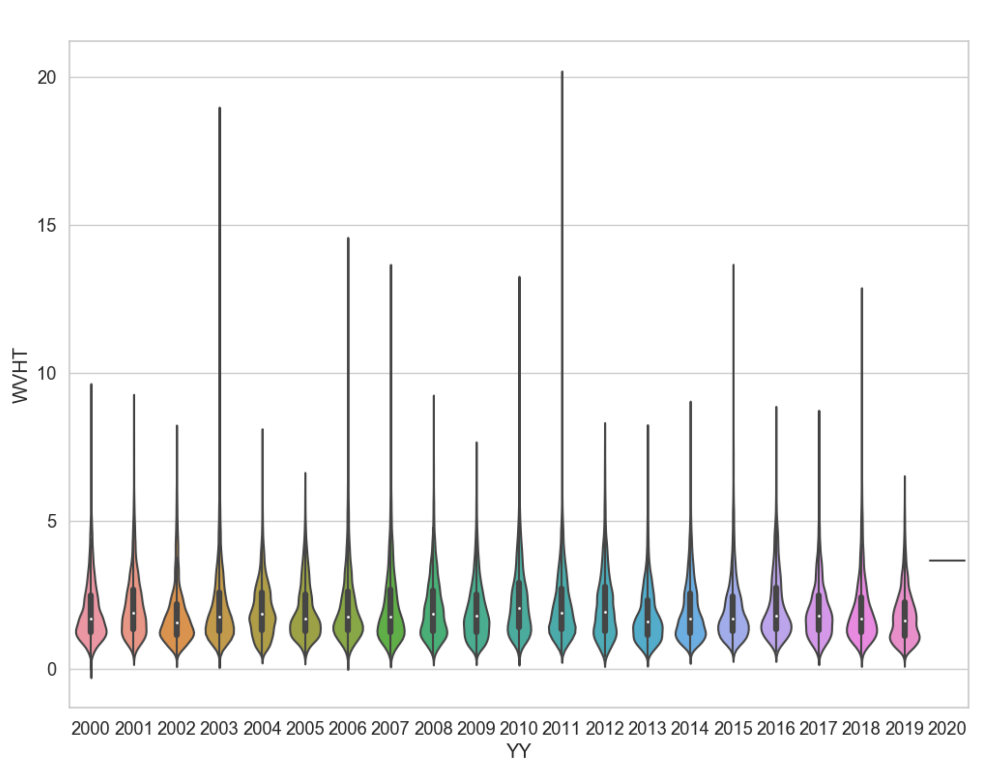

Figure 58: Annual Violin Plot of Wave Height from 2000 to 2020

5.3.2.2 Model Results

Comparisons of the 10-year average annual morphological changes of the tidal flats between the InSAR data and the model results are presented in Figure 59 for Grays Harbor and in Figure 60 for Willapa Bay, respectively. The results are only shown where the InSAR data is available. It should be noted the comparison is qualitative as it is beyond the model accuracy to capture the millimeter-scale changes from the InSAR data. Breakdown comparison for different regions (grey polygons in Figure 59 and Figure 60) are described below:

Grays Harbor

- Region A: this region is located on the west side of the harbor. The model generally captures the depositional area from the InSAR data on the south side of this region and erosional area toward the north corner; however, the model predicts erosion along the eastern edge of this region adjacent to a channel that is opposite to the InSAR data.
- Region B: This region is the northwestern portion of the harbor. The model captures well the overall depositional trend from the InSAR data in this region except the southern edge of this region adjacent to channels where the model predicts erosion.

- Region C: This region covers the northeast portion of the harbor. The model captures the erosional area near the Humptulips River from the InSAR data but predicts deposition along the shoreline that is different from the InSAR data. The model also captures overall depositional areas from the InSAR data in this region.
- Region D: This region covers the southern portion of the harbor. The model captures well the general depositional trend from the InSAR data with exceptions of a few localized erosional areas.
- Region E: This region is located on the west side of the harbor. The majority of the InSAR data is over an island. Otherwise, the model results compare well with the InSAR data.

Willapa Bay

- Region A: This region covers the northwestern corner of the bay north of the Willapa River Estuary. The model captures well the depositional and the erosional areas from the InSAR data.
- Region B: This region covers the northeastern portion of the bay on both sides of the Willapa River Estuary. The model captures well the patterns of morphological change from the InSAR data except the north corner of this region, where the model predicts deposition as opposed to the erosion from the InSAR data due to weak dynamics in the sheltered areas.
- Region C: This region encompasses the tidal flats directly facing the inlet. The model captures the overall depositional trend from the InSAR data except along the edge of the region, where the model predicts erosion.
- Region D: This region is the middle western portion of the bay. The model captures well the overall depositional trend from the InSAR data.
- Region E: This region is the middle eastern portion of the bay. The model captures well the overall depositional trend from the InSAR data except for a few localized erosional areas.
- Region F: This region is mainly the Long Island areas. The InSAR data are over the island for this region; otherwise, the model predicts the depositional trend along the shoreline of the island.
- Region G: This region covers the southern portion of the bay. The model captures the overall depositional trend from the InSAR data. The magnitude of the morphological changes in this area predicted by the model seems to be weaker than that of the other locations.

In general, the model predicts the morphological change patterns with a good degree of accuracy especially given the coarse resolution of the sediment data, limitations/challenges of the morphological model itself, and the high detail of the InSAR data used for the comparison. The discrepancy is mainly at areas adjacent to the channel system and from some localized areas that require finer mesh resolution and better sediment data with higher spatial resolution.

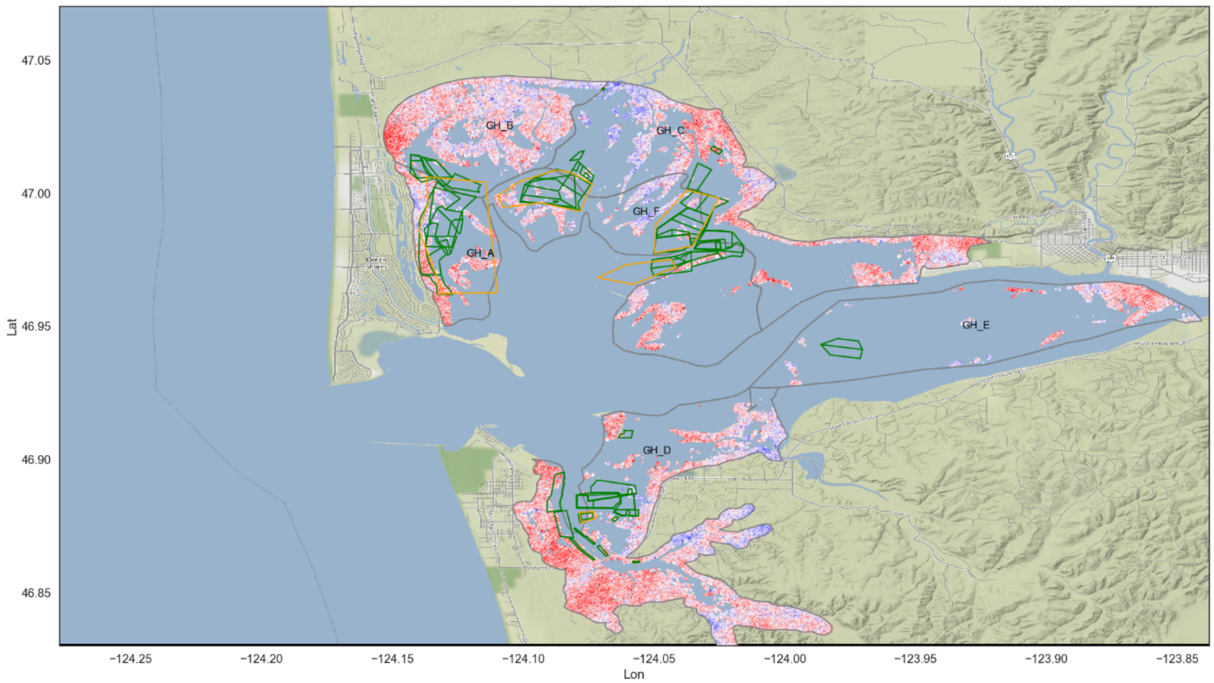

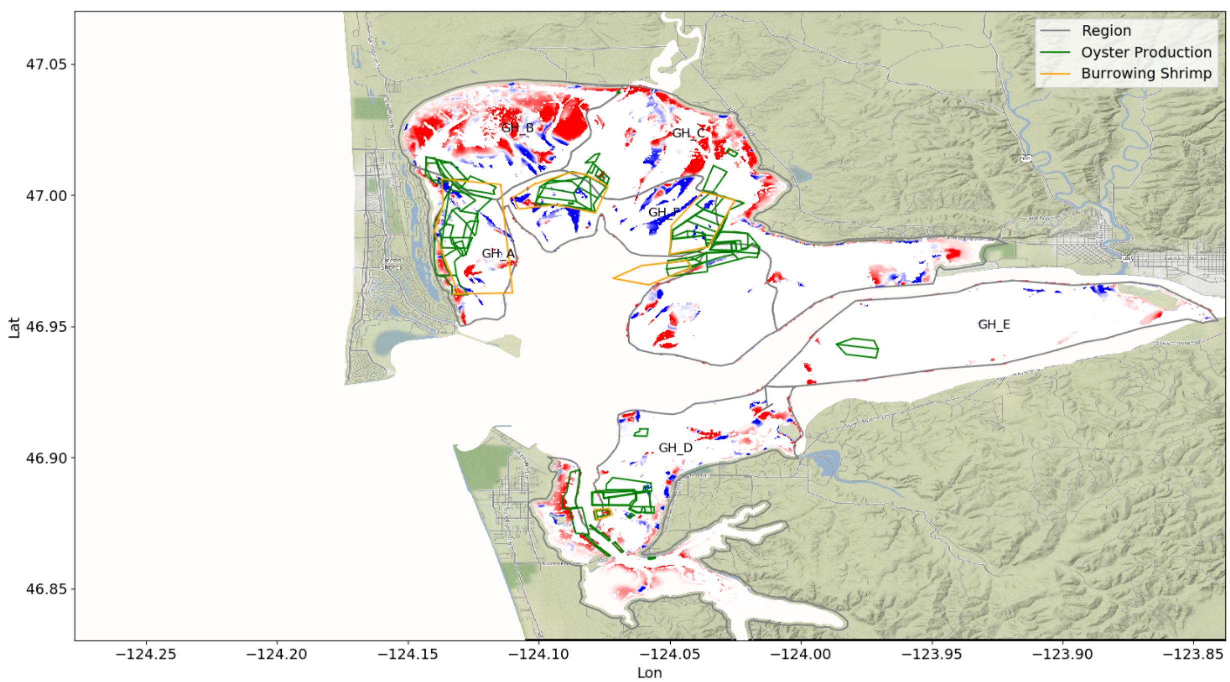

Figure 59: Comparison of Annual Morphological Changes over Tidal Flats Between the InSAR Data (Top) and Model Results (Bottom), Grays Harbor

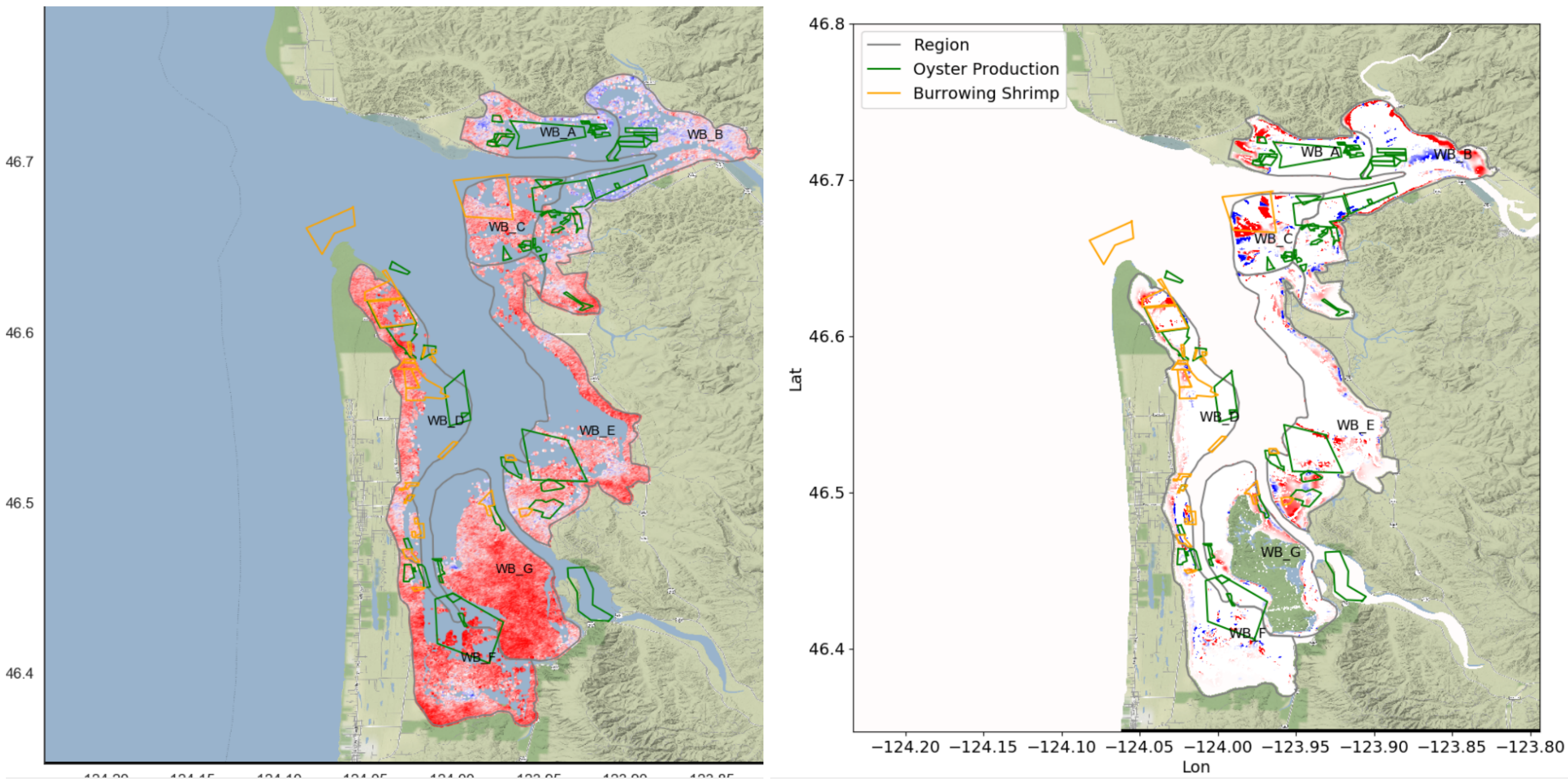

Figure 60: Comparison of Annual Rate of Morphological Changes over Tidal Flats Between the InSAR Data (Left) and Model Results (Right), Willapa Bay

5.4 GRAYS HARBOR

5.4.1 Overall Morphodynamics

The 10-year average annual morphological changes in Grays Harbor predicted by the model are shown in Figure 61, with red indicating accretion and blue indicating erosion. The oyster production farms from the stakeholder survey are shown as green polygons. The observations regarding the morphodynamics in Grays Harbor are summarized below:

- The inlet has a very strong morphodynamic response, with greater than 3 m of annual deposition southeast of Damon Point abutting an erosion zone toward the navigation channel, causing the channel to migrate to the southeast.
- The navigation channel is generally accreting, with an average annual deposition of over 1 m in the Outer Harbor reach and less than 0.5 m per year in the Inner Harbor reach; this generally matches the historical average dredging required to maintain the navigation channel depth.
- Tidal flats consist of subsidence areas adjacent to accretional areas farther landward, with an annual rate of change on the order of centimeters.
- The channel system inside the harbor seems to be widening, which matches observations using historical satellite images.

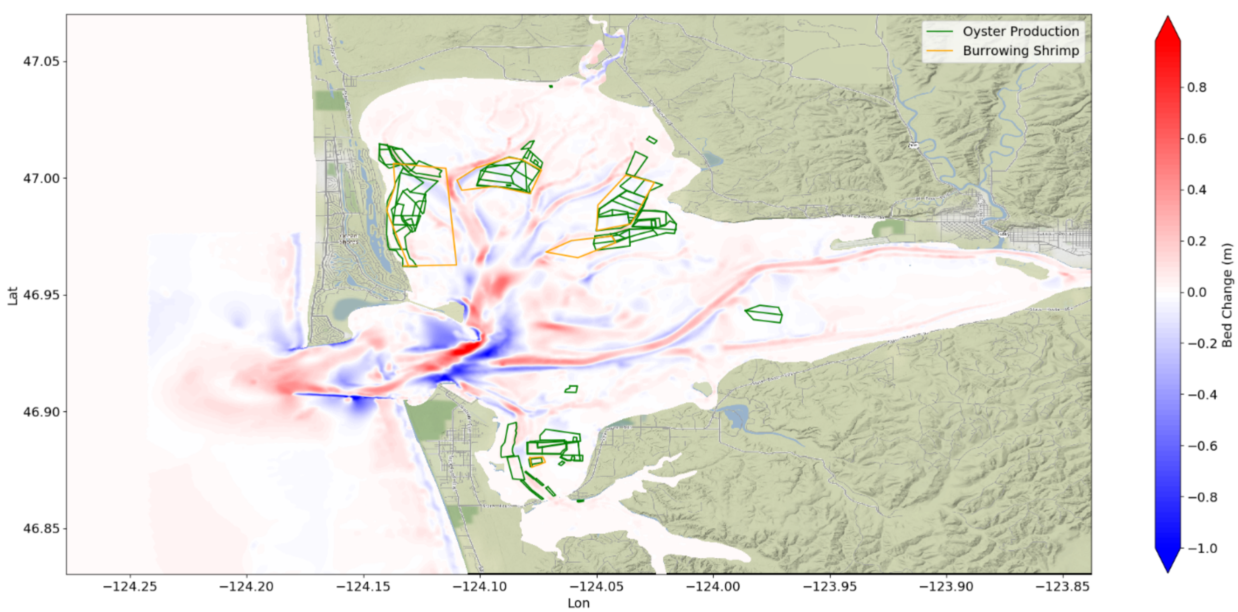

Figure 61: 10-year Average Annual Morphological Changes in Grays Harbor

5.4.2 Seasonal Variations

The morphological response over tidal flats in Grays Harbor exhibit seasonal variations in response to the seasonal wind conditions. Figure 62 shows the morphological change over tidal flats (areas with depth greater than 1.5 m are not shown) for one morphological tide cycle during typical summer conditions with NW wind and typical winter conditions with S wind, respectively. The morphological response is weaker in summer than in winter. Northerly directed strong wind during winter causes erosion of the tidal flats with sediments being deposited farther landward. During the winter storm conditions with strong offshore waves, tidal flats are experiencing overall deposition, which is shown in Figure 63.

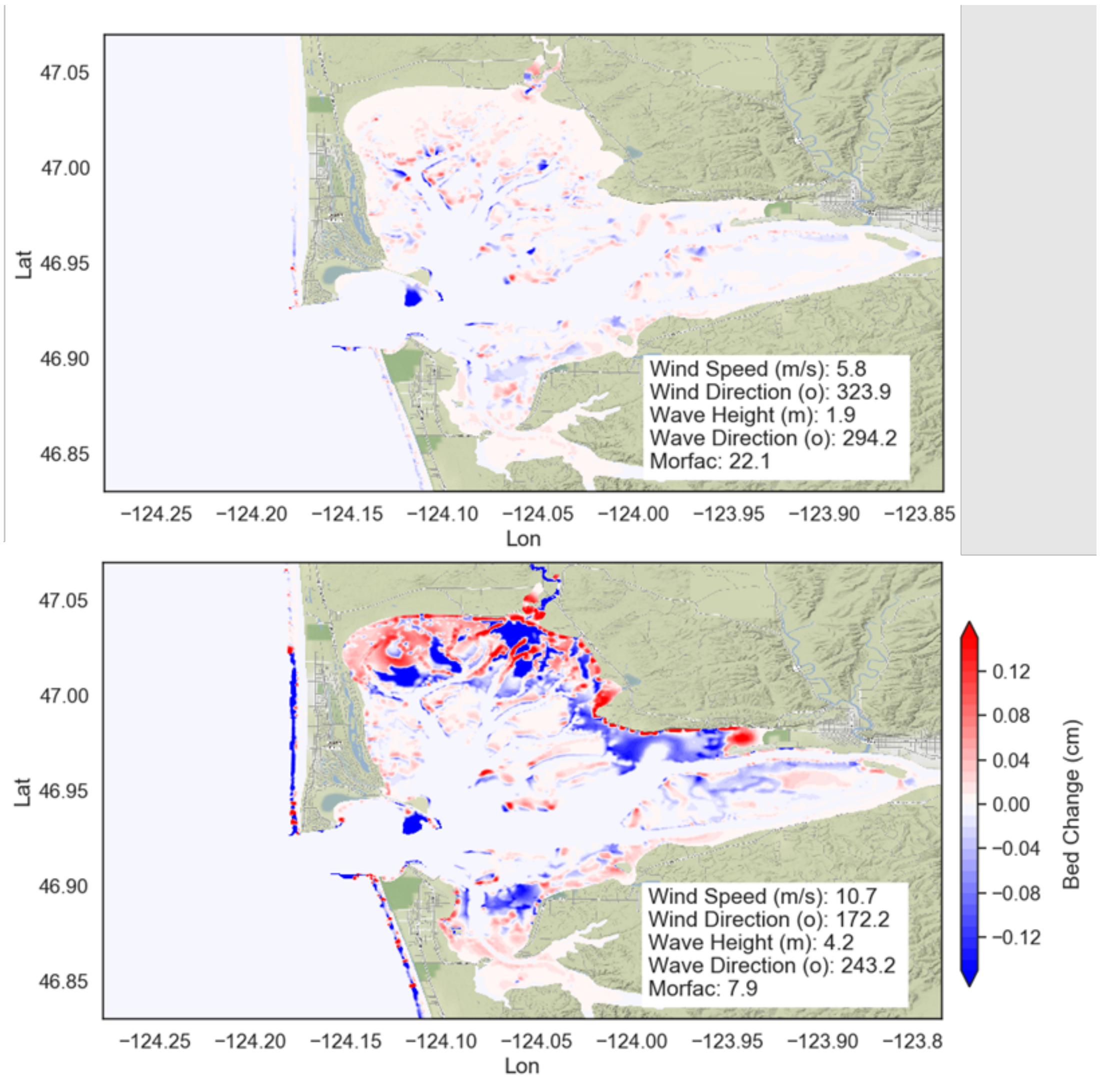

Figure 62: Morphological Change over One Morphological Tidal Cycle, Typical Summer Conditions with N Winds (Top) versus Typical Winter Conditions (Bottom), Grays Harbor.

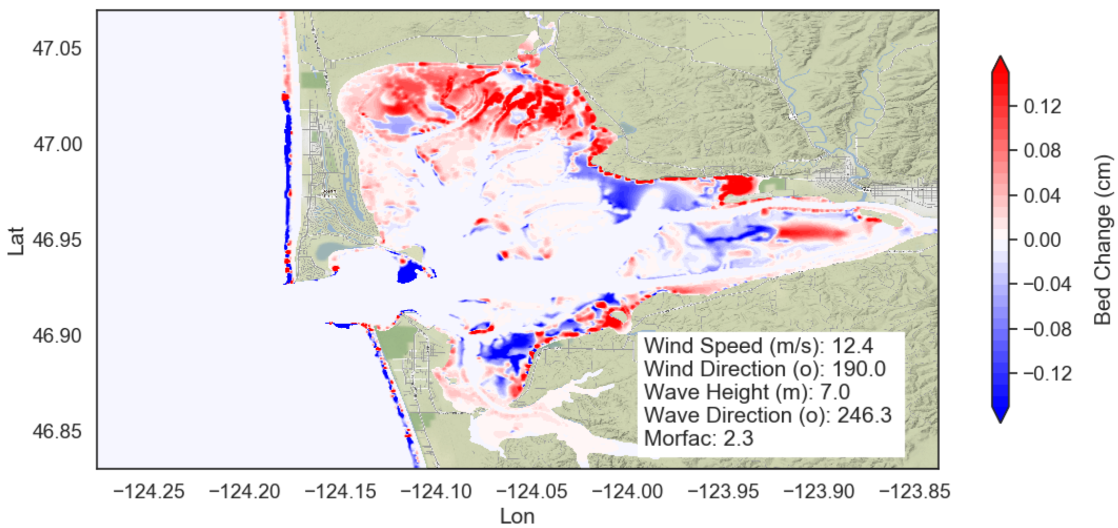

Figure 63: Morphological Change over One Morphological Tidal Cycle, Winter Storm Conditions with S Winds, Grays Harbor

5.5 WILLAPA BAY

5.5.1 Overall Morphodynamics

The 10-year average annual morphological changes in Willapa Bay predicted by the model are shown in Figure 64, with red indicating accretion and blue indicating erosion. The oyster production farms and burrowing shrimp areas from the stakeholder survey are shown as the green and orange polygons, respectively. The following observations regarding the overall morphodynamics in Willapa Bay are made:

- The inlet has a very strong morphodynamic response, with greater than 3 m of annual deposition. Water largely leaves the bay at three locations, indicated by three erosion areas, signifying a very dynamic inlet. This is consistent with the historical channel migration as discussed in Section 3.10.2.
- Based on the morphological change in 2018 (included in the deliverable), the North Channel is currently migrating southward across the ebb shoal with current exit closing up connecting the ebb shoals to the Cape Shoalwater.
- The South Channel is migrating northward, encroaching the tidal shoals to the north, which seems to be matching the observation from the stakeholders.
- There is deposition in the channel system with an average annual magnitude around 0.5 m.
- Tidal flats near shore are generally in accretion, with subsidence zones adjacent to the channel; the annual rate of change is on the order of centimeters.

- The channel system inside the bay seems to be widening, which matches observations using the historical satellite images.

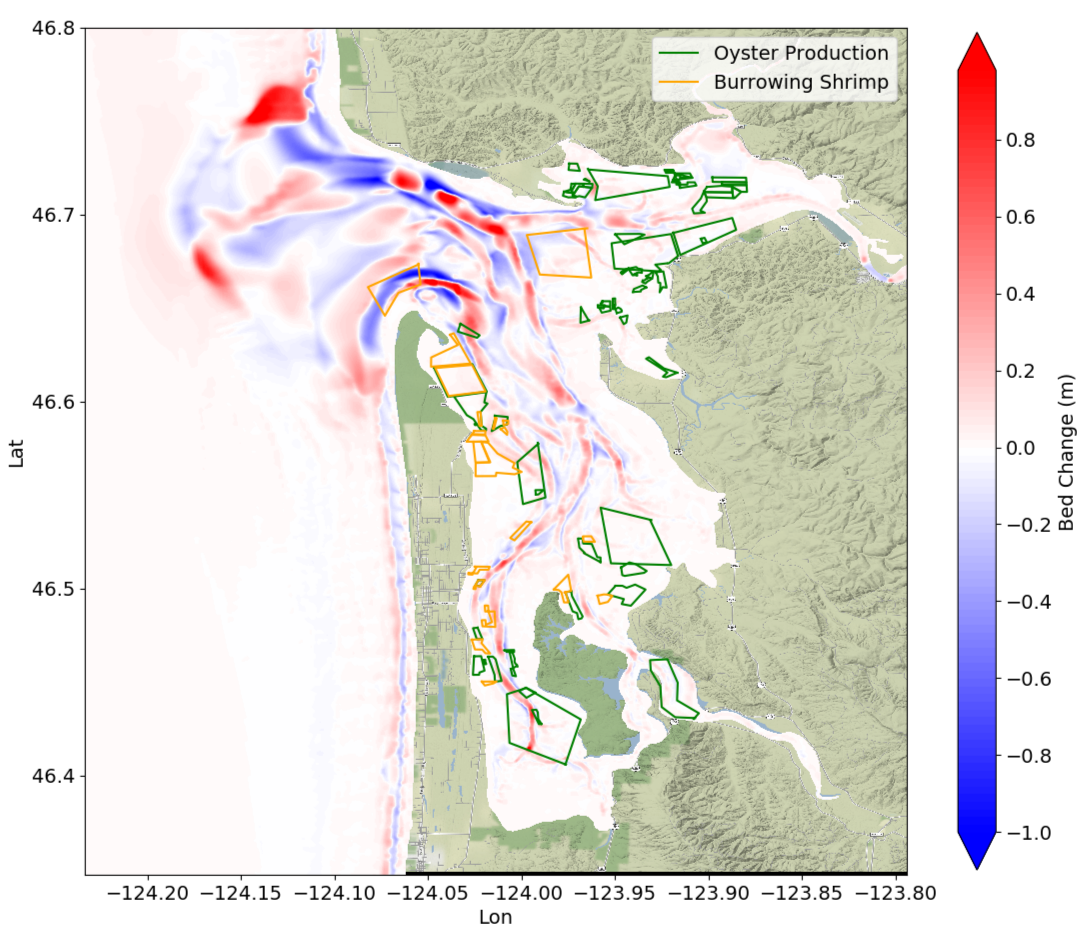

Figure 64: 10-year Average Annual Morphological Changes in Willapa Bay

5.5.2 Seasonal Variations

The morphological response over the tidal flats in Willapa Bay also exhibit seasonal variations in response to the seasonal wind conditions. Figure 65 compares the morphological change over tidal flats (areas with depth greater than 1.5 m are not shown) for one morphological tide cycle during typical summer conditions with NW winds versus typical winter conditions with S winds, respectively. The morphological response is weaker in summer than in winter. Northerly directed strong winds during winter cause erosion of tidal flats along the bay, with sediments being deposited farther landward. During winter storm conditions with strong offshore waves, the tidal flats are experiencing overall deposition except middle eastern portion and northeast corner north of the Willapa River estuary, which is shown in Figure 66.

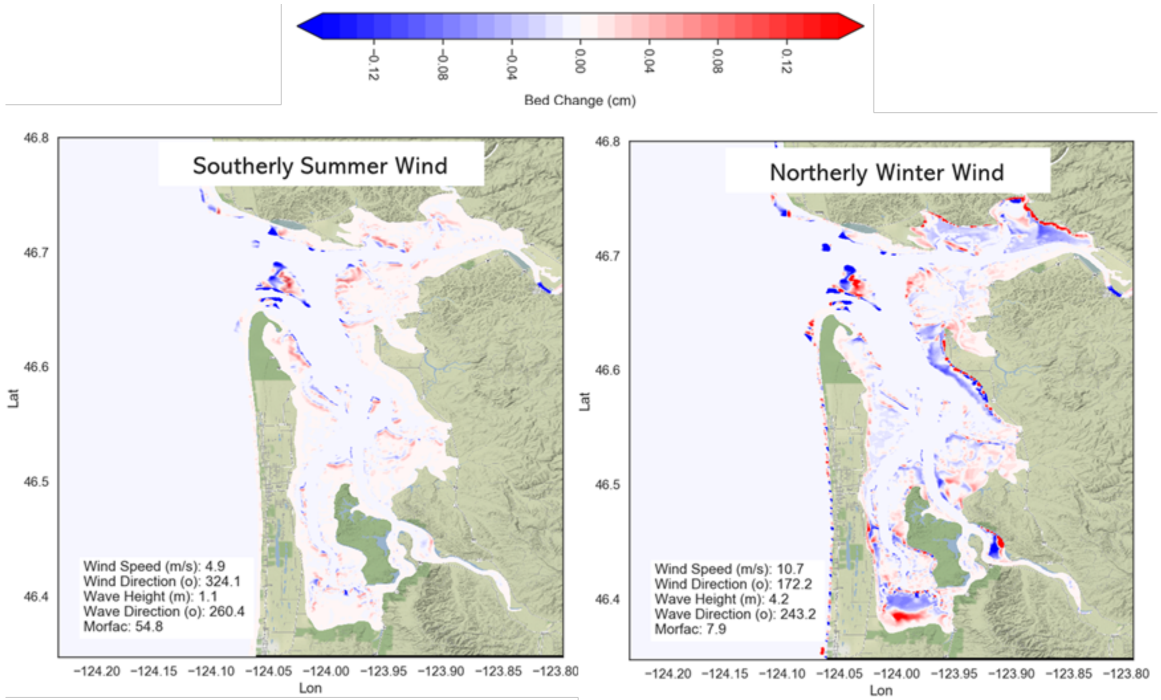

Figure 65: Morphological Change over One Morphological Tidal Cycle, Typical Summer Conditions with N Winds (Left) versus Typical Winter Conditions with S Winds (Right), Willapa Bay

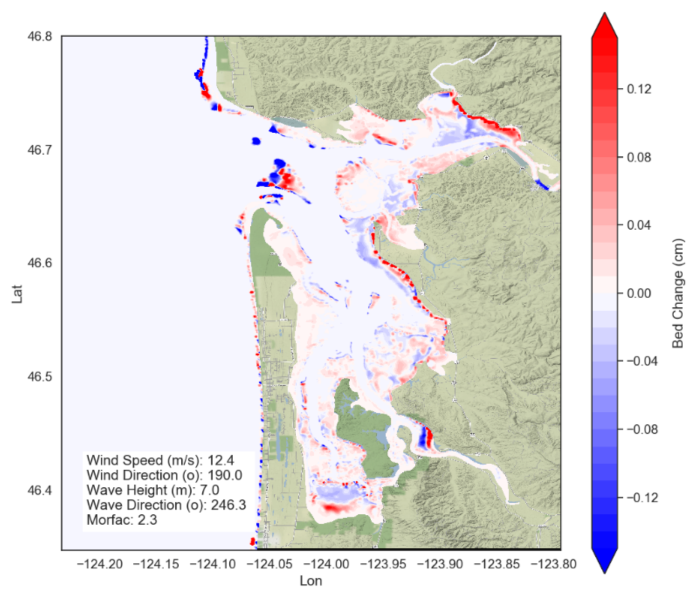

Figure 66: Morphological Change over One Morphological Tidal Cycle, Winter Storm Conditions with S Winds, Willapa Bay

6.0 O&M DREDGING IMPACTS

An overview of the Grays Harbor Federal Navigation Project, delineating the channel reaches, disposal sites, and other features, can be found in Figure 4. O&M dredging was performed in recent years on an annual basis to maintain the navigation depth. The most recent dredging information available is from 2018, and the dredged volumes are summarized in Table 9. Including the deepening to -42 ft MLLW, a total of 4,162,538 yd^3 of sediment was dredged, with suitable material placed at the Point Chehalis disposal site. This occurred over the course of 2 years, with the annual average dredge volume similar to the long-term annual average volume of close to 2,000,000 yd^3.

The impact from O&M dredging activities was analyzed using the sediment transport model described in Section 5.0, where the ambient conditions were turned off to isolate the sediment processes from the dredging itself. Dredging activity in the model was parameterized as a time series of point discharges based on the average volume dredged in each reach, the length and width of the reach, and the typical time required to complete dredging activities. This information was found in Table 9, Table 17, and Section 7.9.1.1 of USACE (2014); other parameters, such as cut width, loss rates, and concentrations, were adapted from past similar work. The parameterization accounts for different dredging methods being used, i.e., clamshell vs. hopper, which are discussed in Section 6.1.1 and 6.1.2, respectively. The impact from O&M dredging also was analyzed from the perspective of sediment release and resuspension at the disposal site. The fate of sediments from the disposal site was analyzed by a particle tracking model and the sediment transport model, which is discussed in Section 6.2.

Table 9: O&M Dredge Volumes (yd^3) in the Grays Harbor Channel, 2018

2018 Dredging	Cow Point / Turning Basin	Hoquiam Reach	North	Crossover Reach	South Reach
O&M (-38)	1,124,902	288,500	65,380	463,691	6,425
Deepening (-42)	614,989	398,400	284,799	698,802	216,650
Total	1,739,891	686,900	350,179	1,162,493	223,075

A total of 4,162,538 yd^3

Suitable material placed at Point Chehalis disposal site

6.1 DREDGING ACTIVITIES

6.1.1 Clamshell Dredge

Figure 67 and Figure 68, respectively, illustrate the peak SSC and bed level change from the modeled clamshell dredge operations. Notable SSC values extend from the inlet to upstream of Aberdeen, typically 30 milligrams per liter (mg/L) or less. The highest peak SSCs, about 90 mg/L, are confined to the North Channel and Crossover Reach. Maximum deposition is roughly 3 centimeters (cm) in Crossover Reach and less than 0.5 cm elsewhere; the largest changes are within the channel, and in reality, more than offset by the change in elevation caused by the dredging itself. In summary, sediment activities due to clam shell dredging do not have significant negative impact on the aquaculture resources within Grays Harbor.

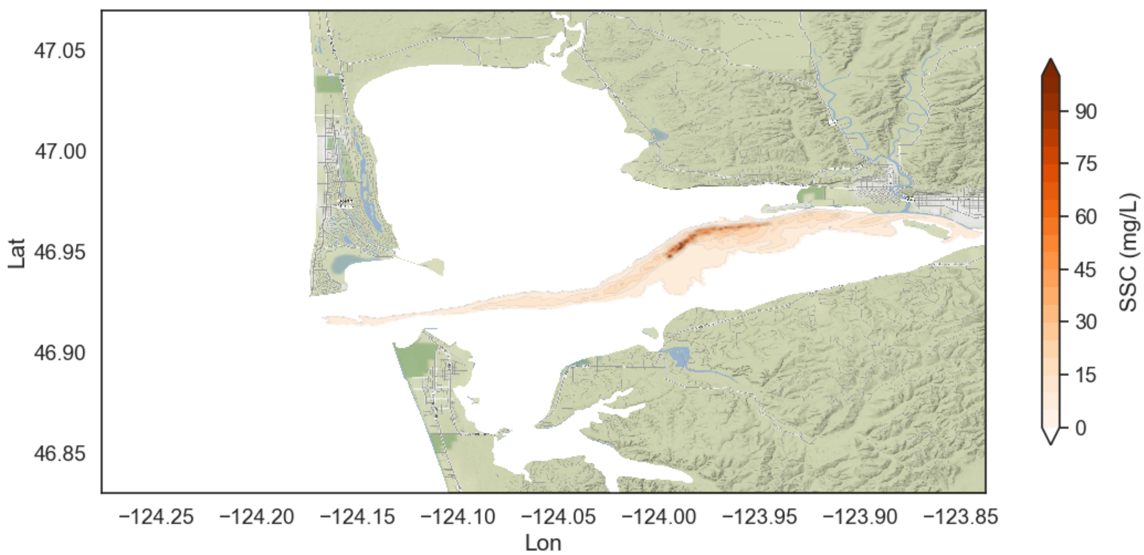

Figure 67: Modeled Peak SSC, Clamshell Dredge Operation

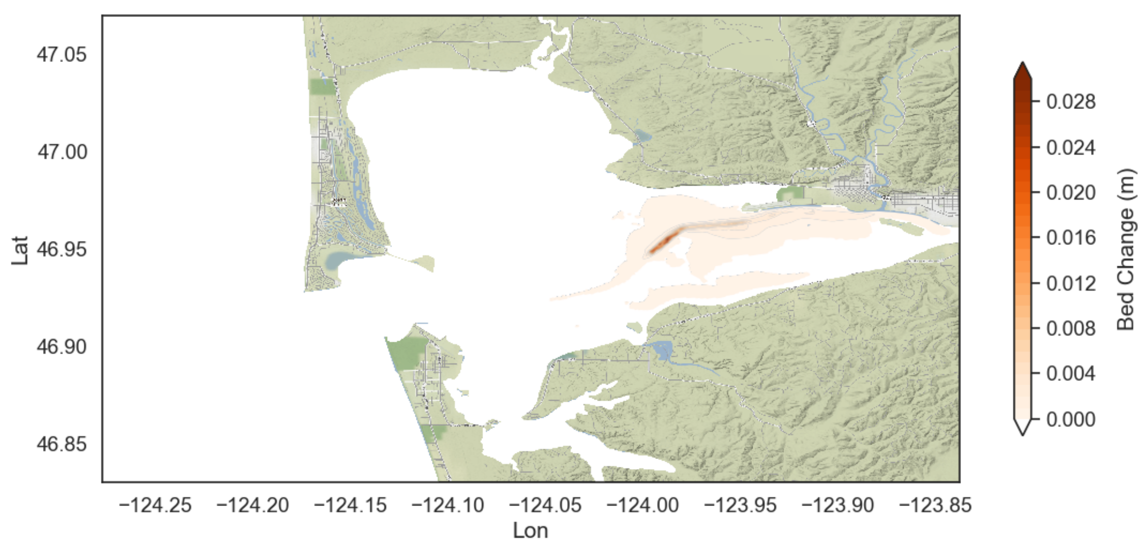

Figure 68: Modeled Bed Level Change, Clamshell Dredge Operation

6.1.2 Hopper Dredge

Figure 69 and Figure 70, respectively, illustrate the peak SSC and deposition from the modeled hopper dredge operations. Notable SSC levels are largely confined to the channel between the inlet and North Reach, with a maximum of 30 mg/L. Bed level change is as high as 3 cm in the Crossover Reach channel, more than offset by the change in elevation caused by the dredging itself. In summary, sediment activities due to clam shell dredging do not have significant negative impact on the aquaculture resources within Grays Harbor.

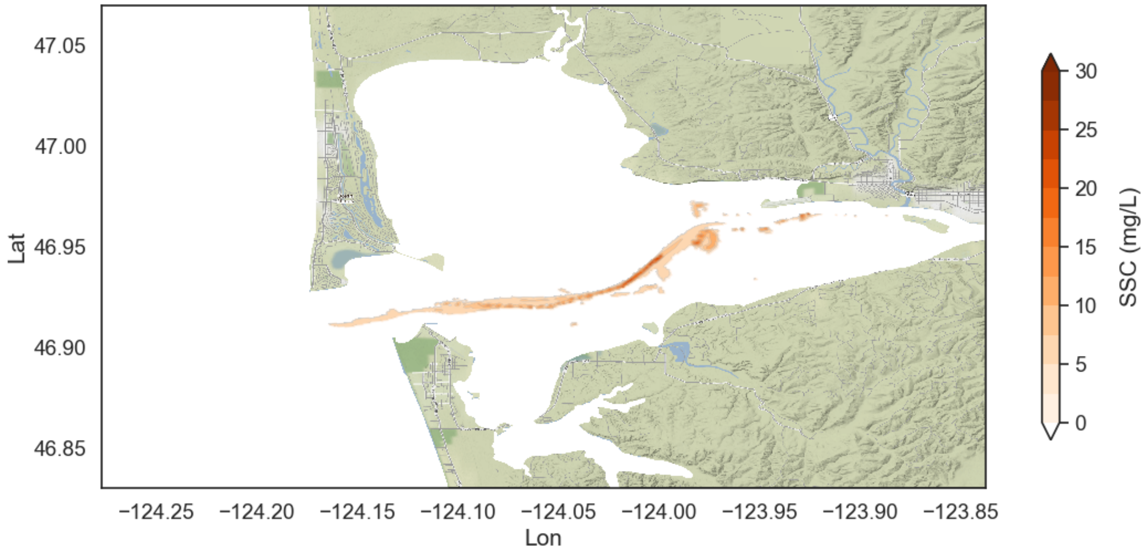

Figure 69: Modeled Peak SSC, Hopper Dredge Operation

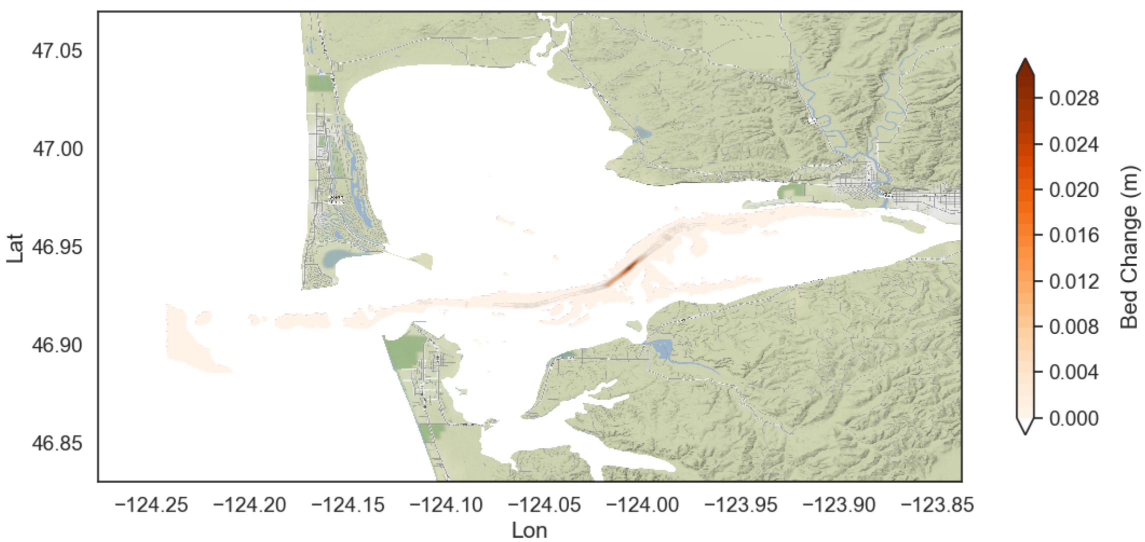

Figure 70: Modeled Bed Level Change, Hopper Dredge Operation

6.2 DISPOSAL SITE

The fate of sediments from release and resuspension at the disposal site was analyzed using a particle tracking model, which accounts for a finite number of sediment parcels individually and models their movement and dispersion, and the sediment transport model developed previously for the dredging simulation. An alternative location for sediment disposal based on the hydrodynamics of Grays Harbor also was analyzed with the objective of reducing the amount of sediment moving back into the harbor.

6.2.1 Particle Tracking

The particle tracking model was performed with the objective of understanding the pathways of the sediments disposed and/or resuspended at the Chehalis disposal site. Therefore, sediments are modeled as passive particles and do not include the sediment characteristics. Particles are randomly released at the disposal site, and the movement of the particles with tidal flow was monitored.

The particle tracking model results at 6, 12, 18, and 24 hours after sediment release during summer ebb tide are shown in Figure 71. Sediments mobilized from the disposal site first leave the disposal site with ebb tide, then move along the sediment path from North Jetty toward Damon Point and find the way into the northern portion of the harbor with flood tide. During the second tidal cycle, most of the mobilized sediments from the disposal site are transported into the Pacific Ocean to the north of the inlet, with a smaller amount within the inlet and a few remaining in the northern tidal flats of Grays Harbor.

The particle tracking model results at 6, 12, 18, and 24 hours after sediment release during summer flood tide are shown in Figure 72. The released sediments are initially transported into the eastern and northeastern portion of the harbor during flood tide, which then exit the harbor straight into the Pacific Ocean during ebb tide. During the second tidal cycle, flood tide pulls sediments back into the harbor reaching most locations within the harbor, which then leave the harbor during ebb tide exiting into Pacific Ocean to the north.

The particle tracking model results at 6, 12, 18, and 24 hours after sediment release during ‘winter’ (with strong wind/wave event) ebb tide are shown in Figure 73, sediments are transported farther west into the Pacific Ocean. This is perhaps associated more so with a higher tide (spring tide) compared with the tide condition used in summer case. The subsequent flood tide does not send much sediment back into the harbor. This shows that the transport of the resuspended sediments at the disposal site is controlled mainly by tide rather than strong wind/wave conditions.

The particle tracking model results at 6, 12, 18, and 24 hours after sediment release during ‘winter’ (with strong wind/wave event) flood tide are shown in Figure 74. This exhibits a similar pattern to summer flood tide release. Flood tide first sends sediments toward the eastern and northeastern portions of the harbor while the following flood tide transport sediments into most areas within the harbor.

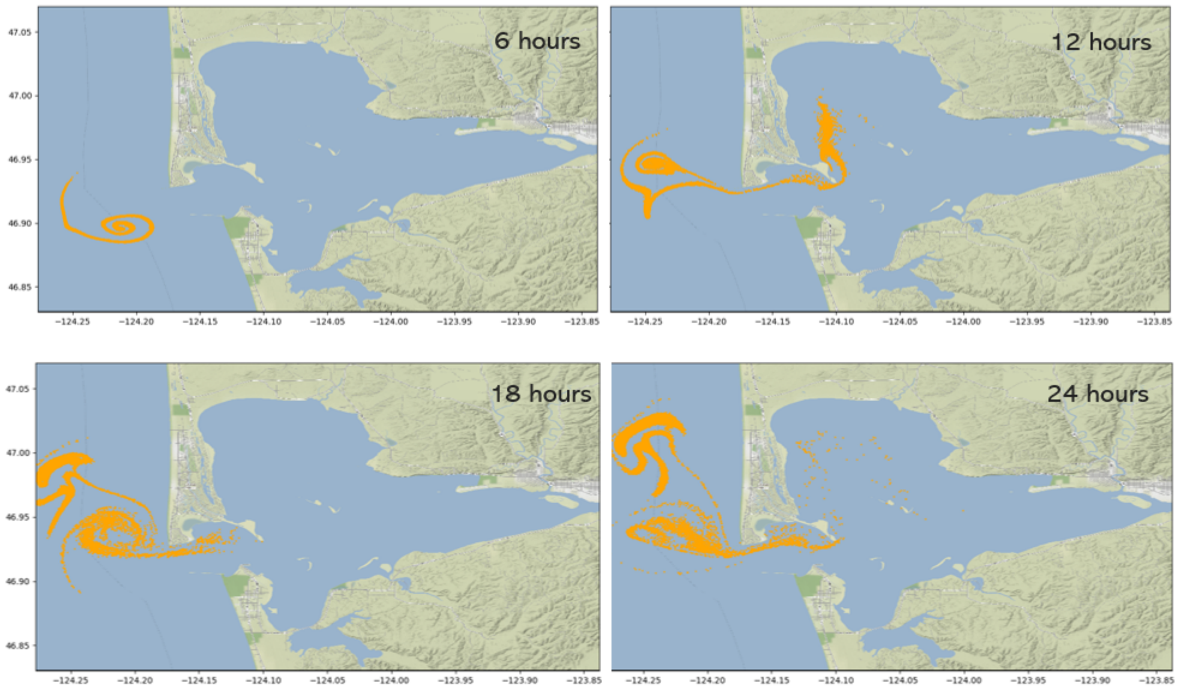

Figure 71: Disposal Site Impact, Particle Tracking Model, Summer Ebb Tide

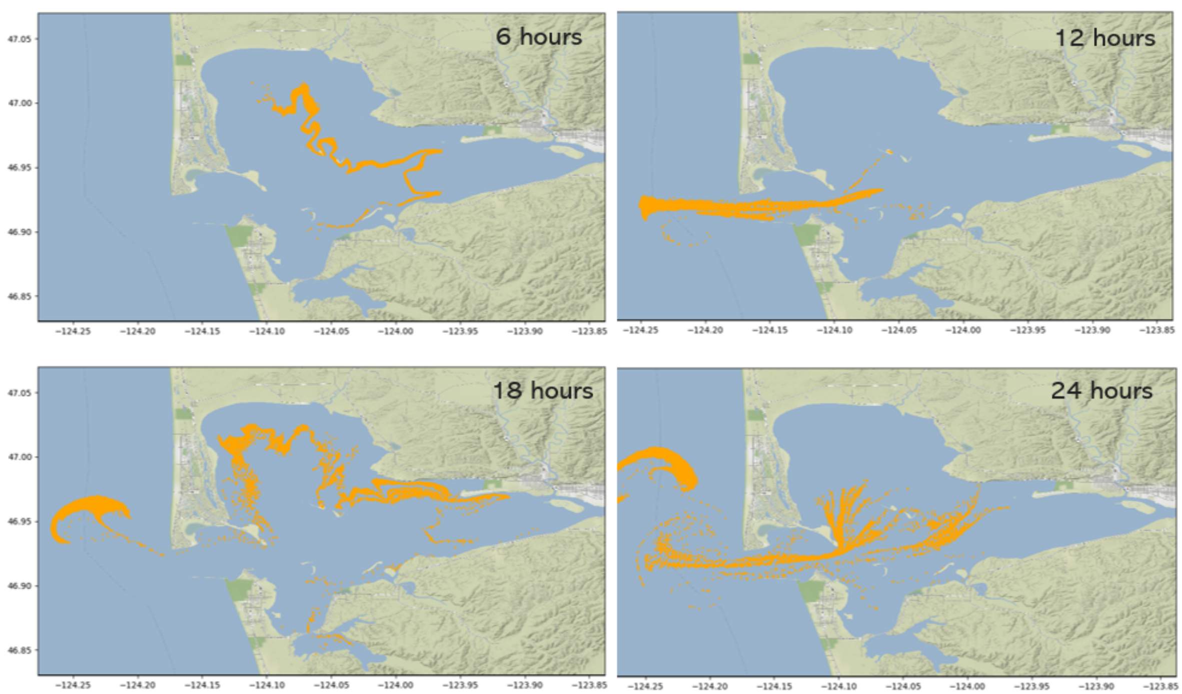

Figure 72: Disposal Site Impact, Particle Tracking Model, Summer Flood Tide

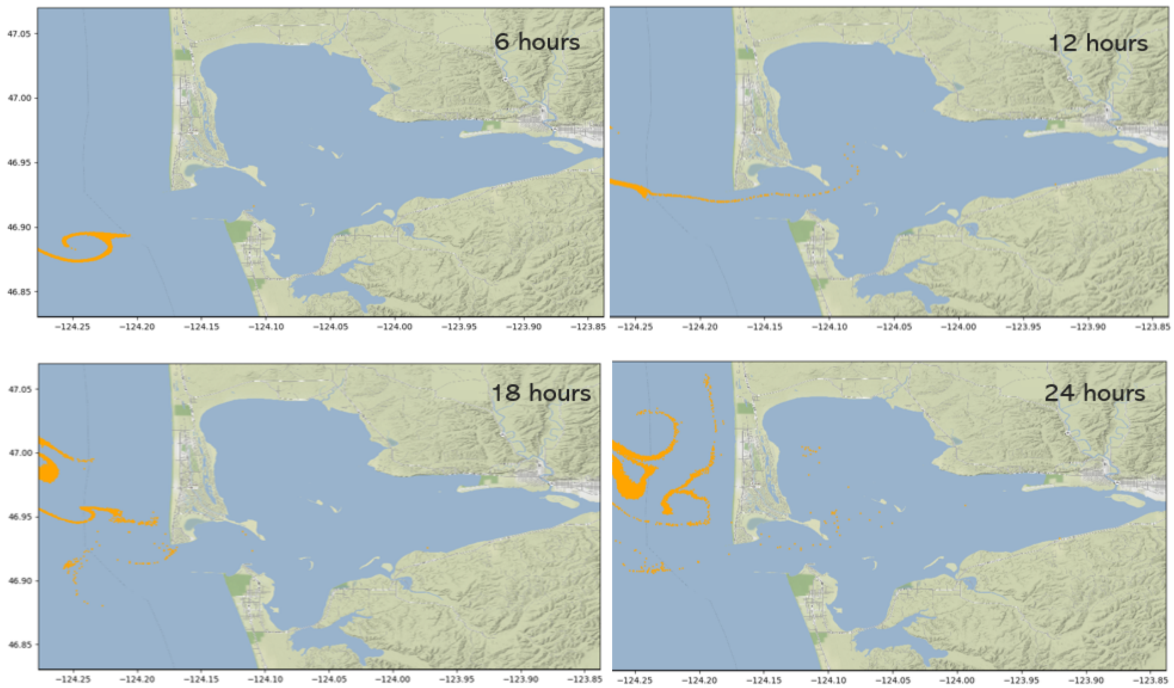

Figure 73: Disposal Site Impact, Particle Tracking Model, Winter Ebb Tide

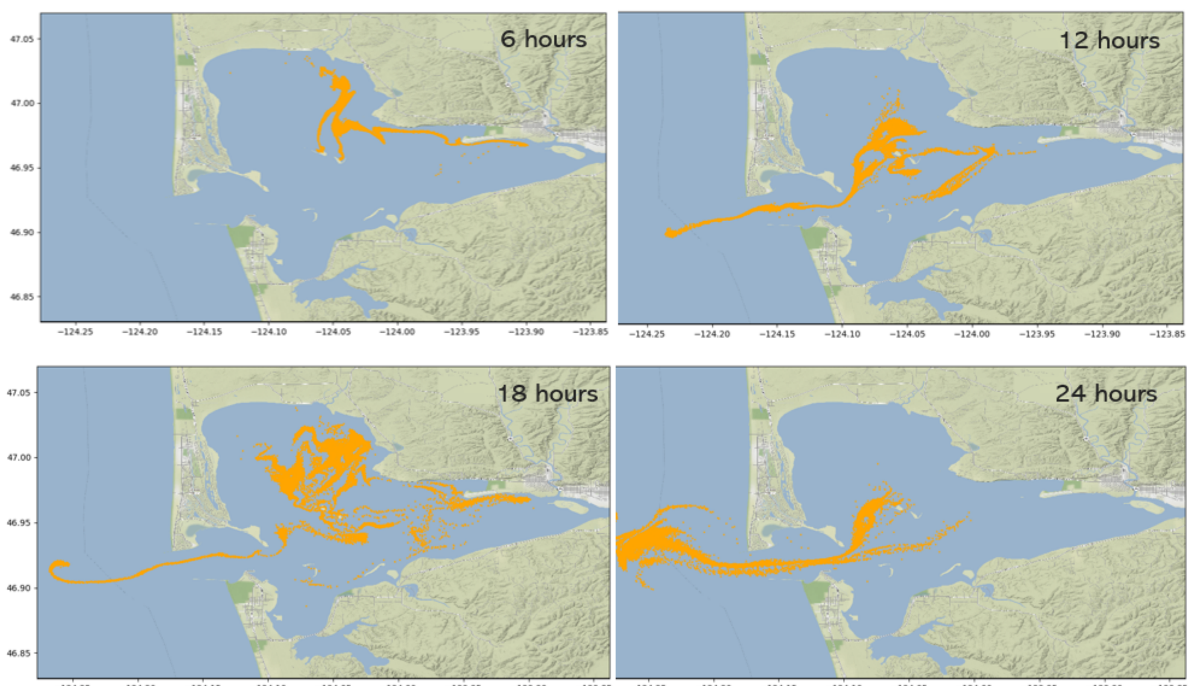

Figure 74: Disposal Site Impact, Particle Tracking Model, Winter Flood Tide

6.2.2 Sediment Transport Model

The sediment fate associated with sediment release and resuspension at the disposal site is a complex process, which requires a detailed understanding of the sequence of the dredging and disposal activities. This is beyond the level of precision of this study. Here, an idealized mass of sediment representing all disposed sediments were initialized at the disposal site, then the hydrodynamics take their course to resuspend and transport the sediment elsewhere. This modeling framework is different from the above particle tracking model, but the final fate of the sediments should be very similar since they are initialized at the same location and transported by the same hydrodynamics.

According to USACE 2018, the annual average dredging volume is 1,885,100 yd^3 with a volume fraction of 0.4, which is consisted of 58 percent of mud and 42 percent of sand. The disposed sediments were initialized at the Chehalis disposal site with a Gaussian shape; see Figure 75. This also is similar to the sediment disposal mound simulated in USACE 2018.

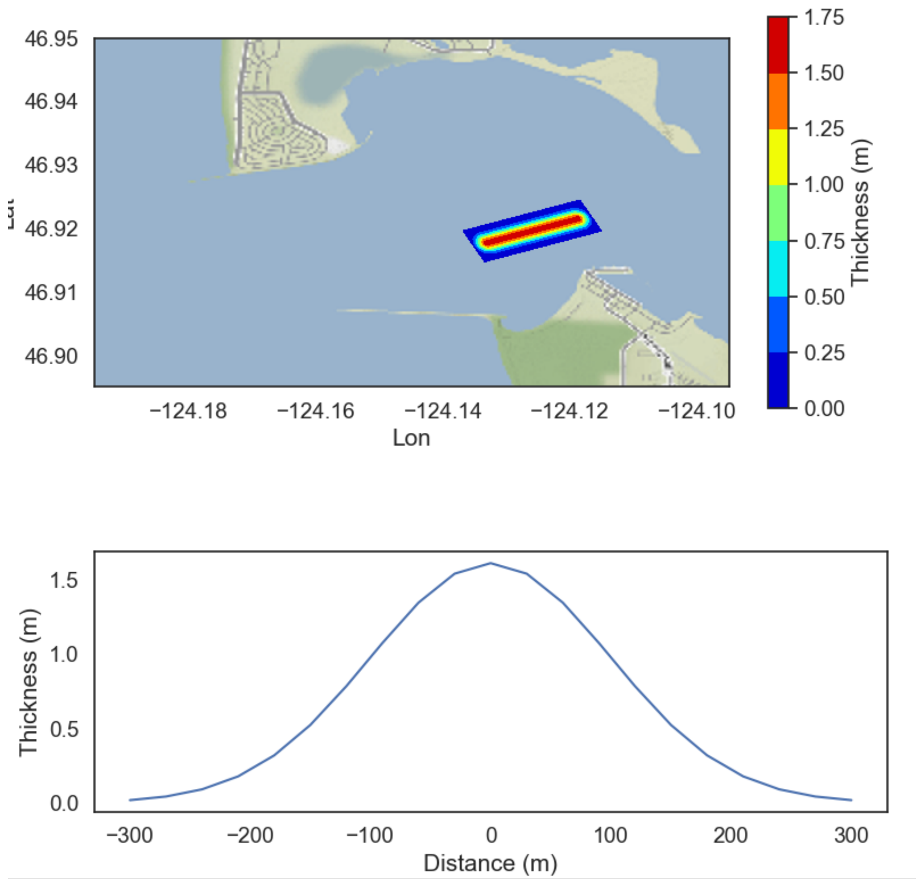

Figure 75: Initial Disposal Site Configuration for Model

The sediment disposal mound at the Chehalis disposal site was incorporated into the model, which are resuspended and transported by the modeled hydrodynamics. The fate of the resuspended sediments as illustrated by the deposition pattern is predicted by the model for both calm summer conditions and active winter conditions. The resuspension and transport processes are similar during both summer and winter conditions due to strong hydrodynamics in the inlet (where the Chehalis disposal site is located), with high velocity and shear stress. The transport process also is mainly controlled by tidally driven flow rather than wind and waves; therefore, the predicted deposition patterns are similar for both summer and winter conditions. Here, only the results for winter conditions are presented in Figure 76. It should be noted that the bed elevation change is shown in millimeters and the scale for erosion (blue) and deposition (red) is different to highlight the deposition over tidal flats.

Figure 76 shows that the largest deposition occurs in the channel just outside of the inlet and farther offshore. A considerable amount of sediment is deposited back into the navigational channel at the Crossover Reach/North Channel transition. The resuspended sediments also find their way to the northern and southern portions of the harbor, with a deposition on the order of millimeters, similar to the naturally occurring range from the InSAR data. The process is likely to be accumulative from year to year with the ongoing dredging/ disposal activities.

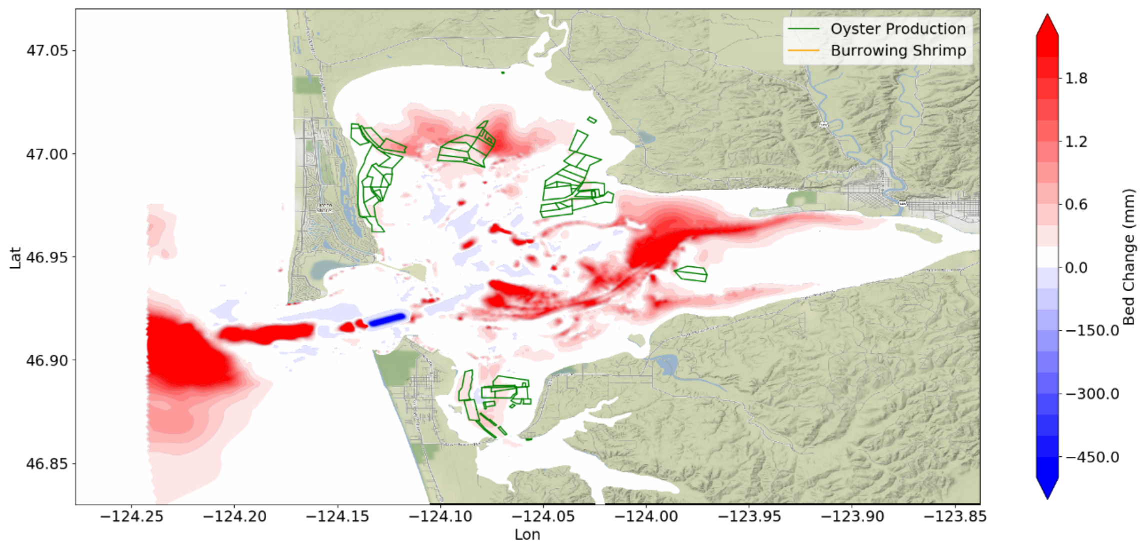

Figure 76: The Fate of Resuspended Sediments at the Chehalis Disposal Site During Active Winter Conditions

6.2.3 Alternative Location

The residual current analysis, presented in Section 4.2.2, suggest two circulation zones just outside the inlet, which offer choices for alternative disposal sites to limit sediment transport back into the harbor. The objective of this analysis is to evaluate the possibility for an alternative sediment disposal site to minimize movement of sediments back into the harbor. It should be noted that other considerations for disposal site selection, such as economy, navigation hazards for dredge vessels, etc., are beyond the scope of this work and are not addressed.

Here, the dredged sediments are assumed to be disposed near the circulation zone outside the inlet to the north as an alternative. This alternative disposal site has a shape of a circle, with diameter of 550 m to match the surface area of the Chehalis disposal site. The disposal mound profile is assumed to be Gaussian in shape. The sediment disposal mound of this alternative option was incorporated into the model, which is then resuspended and transported by the hydrodynamics. The same hydrodynamic conditions used for the Chehalis disposal site analysis were used, and the fate of the resuspended sediments are illustrated by the deposition patterns shown in Figure 77. Similar to the results presented in Figure 76 for the Chehalis disposal site, the bed elevation change is shown in millimeters and the scale for erosion (blue) and deposition (red) is different to highlight the deposition over tidal flats. The scale for deposition (0 to 1 mm) is twice as small for this alternative option as that for the Chehalis disposal site.

The offshore erosion area (blue) in Figure 77 indicates the location of the alternative disposal site, which also is highlighted by a circle. As indicated by the deposition areas (red), only a small portion of sediments find their way along the sediment path from the North Jetty to Damon Point and settle there. A smaller amount of sediments is deposited farther into the northern portion of the harbor over the tidal flats, and the deposition depth is an order of magnitude smaller than the scenario with the Chehalis disposal site. Further, almost no sediment makes its way back into the navigational channel compared to Figure 76 for the Chehalis disposal site.

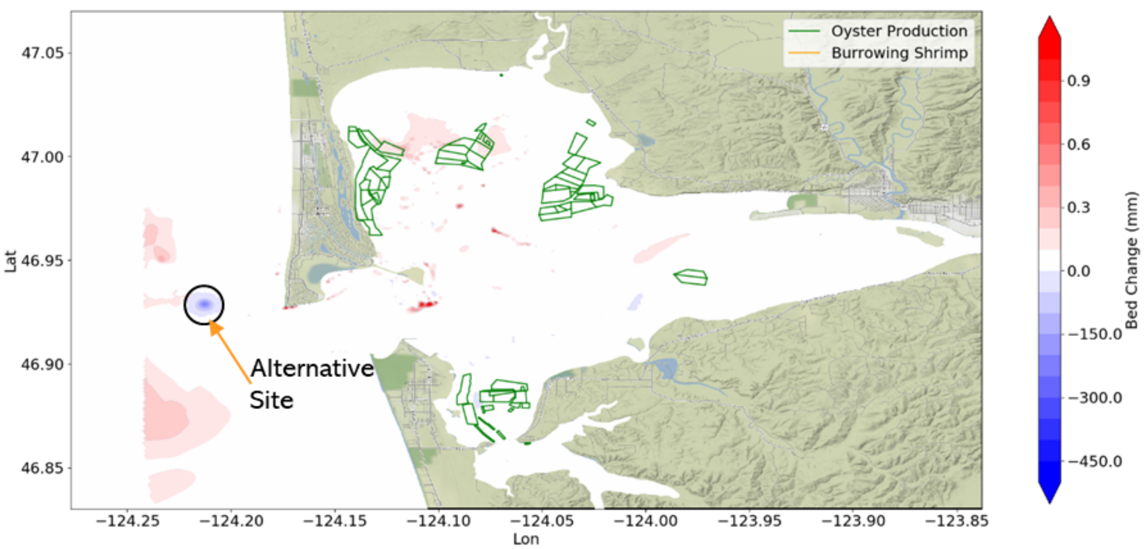

Figure 77: The Fate of Resuspended Sediments if Disposed Further Offshore During 'Winter' Condition

7.0 MITIGATION MEASUREMENT

7.1 OVERVIEW

Strong wave activity and excessive erosion/sedimentation within the Twin Harbors can be mitigated via innovative structures that have minimal environmental impact. For example, the reef cubes by ARC Marine ("Reef Cubes – The Building Block of The Ocean" 2020) can be used. ARC Marine reef cubes are made with an eco-friendly concrete mixture with no plastic fibers or Portland cement, and the mix is carbon neutral at the point of manufacture. The manufacturer also uses local, sustainably sourced sand and aggregate as the primary ingredients of the unique mix. The objectives of using environmentally friendly structures for the mitigation measures are to attenuate waves and create a calmer environment over the cultivated aquaculture beds (discussed in Section 7.2), particularly during winter storms, to reduce rapid morphological variations regarding both erosion and sedimentation (presented in Section 7.3), and to enhance the ecosystem (discussed in Section 8.0).

Although many alternatives exist and achieve the same objective, the mitigation evaluation in this study is based on the dimensions of the ARC Marine reef modules. The ARC Marine reef cubes have a height of 0.63 m and volume of 0.25 m^3, with circular hollows on each side. Two reef cubes are placed at the sea floor as the bottom layer and one on top along the transects as shown in Figure 78; therefore, it has variable height along the placement alignment depending on local bathymetry. For Grays Harbor, two scenarios (alignments) are considered for the locations of the reef cubes, which are shown in Figure 79. In the offshore scenario, reef cubes are placed near the inlet away from the oyster farms and the shoreline. Alternatively, in the nearshore scenario, reef cubes alignments are closer to the oyster farms and the shoreline. Also illustrated in Figure 79, only three representative areas are considered as examples for Willapa Bay as the oyster production farms are on either side of the predominant fetch directions during winter storms. In addition, the alignments of the reef cubes follow certain contours, with gaps to avoid the channels, in order to maintain flushing of the system.

The reef cubes are incorporated in the hydrodynamic, wave, and sediment transport model described in Section 5.0. In the hydrodynamic and sediment transport module, the reef cubes are implemented as fixed weirs in Delft3D-FM. This is an approximation, as it does not consider the porosity of the reef cubes; however, the openings will eventually be obstructed and block any flow. For the wave modeling, the reef cubes are included by assigning transmission coefficients along the alignment to reduce wave energy. The transmission coefficient of reef cubes is related to their heights and the local bathymetry and are estimated based on the studies of wave attenuation by artificial reefs by d'Angremond et al. (1996), Armono and Hall (2003), and Bleck (2006). The transmission coefficient has a value of 0.40, 0.45, and 0.65 for depths of 1.26 m, 1.5 m, and 2.0 m, respectively. The transmission coefficients for other depths are interpolated accordingly. The reef cubes in the offshore scenario have been modeled in deeper water, which results in larger transmission coefficients compared to those in the nearshore scenario. Simulations were performed using the 2018 condition with and without the reef cubes, and the wave height field and morphological change patterns are compared to evaluate the performance of the implemented mitigation measures.

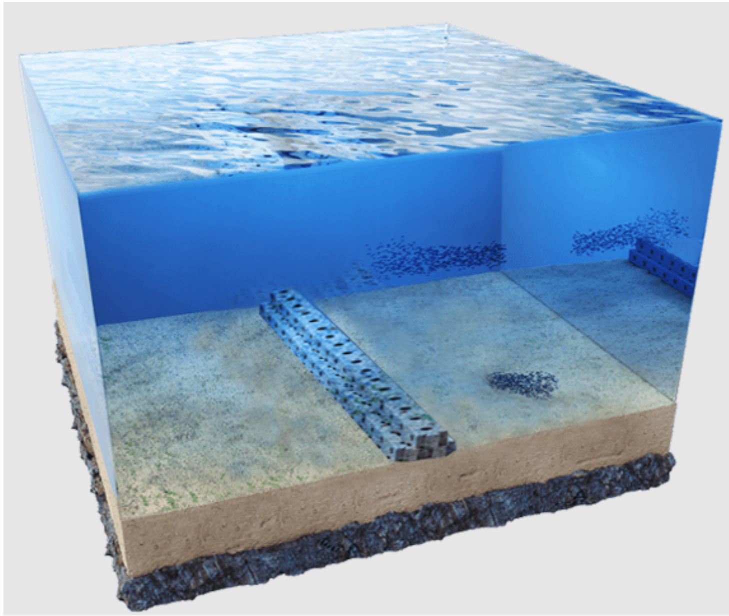

Not to scale.
Modified from “Reef Cubes – The Building Blocks of The Ocean” by ARC Marine 2020 (https://arcmarine.co.uk/reef-cubes/)

Figure 78: Illustration of the Two-layer Reef Cubes

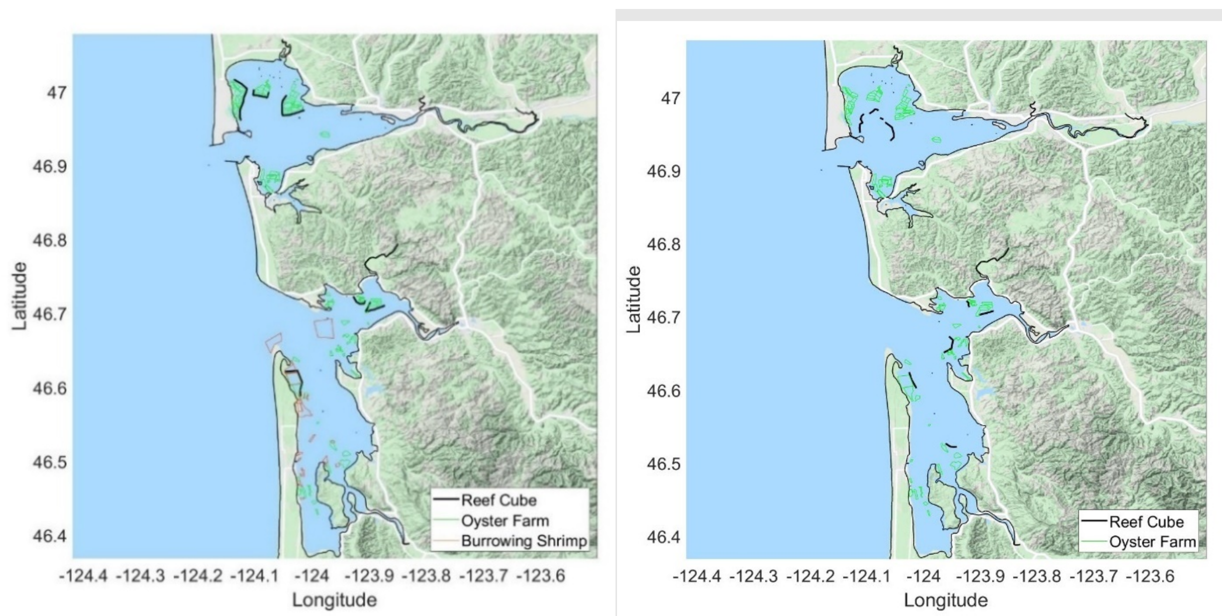

Figure 79: The Locations of Reef Cubes and Oyster Farms for Nearshore Scenario (Left) and Offshore Scenario (Right)

7.2 WAVE ATTENUATION

The percentage wave attenuation was evaluated for typical winter conditions with northerly directed winds. The reduction in wave height (Hs) is divided by the wave height without reef cubes to get the percentage wave attenuation, shown in Figure 80 and Figure 81 for nearshore reef cubes in Willapa Bay, and offshore and nearshore reef cubes in Grays Harbor, respectively.

For the reef cube alignment in Willapa Bay, reef cubes could reduce up to 50 percent of wave height near the structures, creating a relatively sheltered area for aquaculture against strong wave energy with diminishing effect towards the shoreline. For Grays Harbor, the offshore placement of reef cubes attenuate waves up to 35 percent near the structures, which reduces quickly moving landward of the structures. The nearshore placement of reef cubes provides larger wave attenuation with a maximum percentage wave reduction of 50 percent near the structure. Wave heights over the tidal flats toward the northern portion of the harbor are also reduced by 10 to 20 percent. In summary, the reef cubes are very effective for wave attenuation.

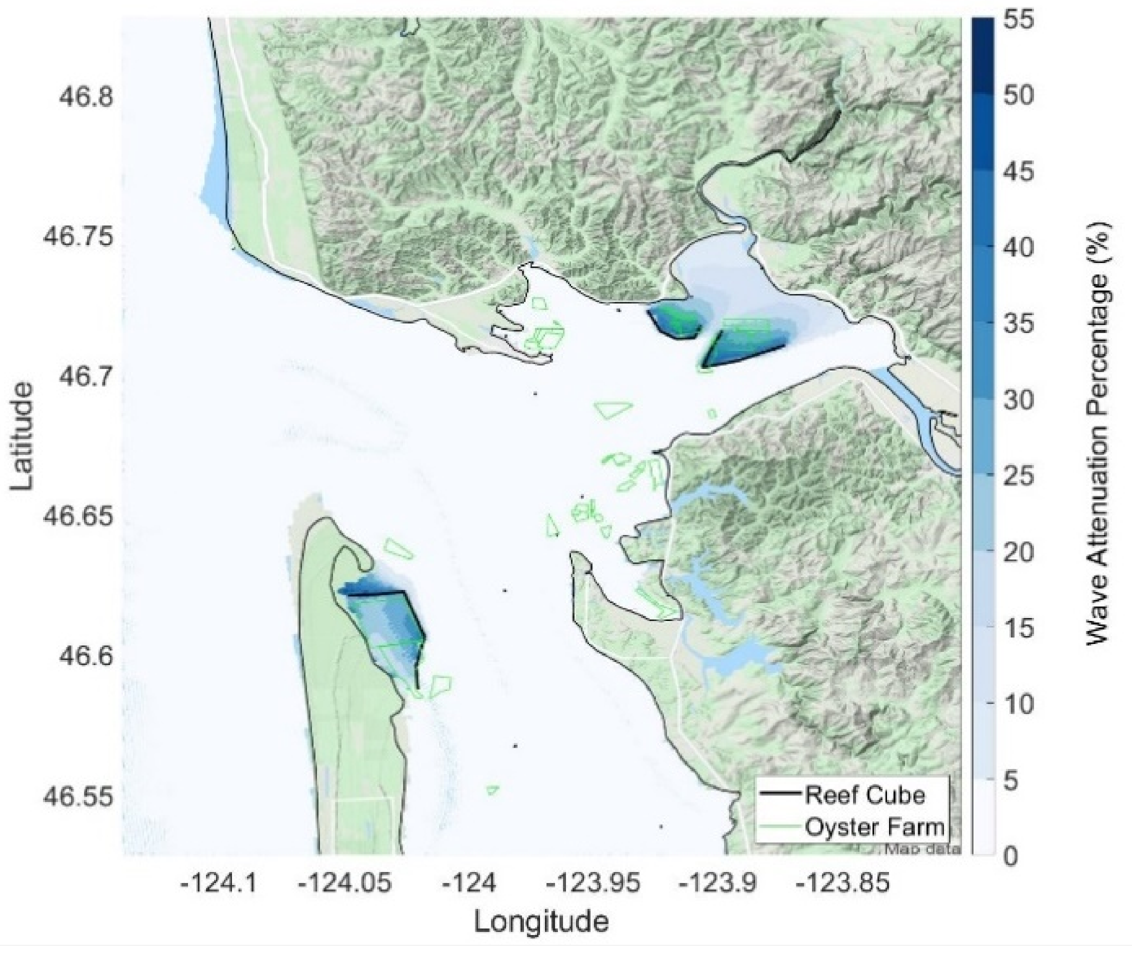

Figure 80: Percentage Wave Attenuation by Reef Cubes in Willapa Bay

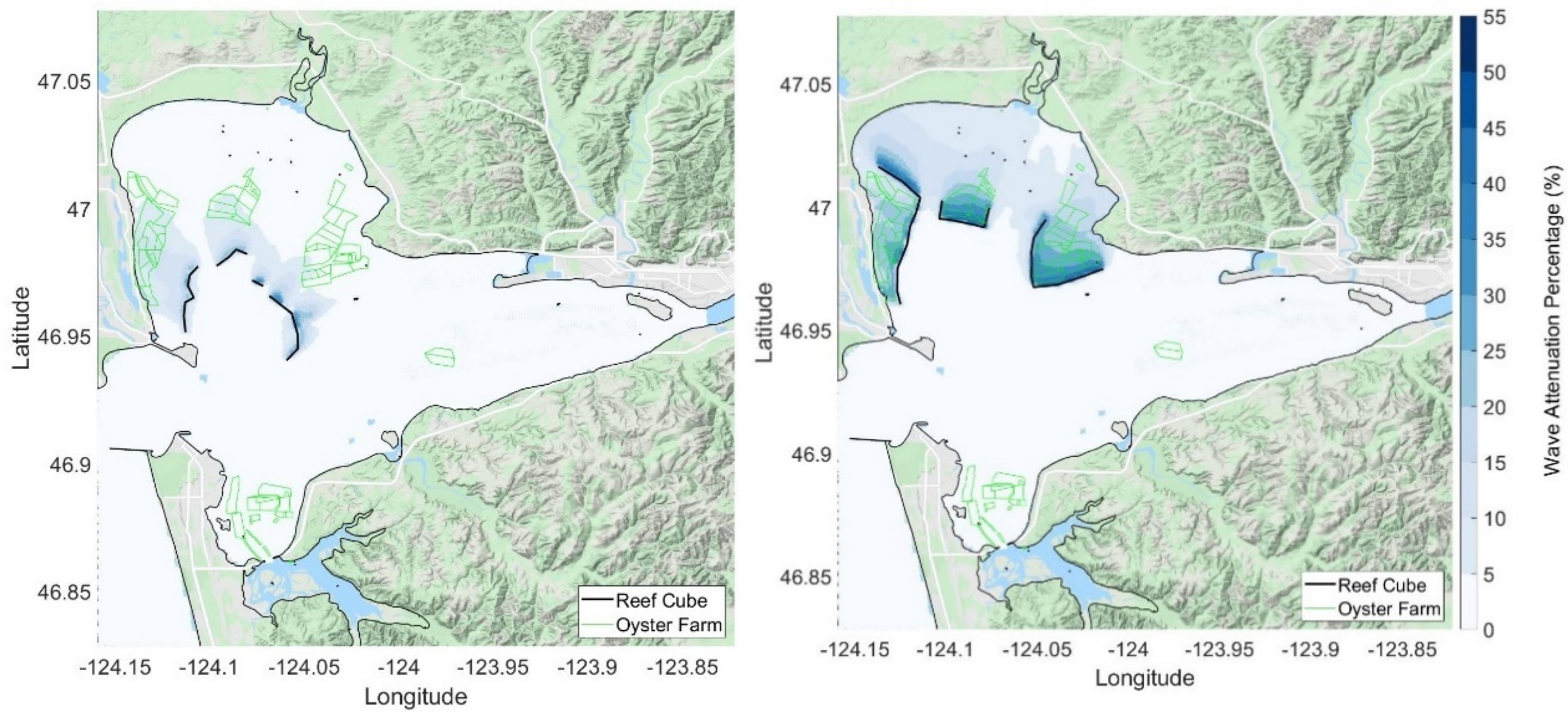

Figure 81: Percentage Wave Attenuation by Offshore Reef Cubes (Left) and Nearshore Reef Cubes (Right) in Grays Harbor

7.3 MORPHOLOGICAL CHANGE IMPACT

The performance of mitigation measures in reducing morphological change also was evaluated, which are measured by the percentage change of the absolute morphological response. The percentage change of the absolute morphological response is calculated by dividing the difference between the absolute bed change (sedimentation or erosion) with and without the reef cubes to the absolute bed changes under the existing condition. A positive value means an increase in the morphological response (i.e., more sedimentation or erosion compared to the existing condition), while a negative value means a decrease in the morphological response (i.e., less sedimentation or erosion compared to the existing condition, which is the objective of the mitigation measures).

Figure 82 shows the percentage change in morphological response by reef cubes in Willapa Bay. The change of the morphological response due to the mitigation measures is complicated. The reef cubes reduce the morphological response behind the structures in general, but at the expense of increased morphological response near and between the structures where flows are constrained. Even behind the structures, increased morphological response is observed for certain areas due to channel crossings of the reef cube alignment that can transport sediments over the tidal flats behind the structures.

Figure 83 shows the percentage change in morphological response by both offshore and nearshore reef cubes in Grays Harbor. The placement of reef cubes offshore close to the inlet in general marginally reduce the morphological response (by roughly 10 percent) for the northern portion of the tidal flats with an increase in the morphological response in between those structures (often in places where channels exist). Alternatively, reef cubes placed at the outer edge of the oyster production farms in the nearshore placement option reduces the morphological response behind the structures by 20 percent to 40 percent, except where the channels cut through the structures. In those areas, drastic increases in morphological response with the reef cubes are observed. This influences a portion of the aquaculture farms adjacent to the channels. However, most of the areas are benefiting from the reef cubes beyond the biological benefits discussed in Section 8.0.

For both Grays Harbor and Willapa Bay, attempts have been made to increase the structure height to a uniform level, which seems to counter react to increase the sedimentation behind the structure since relatively high structures with consistent crest elevation tend to hold sediments back behind the structure. In addition, options with the alignments broken into overlapping segments with gaps in between (i.e., fish gaps) were explored with the objective to enhance the flushing of the semi-enclosed areas by the structures. There seems to be an increased morphological response at the gaps due to increased flow velocity. Further exploration would be required to refine the alignment, opening width, and overlapping distance to achieve the ideal setup, which is beyond the effort at the conceptual level of this study.

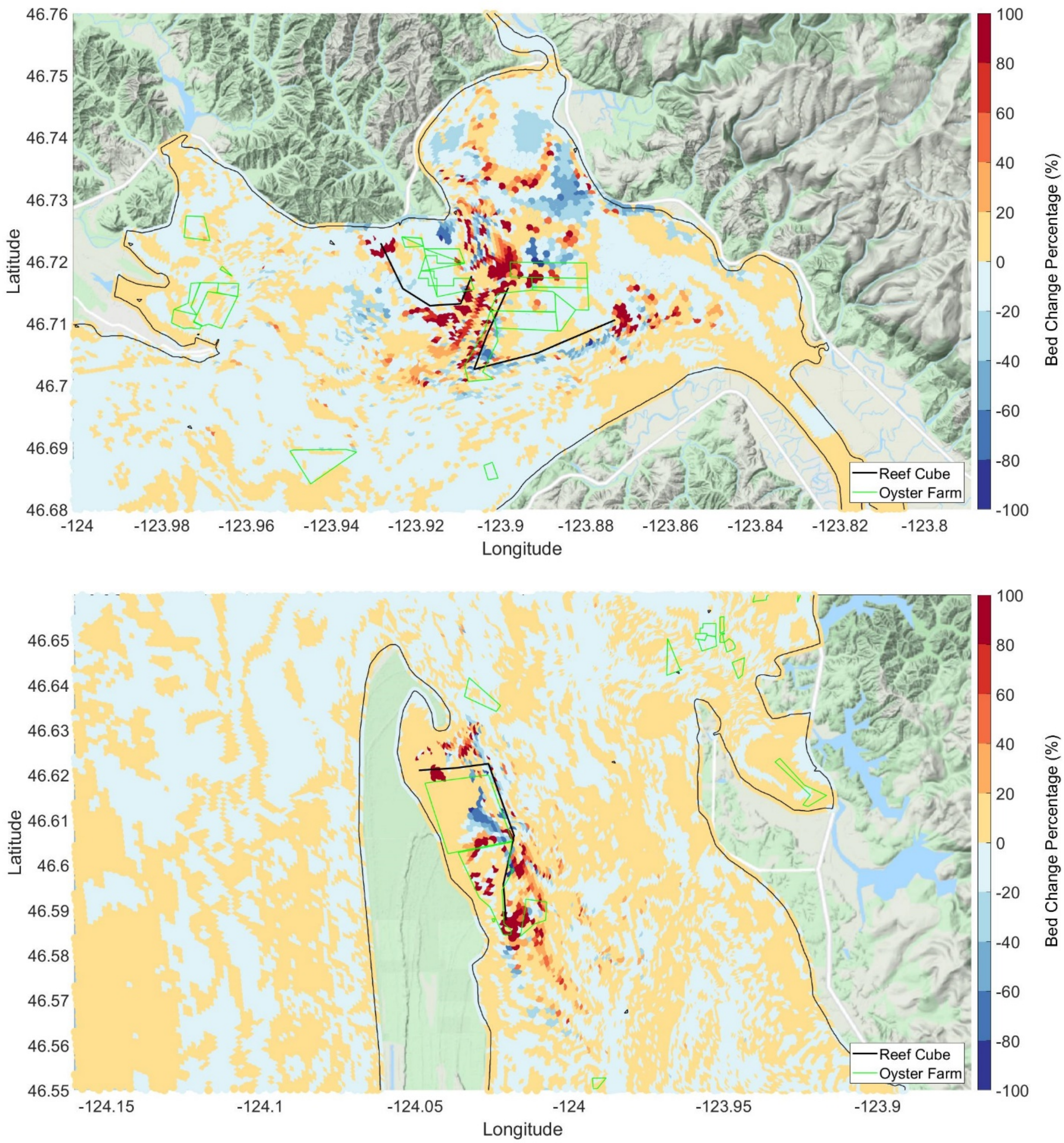

Figure 82: Percentage Sedimentation Reduction by Reef Cubes in Northern Portion (Top) and Western Portion (Bottom) of Willapa Bay

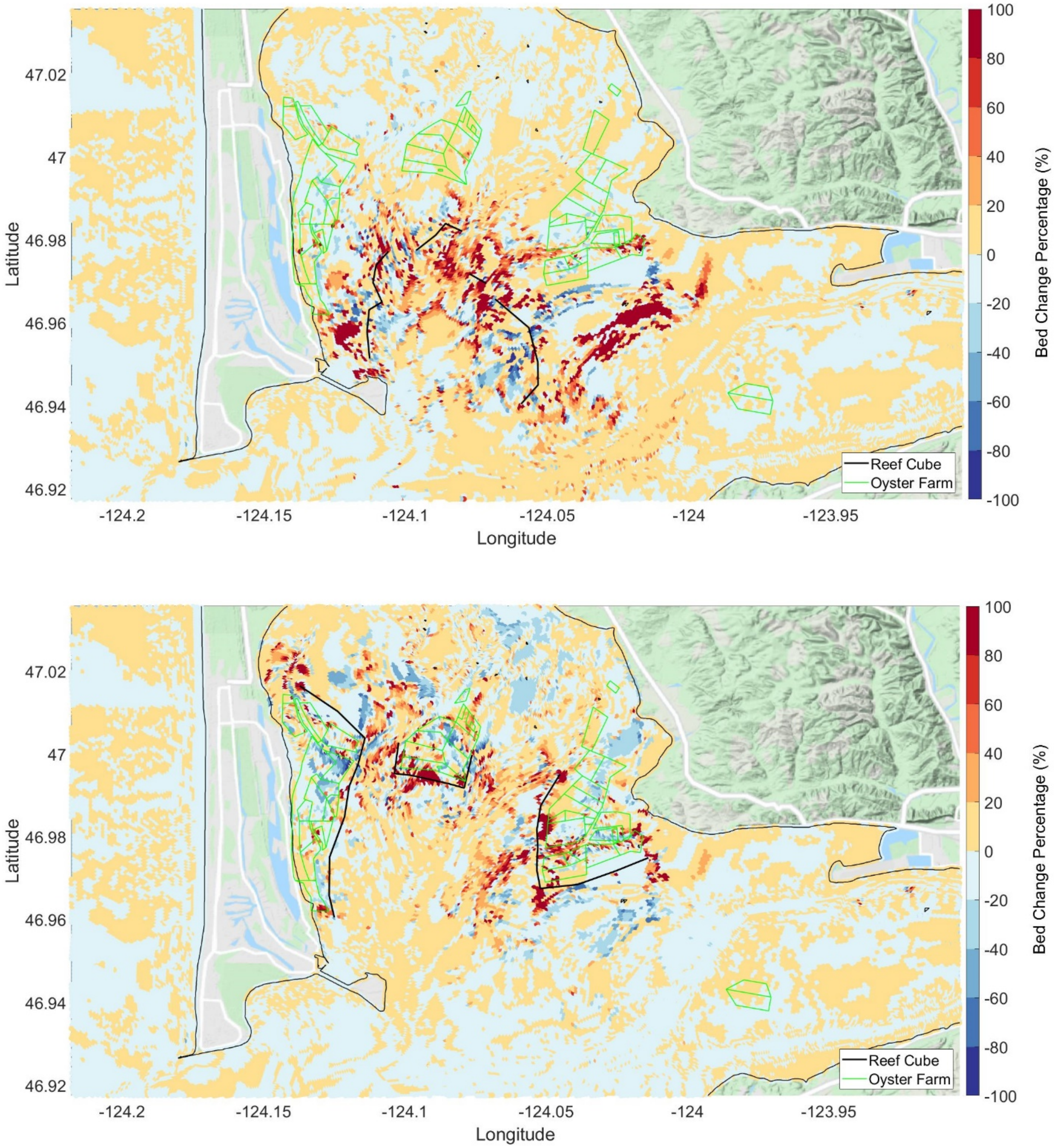

Figure 83: Percentage Sedimentation Reduction by Offshore (Top) and Nearshore (Bottom) Reef Cubes in Grays Harbor

In summary, the morphological responses with the mitigation measures using reef cubes or other alternative structures are complicated, particularly due to the complex channel system in the Twin Harbors. On one hand, the natural channel system serves the purpose of flushing the system and providing necessary nutrients for aquaculture; however, sediments can pass through the channel reaching the tidal flats behind the structures. The recommended approach is to create terrain-conformed structures with variable crest elevation following the existing topography (i.e., a ‘speed bump’) rather than a blockage/barrier for the sediment movement. Although the morphological responses are likely increased where a channel crosses the structures, the mitigation measures work very well for wave attenuation and serve to reduce the morphological changes within the oyster production farms in general. The ecological benefits of the reef cubes are discussed in Section 8.0.

8.0 BIOLOGICAL EVALUATION

8.1 ECOLOGICAL REVIEW OF MODEL RESULTS

8.1.1 Results of Morphodynamic Modeling with WebApp Data

Results of the morphodynamic model reveal each bay shows similar patterns of erosion and deposition on tidal flats, but the location of the effect, and the ramifications on the areas of oyster production, differ within each bay (Figures 84 and 85). Using the webapp data collected, areas of oyster production were plotted along with current areas of burrowing shrimp activity over the 10-year average annual morphological changes for the tidal flats (areas with depth greater than 1.5 m are not shown). Average annual morphological changes for the entirety of each bay are shown in Figures 61 and 64. In general, north-directed winter storm winds and waves cause erosion in the tidal flats that is deposited closer to the shores. Greater erosion also is seen along the edges of the subtidal secondary channels, with heavier deposition accumulating within those subtidal channels, suggesting sediment from the tidal flats is being pulled out on the ebb tide. Compounding sediment movement are increased suspended sediment loads entering the bays from river sources resulting from the winter rain storms that are conveyed via the navigation channel into secondary channels, and potentially out onto the tidal flats and over areas of oyster production.

In Grays Harbor, most of the indicated areas of oyster production are in or near erosion areas in the North Bay region, with losses of 2-4 cm per year on average (Figure 84). In addition, each of these areas coincide with areas of burrowing shrimp activity. Willapa Bay shows the similar patterns on the tidal flats, but mostly in the north end and eastern areas towards the river mouth (Figure 85). The southern portion of the bay is more protected, but erosion appears prevalent along the edges of the subtidal channels, with subsequent heavier deposition in the channels and at the various river mouths. Deposition also shows up along the shorelines at variable rates. Areas of oyster production are found in both erosional and depositional areas. Burrowing shrimp activity appears to be more prevalent in the southern half of the bay, particularly along the western side. Burrowing shrimp are often next to areas of oyster production or in former oyster areas that have been lost to the burrowing shrimp population. Many of the burrowing shrimp areas also contain portions of modeled erosion, with adjacent depositional areas found in a landward direction (Figure 85).

Burrowing shrimp contribute to the increased erosion by destabilizing sediments as they create their burrows and sort through the sediment for food particles. This process removes the binding particles of silt, clay, and organic material from the excavated sand and expels it to the surface (see Section 8.2 for additional discussion). Wind, waves, and storm surges cause erosion and mass transport of this sediment around the bay, suspending it in the water column and depositing it on oyster beds and tidal flats in adjacent areas. The increased sediment mobilization and deposition can have a pronounced effect on oysters and other fauna living on the tidal flats in the bays.

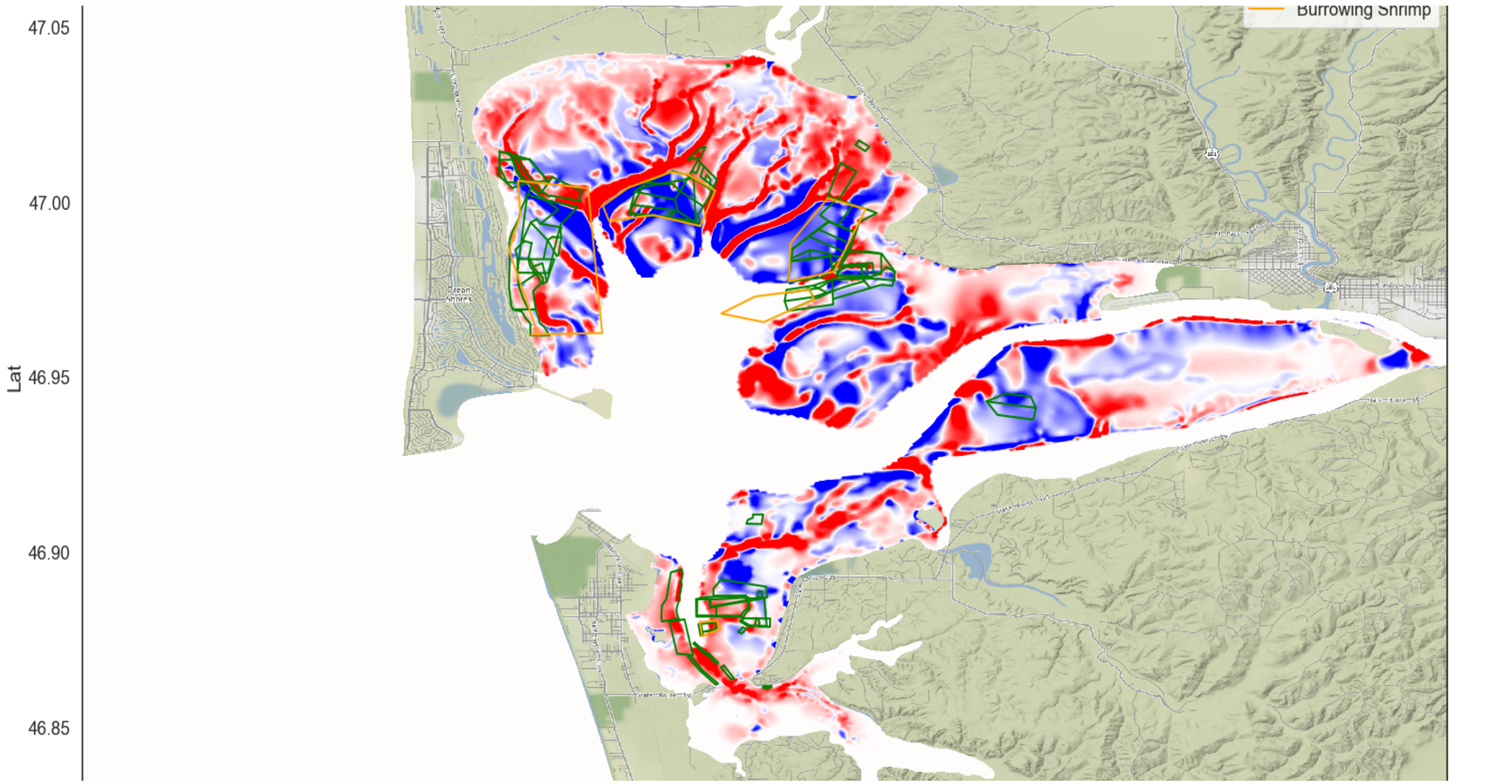

Figure 84: 10-year Average Annual Morphological Changes in Tidal Flat Areas (< 1.5 m Depth) in Grays Harbor in Association with Oyster Production Areas and Burrowing Shrimp Areas from Stakeholder Survey Input

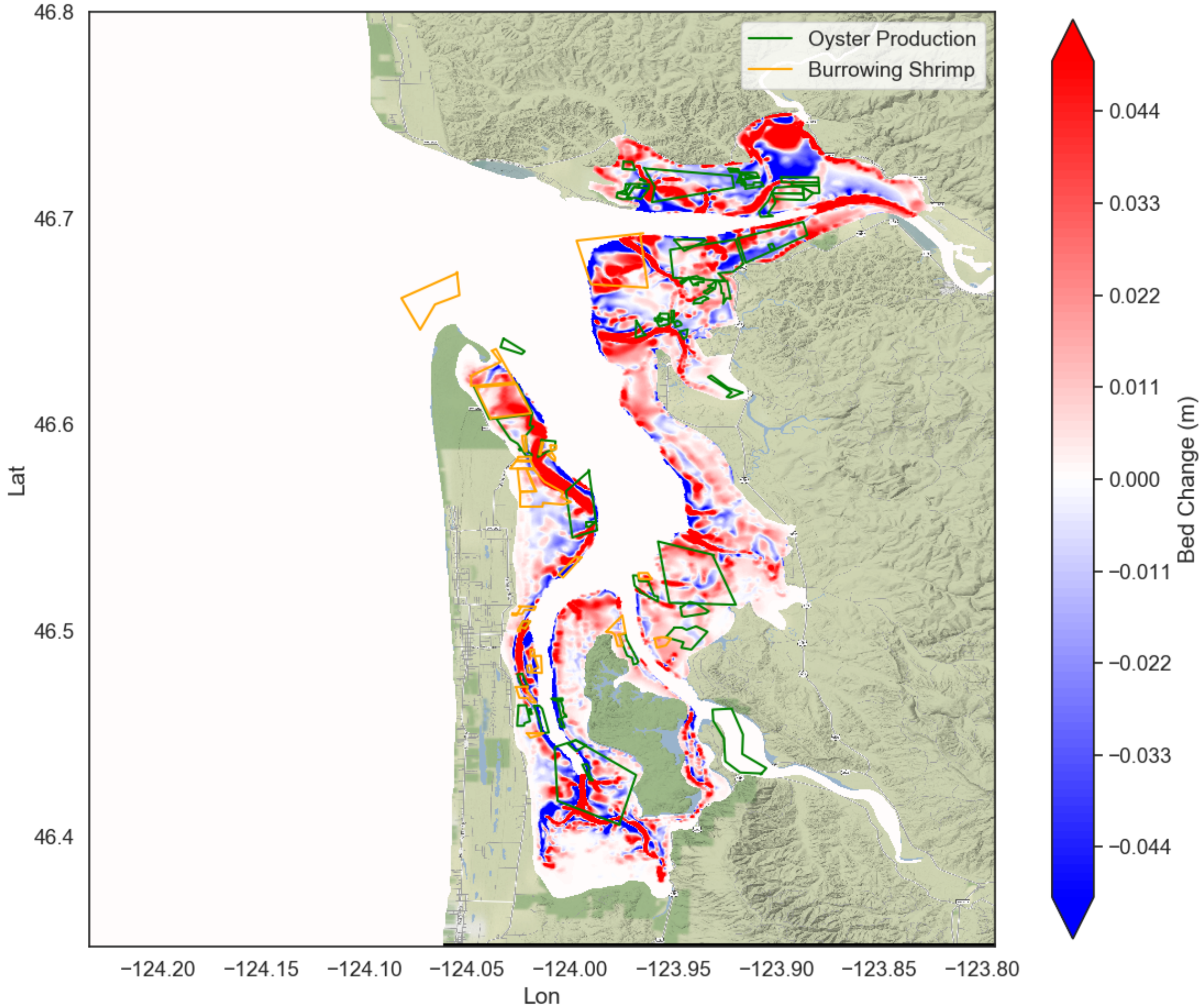

Figure 85: 10-year Average Annual Morphological Changes in Tidal Flat Areas (< 1.5 m Depth) in Willapa Bay in Association with Oyster Production Areas and Burrowing Shrimp Areas from Stakeholder Survey Input

Oysters are generally tolerant of partial burial in terms of survival, and able to tolerate anoxic conditions for days or weeks, depending on the environmental conditions (e.g., temperature, salinity) (Widdows et al. 1989; Hinchey et al. 2006; Comeau et al. 2017). Colden and Lipcius (2015) found that eastern oyster (*Crassostrea virginica*) survival over a 28-day experiment declined significantly when 90 percent or more of an oyster was buried. The critical depth incurring 50 percent mortality was 108 percent of the shell height, and 100 percent mortality was exhibited at a 130 percent burial depth. Other studies on eastern oysters noted that mortality occurs quite rapidly following major (≥25 mm) siltation events (Rose 1973; Kranz 1974; Essink 1999; Comeau et al. 2014). Given these burial limits, the movement of 2-4 cm of fine sediments over oysters with a shell height of 36 mm or less would result in their death.

Even if the oysters are briefly covered, burial can adversely affect their growth and condition. Hinchey et al. (2006) buried juvenile eastern oysters with 2-5 mm of sediment for 6 days. While there was no mortality, no buried oysters produced fecal pellets (biodeposition), and 70 percent showed black discoloring around the shell edges. Colden and Lipcius (2015) noticed a similar lack of biodeposition in oysters buried over 90 percent. Additionally, oysters showed a declining condition index with increasing burial depth, suggesting the deterioration of tissue due to metabolic stress and sustained anaerobic conditions, or to the investment of energy into shell growth when access to food and oxygen are limited by burial (Colden and Lipcius 2015). Oysters buried in muddy habitats often develop an elongated shape, in the attempt to reach the sediment surface to feed and respire; the likely limit to this increased growth is burial that induces mass mortality (Colden and Lipcius 2015).

8.1.2 Results of the Dredge Disposal Modeling

The modeling for dredge disposal in Grays Harbor examined the impacts to sedimentation in three different aspects: impacts of the dredging in the navigation channel, a particle tracking model to show the pathways of suspended sediments coming from the Chehalis disposal site over a 24-hour cycle, and sediment transport model to show the fate of the suspended sediments coming from both the Chehalis disposal site and an alternative offshore disposal location.

For dredge activity, the model evaluated both the clamshell and hopper dredges. Results show that sedimentation from dredging is largely in confined to the navigation channel itself. A maximum bed change increase of 3 cm was indicated in the Crossover Reach channel, with adjacent tidal flats accumulating an estimate of less than 5 mm of sediment. The model shows that a clamshell dredge distributes sediment mostly to the eastern portion of the harbor in the areas adjacent to the navigation channel, whereas the hopper dredge activity distributes sediment mostly within the navigation channel (Figures 68 and 70). There are few oyster production areas in the area of effect from the model results; therefore, dredging activities in the navigation channel do not appear to have a significant negative impact on the aquaculture resources within Grays Harbor. However, frequent dredging operations over a short period of time could potentially compound in the tidal flats of the harbor. Accumulating sediment would be subject to redistribution from wind, wave, and storm surges; would be deposited along shorelines; eroded back into the channel; and possibly redistributed to the northern and southern areas of the bay.

The particle tracking model examines the pathways of suspended sediment particles for ebb and flood tides in both summer and winter (Figures 71 through 74). In general, sediment disposals released at the Chehalis site during an ebb tide shows most of the sediment particle leaving the bay and heading out into the Pacific Ocean and returning to the inlet entrance/disposal area locale with the rising tide cycle. Releases during the summer ebb tide show greater movement of particles into the bay along the North Jetty and Damon Point.

In contrast, disposals released during the flood tide shows increased sediment particle movement into the northeast and eastern portions of the harbor, exiting out to the inlet and South Reach of the navigation channel on the receding tide, and then reentering the harbor and spreading throughout the northern and eastern bays. The majority of the resuspended sediment particles never leave the harbor. This modeled effect is seen in both the summer and winter scenarios. The particle tracking model shows that the transport of the resuspended sediments at the disposal site is controlled mainly by tide rather than strong wind/wave conditions. Dredge sediment disposed during the flood tide introduces an increased chance of being distributed across the tidal flats and oyster production areas in the northern part of the bay; releasing on the ebb tide, preferably in the winter, poses the least risk to sedimentation on aquaculture resources within Grays Harbor.

Results of the sediment transport model shows the greatest deposition of resuspended dredge sediment (2 mm or more) in the main channel outside of the bay entrance and offshore, as well as back into the navigation channel at the Crossover Reach/North Channel transition (Figure 76). Deposition within the northern portion of the bay generally ranges from 0.5-1.0 mm, settling in the tidal flats along the northern shoreline. Several of the northernmost oyster production areas in that part of the bay also would receive close to 1 mm of sediment. The southern extent of the bay is estimated to receive less than 0.5 mm. This sedimentation would accumulate over time with each dredging event. When compounded with burrowing shrimp disruption, storm surges, and increased sediment from freshwater outflows, the risk of increased sedimentation and burial of oysters further increases.

The sediment transport model also shows the use of an alternative disposal site proposed outside of the harbor would effectively reduce sedimentation due to dredge sediment disposal within Grays Harbor (Figure 77). Oyster production areas in the northern portion of the harbor are estimated to accumulate a reduced 0-0.1 mm of sediment, and no accumulations in the navigation channel and much of the rest of the harbor. These modeling results of dredge disposal alternatives show that sedimentation due to dredging activities can be controlled and minimized by changes in timing and location of disposal.

8.2 ECOLOGICAL ASSESSMENT

The erosion of sediments in tidal flats can vary spatially and temporally and is dependent on the interactions between physical processes (water flow, wave energy), sediment properties, and biological processes (Widdows and Brinsley 2002). One of the biologically key components involves ‘ecosystem engineers’ (Jones et al. 1994, 1997), organisms which create, modify, destroy, or maintain a habitat in which they live or frequent. There are two functional groups of ecosystem engineers, the bio-stabilizers and the bio-destabilizers. Bio-stabilizers can influence the hydrodynamics and provide some physical protection to the bed (e.g., mussel beds/oyster reefs, macroalgae, seagrass beds, salt marsh macrophytes), or can enhance cohesiveness and alter the critical erosion threshold (e.g., microphytobenthos, diatoms). In contrast, bio-destabilizers (or bioturbators) such as burrowing shrimp increase sediment erosion/resuspension and turbidity. They also can modify surface sediments by increasing bed roughness and sediment water content or grazing on bio-stabilizers and producing fecal pellets (Paterson and Black 1999; Reise 2002; Widdows and Brinsley 2002; Bouma et al. 2005; Montserrat et al. 2008; Pillay and Branch 2011).

As ecosystem engineers, oysters stabilize the sediment and affect tidal flat morphology to protect the surrounding soft-sediment environment against erosion (Walles et al. 2015). The presence of oyster beds can alter local hydrodynamics in general, slowing water flow close to the substrate while altering surface roughness and turbulence across the top of the bed, thus, altering the patterns of movement by sediments and stabilizing sediments (Padilla 2010; Walles et al. 2015). Oyster shells also increase the biodiversity of an area, supplying new, three-dimensional habitat for many species to colonize, and increasing the total area available for settlement by a variety of species. This three-dimensional, biologically generated habitat can act as a spatial refuge for many species, providing refugia from predators and consumers and a retreat for organisms from desiccation during low tides (Padilla 2010).

Countering this as de-stabilizers are two species of burrowing shrimp, the ghost shrimp (*Neotrypaea californiensis*) and mud shrimp (*Upogebia pugettensis*). Both are members of the infraorder Thalassinidea, decapod crustaceans that live in burrows in mud and sand sediments in oceans and estuaries. Thalassinidean shrimp are recognized as among the most important ecosystem engineers in marine soft sediments, where they influence many ecological processes, including nutrient fluxes and cycling, alteration of geochemical and sediment properties, and modification of community composition across all organismal groups (Pillay and Branch 2011).

Ghost shrimp are selective deposit feeders, sorting food particles such as benthic microalgae and bacteria from the surfaces of sediment particles. They prefer sandy substrates over muddy substrates, and construct complex, deep burrows (0.75 to 1.0 meters deep) as they feed (Dumbauld et al. 1996, 2004). Their burrows are more expansive but less defined than those of mud shrimp. Excavated sediment and feces are deposited at burrow entrances, forming conspicuous mounds that gradually raise the level of the tidal flat. It is estimated that a single ghost shrimp produces 49.1 g of sediment per day (Dumbauld et al. 2004). The continual reworking and turnover of sediments by ghost shrimp removes the binding particles of silt, clay, and organic material, thus softening the sand flat and making it similar to quicksand (Bird 1982; Posey 1986). The shrimp deposit these removed binding particles with the excavated sand as unconsolidated sediment on the surface where it is subject to removal by tides and waves to be suspended in the water and elevating turbidity and is redeposited to adjacent areas (Washington Department of Ecology 2015).

In comparison, mud shrimp are filter feeders, cycling water through their burrows and removing food particles (phytoplankton, zooplankton, bacteria, and detritus) suspended in the water column (Dumbauld et al. 1996; Griffen et al. 2004; D'Andrea and DeWitt 2009). Mud shrimp prefer a muddier habitat with sediments that are less well-sorted than those inhabited by ghost shrimp, and generally more common farther from the mouths of estuaries (Bird 1982). They construct vertically oriented Y-shaped burrows to depths much shallower than ghost shrimp (>50 cm; Swinbanks and Murray 1981; D'Andrea and DeWitt 2009). In addition, the inner walls of *U. pugettensis* burrows are typically lined with mud and mucus (Swinbanks and Murray 1981), which trap and store seston in the water that is pumped through the burrow by the shrimp. Griffen et al. (2004) have shown these burrow wall linings can trap 20 to 30 percent of the total phytoplankton removed during filter feeding. The mud shrimp have been observed to occasionally feed on the trapped material. The burrow wall materials significantly increase the organic content of the sediments with this wall lining, which also are likely sites of high microbial abundances and activities, and harbor bacterial communities distinct from surface sediments (D'Andrea and DeWitt 2009). Because of the less extensive burrows, and their filter feeding behaviors, *U. pugettensis* produces only a moderate amount of sediment (4.1 g/shrimp/day; Dumbauld et al. 2004).

Both ghost shrimp and mud shrimp have been observed with dense populations (up to 400 shrimp per m^2). In Willapa Bay, Dumbauld et al. (1996) observed that the density of *N. californiensis* (up to 450 shrimp per m^2) was always higher than that of *U. pugettensis* (up to 100 shrimp per m2) populations. Mud shrimp also have declined, for several possible reasons. First, research has shown that the timing of past Carbaryl treatments in July and August coincided with the presence of the newly recruited (0+ age class) *Upogebia* juveniles along with the adult *Upogebia* and adult *Neotrypaea*. However, 0+ *Neotrypaea* recruit later in August and September were not killed, so young ghost shrimp were able to recruit back to areas just treated (Dumbauld et al. 1996). Additionally, the decline in mud shrimp populations may be due to the increasing presence of a parasitic isopod (*Orthione griffenis*) that renders female mud shrimp infertile (Dumbauld et al. 2011). Prevalence of this bopyrid isopod parasite in *U. pugettensi*s was high in populations sampled from 2005 to 2009 in Willapa Bay, Tillamook Bay, and Yaquina Bay, infecting 17 to 94 percent of these shrimp (Dumbauld et al. 2011; Chapman et al. 2012). The parasite caused an estimated average 68 percent loss of *U. pugettensis* reproduction in Yaquina Bay, Oregon, over a 5-year period. Given these reductions, and the fact that *Neotrypaea* is a much stronger bioturbator and causes much more significant damage to oyster aquaculture operations, most of the efforts on controlling burrowing shrimp is focused on the ghost shrimp populations.

Erosion in Grays Harbor and Willapa Bay is exacerbated in part by the increase of ghost shrimp and their contribution of fine sediments and decreased cohesiveness of sand-mud matrices they are burrowing through. This increase of fine sediments from ghost shrimp also has caused of the reduction of the bio-stabilizers in the ecosystem. One of the most important bio-stabilizing communities in marine sedimentary ecosystems is that of the biofilm, a complex mixture of diatoms (microalgae), bacteria, and fungi coexisting in a matrix of extracellular polymeric substances they secrete (Pillay et al. 2007; Wilson 2017, 2020, various unpublished reports). This biofilm helps to bind the top sediment layer and maintain smooth or laminar flows over the sediment. The biofilm, especially the diatom component, also serves as food sources for juvenile and adult invertebrate infauna and provide cues for the settlement of metamorphoris of invertebrate larvae (Pillay and Branch 2011; Wilson 2017, 2020). The diatom biofilm essentially serves as the first step in colonization of the tidal flats, creating a stable autotrophic base for the establishment of other flora, thus further stabilizing the sediments, and providing a food source for the invertebrate infauna to follow, which in turn build structures and add to the stability and complexity of the benthic substrates. However, actively burrowing thalassinid shrimp can reduce diatoms and bacterial layers by burial from sediment from their burrows. Diatoms thrive via photosynthesis, so burial deprives them of light, thus killing them. Additionally, because the expelled sediment is finer and more prone to erosion, diatom and bacteria components will be swept into the water column (Pillay et al. 2007; Wilson 2017, 2020).

The reduction and removal of the sediment biofilm has additional negative ramifications to sedentary surface and subsurface fauna as well. Species with limited mobility also will be buried by sediment disturbance associated with bioturbation and die. This would include tube-building and more sedentary species found in these bays, which include spionid polychaetes (e.g., *Spio, Pygiospio, Streblospio* and *Pseudopolydora*), corophiid amphipods (*Corophium acherusicum*), the tanaid *Leptochelia savignyi*, and the cumaceans *Cumella vulgaris* and *Hemileucon comes* (Dumbauld et al. 2001; Ferraro and Cole 2007; Booth et al. 2019), as well as juvenile oysters (Hinchey et al. 2006; Colden and Lipcius 2015; Comeau et al. 2017). *Corophium* is an important keystone species in the Twin Harbors, numbering 10,000 per m² (Wilson 2020). Not only are they important to stabilization and adding complexity and structure to the tidal flat sediments via their tube-building, but they serve as a vital food source to shorebird populations as well (Brennan et al. 1990; Mathot et al 2010; Wilson 2020).

This effect of sediment burial suppressing invertebrate infauna and plant cover on substrate surfaces was demonstrated by Thomsen and McGlathery (2006). They examined bricks contained in constructed cages that trapped drifting macroalgae and facilitated sedimentation (~7 mm per 2 to 3 months). Control bricks (no sedimentation) had high plant richness, high animal and plant cover, and high cover of eastern oysters (*C. virginica*). In comparison, sediment-stressed bricks had low plant richness, low animal and plant cover, and low cover of *C. virginica* (Thomsen and McGlathery 2006). Additionally, the feeding mechanisms of filter-feeders, such as oysters, may become clogged by expelled sediments (Suedel et al. 2014).

More mobile organisms will escape smothering from sediment burial but may face reduced food availability because of the scarcity of biofilm components or be subject to increased predation as they search for more suitable habitat (Posey 1986). In addition, the increased erodibility of the sorted fine sediments may cause increased drift of smaller organisms and early instars into the water column (Pillay and Branch 2011). This is an increasing threat to juvenile Dungeness crab (*Cancer magister*) in Grays Harbor and Willapa Bay. Juvenile Dungeness crab are highly dependent on epibenthic structure, with the highest densities in oyster shell refuge as a result of selective settlement of megalopae larvae (Eggleston and Armstrong 1995) and increased survival of juveniles within the habitat (Armstrong and Gunderson 1985; Fernandez et al. 1993; Armstrong et al. 1995). Feasibility studies have been conducted to assess creating and maintaining intertidal shell habitat to mitigate crab losses due to sedimentation from the dredging of the Grays Harbor navigational channel (Armstrong et al. 1991, 1992). Results have consistently shown young-of-year Dungeness crab densities exceeding 300 juvenile first instar crabs per m^2 in shell habitat but less than 5 crabs per m^2 on bare mud (Armstrong et al. 1992). The various studies also have demonstrated that megalopae, the final larval stage that transitions to juvenile first instar crabs, have a definite affinity for settling in shell habitat for shelter from predation and for the increased supply of food resources present in that habitat (Fernandez et al. 1993; Eggleston and Armstrong 1995). Studies also have found that shell habitat discourages juvenile burrowing shrimp from becoming established (Feldman et al. 1997; Dumbauld et al. 2004). However, it appears that even the relatively low densities of juvenile and adult burrowing shrimp occupying the area of shell deposition can contribute to a substantial loss of shell, with most of the shell deposits sinking or becoming buried by fine sediment (Feldman et al. 1997; Dumbauld et al. 2004). This sedimentation would eliminate suitable habitat for Dungeness megalopae and juveniles, forcing them into open mud flat areas with less food resources and higher predation risks.

Seagrasses are another group of ecosystem bio-stabilizers in estuaries. Seagrass root/rhizome systems stabilize sediments, while foliage modifies local hydrodynamics, trapping organic and inorganic nutrients, thus providing nutrient-rich, sheltered habitats for resident biota (Hemminga and Duarte 2000; Semmens 2008; Pillay and Branch 2011). The effect of burrowing shrimp bioturbation on seagrasses reduces the ecosystem services provided by these plants, and in turn the unique faunal assemblages supported by them. Dumbauld and Wyllie-Echeverria (2003) showed a negative effect of ghost shrimp *N. californiensis* on the eelgrass *Zostera japonica* within Willapa Bay. Using the pesticide carbaryl to eliminate ghost shrimp from experimental plots resulted in greater survival and growth of eelgrass seedlings in plots lacking ghost shrimps. The turnover of sediments from the extensive burrowing of ghost shrimp, along with expulsion of the fine sediments to the surface can smother seagrasses and increases water column turbidity, thus reducing light available for photosynthesis and subsequently seagrass growth (Suchanek 1983; Dumbauld and Wyllie-Echeverria 2003; Pillay and Branch 2011). Conversely, seagrasses can hinder burrowing shrimp activity, with their root-shoot systems acting to bind the sediments and reduce penetrability (Siebert and Branch 2006).

The negative effects of ghost shrimp on the overall estuarine community as compared to other habitats dominated by bio-stabilizers was demonstrated by a benthic fauna-habitat study in Willapa Bay by Ferraro and Cole (2007). This study examined the estuary-wide benthic macrofauna-habitat associations for 4 habitats in 1996: eelgrass (*Zostera marina*), Atlantic cordgrass (*Spartina alterniflora*), mud shrimp, ghost shrimp. In 1998, the study looked at 7 habitats (eelgrass, Atlantic cordgrass, mud shrimp, ghost shrimp, oyster [*Crassostrea gigas*], bare mud/sand, subtidal). In 1996, a total of 172 benthic macrofauna taxa and 44,947 individuals were collected, of which 92 percent were deposit, suspension, or facultative feeders. A total of 144 benthic macrofauna taxa and 22,702 individuals, 92 percent being deposit, suspension, or facultative feeders, were collected in 1998. The results of the analyses showed there were 2 to 4 significantly different habitat groups in terms benthic community structure and diversity, with those differences between the groups often being large (2-100x). Overall, the habitats fell into 3 groups characterized by high (*Zostera*, oyster, *Spartina*), intermediate (*Upogebia*, bare mud/sand), and low (*Neotrypaea*, subtidal) benthic macrofaunal community structure and diversity. *Neotrypaea* and subtidal habitats had similarly depauperate benthic macrofaunal communities, but with different species compositions. These findings by Ferraro and Cole (2007) agree with several previous studies that also found different benthic macrofaunal species composition in *Neotrypaea* and *Upogebia* and lower species richness and abundance in *Neotrypaea* than *Upogebia* (Brenchley 1978; Bird 1982; Dumbauld 1994).

8.3 ASSESSMENT OF MITIGATION MEASURES

8.3.1 Marine Friendly Products

The mitigation proposed and used in Section 7.0's modeling assessment utilizes Reef Cubes, the signature product from UK-based Arc Marine, which specializes in concrete for marine applications (https://arcmarine.co.uk/). Reef Cubes are hollow cubes made from a 100 percent recycled aggregate and low-carbon concrete, ranging in size from 150 mm^2 up to 2 m^2 per side (Figure 86). Advanced casting techniques create a rough surface that encourages marine life to colonize, while the larger openings in each side allow for an interlocking internal space that provide reef-like shelters for fish refuge and crustacean homes. Through testing at University of Plymouth's COAST Laboratory, Reef Cubes were found to disrupt the incoming waves and currents because its shape lowers the force impact by its permeability while also trapping sediment, stabilizing the foundations and the formation. Reef Cubes also can be linked together to form a marine mattress configuration.

Figure 86: Arc Marine Reef Cubes, in Various Sizes and Configurations

In addition, Arc Marine is working with the University of Plymouth to produce solid cubes called Bio Blocks (Firth et al. 2014; Whitehead 2020). Each side of the 1 m^3 Bio Block contains different-sized holes, overhangs, and recesses, and notches to create multiple habitats to provide shade and shelter different-sized marine species (Figure 87).

Figure 87: Arc Marine Bio Blocks as Designed by University of Plymouth Researchers

Alternatively, an Israeli company, ECOncrete Tech Ltd., produces a similar product called ECOncrete (https://econcretetech.com/). The company creates ecologically active concrete coastal infrastructures from a proprietary concrete mix that has a reduced alkalinity in comparison to Portland cement, and includes various additives that decrease the dominance of Portland cement in the mix, making the concrete more hospitable to marine life (Perkol-Finkel and Sella 2014). In addition, their products have an increased surface complexity and design to encourage biological development (Figure 88). ECOncrete's larger ECO Armor Block also can be fitted with screens to fill with oyster shells or rotating stacked oyster hatchery units (Figure 5, top left). The company also produces a marine mattress, the ECO mat, that features the same custom concrete mix and highly texturized surfaces for colonization (Figure 88, bottom).

Figure 88: Examples of ECOncrete Products: ECO Armor Block (Top) and ECO Mats (Bottom)

Both product lines are suitable for the needs of wave attenuation to mitigate the morphological changes with reduction in both erosion and sedimentation in oyster production areas. In addition, the modified concrete mixtures are a marked improvement over Portland cement, which has been shown to be a poor substrate for biological recruitment due to high surface alkalinity (pH ~13 compared to a seawater pH ~8) and the presence of compounds that are toxic to marine life (Sella and Perkol-Finkel 2015).

8.3.2 Review of Mitigation Modeling Results

Results of the modeling of mitigation measures detailed in Section 7.0 used long lines of reef cubes stacked as pictured in Figure 78 (and in Figure 86, left, minus the smaller cube on top). Although pictured as hollow, the model treated the cubes as solid, with the assumption that they would fill with sediment over time. These structures would essentially be considered an artificial reef, a human-created underwater structure, typically built to promote marine life in areas with a generally featureless bottom, to control erosion, block ship passage, block the use of trawling nets, or improve surfing. For the purposes of the mitigation efforts, reef cubes or similar wave attenuation structures would be deployed for the purposes of wave attenuation and erosion management.

Modeling results looked at offshore and nearshore placement of reef cubes in Willapa Bay and Grays Harbor. Results suggest that the reef cubes would be very effective for wave attenuation. The nearshore placements provided a stronger wave attenuation with a maximum percentage wave reduction of 50 percent near the structures (Figures 80 and 81). Wave heights over the tidal flats toward the northern shoreline of Grays Harbor also are reduced by an approximately 10 to 20 percent range (Figure 81). Oyster production areas located behind the nearshore artificial reefs would be relatively sheltered against strong wave energy, which would curtail possible erosion of sediments in those areas, especially if burrowing shrimp densities are high. The reef also may help to reduce the flow of suspended sediments into the area, but calmer waters behind the structures may encourage localized deposition of sediments.

Modeling examining the potential morphological changes to the surrounding areas were more complicated than wave attenuation modeling. In Willapa Bay, the reef cubes reduced morphological changes behind the reefs, but showed an increased change near or between the structures (Figure 82). Since most of those areas behind the reefs showed increased deposition (Figure 85), these model results suggest that sedimentation in those oyster production areas would be generally reduced (10 to 20 percent). However, the model shows an increased morphological response near and between the structures where flows are constrained, or where tide channels are adjacent or interrupt the reef alignment. In Grays Harbor, the artificial reef with nearshore placement could reduce the morphological response behind the structures by a range of 20 to 40 percent (Figure 83). As was seen in the model results for Willapa Bay artificial reef placements, the response is more complicated near the reef structures themselves, especially in those areas adjacent to or interrupted by tidal channels. Oyster production areas adjacent to the channels may therefore experience more erosion, but the majority of the areas located behind the reef barriers would benefit from reduced erosion. The model shows that artificial reef structures can be effective at altering morphological changes to tidal flats, but additional investigations as to the correct locations and configurations will be necessary to find the right combination to most effectively reduce sedimentation in the Twin Harbors.

8.3.3 Effects of Artificial Reefs on Surrounding Sediment and Biota

Studies generally accept that installation and placement of artificial structures will result in the complete loss of habitat directly under the structure, instead focusing on the effects local turbulence may have on benthic habitats in the immediate vicinity (Henkel 2016; Taormina et al. 2018; Hemery 2020). The initial model results on morphological responses of the reef cubes suggests a similar shift in sediments may occur in and around the artificial reef structures. Confirming this potential effect, several studies looking at the effects of artificial reef structures on the surrounding sediments and, in turn, the biota have noted changes closer to the artificial reef.

Ambrose and Anderson (1990) investigated the influence of the Pendleton Artificial Reef (PAR) in Southern California on the abundance of infauna in the surrounding sand bottom. PAR was constructed in 1980 of quarry rock placed in eight piles, or modules. The study found the artificial reef altered the grain-size distribution of sediments around the reef; sediments close to the modules were coarser than those 10 or 20 m away from the modules. This change impacted two species of polychaetes, with *Spiophanes* spp. increasing in abundance adjacent to the artificial reef structures, but *Prionospio pygmaeus*, nemerteans, and cumaceans were more abundant away from the Reefballs. The study concluded that while densities of some species changed around the reef, the overall effect of the artificial reef on the surrounding infauna was limited to a small area near the structures.

In a more local study, Mendoza and Henkel (2017) deployed stacked pyramids of 45 cinderblocks (1.2 m × 1 m and 1 m tall) in Yaquina Bay, Oregon, in pairs approximately 100 m apart. They found median grain size increased significantly with proximity to their structures and a trend of increasing fine sediment with increasing distance from a structure, the detectable effect ending at 5 m from the structures. Infaunal abundances were higher closer to the artificial structures; however, measures of diversity or richness did not differ in relation to distance from the structures or the reference areas. They concluded that any effects on infauna were localized and smaller than differences between different regions of the estuary.

Other studies have found the opposite trend, with finer sediments accumulating near the artificial reef. Fabi et al. (2002) monitored the effects of an artificial reef along the Italian coast in the Adriatic Sea. The reef was comprised of 29 pyramids, each of five 8 m^3 concrete blocks, at a distance of about 15 m from each other. This grid-pattern configuration caused siltation and accumulation of organic matter inside the reef area, favoring the settlement of deposit and suspension feeders, mainly polychaetes. Outside the reef, mollusks were numerically dominant, with an increasing proportion of sandy-bottom species with increasing distance from the structures.

Yang et al. (2019) deployed large concrete boxes (1.8 m × 1.8 m × 1.7 m) approximately 10 m apart in Xiangyun Bay, Bohai Sea, China. Their results showed increased fine sediment, higher levels of total organic matter, chlorophyll-a, and carbon and nitrogen content next to the artificial reefs as compared to up to 5 m away. The increased food resources accumulating around the artificial reef structures, possibly contributed by the increased colonization of bivalves and kelps, resulted in higher meiofaunal abundances adjacent to the structures at all three sampling sites.

Zalmon et al. (2014) placed triads of Reefballs 0.5, 5, and 15 m apart on a sandy bottom shoreline on the northern coast of Brazil. The arrangements at shorter distances (0.5 and 5 m) showed reduced fine sediment and nutrient deposition compared to those spaced 15 m apart. This, in turn, affected the infauna types colonizing the structures, with a lower density of deposit feeders in the infauna at closer-spaced groupings compared with the 15 m group, which had a greater number of predators and suspension feeders.

These studies demonstrate that although there is a given loss of habitat and biota directly beneath artificial reef structures, the reef itself alters flows and turbulence around itself, and changes sediments and infauna in areas affected. In areas with less diverse habitat, such changes can introduce more complexity that in turn supports a more diverse community of organisms.

8.3.4 Artificial Reef Structures as New Hard Substrate Habitat

Artificial reefs are most often used to promote marine life in areas with a generally featureless and biologically depressed bottom. Regardless of construction method or intended purpose, artificial reefs generally provide hard surfaces where algae and invertebrates such as barnacles, corals, and oysters attach; the accumulation of attached marine life in turn provides intricate structure and food for assemblages of marine species. While assemblages will vary according to geography, habitat, devices, and components, the colonization starts with a biofilm of marine diatoms, bacteria, and fungi followed over time by successions of initial (e.g., barnacles, hydroids, tube-building corophiids, and tubeworms) and then secondary colonizers (e.g., anemones, ascidians, and mussels) (Hemery 2020). Thus, despite the loss of habitat directly under the structure, significantly more habitat is made available on the new reef structure itself. The increased complexity of the reef structures also supports a more diverse community.

Many of these colonizers contribute to the reef via biogenic buildup, a natural process in which engineering species like oysters, serpulid worms, barnacles, and corals deposit calcium carbonate skeletons onto hard surfaces, thus creating valuable habitat to additional organisms (Jones et al. 1994). This biogenic layer also protects the structure from mechanical erosion caused by constant abrasions of sand and floating debris, and increasing its strength, stability, and durability. Risinger (2012) examined the influence of oyster growth on concrete strength, and found that concrete covered with marine growth, especially oysters, showed a significant 10-fold increase in flexural strength over a 2-year period.

In response, the artificial reef may potentially attract mobile organisms like decapods, demersal and pelagic fish, and apex predators (Hemery 2020). Artificial reef structures are considered to be ecologically positive because the artificial reef increases habitat complexity and functions as an additional food source, refuge for endangered species, and nursery ground (Firth et al. 2014; Sella and Perkol-Finkel 2015; Taormina et al. 2018, Hemery 2020; Taormina et al. 2020). The increased diversity of organisms creates a richer selection of forage items, attracting invertebrates such as Dungeness crabs, local fish such as Pacific salmon smolts, and a variety of marine waterfowl (Brennan et al. 1990; Mathot et al. 2010). Conversely, these structures also can lead to negative effects by facilitating the introduction of non-native species or causing important shifts in local communities (Dannheim et al. 2020; Loxton et al. 2017).

Ambrose and Anderson (1990) noted that the tube-dwelling worm *Diopatra ornata* occurred only within the artificial reef modules. In addition, total infaunal density and the densities of decapods, echinoderms, and sipunculids were higher within *D. ornata* beds than outside the beds. Total infaunal density was significantly higher in *D. ornata* beds (13,240 individuals/m^2) than outside *D. ornata* beds (4,947 individuals/m^2). These density differences were mostly due to hermit crabs (*Pagurus* spp.) and the polychaete *Gyptis brevipalpa*. In addition, *D. ornata* beds hosted twice as many decapod species as outside them (12 vs. 6). *D. ornata* is a large tube worm, and frequently occurs near hard substrates, which the reef piles provided in soft sediment-dominated habitat. Its tube, covered with fragments of shells and algae, extends above the sediment surface, and provided substrate stabilization, habitat for other infauna, and protection from predation.

Walles et al. (2015) constructed 200-m-long reefs made of 25-cm-high gabions filled with Pacific oyster shells, which provided substrate for the settlement of new oyster recruits. The reefs were positioned perpendicular to the dominant wave direction at three different elevations: 23 percent, 35 percent, and 50 percent emersion time (Walles et al. 2016). Over a 5-year period, the development of these reefs and their effect on tidal flat morphology (erosion/sedimentation) were monitored. The 23 percent tidal emersion turned out to have the best survival and condition, with sufficient recruitment to maintain the reef structures. A vertical accretion of the reef base was expected to grow 7.0–16.9 mm per year; over the course of 5 years, this reef increased an average of 10 cm. This growth effectively reduced erosion leeward of the reef, as was predicted (Walles et al. 2015). Up to 90 m leeward of the reef, there was a reduction of 51 ± 29 percent in the erosion measured.

Recent attention has focused on utilizing the principles of ecological engineering (Firth et al. 2014; Sella and Perkol-Finkel 2015) to enhance the biological and ecological value of these coastal and marine infrastructures. To date, enhancement measures concentrated on design or surface texture aspects, aimed at attracting more abundant and diverse natural assemblages (Firth et al. 2014; Perkol-Finkel and Sella 2014), yielding ecological and structural advantages. More complex substrata provide more ecological niches, which may allow more animals to recruit and thus may lead to a higher local biodiversity (Langhamer et al. 2009).

As an example of the difference these types of enhancements and improvements can make with colonization of artificial reef structures, Sella and Perkol-Finkel (2015) conducted a 24-month monitoring study of two breakwater sections in Haifa Bay, Israel, comparing the community structure developing on standard Portland cement based armoring units (Standard Antifers – SA) compared to that developing on ecologically enhanced units (ECOncrete Antifers – EA). Results showed that the enhanced EA units significantly differed from the Portland based SA, exhibiting greater live cover, higher species richness, and higher diversity. Typical coverage of benthic flora and fauna on SA was dominated mostly by turf algae and barnacles, which were concentrated mainly on the edges of the units. In contrast, the EA units displayed a more diverse faunal assemblage composed of oysters, sponges, Sabellidae, Serpullidae, tunicates, bryozoans, and coralline algae that are considered engineering species. Considering invasive species, smaller ratio between invasive and local species on EA units was much smaller than the one found on the SA units (1/3 vs. 2/3).

Higher surface complexity, along with a variety of spaces for refuge from predators, and an ample supply of prey fauna can potentially increase fish use and diversity around artificial reef structures. Sherman et al. (2002) installed Reef Balls with and without concrete blocks placed in the central void space to examine if manipulating the inner structural complexity of the artificial reef structures would have an effect on enhancing fish abundance, species richness, and biomass. Results showed that reefs with less void space and more structural complexity had greater fish abundance, species richness, and biomass than similar reefs with more void space. Other studies also have found that the number and size of refuges available positively affected the number, biomass, and species richness of fishes in reef structures (Hixon and Beets 1989; Eklund 1996). These results highlight the importance of structural complexity in artificial reefs designed to enhance fish recruitment, aggregation, and diversity. In terms of Reef Cubes, while they may have more surface area in total, the interior void of the cube would not provide greater complexity alone and would perhaps be less apt to attract salmon smolts but could serve as an attractant to larger fish and potential predators to smolts. Alternatives such as the Bio Block or ECO Armor Block offer more surface complexity, but less overall inner void space, unless some of the additional features are installed.

8.3.5 Burrowing Shrimp Control Options

From the overall assessment of the model results, it is clear that the burrowing shrimp population, specifically that of ghost shrimp, contributes to the sedimentation issues of the two embayments. In their role as ecosystem engineers, ghost shrimp destabilize oyster production grounds. With the ceasing of Carbaryl applications, and the denial of Imidacloprid use, many alternative control methods have been investigated (Dumbauld et al. 2004; Booth 2007; Dumbauld and Harlan 2009; Patten 2017); most have proven ineffective. Biological control using Dungeness crab and Red Rock crab were assessed, but results indicated their predation was insufficient to provide any practical control (Patten 2017). Green sturgeon was found ineffective for burrowing shrimp control. Mechanical and cultural control methods such as suction harvesting, surface air bubble harvesting, heating the sediment surfaces with a propane torch, covering the surface with plastic, electrofishing, high pressure-low volume water injections, and low-pressure-high volume water injections were all investigated and were not found to be effective in reducing shrimp densities. In many cases, they were deemed impractical and highly destructive to the habitat (Patten 2017).

One solution would be the addition of shell materials to the surface, as was done to enhance Dungeness crab populations to mitigate for dredging impacts in Grays Harbor (Armstrong et al. 1992). Oyster shell material is beneficial to Dungeness crab recruitment, oyster and clam recruitment and colonization, and generally provides a good surface area for a diverse infauna (diatoms, corophids, macroalgae), but was found to be ineffective at preventing ghost shrimp recolonization once it becomes covered by sediment (Feldman et al. 1997; Dumbauld et al. 2004). Because burrowing shrimp soften the sediments, materials easily sink up to 30 to 70 cm over the course of time or would be covered by the erosion of those finer sediments from nearby shrimp beds (12 to 20 weeks according to Dumbauld et al. 2004). Feldman et al. (1997) noted that shell deposits sunk or had been covered with sediments within 3 months. For these reasons, augmenting tidal flats with oyster shells is not an effective or viable treatment for preventing burrowing shrimp infestations.

Dumbauld and Harlan (2009) experimented with electrofishing to control burrowing shrimp in oyster aquaculture beds, hoping to use the Direct Current (DC) to draw them to the surface from their burrows. Unfortunately, the electrofishing current drove them towards the bottom of their burrows instead. Further experiments were investigated to induce mortality. While it was possible to achieve paralysis or tetany by use of higher power with DC, pulsed DC, and Alternative Current, the animals recovered unless a combination of high voltage and frequency were applied for 60 to 100 seconds. Dumbauld and Harlan (2009) concluded that those sustained levels would be difficult to achieve in the field due to the substrate, depth of the shrimp burrows, and high power necessary to obtain adequate field strength.

Patten (2017) details an experiment looking at crushing burrowing shrimp in their burrows by driving several amphibious platforms over test plots of burrowing shrimp populations. A four-wheeled Rolligon and a tracked unit were repeatedly driven over affected ground and population changes of shrimp were monitored over time. The sediment compaction treatment reduced the number of burrows per m^2 in the year of treatment, but burrow density rebounded above the 10 burrows per m^2 threshold 1 year later.

Washington Department of Natural Resources (WDNR) completed a Proof of Concept (POC) study at Grassy Island, using a “dry harrowing” method of applying two passes of a shrimp-infested plot with a large “roller-chopper” harrow implement towed behind an amphibious vehicle, combining the sediment compaction treatment with deeper ground disturbance (WDNR 2018). During the POC experiment completed in May, two passes of the dry harrow treatment took an average of 28 minutes/half acre and yielded 67 percent shrimp control from biomass (WDNR 2018). A POC supplement study was conducted to further assess the success of dry harrowing, assess whether a more intense application would be more successful, and document any recolonization of shrimp to the treated plots.

The follow-up study implemented a four-pass treatment, which took an average of 41.5 minutes/half acre to treat and yielded an estimated 79 percent initial reduction in biomass (g/core) after the first 20-day period (t1). Shrimp density in dry harrowed plots dropped significantly from pre-treatment densities (by an average of 89 percent after the first 20-day period). After another 4 weeks (6 weeks post-treatment, t2) this low shrimp density (0.73 ± SE 0.23) shrimp/core persisted. Burrow density was reduced 77 percent from 49 burrows/m² to 11.38 burrows/m² pre- and post-supplemental treatment (25 percent within control plots, from 54.3 to 40.68 burrows/m²). Burrow density fell another 5 percent, from 11.38 to 8.88 burrows/m² in treated plots when sampled in September at t2 (21% within control plots, from 40.68 to 29.33 burrows/m²).

Investigations also observed no evidence of lateral movement of shrimp from adjacent plots after both 20 days and 12 weeks. However, sampling showed that by the September sampling, 20 weeks after treatment, a higher proportion of extra small shrimp (XS size class, CL 4.5 to 8 mm) were observed to dominate the population distribution. This suggests that the dry harrowing treatment in April or May will miss these XS class of recruits. It was suggested that later summer to early fall treatments would be the most effective time to treat, as it would then affect both this smallest size class as well as newly recruited shrimp, as well as actively burrowing adult *N. californiensis* that would be closer to the substrate surface, and more easily impacted by methods of control (Dumbauld et al. 1996). This timing provides decent windows of daytime low tides that can be utilized for dry harrowing.

However, the estimates are, that due to the life cycle of the ghost shrimp, this treatment would be necessary roughly every 2 years. The process is fairly labor intensive and requires a heavy amphibious tracked vehicle (Marsh Master-2LX) and a 700-pound steel roller with a series of flat plates welded to it that penetrate 30 cm into the sediment. While it may be effective at compaction and reducing shrimp densities, its effectiveness is dependent on the timing of the treatment. It also is a treatment that has only been applied on a limited scale; it is unclear if dry harrowing with up to four passes is economically viable on a larger, commercial scale. Also, the treatment can be fairly destructive to the tidal flat, which may loosen the surface sediment in the short term far more than burrowing shrimp activities, thus increasing the risks of sediment erosion and sediment movement to other areas of the tidal flat in the bay. It also is unclear if this degree of disturbance would be compatible with shellfish ground culture.

One important characteristic that separates ghost shrimp and oysters is their preferences for substrates. Oysters prefer to attach to hard substrates, whereas ghost shrimp will actively avoid burrowing around hard substrates. As mentioned previously, the application of oyster shell material as a base layer of substrate to deter burrowing shrimp was not effective due the shell layer sinking into the sediment in the matter of a few months. Once the shells are covered by sediment, they are no longer effective as a deterrent.

The key element to deterring burrowing shrimp could be establishing a hard substrate layer. Aside from shell deposits and smaller experiments with a thin layer of quick-crete (Patten 2017), no studies have examined the effects of installing a layer of artificial substrate material as a base layer to areas with shrimp burrows. Utilizing the marine-friendly concrete products such as Reef Cubes or the ECO Mat, a larger marine mattress would provide a layer of hard substrate with extra surface complexity that would encourage colonization of a diatom biofilm, invertebrate infauna such as *Corophium*, as well as mussels and, most importantly, oyster attachment. The increased presence of mussels also would attract and support marine waterfowl. Gaps in between the blocks add further habitat complexity, offering refuge for Dungeness crab megalopae and juvenile crabs. Depending on the condition of the sediment, the mattress may sink into the sediment, but by doing so, it may create an effective layer that could impede ghost shrimp as they attempt to burrow down into the sediments, making that area unsuitable for recolonization.

The application of marine friendly concrete marine mattresses as a treatment for controlling burrowing shrimp activity would require a pilot study to investigate both the logistics of installation, but also several other factors, including the rate of sinking, effectiveness, area of influence, colonization rates of diatoms and infauna, and the efficacy of the treatment in combination with dry harrowing. To determine where the best locations are for treatment, a mapping and inventory of burrowing shrimp presence is necessary, so that management decisions can be best informed on where the problem areas are located. The Pacific Conservation District applied for a Washington State Department of Agriculture Integrated Pest Management Grant in 2020 to fund the District's study to refine newly developed remote sensing capabilities to efficiently monitor burrowing shrimp densities in intertidal tidelands of Willapa Bay and Grays Harbor. The system entails specialized instrument platforms operated from low flying unmanned aerial vehicles (UAV = drones). The instrument packages are varied and include LiDAR to measure microtopography and surface roughness, hyperspectral imagery for object identification, and high-resolution visible imagery used for orthographic mosaics. By repeated measurements over time, changes in the spatiotemporal demographics can be calculated (e.g., determine if shrimp bed area is increasing or decreasing; map where the critical density of 10 burrow holes per m^2 has been exceeded). Such a monitoring program will be critical in quantifying the large-scale burrowing shrimp density distribution in the two embayments and helping to identify where to implement mitigation measures.

8.4 SUMMARY AND RECOMMENDATIONS

Modeling efforts have shown that winter storm winds and waves cause erosion in the tidal flats that is deposited closer to the shores. Greater erosion also is seen along the edges of the subtidal secondary channels, with heavier deposition accumulating within those subtidal channels, suggesting sediment from the tidal flats is being pulled out on the ebb tide. Compounding these sediment movements are increased suspended sediment loads entering the bays from river sources resulting from the winter rainstorms, which are conveyed via the navigation channel into secondary channels, and potentially out onto the tidal flats and over areas of oyster production. Additionally, modeling of dredge disposal activity in Grays Harbor shows that disposal of dredged sediments at the Chehalis disposal site during flood tides can distribute resuspended sediments throughout the harbor and adds to the sedimentation issues in oyster production areas in the north part of the harbor.

Results of the 10-year average annual morphological changes for the tidal flats (areas 1.5 m depth or less) were plotted with the webapp data showing areas of oyster production and current areas of burrowing shrimp activity. The overlay revealed increased erosion in areas with burrowing shrimp activity, with indications of increased deposition in adjacent areas. Burrowing shrimp were often next to areas of oyster production or in former oyster areas that have been lost to the burrowing shrimp population. Literature reviews provided additional insights into the role that burrowing shrimp can play as ecosystem engineers, and their ability to de-stabilize the ecosystem and counteract the stabilizing influences of other ecosystem engineers, such as oysters, seagrasses, and tidal flat diatoms and invertebrate fauna. Burrowing shrimp activities result in a contribution of fine sediments and decreased cohesiveness of sand-mud matrices they are burrowing through that exacerbates the erosion in Grays Harbor and Willapa Bay, burying oysters and other flora and fauna and reducing biological diversity on tidal flats.

Several measures to have been proposed and investigated in this report that have the potential to help mitigate the increased sedimentation and erosion observed in the Twin Harbors. The use of artificial reefs was evaluated for their effects on the infauna and tidal flat sediments, and particularly on oysters and early life stages of Dungeness crabs. Their value as additional habitat for infauna and flora also was detailed. A review of alternative burrowing shrimp control methods revealed that there has been limited success, but also little examination at applying a more substantive hard substrate layer or barrier to suppress shrimp presence. The review of artificial reef structures provided a potential solution with the installations of marine-friendly concrete mattresses as a hard substrate barrier layer to suppress burrowing shrimp.

Stantec's recommendations are to proceed with the following pilot studies, to further examine their potential and effectiveness:

1. **Artificial Reefs for Wave Attenuation and Erosion Control**: The study would continue the modeling effort, re-running the scenarios to investigate the most advantageous configurations of reef structure alignment, height, spacing, and positions that derive the most benefits to oysters in the Twin Harbors, and then conduct a field investigation that would construct the reef design and measure the effects of sedimentation on tidal flats and oyster beds to validate the model.

2. **Adjustment of the Timing of Dredge Disposal Activities and Relocation of the Dredge Disposal Site**: The study would continue the modeling effort, simulating the dynamic cycle of O&M dredging and disposal activities on the morphological changes within Grays Harbor. The study would then require ground-truthing via field measurements. Investigators would work with the USACE to monitor dredge disposal activities occurring during ebb tides and would monitor suspended sediment levels and deposition at multiple locations within Grays Harbor to confirm the model results. The study also would work with the USACE to conduct a disposal at an alternative offshore disposal location and would monitor suspended sediment levels and deposition at multiple locations within Grays Harbor to confirm the model results.

3. **Use of Marine Friendly Concrete Mattresses for Burrowing Shrimp Control:** The study would install ECOncrete ECOmats or a similar marine-friendly concrete product on selected high-density burrowing shrimp areas to investigate their performance at suppressing the shrimp population and reoccurrence at the site, and measure colonization of diatoms and invertebrate infauna on the mattress and effects on sediments around the mattresses. Installations could be coordinated with future dry harrowing studies to investigate if the combinations of the two treatments (harrowing followed by mattress installations) increase the long-term effectiveness of shrimp suppression.

9.0 SUMMARY

The GHCD initiated a three-phased process in 2015 to investigate the decline of shellfish aquaculture in the Twin Harbors, thought to be the result of excessive sediment movement due to geomorphological changes associated with anthropogenic activities and from biological processes such as overpopulation of the burrowing shrimp. Following the literature review and recommendations from the Phase I study, this Phase II study performed a comprehensive data investigation and analysis and developed/calibrated a hydrodynamic and sediment transport model using Delft3D-FM. The calibrated model was then used to understand the hydro- and morpho-dynamics within the Twin Harbors, evaluate the impact of the USACE O&M dredging within Grays Harbor, and to define/evaluate mitigation measures to offset impacts to shellfish growing beds in the Twin Harbors.

The data investigation involves four simultaneous data collections, including an online data search, InSAR data generation, a stakeholder survey, and a USACE literature review, which are summarized below:

- Current and historical topographic/bathymetric data, historical records of water level, wind, waves, riverine discharge, sediment load, as well as historical samples of bed sediments within the Twin Harbors were collected from different agencies through the online data search. Those datasets were analyzed to understand the regional behaviors and seasonal variations of wind/wave climates, river discharge and sediment load, and the sediment distribution within the Twin Harbor. Those datasets also were used for the model development and calibration.
- The recent annual rate of morphological change over massive tidal flats within the Twin Harbors was generated using the InSAR process based on historical satellite images. The InSAR data was used to verify the morphological model, which avoided the time and expense (which otherwise would be required) of an extensive field survey.
- Digital map layers (in ESRI Geodatabase) of oyster production farms, burrowing shrimp, substrate information, and wetlands were developed with the participation of major stakeholders and shellfish growers through an interactive webapp. This unified map product was used in the biological assessment in this study, which also can be used for planning purpose in the future.

A preliminary understanding of the hydro- and morpho-dynamics within the Twin Harbors, as well as a broader region of the North Pacific Ocean, including regional wind/wave patterns, climate, and circulation, was acquired through a comprehensive literature review of the studies of the Twin Harbors performed by USACE. The USACE literature review also provided information about the history of the navigation and O&M dredging activities within Grays Harbor. The knowledge gained through this literature review was leveraged to support the development of the numerical model.

The numerical model is created with Delft3D-FM, developed by Deltares. Delft3D-FM is a process-based integrated modeling suite capable of simulating tides, storm surge, wind-generated waves, sediment transport, water quality, etc. The model dynamically couples the hydrodynamic and wave components, accounting for their two-way interactions during the simulation. The model development and calibration are summarized below:

- Benefiting from the flexible mesh configuration, the hydrodynamic model covers the Northeastern portion of the Pacific Ocean with coarse resolution on the order of approximately 1,000 m and the Twin Harbors with high spatial resolution of 60 m to 180 m. The hydrodynamic model was driven by the tidal constituents from a regional tidal database at the offshore boundary, riverine discharge from USGS at major rivers, and temporally and spatially varying wind and pressure fields from the NCEP CFSR climate model throughout the domain.

- The wave model has a uniform resolution of about 100 m and covers the Twin Harbors, a portion of the Columbia River, and extends offshore to the CDIP 026 buoy where long-term measurements of wave data are available to drive the model. The water levels and currents from the hydrodynamic model and wave parameters and radiation stresses from the wave model are dynamically coupled between both model components to account for their interaction and feedback.

- The hydrodynamic and wave model was calibrated using water level data from NOAA for two periods in 2010. The model skill in reproducing the measured water levels, currents, waves, and SSC was validated and evaluated using the USACE 1999 survey at the Grays Harbor inlet. The model skill, as measured by a score ranging from 0 (worst) to 1 (best) proposed in Taylor 2001, is greater than 0.9 with a mean close to 0.95 for water level, and greater than 0.9 for currents except one location, and greater than 0.8 for wave height in general, which exceeds typical engineering standards for numerical modeling.

- The measured data from the USACE 1999 survey at the Grays Harbor inlet also was used to validate the model's ability to replicate the measured SSCs. Since the measured data has a high level of uncertainty, qualitatively, the model is able to capture the variations in SSC.

- The validation of the model for morphological change prediction at the inlet was performed using the historical morphological changes from the USACE studies. Modeled morphological change at the Grays Harbor inlet from June 2009 to February 2010 compares well to the measurements for the same period. Quantitatively, modeled morphological changes at the Willapa Bay inlet were compared to the measurements at different period, and the model produces similar patterns of morphological change.

- The validation of the model for morphological change prediction over tidal flats was performed using the InSAR data generated in this study, and overall, the model was consistent with the observed patterns.

9.1 KEY CONCLUSIONS

The hydrodynamics within the Twin Harbors were analyzed by examining the residual currents for two conditions: typical calm summer conditions and active winter conditions. The following observations were made:

- The residual current at the inlets for both Grays Harbor and Willapa Bay exhibits a net outward flow through the channel associated with complex circulation patterns on either side of the net flow stream.
- The northerly-directed longshore current in winter is stronger than the southerly-directed longshore current in summer, leading to a net northward flow on an annual basis; this is consistent with the observed longshore sediment transport.
- Specifically, for Grays Harbor:
  - The circulation pattern north of the inlet entrance potentially sends sediments exiting the harbor back towards Ocean Shores due to the presence of a stronger ebb current.
  - The circulation pattern within the inlet indicates a potential sediment pathway from North Jetty to Damon Point, and an eastward sediment pathway within Half Moon Bay.
- Specifically, for Willapa Bay:
  - Net tidal flows ebb through the inlets and flood over the shoals due to breaking waves.

The morphodynamics within the Twin Harbors were evaluated by determining the 10-year average annual morphological changes using the data from the numerical model:

- The inlets for both Grays Harbor and Willapa Bay have a very strong morphodynamic response, with a high annual rate (greater than 3 m) of morphological change.
- The interior channel system seems to be widening, which matches the observations from historical satellite images.
- Specifically, for Grays Harbor:
  - A highly erosional area southeast of Damon Point abuts an erosion zone toward the navigation channel, which are causing the channel to migrate to the southeast.
  - The navigational channel is generally in deposition with an average annual deposition of over 1 m in the Outer Harbor reach and less than 0.5 m per year in the Inner Harbor reach; this generally matches the historical average dredging required to maintain the navigation channel depth.
  - Tidal flats consist of subsidence areas adjacent to accretion areas farther landward, with an annual rate of change on the order of centimeters.

- Specifically, for Willapa Bay:
    - Water generally leaves the bay through the inlet at three locations, indicating a very dynamic inlet. This is consistent with the historical channel migration. The North Channel is currently migrating southward across the ebb shoal with current exit closing up connecting the ebb shoals to the Cape Shoalwater.
    - The South Channel is migrating northward, encroaching the tidal shoals to the north, which seems to be matching the observation from the stakeholders.
    - There is deposition in the channel system with an average annual deposition around 0.5 m.
    - Tidal flats near shore are generally in accretion, with subsidence zones adjacent to the channel; the annual rate of change is on the order of centimeters.

The impact from the O&M dredging was evaluated from two perspectives, i.e., temporary perturbation of the bed sediments from the dredging and the fate of the sediments released/resuspended at the disposal site. The following conclusions were made:

- The peak SSC associated with clamshell and hopper dredging was estimated to be 90 mg/L and 30 mg/L, respectively, which are confined to the channel. The maximum modeled deposition is 3 cm, which is confined largely to the channel for both clamshell and hopper dredging. Both clamshell and hopper dredging do not appear to have negative impacts on sedimentation behaviors and the aquaculture within Grays Harbor.
- The particle tracking model for sediment release at the Chehalis disposal site shows that:
    - If released during ebb tide, sediments firsty leave the disposal site, then move with flood tide along the sediment path from North Jetty toward Damon Point and find their way into the northern portion of the harbor. During the second tidal cycle, the majority of the mobilized sediments from the disposal site are transported into the Pacific Ocean to the north of the inlet, with a smaller amount remaining within the inlet and some in the northern tidal flats of Grays Harbor.
    - If released during flood tide, sediments are initially transported into the eastern and northeastern portion of the harbor during flood tide, then exit the harbor into the Pacific Ocean during ebb tide. During the second tidal cycle, the flood tide transports sediment back into the harbor, reaching most locations within the harbor; finally, they exit the harbor with ebb tide into Pacific Ocean to the north.
- The predicted fate of the sediments from the Chehalis disposal site from a simplified model indicates that:
    - The largest deposition occurs in the channel just outside of the inlet and farther offshore.
    - Appreciable amounts of sediment are deposited back into the navigational channel at the Crossover Reach/North Channel transition.

- The resuspended sediments also find their way to the northern and southern portions of the harbor with a deposition on the order of millimeters, similar to the naturally occurring range from the InSAR data. The process is likely to be accumulative from year to year with the ongoing dredging/ disposal activities.

- The model run with an alternative disposal area at the circulation zone to the north of the inlet indicates that:
  - Only a small portion of sediments are transported along the sediment path from the North Jetty to Damon Point and deposited there.
  - An even smaller amount of sediment is deposited farther over the tidal flats in the northern portion of the harbor, and the deposition depth is an order of magnitude smaller than that with the Chehalis disposal site.
  - Rarely do any sediments make their way back into the navigational channel as observed for the Chehalis disposal site.

A preliminary mitigation measure using reef cubes (applicable to other structure alternatives without loss of generality) was developed and evaluated. The following conclusions or recommendations were made.

- The mitigation measures using reef cubes works very well for wave attenuation, with a maximum reduction in wave height of 50 percent close to the structure, with diminishing affect landward.
- Morphological responses with the mitigation measures using reef cubes or other alternative structures are complicated, particularly due to the complex channel system in the Twin Harbors. The natural channel system serves to flush the system and provide necessary nutrients to local aquaculture; however, it also allows sediments pass through the channel and reach the tidal flats behind the structures.
- The recommended approach is to create terrain-conformed structures with variable crest elevation following the existing topography (i.e., a ‘speed bump’) rather than a blockage/barrier for the sediment movement.
- With the recommended approach, the mitigation measures reduce the morphological response behind the structure in general; however, increase of morphological response in channel crossings and between structures is expected, which should be taken into consideration in implementation and planning for oyster production areas.

9.2 LIMITATIONS AND RECOMMENDATIONS

The model skill in reproducing the measured water levels, currents, waves, and SSC was measured by a score ranging from 0 (worst) to 1 (best) proposed in Taylor 2001, which is greater than 0.9 with a mean close to 0.95 for water level, and greater than 0.9 for currents except one location, and greater than 0.8 for wave height in general, which exceeds typical engineering standards for numerical modeling. The model also performs well to resolve the morphological change pattern at the inlet as compared with the measurements and over the tidal flats as compared with the InSAR data. However, like any other models, there are limitations associated with the model due to assumptions used in the model as well as the quality and coverage/resolution of the data used to support the model development. Those limitations are summarized below:

- The bathymetry data from NOAA used in the model is compiled from a series of most recent bathymetry data for different regions that were collected at different times; therefore, it does not represent the latest bathymetry condition.
- The bathymetry data used in the model does not cover river mouth conditions discharging into the Twin Harbors. The discharge from those rivers is considered from a mass balance point of view. The dynamics within those rivers are not resolved by the model. The exception is the Columbia River, where bathymetry data is available but resolved at a coarse resolution.
- Data from the 1999 USACE survey were used to validate the model to reproduce water level, current, waves, and SSC, which are only available near the inlet. A basin wide calibration may be desired to reassure the accuracy of the model for hydrodynamic and sediment transport modelling.
- The model validation for SSC is qualitative as the SSC from the 1999 USACE survey used for the model validation have high uncertainty.
- Wind/pressure data (i.e., NCEP CFS dataset) used in the model calibration are from a hindcast model, which are subjective to the accuracy and limitations of the model used to derive those datasets.
- The bed sediment data used to specify the spatially varying sediment characteristics are compiled from a series of historical surveys, which may be outdated, and most importantly, is sparsely distributed.
- The riverbed sediment transport data for rivers discharging into the Twin Harbors are not available; the sediment distribution in the river is overly simplified to account for the detail sediment transport in those rivers.
- Only three sediment classes were included in the model to represent the full range of sediment characteristics.
- The morphological acceleration provides an efficient way to evaluate long-term morphological change, which has the following limitations:
    - The model was driven by the morphological tide and representative binned wind/wave derived from their time series, which represents a balance between the computational efficiency and accuracy.

- Time series of discharge and sediment load from rivers are condensed into a reduced time frame for morphological modeling, which may result in a loss of accuracy.
- Spatially uniform wind was specified in correspondence to the binned waves, which may result in over- or under-estimation of morphological response at certain areas.

- The evaluation of the O&M dredging impact at the disposal site does not address the dynamic dredging and disposal process; instead, it simply considers the resuspension of the sediments at the disposal site. Although the fate of those sediments should be similar, it may be interesting to resolve the full dynamic cycle of the dredging and disposal activities.
- The evaluation of the mitigation measurement is at the conceptual level with considerations to a few scenarios, which should be advanced in the future by looking at more alignment, layout of the placement, etc.

Acknowledging the limitations of the model developed in this study, the following recommendations were made:

- A basin-wide survey should be performed to collect the latest bathymetry data and sediment data. Data collected and input to the model should include major river discharge, sediment transport from river sources, and water quality parameters that may affect the Twin Harbors. One objective of this study is to better understand the dynamics of sediment transport processes in those rivers improve the hydrodynamic model to address river discharge impact on the overall morphological change in the Twin Harbors.
- For the sediment data, sieve analysis and erodibility analysis should be performed to determine the sediment characteristics, including the particle size distribution, settling velocity, critical shear stress for erosion, and erosion parameter. The location for sediment data can be strategically determined to supplement the historical data as well as at duplicated locations where historical samples are available to verify the historical data.
- InSAR data should be updated as more satellite images become available, which will increase its accuracy and provide a quick and economic way to track morphological change over tidal flats.
- A strategic basin-wide survey plan should be developed and performed to collect the water level, currents, waves, and SSC at different locations throughout the Twin Harbors such as over tidal flats and in the complex channel system to supplement the data available at the inlet from the USACE survey. Those datasets can be used to further improve the accuracy of the model to resolve the hydrodynamic and sediment transport processes.
- Long-term direct simulation (without using the morphological acceleration) should be performed to cross verify the prediction of the morphological changes if the computational efficiency and expense are allowable.

- It also is suggested to simulate the dynamic cycle of O&M dredging and disposal activities on the morphological changes within Grays Harbor as opposed to the simplified approach used here.
- The evaluation of the mitigation measures using reef cubes is at a conceptual level and forms the basic evaluation framework, which should be refined in the next phase to identify the optimal layout of the structures, including alignment, opening width and overlapping distance for flushing purposes.

9.3 DELIVERABLES

The following data are included as the digital deliverables:

1. WebApp Database:

- Layers of oyster production areas, burrowing shrimp, and wetlands collected from the Stakeholder in ESRI Geodatabase.

2. InSAR Data:

- Annual rate of elevation change for tidal flats and for the entirety of Pacific County and Grays Harbor County in GIS raster format.

3. Model Data:

- Hydrodynamics
  - X- and Y-component of the residual currents for both typical summer and winter conditions in GIS raster format.
- 2018 morphological modeling:
  - Predicted wave height field associated with the 13 representative wave conditions developed for the 2018 morphological modeling in GIS raster format.
  - Predicted morphological change for each of the 13 representative wave conditions over one morphological tidal cycle in GIS raster format.
  - Predicted 2018 morphological change in GIS raster format.
- 10-year morphological change:
  - Predicted annual morphological change for each of the 10 years in GIS raster format.
  - Predicted 3-, 5-, and 10-year cumulative morphological change in GIS raster format.
  - Predicted 10-year average annual morphological change in GIS raster format.

10.0 REFERENCES

Ambrose, R. F., and T. W. Anderson. 1990. Influence of an artificial reef on the surrounding infaunal community. Marine Biology 107: 41-52.

Armono, H. D. and K. R. Hall. 2003. Wave transmission on submerged breakwaters made of hollow hemispherical shape artificial reefs. Canadian Coastal Conference: 313-322.

Armstrong, D. A., and D. R. Gunderson. 1985. The role of estuaries in Dungeness crab early life history: a case study in Grays Harbor, Washington. Pages 145–170 in: Proceedings of the Symposium on Dungeness Crab Biology and Management. Alaska Sea Grant Report No. 85-3.

Armstrong, D. A., K. A. McGraw, P. A. Dinnel, R. M. Thom, and O. Iribarne. 1991. Construction Dredging Impacts on Dungeness Crab, Cancer magister, in Grays Harbor, Washington and Mitigation of Losses by Development of Intertidal Shell Habitat. FRI-UW-9110. Final Report for Seattle District, U.S. Army Corps of Engineers. University of Washington, School of Fisheries, Fisheries Research Institute, Seattle, Washington. 63 p.

Armstrong, D. A., O. O. Iribarne, P. A. Dinnel, K. A. McGrabv, A. Shaffer, R. Palacios, M. Fernandez, K. Feldman, and G. Williams. 1992. Mitigation of Dungeness crab, *Cancer magister*, losses due to dredging by development of intertidal shell habitat: pilot study during 1991. FRI-UW-9205. Final Report for Seattle District, U.S. Army Corps of Engineers. University of Washington, School of Fisheries, Fisheries Research Institute, Seattle, Washington.

Armstrong, J., D. A. Armstrong, and S. Mathews. 1995. Food habits of estuarine staghorn sculpin, *Leptocottus armatus,* with focus on consumption of juvenile Dungeness crab *Cancer magister*. Fish. Bull. 93(3): 456–470.

Anderson, W. B., and A. R. Foster. 1979. QUTR: Desk top survey of the inner continental shelf from Grays Harbor to Destruction Island. Research and Engineering Department, Naval Undersea Warfare Engineering Station, Keyport, WA.

Barnes, C. A., Duxbury, A. C., and Morse, B. A. 1972. Circulation and selected properties of the Columbia River effluent at Sea, Chapter 3, A. T. Pruter and D. L. Alverson (eds.), The Columbia River Estuary and Adjacent Ocean Waters: Bioenvironmental Studies. University of Washington Press, Seattle.

Bird, E. M. 1982. Population dynamics of thalassinidean shrimps and community effects through sediment modi!cation. PhD thesis, University of Maryland, College Park, Maryland.

Bleck, M. 2006. Wave attenuation by artificial reefs. PIANC. Accessed at: http://resolver.tudelft.nl/uuid:046d43c0-b8d9-470f-8d7d-ffe65aad793e

Booth, S. 2007. Development and implementation of integrated pest management of burrowing shrimp on Washington State commercial oyster beds - 2007 Final Report. Sustainable Agriculture Research and Education. Accessed at: https://projects.sare.org/project-reports/sw03-046/.

Booth, S. R., K. Patten, and L. New. 2019. Response of estuarine benthic invertebrates to field applications of insecticide. Estuarine, Coastal, and Shelf Science 218: 86-94.

Bouma, T. J., M. B. De Vries, E. Low, G. Peralta, I. C. Tanczos, J. Van De Koppel, and P. M. J. Herman. 2005. Trade-offs related to ecosystem-engineering: a case study on stiffness of emerging macrophytes. Ecology 86: 2187-2199.

Brenchley, G. A. 1978. On the regulation of marine infaunal assemblages at the morphological level: a study of the interactions between sediment stabilizers, destabilizers and their sedimentary environment. PhD thesis, The Johns Hopkins University, Baltimore, Maryland.

Brennan, L. A., M. A. Finger, J. B. Buchanan, C. T. Schick, and S. G. Herman. 1990. Stomach contents of dunlins collected in Western Washington. Northwestern Naturalist 71: 99-102.

Chapman, J. W., B. R. Dumbauld, G. Itani, and J. C. Markham. 2012. An introduced Asian parasite threatens northeastern Pacific estuarine ecosystems. Biological Invasions 14: 1221-1236.

Clifton, H. E., and R. L. Phillips. 1980. Lateral trends and vertical sequences in estuarine sediments, Willapa Bay, WA. Pacific Coast Paleogeography Symposium 4.

Colden, A. M., and R. N. Lipcius. 2015. Lethal and sublethal effects of sediment burial on the eastern oyster *Crassostrea virginica*. Mar. Ecol. Prog. Ser. 527: 105–117.

Comeau, L. A., A. Mallet, C. Carver, and T. Guyondet. 2014. Impact of high-density suspended oyster culture on benthic sediment characteristics. Aquac. Eng. 58: 95–102.

Comeau, L. A., A. Mallet, C. Carver, J-B. Nadalini, and R. Tremblay. 2017. Behavioural and lethal effects of sediment burial on quiescent Eastern oysters Crassostrea virginica. Aquaculture 469: 9-15.

D'Andrea, F. D. and T. H. DeWitt. 2009. Geochemical ecosystem engineering by the mud shrimp *Upogebia pugettensis* (Crustacea: Thalassinidae) in Yaquina Bay, Oregon: Density-dependent effects on organic matter remineralization and nutrient cycling. Limnol. Oceanogr. 54(6): 1911–1932.

d'Angremond K., J. W. van der Meer, and R. J. de Jong. 1996. Wave transmission at low crested structures. Proc. 25th Int. Conf. on Coastal Engineering, ASCE, 3305-3318 (20).

Dannheim, J., L. Bergström, S. N. R. Birchenough, R. Brzana, A. R. Boon, J. W. P. Coolen, J.-C. Dauvin, I. De Mesel, J. Derweduwen, A. B. Gill, Z. L. Hutchison, A. C. Jackson, U. Janas, G. Martin, A. Raoux, J. Reubens, L. Rostin, J. Vanaverbeke, T. A. Wilding, D. Wilhelmsson, and S. Degraer. 2020. Benthic effects of offshore renewables: identification of knowledge gaps and urgently needed research. ICES Journal of Marine Science 77: 1092–1108.

Deltares. 2020. Delft3D-FLOW: Simulation of multi-dimensional hydrodynamic flows and transport phenomena, including sediments. User Manual. Deltares, the Netherlands.

Dumbauld, B. R. 1994. Thalassinid shrimp ecology and the use of carbaryl to control populations on oyster ground in Washington coast estuaries. PhD thesis, University of Washington, Seattle, Washington.

Dumbauld, B. R., D. A. Armstrong, and K. L. Feldman. 1996. Life-history characteristics of two sympatric thalassinidean shrimps, *Neotrypaea californiensis* and *Upogebia pugettensis*, with implications for oyster culture. Journal of Crustacean Biology 16(4): 689-708.

Dumbauld, B. R., K. M. Brooks, K. M. & M. H. Posey. 2001. Response of an estuarine benthic community to application of the pesticide carbaryl and cultivation of Pacific oysters (Crassostrea gigas) in Willapa Bay, Washington. Marine Pollution Bulletin 42: 826–844.

Dumbauld, B.R., K. Feldman, and D. Armstrong. 2004. A comparison of the ecology and effects of two species of thalassinidean shrimps on oyster aquaculture operations in the eastern North Pacific. Pages 53-61 *in* Editor A. Tamaki, Symposium on "Ecology of large bioturbators in tidal flats and shallow sublittoral sediments-from individual behavior to their role as ecosystem engineers." Nagasaki: Nagasaki University.

Dumbauld, B. R., J. W. Chapman, M. E. Torchin, and A. M. Kuris. 2011. Is the Collapse of Mud Shrimp (*Upogebia pugettensis*) Populations along the Pacific Coast of North America caused by Outbreaks of a Previously Unknown Bopyrid Isopod Parasite (*Orthione griffenis*)? Estuaries and Coasts, 34: 336–350.

Dumbauld, B., and L. Harlan. 2009. The potential use of electricity to control burrowing shrimp in oyster aquaculture beds. North American Journal of Aquaculture 71: 178-188.

Dumbauld, B. R. and S. Wyllie-Echeverria. 2003. The influence of burrowing thalassinid shrimps on the distribution of intertidal seagrasses in Willapa Bay, Washington, USA. Aquatic Botany 77: 27–42.

Eklund, A. 1996. The effects of post-settlement predation and resource limitation on reef fish assemblages. Dissertation. University of Miami, Miami, Florida, USA.

Eggleston, D., and D. A. Armstrong. 1995. Pre- and post-settlement determinants of estuarine Dungeness crab recruitment. Ecol. Monogr. 65(2): 193–216.

Essink, K. 1999. Ecological effects of dumping of dredged sediments; options for management. J Coast Conserv 5: 69−80

Fabi, G., F. Luccarini, M. Panfili, C. Solustri, and A. Spagnolo. 2002. Effects of an artificial reef on the surrounding soft-bottom community (central Adriatic Sea). – ICES Journal of Marine Science, 59: S343–S349.

Feldman, K.L., D.A. Armstrong, D.B. Eggleston, and B.R. Dumbauld. 1997. Effects of substrate selection and post-settlement survival on recruitment success of the thalassinidean shrimp *Neotrypaea californiensis* to intertidal shell and mud habitats. Marine Ecology Progress Series 150: 121–136.

Fernandez, M., O. Iribarne, and D. Armstrong. 1993. Habitat selection by young-of-the-year Dungeness crab Cancer magister and predation risk in intertidal habitats. Marine Ecology Progress Series 92: 171-177.

Ferraro, S. P. and F. A. Cole. 2007. Benthic macrofauna-habitat associations in Willapa Bay, Washington, USA. Estuarine, Coastal and Shelf Science 71 (2007): 491–507.

Firth, L. B., R. C. Thompson, K. Bohn, M. Abbiati, L. Airoldi, T. J. Bouma, F. Bozzeda, V. U. Ceccherelli, M. A. Colangelo, A. Evans, F. Ferrario, M. E. Hanley, H. Hinz, S. P. G. Hoggart, J. E. Jackson, P. Moore, E. H. Morgan, S. Perkol-Finkel, M. W. Skov, E. M. Strain, J. van Belzen, and S. J. Hawkins. 2014. Between a rock and a hard place: environmental and engineering considerations when designing coastal defence structures. Coast. Eng. 87: 122–135.

Griffen, B. D., T. H. DeWitt, and C. Langdon. 2004. Particle removal rates by the mud shrimp *Upogebia pugettensis*, its burrow, and a commensal clam: effects on estuarine phytoplankton abundance. Marine Ecology Progress Series 269: 223-236.

Hemminga, M. A., and C. M. Duarte. 2000. Seagrass Ecology. Cambridge, UK: Cambridge University Press.

Hemery, L. G. 2020. Changes in Benthic and Pelagic Habitats Caused by Marine Renewable Energy Devices. Pages 104-125, In A.E. Copping and L.G. Hemery (Eds.), OES-Environmental 2020 State of the Science Report: Environmental Effects of Marine Renewable Energy Development Around the World. Report for Ocean Energy Systems (OES).

Henkel, S. 2016. Assessment of Benthic Effects of Anchor Presence and Removal. Report by Northwest National Marine Renewable Energy Center for Oregon Wave Energy Trust, Portland, Oregon.

Hickey, B. M. 1979. The California current system – hypotheses and facts. Progress in Oceanography 8.

Hinchey, E., L. Schaffner, C. Hoar, B. Vogt, and L. Batte. 2006. Responses of estuarine benthic invertebrates to sediment burial: the importance of mobility and adaptation. Hydrobiologia 556: 85-98.

Hixon, M. A., and J. P. Beets. 1989. Shelter characteristics and Caribbean fish assemblages: experiments with artificial reefs. Bulletin of Marine Science 44: 666–680.

Jarrett, J. T., 1976. Tidal prism-inlet area relationships, GITI Report 3, U.S. Army Engineer Waterways Experiment Station, Vicksburg, MS.

Jones, C. G., J. H. Lawton, M. Shackak, 1997. Ecosystem engineering by organisms: Why semantics matters. Trends in Ecology and Evolution 12: 275-276.

Jones, C. G., Lawton, J. H. and Shackak, M. 1994. Organisms as ecosystem engineers. Oikos 69: 373–386.

Kaminsky, G. M., P. Ruggiero, and M.C., Buijsman. 2010. Historical evolution of the Columbia River littoral cell. Marine Geology, 273.

Karlin, R. 1980. Sediment sources and clay mineral distributions off the Oregon coast. Journal of Sedimentary Petrology 50(2).

Kranz, P. M. 1974. The anastrophic burial of bivalves and its paleoecological significance. J Geol 82: 237−265.

Kraus, N. C. and H. T. Arden. 2003. North Jetty Performance and Entrance Navigation Channel Maintenance, Grays Harbor, Washington. Volume 1: Main Text. ERDC/CHL TR-03-12, Coastal and Hydraulics Laboratory, U.S. Army Engineer Research and Development Center, Vicksburg, MS.

Landerman, L. A., C. R. Sherwood, G. Gelfenbaum, J. Lacy, P. Ruggiero, D. Wilson, T. Chisholm, and K. Kurrus. 2004. Grays Harbor Sediment Transport Experiment Spring 2001—Data Report. Data Series 98, U.S. Geological Survey, Reston, VA.

Landry, M. R., J. R. Postel, W. K. Peterson, and J. Newman. 1989. Broadscale distributional patterns of hydrographic variables on the Washington/Oregon shelf," Coastal Oceanography of Washington and Oregon, M. R. Landry and B. M. Hickey, ed., Elsevier Oceanography Series, Amsterdam, Chapter 1.

Langhamer, O., D. Wilhelmsson, and J. Engström. 2009. Artificial reef effect and fouling impacts on offshore wave power foundations and buoys – a pilot study. Estuarine, Coastal and Shelf Science 82: 426-432.

Le Provost, C., M. L. Genco, F. Lyard, P. Vincent, and P. Canceill. 1994. Spectroscopy of the world tides from a hydrodynamic-finite element model, Journal of Geophysical Research, 99 (Cl2).

Loxton, J., A. K. Macleod, C. R. Nall, T. McCollin, I. Machado, T. Simas, T. Vance, C. Kenny, A. Want, and R. G. Miller. 2017. Setting an agenda for biofouling research for the marine renewable energy industry. International Journal of Marine Energy 19: 292-303.

Mathot, K. J., D. R. Lund, and R. W. Elner. 2010. Sediment in stomach contents of Western Sandpipers and Dunlin provide evidence of biofilm feeding. Waterbirds 33(3): 300-306.

McCowen, C., L. V. Weatherdon, J. Bochove. 2017. A global map of saltmarshes (ver 6.0). Biodiversity Data Journal 5: e11764.

Mendoza, M. and S. K. Henkel. 2017. Benthic effects of artificial structures deployed in a tidal estuary. Plankton & Benthos Research 12(3): 179-189.

Montserrat F., C. Van Colen, S. Degraer, T. Ysebaert, and P. M. J. Herman. 2008. Benthic community-mediated sediment dynamics. Marine Ecology Progress Series 372: 43-59.

MRLC. 2016. National Land Cover Database (CONUS). https://www.mrlc.gov/data/nlcd-2016-land-cover-conus

Nittrouer, C. A. 1978. The process of detrital sediment accumulation in a continental shelf environment: an examination of the Washington shelf: Thesis, University of Washington, Seattle, WA.

Osborne, P. D. 2003. Dynamics of Whitcomb Flats, Grays Harbor. Prepared for Port of Grays Harbor in coordination with the CoastalCommunities of Southwest Washington. Pacific International Engineering, PLLC, Edmonds, WA.

Padilla, D. K. 2010. Context-dependent Impacts of a Non-native Ecosystem Engineer, the Pacific Oyster *Crassostrea gigas*. Integrative and Comparative Biology 50(2): 213–225.

Paterson, D. M. and K. S. Black. 1999. Waterflow, sediment dynamics and benthic biology. Adv. Ecol. Res. 29: 155-193.

Patten, K. 2017. A review of the past decade of research on non-chemical methods to control burrowing shrimp. Unpublished, Exhibit C. pp. 1-7. Retrieved from https://protectwillapabay.org/wp-content/uploads/2017/09/Researchers-tested.pdf

Perkol-Finkel, S. and I. Sella. 2014. Ecologically active concrete for coastal and marine infrastructure: innovative matrices and designs. Pages 1139–1149. In: Allsop, W., Burgess, K. (Eds.), From Sea to Shore – Meeting the Challenges of the Sea. ICE Publishing.

Pillay, D. and G. M. Branch. 2011. Bioengineering effects of burrowing thalassinidean shrimps on marine soft-bottom ecosystems. Oceanography and Marine Biology: An Annual Review 49: 137–192.

Pillay, D., G. M. Branch, and A. T. Forbes. 2007. Effects of *Callianassa kraussi* on microbial biofilms and recruitment of macrofauna: a novel hypothesis for adult-juvenile interactions. Marine Ecology Progress Series 347: 1–14.

Posey, M. H. 1986. Changes in a benthic community associated with dense beds of a burrowing deposit feeder *Callianassa californiensis*. Marine Ecology Progress Series 31: 15–22.

Reise, K. 2002. Sediment mediated species interactions in coastal waters. Journal of Sea Research 48: 127-141.

Risinger, J. D. 2012. Biologically dominated engineered coastal breakwaters. PhD Thesis. Louisiana State University and Agricultural and Mechanical College.

Roberts, R. W. 1974. Marine sedimentological data of the Washington continental shelf: University of Washington, Department of Oceanography Special Report 57.

Rose, C. 1973. Mortality of market-sized oysters (Crassostrea virginica) in the vicinity of a dredging operation. Chesap. Sci. 14: 135-138.

Saha, S., Moorthi, S., Pan, H., Wu, X., Wang, J., and Coauthors. 2010. The NCEP Climate Forecast System Reanalysis. Bulletin of the American Meteorological Society, 91.

Scheidegger, K. F. and J. B. Phipps. 1976. Dispersal patterns of sands in Grays Harbor estuary, WA. Journal of Sedimentary Petrology. 46(1).

Scheidegger, K. F. and P. D. Komar. 1984. Sediment composition and hydrography in six high-gradient estuaries of the northwestern United States. Journal of Sedimentary Petrology 54: 86-97.

Sella, I. and S. Perkol-Finkel. 2015. Blue is the new green – Ecological enhancement of concrete based coastal and marine infrastructure. Ecological Engineering 84: 260–272.

Semmens, B. X. 2008. Acoustically derived fine-scale behaviors of juvenile Chinook salmon (*Oncorhynchus tshawytscha*) associated with intertidal benthic habitats in an estuary. Canadian Journal of Fisheries and Aquatic Sciences 65: 2053-2062.

Sherman, R. L., D. S. Gilliam, and R. E. Spieler. 2002. Artificial reef design: void space, complexity, and attractants. ICES Journal of Marine Science 59: S196-S200.

Siebert, T. and G. M. Branch. 2006. Ecosystem engineers: interactions between eelgrass Zostera capensis and the sandprawn *Callianassa kraussi* and their indirect effects on the mudprawn *Upogebia africana*. Journal of Experimental Marine Biology and Ecology 338: 253–270.

Suchanek, T. H. 1983. Control of seagrass communities and sediment distribution by Callianassa (Crustacea, Thalassinidea) bioturbation. Journal of Marine Research 41, 281–298.

Suedel, B. C., J. U. Clarke, J. Wilkens, C. H. Lutz, and D. G. Clarke. 2014. The effects of a simulated suspended sediment plume on eastern oyster (Crassostrea virginica) survival, growth and condition. Estuar Coast 38: 578−589.

Swinbanks, D. D. and J. W. Murray. 1981. Biosedimentological zonation of Boundary Bay tidal flats, Fraser River Delta, British Columbia. Sedimentology 28: 201–237.

Taormina, B., J. Bald, A. Want, G. Thouzeau, M. Lejart, N. Desroy, and A. Carlier. 2018. A review of potential impacts of submarine power cables on the marine environment: Knowledge gaps, recommendations, and future directions. Renewable and Sustainable Energy Reviews 96: 380-391.

Taormina, B., M. Laurans, M. P. Marzloff, N. Dufournaud, M. Lejart, N. Desroy, D. Leroy, S. Martin, and A. Carlier. 2020. Renewable energy homes for marine life: Habitat potential of a tidal energy project for benthic megafauna. Marine Environmental Research 161: 105131.

Taylor, K. E., 2001. Summarizing multiple aspects of model performance in a single diagram. Journal of Geophysical Research. 106(D7).

Thomsen, M. S. and K. McGlathery. 2006. Effects of accumulations of sediments and drift algae on recruitment of sessile organisms associated with oyster reefs. Journal of Experimental Marine Biology and Ecology 328: 22-34.

Twitchell, D. C., V. A. Cross, and K. F. Parolski. 2000. Sidescan-sonar Imagery, Surface Sediment Samples, and Surficial Geologic Interpretation of the Southwestern Washington Inner Continental Shelf Based on Data Collected During Corliss Cruises 97007 and 98014. USGS, Woods Hole, MA.

USACE. 1973. Grays Harbor (Chehalis andHoquiam Rivers) North Jetty Rehabilitation Report. Seattle, WA.

_______. 1974. Grays Harbor (Chehalis and Hoquiam Rivers) North Jetty Rehabilitation. Technical Design Memorandum, Seattle, WA.

_______. 2000. Study of Navigation Channel Feasibility, Willapa Bay, WA. USACE ERDC/CHL-TR-00-6. Vicksburg, MS.

----------. 2002. Study of Navigation Channel Feasibility, Willapa Bay, WA – Report 2: Entrance Channel Monitoring and Study of Bay Center Entrance Channel, WA. USACE ERDC/CHL-TR-00-6. Vicksburg, MS.

----------. 2003a. North Jetty Performance and Entrance Navigation Channel Maintenance, Grays Harbor, Washington. USACE, ERDC/CHL TR-03-12. Vicksburg, MS.

----------. 2003b. South Jetty Sediment Processes Study, Grays Harbor, WA: Evaluation of Engineering Structures and Maintenance Measures. USACE, ERDC/CHL TR-03-4. Vicksburg, MS.

----------. 2006. Breach History and Susceptibility Study, South Jetty and Navigation Project, Grays Harbor, WA. USACE ERDC/CHL TR-06-22. Vicksburg, MS.

----------. 2010. Waves, Hydrodynamics and Sediment Transport Modeling at Grays Harbor, WA. USACE, ERDC/CHL TR-10-13. Vicksburg, MS.

----------. 2012. Dredged Material Placement Site Capacity Analysis for Navigation Improvement Project at Grays Harbor, WA. USACE, ERDC/CHL TR-12-18. Vicksburg, MS.

----------. 2019. Sea Level Rise Change Curve Calculator (Version 2019.21). Vicksburg, MS. http://corpsmapu.usace.army.mil/rccinfo/slc/slcc_calc.html

USACE Seattle District. 1971. Feasibility report, navigation and beach erosion, Willapa River and Harbor and Naselle River, Washington; Exhibit D, fish and wildlife in relation to the ecological and biological aspects of Willapa Bay - Estuary, Washington, Seattle, WA.

----------. 1989. Appendix B: Design analysis in General Design Memorandum and Environmental Impact Statement Supplement: Grays Harbor, WA, Navigation Improvement Project, Volume 1, TC 202.S42 G72, Seattle, WA.

----------. 1995. Willapa Bay, Washington, FY 95 Bar Maintenance Dredging Evaluation, Unpublished memorandum, Seattle, WA.

----------. 2014. Grays Harbor, Washington Navigation Improvement Project General Investigation Feasibility Study - FINAL Limited Reevaluation Report. Seattle, WA.

----------. 2018. Final Environmental Assessment and Clean Water Act, Section 404 Public Interest Review Grays Harbor and Chehalis River Federal Navigation Channel Maintenance Dredging and Placement 2018-2033 Grays Harbor County, WA. Seattle, WA.

----------. 2019. Semiannual Dredging Meetings https://www.nws.usace.army.mil/Missions/Civil-Works/Navigation/Semiannual-Dredge-Meetings. Seattle, WA.

USGS. 2000. Grays Harbor Wave Refraction Experiment 1999: Data Report. Reston, VA.

_______. 2004. Grays Harbor Sediment Transport Experiment Spring 2001. Reston, VA.

_______. 2019. USSEABED Database. Reston, VA. Internet website: https://www.usgs.gov/natural-hazards/coastal-marine-hazards-and-resources/science/usseabed?qt-science_center_objects=0#qt-science_center_objects

Washington Department of Natural Resources (WDNR). 2018. Willapa Bay Mechanical Management of Burrowing Shrimp Supplement. Technical Report, Aquatic Assessment and Monitoring Team, Aquatic Resources Division, Olympia, Washington.

Washington Department of Ecology. 2015. Final Environmental Impact Statement: Control of Burrowing Shrimp using Imidacloprid on Commercial Oyster and Clam Beds in Willapa Bay and Grays Harbor, Washington. Publication 15-10-013. Olympia, WA. April 9, 2015.

Walles, B., J. S. de Paiva, B. C. van Prooijen, T. Ysebaert, and A. C. Smaal. 2015. The Ecosystem Engineer *Crassostrea gigas* Affects Tidal Flat Morphology Beyond the Boundary of Their Reef Structures. Estuaries and Coasts 38: 941–950.

Walles, B., K. Troost, D. van den Ende, S. Nieuwhof, A. C. Smaal, and T. Ysebaert. 2016. From artificial structures to self-sustaining oyster reefs. Journal of Sea Research 108: 1-9.

Widdows J, R. I. E. Newell, and R. Mann. 1989. Effects of hypoxia and anoxia on survival, energy, metabolism, and feeding of oyster larvae (*Crassostrea virginica*, Gmelin). The Biological Bulletin 177: 154−166.

Widdows, J. and M. Brinsley. 2002. Impact of biotic and abiotic processes on sediment dynamics and the consequences to the structure and functioning of the intertidal zone. Journal of Sea Research 48: 143-156.

Whitehead, T. 2020. Innovation: Bio Blocks. Concrete Quarterly. Autumn/Winter 2020. Issue 273: 3.

Wilson, R. 2017. Comments on Draft SEIS on the use of the nicotine based pesticide imidacloprid to control burrowing ghost shrimp (*Neotrypaea californiensis*) in Willapa Bay and Grays Harbor. Attachment A in Willapa/Grays Harbor Oyster Growers Association ("WGHOGA") Comments to Derek Rockett, Ecology Water Quality Program, in support of the Draft Supplemental Environmental Impact Statement for Control of Burrowing Shrimp using Imidacloprid on Commercial Oyster and Clam Beds in Willapa Bay and Grays Harbor, Washington. November 1, 2017.

Wilson, R. 2020. Comments on the critical importance of shellfish farms in providing the habitat requirements for the microphytobenthos (mainly diatoms) critical to Willapa Bay productivity. Bay Center Mariculture Co.

Wilson, R. (unpublished). Various reports and comments on Willapa Bay and estuary food webs, and ghost shrimp. Available at: https://www.flickr.com/photos/76798465@N00/albums/with/72157644330726062

Yang, X., C. Lin, X. Song, M. Xu, and H. Yang. 2019. Effects of artificial reefs on the meiofaunal community and benthic environment - A case study in Bohai Sea, China. Marine Pollution Bulletin 140(2019): 179-187.

Zalmon, I. R., F. S. de Sa, E. J. D. Neto, C. E. de Reze, P. M. Mota, and T. C. M. de Ameida. 2014. Impacts of artificial reef spatial configuration on infaunal community structure – Southeastern Brazil. Journal of Experimental Marine Biology and Ecology 454 (2014): 9-17.

APPENDIX

Appendix A USACE LITERATURE REVIEWS

A.1 WILLAPA BAY NAVIGATIONAL CHANNEL FEASIBILITY STUDY (2000, 2002)

USACE. 2000. Study of Navigation Channel Feasibility, Willapa Bay, Washington. USACE ERDC/CHL-TR-00-6

USACE. 2002. Study of Navigation Channel Feasibility, Willapa Bay – Report 2: Entrance Channel Monitoring and Study of Bay Center Entrance Channel, Washington. USACE ERDC/CHL-TR-00-6

A.1.1 Background

The shifting channels at the entrance to Willapa Bay make navigation unreliable (USACE 1971, 1995), and the local port cannot maintain or attract commercial users. Local interests have obtained Congressional support to determine if an economical channel can be established through the entrance bar. On behalf of the Seattle District, USACE ERDC conducted the Study in the Reference (SR) to determine the technical feasibility of maintaining a reliable channel with a 28-ft depth, including advance dredging and over dredging allowance over the entrance bar and into Willapa Bay. The channel reliability refers to stability of location and depth of the channel for an acceptable construction and maintenance cost, as well as hydrodynamic conditions for safe passage.

Based on examination of historical maps of the inlet, three basic alternative groups were proposed corresponding to the three natural channels that occurred historically in the inlet. Each alternative group has different variations with different cross section dimensions and horizonal alignments. The SR was performed to evaluate the performance of those design alternatives.

A.1.2 Method

The SR was developed as a simultaneous effort in two major tasks involving data collection and analysis, and analytical and numerical studies. The data collection is summarized under Section 2.1.3 of this report. The numerical studies include a circulation and transport modeling effort with the objective of evaluating the alternatives for a safe and reliable entrance channel in Willapa Bay. The circulation and transport model is a coupled wave and circulation/transport (salinity and sediment) model with the following components:

- STWAVE: This model is a steady-state finite-difference wave model based on the wave action balance equation, which is developed by the USACE Waterways Experiment Station. STWAVE was used to describe quantitatively the change in wave parameters (wave height, period, direction, and spectral shape) between the offshore and the nearshore regions. The model domain extends 30 km (west to east) by 51 km (south to north). The computational grid is a rectilinear grid with a resolution of 100 m including 301 grid cells across the shore and 511 cells along the shore. The model was driven by the wave spectrum derived from the field survey, while the effects of wind were not included.

- ADCIRC: This model is a multidimensional, depth-integrated finite element hydrodynamic circulation model developed at University of North Carolina Chapel Hill. ADCIRC was used for the tide circulation modeling. The model domain encompasses a regional area extending from 40.8 to 51.2°N and from 130.5 to 122.7°W. The computational grid contains 24,170 nodes and 46,250 elements. The model was forced with river discharge from Naselle and Willapa Rivers, and eight tidal constituents (K1, O1, M2, N2, S2, K2, P1, and Q1) at the open boundary. The tidal constituents were obtained from the LeProvost et al. (1994) tidal constituent database. Wind data obtained from NCEP were applied as meteorological forcing for simulations. Wave-induced currents were calculated by including wave stresses from the STWAVE model in the momentum equations within ADCIRC. The model was calibrated using the 1998 field survey. A constant friction factor of 0.0025 was used throughout the model domain, which was not adjusted in the calibration process.

- ADTRANS: This model calculates the concentration of specified parameters by application of the convection diffusion equation. ADTRANS, in conjunction with ADCIRC, was used to simulate salinity in this study.

A.1.3 Conclusion

The alternatives were evaluated by comparing their relative impact on the crosscurrents for navigational safety, the material deposition into the channel for the maintenance requirement, and the salinity for aquaculture considerations. The conditions for the evaluation include a fair-weather condition between September 4 to October 6, 1998, and a storm condition during January 1998. The following key observations and/or conclusions were made:

- The three most favorable alternatives were determined, which produced less than 3.2 ft/s crosscurrents and the least amount of material deposition into their channels during the storm.

- All engineering alternatives have no significant impact on the salinity as compared with the existing condition.

A.2 NORTH JETTY STUDY PERFORMANCE AND ENTRANCE NAVIGATIONAL CHANNEL MAINTENANCE (2003)

USACE. 2003a. North Jetty Performance and Entrance Navigation Channel Maintenance, Grays Harbor, Washington. USACE, ERDC/CHL TR-03-12.

A.2.1 Background

The Grays Harbor and Chehalis River Navigation Project is a federally constructed and maintained navigation channel that supports deep-draft shipping through the outer bar, Grays Harbor estuary, and the Chehalis River to Cosmopolis. The authorized depth of the outer harbor navigation channel tapers from 46 ft MLLW at the Bar Reach to 36 ft MLLW at the South and Crossover Reaches. The north and south jetties were constructed to provide a reliable, safe, and low-maintenance navigable channel over the Bar, Entrance, Point Chehalis, South, and Crossover Reaches. However, the seaward ends of both the north and south jetties have been deteriorating in the century since they were constructed. Although portions of the jetties have been rehabilitated a number of times, the seaward portions have been allowed to sink and now provide minimal obstruction to waves, longshore current, and longshore sand transport.

The Seattle District has formulated a maintenance dredging and disposal program for the Grays Harbor and Chehalis River Navigation Project to reduce dredging volumes and cost. The navigation channel deepening and improvement project was complete in 1990 with an expectation that the tidal prism and reduction of sediment around the pre-jetty ebb shoal would result in a self-scouring channel with little input. It was projected that outer harbor channel dredging requirements would diminish to zero 10 years after construction, which has not happened. An estimated 1.1 million yd^3 of sediment was dredged annually from the outer harbor and will continue to be necessary for the foreseeable future, resulting in continued adverse environmental conditions for Dungeness crab, the most commercially significant crab in Washington State territorial waters.

Based on a simple empirical relationship between channel dredging volume and jetty length before and after jetty rehabilitation with limited data, the Seattle District (USACE 1973, 1974) concluded that significantly lengthening the North Jetty (by 6,000 to 7,800 ft) would reduce annual maintenance dredging in the South and Crossover Reaches by as much as 360,000 to 660,000 yd^3, respectively. To that end, numerous alternatives were proposed through the SR, six of which passed through the screening. They include long rubble mound submerged jetty spur, short rubble mound submerged jetty spur, partial rehabilitation of North Jetty, full rehabilitation of North Jetty, and a combination of short spur and partial rehabilitation. A potential secondary benefit of such a project would be protection of the North Jetty from scour during times of beach erosion and shoreline recession. The purpose of the SR is to identify and evaluate those engineering alternatives for reducing annual maintenance of the Federal navigation channel by reducing the amount of sand bypassing the North Jetty.

A.2.2 Method

The SR performed a comprehensive review of the literature and engineering activities, including the dredging records, and the relationship between maintenance of the outer harbor channel and the condition of the beach adjacent to the North Jetty. The SR also analyzed the historical bathymetry datasets to understand long-term evolution and behavior of inlet morphology, including the ebb-tidal shoal, channels, nearshore, and shoreline change, leading to development of historical and existing-condition inlet sediment budgets and quantification of inlet sediment pathways. Ultimately, physical models and numerical models were used to evaluate the performance of the design alternatives. The physical model was developed for the waves and circulation along the beach north of the North Jetty, together with inferences of wide-area currents and sediment transport through dye and tracer studies. Relevant to this study, the numerical model developed in the SR includes the following components:

- STWAVE: This model was used to describe quantitatively the change in wave parameters (wave height, period, direction, and spectral shape) between the offshore and the nearshore regions. The wave model domain extends from approximately 3.7 miles south of the North Jetty to about 10.9 miles to the north in the alongshore direction and 8.6 miles in the cross-shore direction. The large domain ensures that the influence of the ebb-shoal bathymetry is considered in the nearshore wave transformation. The individual grid cells are 82 ft by 82 ft. The model was calibrated using the 1999 field survey as discussed Section 2.1.3.

- ADCIRC: This model was used to simulate the tidal circulation. The computational domain encompasses a regional area extending from 40.8 to 51.2°N and 130.5 to 122.7°W. The computational grid has 30,254 nodes and 58,231 elements with mesh resolution ranging from 25 m near the North Jetty to 60 km in the open ocean. The model was forced with eight tidal constituents (K1, O1, M2, N2, S2, K2, P1, and Q1) at the open boundary obtained from the LeProvost et al. (1994) tidal constituent database. The temporally and spatially varying winds obtained from NCEP wind data from NOAA also were applied. The model was calibrated using the 1999 field survey as discussed Section 2.1.3. A spatially varying friction factor that increases exponentially as the water depth was applied through the model calibration.

- PSed: This model is a Lagrangian sediment transport model developed at the Canadian Hydraulics Centre of the National Research Council of Canada. PSed was used to analyze sediment pathways in the estuary and identify changes in sediment pathways in response to project alternatives. In the model, sediment entrainment, mobility, advection, and deposition are predicted in a particle-based approach. The water levels and currents from the ADCIRC model were used to force the model.

- GENESIS-T: This model is a 1-D shoreline response numerical modeling system based on the assumption that the beach profile remains in a state of quasi-equilibrium over the long term, which is the official shoreline change model of USACE. GENESIS-T was used to estimate the existing longshore transport rates, particularly near the North Jetty, and evaluate the longshore transport and shoreline change in response to the various structural alternatives. The north boundary extends 3.7 miles from the North Jetty while the south boundary is located at the North

Jetty with the jetty-gated boundary. The model was forced by the water level data from the NOAA Westport tide gauge and wave data from CDIP station 036. The GENESIS-T model was calibrated by comparison to the change in measured shoreline positions from September 1976 to August 1985 and verified by simulating shoreline change from September 1985 to August 1995.

A.2.3 Conclusion

The GENESIS-T model was performed to evaluate various alternatives for reducing sediment bypassing and shoreline recession for short-term (5-year) and long-term (30-year) conditions. The following key observations and/or conclusions were made:

- Approximately 10 to 15 percent of the sediment that bypasses the North Jetty is attributable to longshore transport.
- All of the proposed structural alternatives produce greater than 10 percent change in the longshore transport rate only within 0.5 miles of the jetty.

The effectiveness of five structural alternatives at modifying current patterns and sediment transport at Grays Harbor was evaluated by numerical simulations of tidal and wave-induced currents and sediment movement. Major observations and conclusions are summarized below:

- The overall current patterns for the project site exhibit a strong southward current around the North Jetty tip.
- A sediment pathway exists from the North Jetty to Damon Point.
- Changes in current magnitude may be large, local to the structural alternative, and usually indicate a shift in the location of maximum flow, and only a minor perturbation to the overall circulation within 0.6 to 1.2 miles of the North Jetty at Grays Harbor was observed.
- The proposed jetty rehabilitation alternatives were predicted to cause an overall decrease in sediment entering the inner estuary, whereas the spur alternatives were predicted to increase sediment entry to the inner estuary.

A.3 BREACH HISTORY AND SUSCEPTIBILITY STUDY

USACE. 2006. Breach History and Susceptibility Study, South Jetty and Navigation Project, Grays Harbor, Washington. USACE ERDC/CHL TR-06-22.

A.3.1 Background

In December 1993, the south barrier spit at Grays Harbor, Washington, experienced a breach adjacent to the South Jetty, and from October to December 1994, the Seattle District closed it with sand dredged from the navigation channel. In 2001, breaching at the same location became imminent. In response, the Seattle District restored the breach fill by placing sand from an upland stockpile and planting native American dune grass to prevent wind and rain erosion of the restored area. USACE ERDC conducted this study to analyze the December 1993 breach at Grays Harbor, Washington, and assess the threat to the Federal Navigation Project had the breach not been filled the following fall.

Seven bathymetry configurations were considered including pre-breach condition and six different breach configurations representing the progression of the 1993 beach from December 1993 to August 1994, a hypothetical probable maximum breach condition and its two variations. The purpose of the SR was to illustrate the relative change in circulation patterns and peak velocities at the breach, in the navigation channel, and in the inlet throat for a series of tide and wave conditions.

A.3.2 Method

The SR was conducted by quantifying evolution of breach morphology; numerically simulating the ocean wave and water level conditions producing the current through such a breach including investigation of wide-area implications for the current in Grays Harbor; and numerical modeling of the breach evolution. Relevant to this study, the SR implemented a numerical model using M2D for hydrodynamics and STWAVE for short waves as discussed below:

- M2D: This is a finite-volume numerical representation of the two-dimensional depth-integrated continuity and momentum equations of water motion. The model domain only covers the entrance of Grays Harbor with a 60-ft resolution rectangular grid for the breach areas, which is nested within a 300-ft resolution grid. The offshore boundary conditions were obtained from the ADCIRC model previously applied at the site, which was discussed in Section 4.2.
- STWAVE: This model was applied for nearshore wave transformation. The model domain and mesh resolution are similar to the M2D model. The model was validated against the 1999 field survey data.
- Breach Model: This model was developed by CIRP, a research and development program conducted for USACE. This model is based on the classical depth averaged 1-D inlet hydrodynamic equations and accounts for the effect of waves and the rate of sediment transport thought the inlet. The morphological model is simply based on mass balance assuming a specified cross-sectional geometry. The model was calibrated against measurements of breach width and depth at Grays Harbor.

A.3.3 Conclusion

The validated M2D-STWAVE model was applied to examine the magnitude, duration, and spatial extent of combined tidal and wave-induced flow through the breach for the different bathymetric conditions as listed in the background. The results from the model (here only the historical breach conditions are included) show that:

- The flood and ebb currents are on the order of 3 ft/s through the breach under normal conditions, which are nearly doubled during a storm condition, predominantly in the flood direction.
- There is an increase in peak storm current, spatial extent of the current, and duration of breach flow of the tidal cycle from Dec 1993 to Aug 1994, which are indicators of breach growth and potential for continued growth.
- There is an increased capacity for sediment transport out of Half Moon Bay toward the navigation channel and a decrease in both the strength and duration of the ebb current in the area of the breach, which would reduce sediment scouring in the navigation channel and increased scour potential at the landward terminus of the South Jetty.
- Much of the sediment eroded from the barrier island when the breach opened, which was subsequently transported through the breach and deposited in Half Moon Bay, a historically erosional area. A portion of the sediment removed from Half Moon Bay would enter the navigation channel.
- Simulations of breach evolution with the average annual rate of longshore sediment supply to the north, and also with reduced and increased supplies, all indicated that the breach would have continued to grow in depth and width had it not been mechanically closed.

A.4 SOUTH JETTY SEDIMENT PROCESS STUDY (2003)

USACE. 2003b. South Jetty Sediment Processes Study, Grays Harbor Washington: Evaluation of Engineering Structures and Maintenance Measures. USACE, ERDC/CHL TR-03-4.

A.4.1 Background

In December 1993, persistent shoreline erosion near the South Jetty culminated in the formation of a breach between the jetty and the adjacent South Beach. A series of measures were undertaken by the USACE Seattle District, which includes:

- A temporary measure in 1994 to fill the breach with 600,000 cy of sand dredged from the navigation channel to protect the Grays Harbor navigation project and alleviate local concerns.
- Extension of the Point Chehalis revetment and fill from November 1998 to March 1999.
- Construction of a wave diffraction mound, and placement of about one-third of a recommended design for a transition gravel beach with cobble material on a subsequent fill of the breach in 1999.

Each of these measures was designed to prolong the life of the breach fill and provide beach erosion protection. However, a series of winter storms in 2001-2002 damaged the South Beach and modified the Half Moon Bay shoreline, re-emphasizing the temporary nature of the sand fill. The greatly reduced scope of the transition gravel beach with cobble was required to alleviate concerns about environmental resources and access impacts of placing gravel on a sandy beach.

The USACE ERDC, CHL coordinated with the Seattle District to develop a plan of action to evaluate the engineering features and maintenance measures in the vicinity of the South Jetty. The purpose of the study was to evaluate the performance of engineering and maintenance measures that have been implemented to control breaching of the South Jetty, reduce shoreline erosion in Half Moon Bay, and alleviate erosion via placement of dredged material.

A.4.2 Method

The study documented the history of the South Jetty and related engineering structures and reviewed the dredging and disposal activities associated with O&M dredging of the federal navigational channel. The following analyses were performed to evaluate the performance of each engineering features and maintenance measure discussed above:

- Analysis of O&M dredging and disposal in Half Moon Bay based on review of intertidal topography and nearshore bathymetry surveys, and shoreline changes identified from aerial imagery.
- Analysis of the wave diffraction mound performance in terms of the consequences of wave approach to the Half Moon Bay shoreline through a physical model as well as a numerical model using CGWAVE.

- Identification of sediment pathways and development of a sediment budget with measurements of currents, waves, and suspended sediment concentration at the site using a numerical model based on the coupled ADCIRC+STWAVE wave and current model as discussed in Section 4.2.

A.4.3 Conclusion

The sediment transport, sediment mobility, and transport path analysis revealed the following key observations and conclusions:

- Strong ebb currents dominate the tidal current and sediment transport regime in the study area.
- In response to the hydrodynamics, fine to medium sands tend to be transported out of the Half Moon Bay/South Jetty area to the west and southwest, while medium and coarse sand fractions may remain for a longer time in both inner and outer Half Moon Bay.
- Wave diffraction and refraction in Half Moon Bay create longshore and cross-shore currents, which flow from the west end of the bay to the northeast.
- The pattern of erosion and redistribution of gravel suggests that sediment in general is transported from the west end of the Half Moon Bay beach eastward along the shoreline, where it may eventually be delivered to the tidal stream in the main channel.

The sediment budget analysis indicated the following key conclusions:

- Half Moon Bay area has a small positive budget over the study period, which is associated mainly with dredged sediment disposal.
- Sediment gain in outer Half Moon Bay correlates well with losses from the Point Chehalis reach and the central inlet that includes large sand waves which migrate to the southwest.
- It was recommended that the priority for sediment management in terms of disposal of dredged sediment should be in Half Moon Bay disposal sites and on the southeast edge of the Point Chehalis disposal site to minimize a sand deficit that would otherwise exist at Half Moon Bay.

The physical model and subsequently the numerical model CGWAVE demonstrated that:

- Waves wrap around the rubble-mound structure so that they arrive at the Half Moon Bay shoreline more perpendicularly than they do without the rubble mound.
- Waves approach the shoreline similar to or at a more perpendicular angle with the jetty remnant in place and wave heights along the Half Moon Bay shoreline change by less than 0.4 ft for large inner harbor waves.

A.5 GRAYS HARBOR NAVIGATIONAL IMPROVEMENT STUDY

USACE. 2010. Waves, Hydrodynamics and Sediment Transport Modeling at Grays Harbor, WA. USACE, ERDC/CHL TR-10-13.

USACE. 2012. Dredged Material Placement Site Capacity Analysis for Navigation Improvement Project at Grays Harbor, WA. USACE, ERDC/CHL TR-12-18.

A.5.1 Background

The Grays Harbor and Chehalis River Navigation Project is a federally constructed and maintained navigation channel that supports deep-draft shipping through the outer bar, Grays Harbor estuary, and the Chehalis River to Cosmopolis. The currently maintained depth is 36 ft MLLW with a full legislatively authorized project depth of 38 ft MLLW. USACE conducted a series of feasibility studies on the navigation improvement project, which would deepen the inner harbor channel reaches (South Reach, Crossover Reach, North Reach, Hoquiam Reach, and Cow Point) up to 2 additional feet to reach the authorized project depth of 38 ft MLLW. This would require dredging up to an additional 1.7 million cy in addition to the 2.8 million cy available for dredging through the O&M program. This additional volume of dredged material would need to be placed within the current open water Dredge Material Placement sites or one of the existing offshore placement sites utilized during phase 1 of the deepening completed in 1990. In addition, historical trends in survey data indicate that Point Chehalis/Entrance reach is naturally scouring a new thalweg, and the Seattle District was evaluating Grays Harbor navigation channel realignment in this reach. The realigned channel would take advantage of this new thalweg developing just north of the present channel. Relocating the channel is hypothesized to reduce annual dredging quantities. The objective of the SR was to address short-term and mid-term dredge material management issues for the federal navigation project and to support the navigation improvement project at Grays Harbor, Washington.

A.5.2 Method

USACE ERDC and CHL developed a series of numerical models to assess the impact of the existing and alternative dredged material placement sites on channel maintenance with different channel depths and/or realignments. The model components include:

- CMS-Wave: This model is a two-dimensional spectral wave model developed by USACE. The model is based on the wave-action balance equation that includes wave refraction, shoaling, diffraction, reflection, breaking, and dissipation. CMS-Wave was used to compute wave transformation from offshore to nearshore. The CMS-Wave model domain is oriented East-West, with the offshore boundary at the 130-ft-depth contour, and extends eastward to Aberdeen, Washington. The CMS-Wave model has 94,000 cells (68,000 computational cells and 26,000 non-computational cells) with the largest and smallest cell sizes of 6,500 ft and 100 ft, respectively.

- ADCIRC: This model was used to simulate the tidal circulation. The extent of the domain was confined in a geographic range defined by longitude of 130.5 to 122.7°W and latitude of 40.7 to

51.2°N. The open ocean boundary is located in the deep ocean, outside the resonant basins and is not located near the tidal amphidromes. The ADCIRC mesh contains approximately 40,000 nodes and 77,000 elements. Mesh resolution varies from 31 km in the deep Pacific Ocean to about 165 ft in the bay. The model was forced with eight tidal constituents (K1, O1, M2, N2, S2, K2, P1, and Q1) at the open boundary obtained from the LeProvost et al. (1994) tidal constituent database. The temporally and spatially varying winds obtained from NCEP wind data from NOAA also were applied. River flow influxes are not considered since the emphasis in this study is on the sediment issues at the outer navigation channel caused by tides and waves. The model was calibrated using the 1999 field survey as discussed Section 2.1.3.

- GTRAN: This model estimates combined wave-current bed stresses and resulting sediment transport of noncohesive sediment at a point. The utility of GTRAN for the SR is to rapidly assess sediment transport pathways for various candidate placement sites and channel alignment alternatives.
- MPFATE: The Multiple Placement Fate of Dredged Material (MPFATE) model simulates the initial release and convective descent of dredged material to the bottom to estimate the resulting bathymetry change within and around the placement site. The MPFATE model was used to provide initial bathymetric conditions following dredged material placement at the disposal sites for the subsequent sediment transport modeling.
- LTFATE: The Long-term Fate of Dredged Material (LTFATE) model includes a combined hydrodynamic and sediment transport model for the long- and short-term stability of dredged material mounds.
    - The hydrodynamic model in LTFATE is the Environmental Fluid Dynamics Code (EFDC) surface water modeling system, which can be used for 1-D, 2-D laterally averaged (2-DV), 2-D vertically averaged (2-DH), or 3-D simulations of rivers, lakes, reservoirs, estuaries, and coastal seas.
    - The sediment transport in LTFATE is SEDZLJ, which is an advanced sediment bed model that represents the dynamic processes of erosion, bedload transport, bed sorting, armoring, consolidation of fine-grain sediment dominated sediment beds, settling of flocculated cohesive sediment, settling of individual noncohesive sediment particles, and deposition.

The model domain and grid are the same as that for the CMS-Wave model. Although Grays Harbor is not completely vertically well-mixed for most of the tidal cycle, measurements by Landerman et al. (2004) showed that the maximum difference between surface and bottom salinities at several nearshore stations was approximately three psu. The hydrodynamic model was run in depth-averaged mode. This model was forced by the water levels derived from the ADCIRC model at the open boundary, and inflows from the Chehalis and Humptulips Rivers. A salinity of 31 psu was assumed at the three ocean boundaries of the model domain, and salinities of 0 psu were used for the river inflows.

Grain size distributions at multiple locations inside and at the mouth of Grays Harbor, the lower Chehalis River, and offshore locations were reported by SAIC (2007) and SAIC (2009). These distributions were used to determine the initial composition of the marine, river, mixed marine and river sediments, summarized in Table 10. Bulk density, settling velocity, and critical shear stress for erosion were determined in Sedflume, which is a field- or laboratory-deployable flume for quantifying cohesive sediment erosion. The bulk density was measured to be approximately 1.4 g/cm^3 at the surface, which steadily increases through the surface 15 cm of the core to 1.53-1.54 g/cm^3 for fully consolidated sediments below 15 cm sediment depth. By assuming an erosion rate of 1×10^{-4} cm/s, the critical shear stress for erosion was determined to be approximately 0.2 Pa for the surface sediments, which increases rapidly to approximately 0.8 Pa for denser sediments at 15 cm below the surface. Settling velocity was measured by the image processing and particle tracking software. The median settling velocity of bed aggregates was found to be relatively constant across all experiments ranging between 0.8 to 1.6 mm/s with a mean of 1.1 mm/s. Floc settling velocities were notably slower, ranging between 0.1 to 0.7 mm/s with a mean of 0.35 mm/s. Settling velocities velocity for sand are on the order of 15 to 20 mm/s or faster.

Table 10: Sediment Composition of the Five Sedflume Cores

Sedflume Cores	Sediment Diameter (µm)					
Sediment Diameter (µm)	10	22	222	375	750	4000
Riverine Sediments	13	57	24	5	1	
Mixed Riverine and Marine Sediments	6	28	62	3	1	
Marine Sediments	1	1	80	15	2	1
Offshore Sediments	1	1	95	2	1	0
Chehalis River Sediments	53	7	1	22	17	

A.5.3 Conclusion

The simulation was performed for a 10-month period and the hydrodynamic model revealed the following key observations:

- Flood and ebb currents have similar magnitude and pattern of variation along the channel with the magnitude of flood current being slightly stronger than ebb current.
- Hydrodynamics in and around the navigation channel were weakly affected by short-term bathymetric changes caused by dredging operations or natural sedimentation processes occurring in the entrance and back-bay area.
- There is essentially no difference in current magnitude between the realigned channel and the existing channel in either unfilled or filled alternatives.

The GTRAN model reveals the following transport pathways for sand:

- Circulation cells are present north of the Point Chehalis placement site and near the end of the North Jetty as indicated by the transport streamlines.
- The transport of sand on the northern half of the entrance is flood-dominated, while the transport of sand on the southern half of the entrance is ebb-dominated. Transport at the Point Chehalis placement site is slightly ebb-dominant and transport at the South Jetty placement site is strongly ebb-dominant.
- The transport of sand at the dredged material placement sites is generally bimodal for both the existing and realigned channel. The Half Moon Bay placement site has a weak flood-directed transport.
- Transport magnitudes generally showed a slight increase with the realigned channel compared to magnitudes with the existing channel.

The percentage erosion of the dredged placement sediments, the residence time as determined as the time it took to achieve 25 and 50 percent of the erosion, and the fate of the eroded sediments at the three existing placement sites were analyzed with the LTFATE sediment transport modeling of Grays Harbor, which reveals the following key observations

At the Point Chehalis Site:

- The percentage erosion of the placed sediments is 6 to 53 percent with the existing channel, whereas less than 7 percent of the placed sediment eroded with the realigned channel.
- Approximately 20 percent of the eroded mass deposits within the navigation channel during the simulation period, with the Point Chehalis reach receiving the vast majority of the sediment that erodes from this site.

At the South Jetty Site:

- Mass eroded does not vary significantly with offshore wave conditions. The percentage of erosion of the placed sediments is 90 to 100 percent for both channel configurations.
- The 25 and 50 percent residence times for the realigned channel configuration was slightly to significantly greater than those for the existing channel configuration depending on the study periods.
- The largest fraction of dredged material eroded from the South Jetty Site deposit at the Point Chehalis and South Channel reaches, although the total amount deposited is very low at 2 to 3 percent. Insignificant fractions deposited in the Entrance and Crossover reaches. Most of the sediments that eroded during the simulations for both channel configurations deposited elsewhere, i.e., not in these four-navigation channel reaches.

At the Half Moon Bay site:

- Like the South Jetty site, eroded sediments are mostly insensitive to incident wave climate. The percentage of erosion of the placed sediments is 80 to 100 percent with the existing channel, whereas 60 to 97 percent eroded with the realigned channel.
- The residence times were consistently greater for the realigned channel configuration than for the existing channel configuration.
- Very little (less than 1.5 percent) of the sediment that erodes from the Half Moon Bay site deposits in any of these four-navigation channel reaches.

Appendix B HISTORICAL ENGINEERING ACTIVITIES

Date	Engineering Activities
3 June 1896	The River and Harbor Act authorized the original Grays Harbor navigation project, including a channel across the bar (self-scouring to a depth of about 18 ft Mean Lower Low Water [MLLW]) and construction of a single jetty extending 18,154 ft seaward from Point Hansen (now called Point Chehalis) peninsula along the southern margin of the entrance to Grays Harbor. At this time, predominant longshore transport was determined to be from south-to-north, and the South Jetty was considered responsible for preventing shoaling in the navigation bar channel (USAED, Seattle, 1965).
1898 – 1902	The South Jetty was constructed between May 1898 and September 1902. It was completed to a height of +8 ft MLLW and a total length of 13,734 ft, of which 11,950 ft extended seaward of the high-water line in 1902. During construction, the channel adjacent to the jetty undermined the structure causing material overruns that depleted project funds before the design length of 18,154 ft could be reached. A groin (spur) pointing into the channel was constructed 11,952 ft from the high-water line in 1902.
1902 – 1906	Between 1898 and 1904, depth over the ebb-shoal increased from 12 to 22 ft MLLW as a result of jetty construction, meeting the stated purpose of the project. In addition, the beach south of the jetty accreted, creating a 3,000-ft seaward progradation of the high-water shoreline. However, deterioration of the jetty began around 1904. By 1906, the South Jetty had settled due to scour, and the bar channel began to widen and shoal. This unfavorable shoaling led to construction of the North Jetty (USACE 1934).
March 1907	The River and Harbor Act authorized construction of the North Jetty 9,000 ft long from the ordinary high-water line to an elevation of +5 ft MLLW and an 18-ft deep navigation channel.
1907 – 1910	Construction of 10,000 ft of the North Jetty completed to +5 ft MLLW.
25 June 1910	The River and Harbor Act authorized an extension of 7,000 ft to the North Jetty.
1910 – 1913	The North Jetty was completed to a project length of 16,000 ft and an elevation of +5 ft MLLW.
1913 – 1916	The North Jetty was reconstructed to +8 ft MLLW and extended to a length of 17,204 ft. Construction period for the entire jetty extends from May 1907 to January 1916. After reconstruction of the North Jetty, the channel adjacent to the South Jetty shoaled, and a new wider and deeper channel developed north of the old channel to about -24 ft MLLW. Depth over the bar was again about -22 ft MLLW, and it remained that way until about 1924.
August 1917	River and Harbor Act authorized dredging of the bar channel.
1916	As jetties continued to deteriorate and were inadequate to maintain project dimensions in the bar channel, dredging commenced (57,000 cy) and continued at regular intervals until 1926 (except for 1918 and 1919).
1926 - 1942	The bar channel required almost continuous dredging between 1926 and 1942. The total quantity dredged from the entrance between 1916 and 1942 was approximately 22 x 10^6 cy; maximum dredging occurred between 1934 and 1936. The minimum quantity dredged in a year was 22,000 cy, and the maximum was 1,964,000 cy (Committee on Tidal Hydraulics 1967).
1933	By 1933, the South Jetty had subsided to an average depth of 5 to 10 ft below MLLW (+6 ft MLLW at the high-water shoreline and -10 ft MLLW at the outer end).
1934	The outer 8,000 ft of the North Jetty, between the high-water shoreline and the tip of the jetty, subsided to approximately -1.5 ft MLLW.
August 1935	River and Harbor Act authorized reconstruction of the north and south jetties and maintenance of a 26-ft deep channel below Aberdeen.
1936 – 1939	A 12,656-ft section of the South Jetty (about sta 80+00 to 220+00) was reconstructed to an elevation of +20 ft MLLW. Jetty reconstruction blocked the supply of sand to Point Chehalis, causing serious erosion of Point Chehalis. A 32-ft section of the jetty was removed to try to restore the supply of sand, but it was quickly blocked by accretion south of the jetty.

Date	Engineering Activities
1939 – 1946	The outer 900 ft of the South Jetty was destroyed, and crest rock was displaced to +2 ft MLLW over the next 2,656 ft.
1940	The inner 7,300 ft of the North Jetty, shoreward of the high-water shoreline, was impounded with sand.
1941 - 1942	The North Jetty was reconstructed between February 1941 and May 1942 to +20 ft MLLW for 7,700 ft seaward of the high-water shoreline, then +30 ft MLLW for an additional 528 ft. A 412 ft segment seaward of the reconstructed section was at MLLW and was not restored. The structure landward of the high-water shoreline was not rebuilt.
1942	Maintenance dredging of the bar and entrance channels was no longer required due to scouring effects of the jetties.
1942 – 1949	The outer 325 ft of the North Jetty was leveled, and about 400 ft of the reconstructed section was lowered 4 ft below grade.
1946 – 1951	An additional 900 ft of the South Jetty was destroyed, and the next 4,100 ft subsided to 0 to +10 ft MLLW.
1951 – 1953	An additional 900 ft of the outer South Jetty was destroyed, and the next 4,500 ft subsided to 0 to 2 ft MLLW. The next 2,400 ft subsided to +4 ft MLLW.
1949 - 1953	An additional 325 ft of outer end of the North Jetty was leveled, and more than 1,000 ft of the remaining section subsided to +10 ft MLLW.
1952 - 1954	More than 300 ft of the South Jetty (between sta 70+00 and 80+00) was dismantled, and the rock used for construction of the Point Chehalis revetment.
1959	An additional 30 x 106 cy of sand had accumulated north of the North Jetty as a result of jetty reconstruction completed in 1942.
1961	Only 2,100 ft of the reconstructed portion of the North Jetty remained at or near grade (+20 ft MLLW).
1962	By April 1962, average elevation of the South Jetty between 135+00 and 198+00 (6,300 ft) was about MLLW; seaward of this point from 198+00 to 220+00 (2,200 ft), crest elevation ranged from -6 ft MLLW to -48 ft MLLW. The landward section from about 88+00 (high-water shoreline) to 135+00 (4,700 ft) was near grade.
1966	A 4,000-ft section of the South Jetty (from sta 110+00 to 150+00) was rehabilitated to +20 ft MLLW, leaving the outer 7,000 ft in a degraded condition (-10 ft MLLW or deeper).
1974	A section of the North Jetty, about 1,300 ft seaward of the high-water shoreline, ranged from +3 to +14 ft MLLW. The jetty seaward of this point was below MLLW.
1975 - 1976	A 6,000-ft section of the North Jetty, from the high-water shoreline seaward, was rehabilitated to an elevation of +20 MLLW.
1991	Maintenance dredging of the bar and entrance channel reactivated.
December 1993	A breach occurred between the ocean and Half Moon Bay adjacent to the South Jetty. The breach was filled with 600,000 cy of sand dredged from the channel in 1994.
March 1999	Storm lowered a 200 ft section of the South Jetty to about +9 ft MLLW and damaged the jetty where it intersected the shoreline.
2000	A 3,500-ft section of the South Jetty seaward of the high-water shoreline was raised to an elevation of +23 ft MLLW. Approximately 5,000 ft of the North Jetty landward of the high-water line was raised to an elevation of +23 ft MLLW.
2013	Repaired another 300-ft section of the Point Chehalis Revetment which had been damaged by wave overtopping

Appendix C 10 YEAR WAVE BINS

ID	Wind		Waves			Morfac
	Speed (m/s)	Direction (o)	Height (m)	Period (s)	Direction (o)	
1	5.4	216.4	2.4	11.4	265.3	10.1
2	5.4	290.4	2.2	10.0	295.1	14.3
3	5.2	324.2	1.3	8.6	295.8	43.2
4	4.5	324.2	1.0	11.7	254.7	51.2
5	10.4	182.7	5.1	13.8	252.9	5.8
6	7.0	252.9	4.0	14.0	283.0	9.4
7	5.2	324.2	1.7	11.5	287.0	61.0
8	6.1	145.8	3.1	13.5	273.1	15.8
9	6.6	145.2	1.9	11.9	248.9	51.6
10	5.0	145.7	1.9	13.2	272.9	46.0
11	5.4	145.2	2.8	12.7	285.8	20.5
12	7.9	164.4	3.2	11.9	246.6	17.0
13	6.8	215.4	4.6	15.0	273.1	6.6
14	4.8	323.5	1.1	10.6	258.0	44.6
15	5.5	324.7	1.9	9.3	294.8	16.1
16	6.6	182.3	2.1	10.5	257.8	12.1
17	5.2	324.1	1.2	8.2	293.4	46.1
18	9.2	282.7	4.0	13.0	282.3	10.8
19	11.9	168.3	4.3	11.8	237.5	10.1
20	10.2	238.1	4.8	14.6	267.3	6.5
21	7.4	143.6	2.8	12.4	283.7	22.8
22	8.8	148.2	2.2	10.8	239.2	41.5
23	8.1	182.4	3.4	13.7	268.7	14.1
24	13.1	190.7	6.4	14.7	241.9	3.6
25	5.9	144.7	1.6	11.5	284.7	75.3
26	6.7	73.5	1.8	13.3	268.2	49.1
27	5.9	323.9	1.9	9.1	294.4	16.9
28	4.7	324.1	1.1	10.3	262.3	44.9
29	4.3	324.1	1.2	8.6	293.6	42.8
30	5.6	320.7	1.9	11.1	269.0	14.3
31	6.9	287.8	2.8	13.0	282.4	19.1
32	9.7	284.4	4.6	14.3	282.1	6.8
33	11.0	179.1	5.5	14.5	249.3	4.5
34	6.7	287.2	2.9	14.2	272.3	16.6
35	9.2	157.9	3.6	12.4	253.8	12.2
36	6.8	144.7	1.8	11.7	252.9	50.7

Appendix C 10 year Wave bins

ID	Wind		Waves			Morfac
	Speed (m/s)	Direction (o)	Height (m)	Period (s)	Direction (o)	
37	9.6	196.3	4.4	14.6	272.2	7.2
38	5.4	324.1	1.5	11.7	285.8	71.8
39	5.6	145.3	1.8	13.9	272.4	45.1
40	6.0	323.2	2.0	10.3	292.0	13.3
41	6.5	323.7	1.9	11.5	258.5	13.6
42	5.4	324.1	1.2	8.4	294.9	47.6
43	5.4	144.2	1.0	11.6	249.0	44.4
44	8.6	232.2	4.8	15.0	274.8	5.5
45	7.9	286.8	4.1	12.9	285.7	8.9
46	5.3	1.0	1.6	11.5	287.4	65.0
47	6.2	286.0	3.1	14.2	274.7	13.9
48	5.1	144.7	1.8	13.8	274.7	41.6
49	7.9	213.0	4.4	14.1	257.3	7.0
50	6.1	145.1	1.7	12.8	253.1	53.2
51	8.2	178.8	3.0	12.5	251.9	17.0
52	5.8	288.3	2.7	12.2	286.7	21.7
53	6.5	324.2	2.2	11.5	287.1	13.0
54	4.8	324.2	1.2	10.6	260.8	45.6
55	8.2	160.0	2.9	11.8	257.1	7.2
56	4.9	324.2	1.2	9.0	292.4	53.1
57	12.6	173.9	5.4	12.9	239.3	8.8
58	6.3	145.8	2.2	12.9	267.1	52.8
59	7.2	181.0	3.3	13.7	281.5	21.2
60	5.8	324.2	2.0	12.4	283.6	68.9
61	8.5	144.0	3.7	14.3	268.1	16.2
62	8.8	84.6	4.5	11.8	240.8	13.7
63	7.4	179.6	5.3	14.7	280.1	8.0
64	8.3	173.7	5.5	15.2	266.1	6.9
65	8.7	178.3	2.8	11.3	237.1	37.3
66	10.4	209.3	3.0	11.1	255.5	6.6
67	5.5	323.8	1.1	11.5	262.2	46.8
68	6.1	323.8	2.1	9.3	294.7	15.7
69	4.8	324.0	1.3	8.4	296.7	49.7
70	6.2	181.3	1.7	11.9	284.4	66.0
71	6.8	180.3	3.1	13.9	268.3	17.5
72	11.9	167.9	5.1	12.6	237.6	7.4
73	8.3	235.3	5.0	15.5	267.9	6.1
74	5.7	144.8	2.1	13.1	268.9	41.3
75	6.6	182.8	2.9	13.0	281.9	22.4

Appendix C 10 year Wave bins

ID	Wind		Waves			Morfac
	Speed (m/s)	Direction (o)	Height (m)	Period (s)	Direction (o)	
76	9.0	166.6	4.1	12.9	283.2	11.2
77	8.3	144.1	2.2	10.2	234.4	46.8
78	9.8	173.0	3.7	11.3	236.4	15.1
79	5.1	323.8	1.3	9.0	290.1	44.5
80	5.4	322.7	2.0	10.6	288.3	15.0
81	4.8	323.9	1.1	12.2	257.6	45.2
82	5.5	223.3	2.0	11.2	268.9	14.1
83	5.8	145.0	1.9	13.4	271.3	47.3
84	5.3	143.9	2.9	13.3	282.8	19.9
85	9.0	181.7	3.5	11.7	245.7	15.7
86	11.5	177.8	5.1	13.4	247.6	6.5
87	6.5	182.9	3.3	13.8	271.2	15.2
88	7.5	249.8	4.8	14.8	270.3	6.8
89	8.1	247.0	4.2	14.4	283.1	9.0
90	5.5	324.2	1.7	12.0	282.6	63.3
91	7.5	144.5	2.0	11.9	247.5	50.2
92	5.2	324.1	1.2	8.2	293.4	46.1
93	6.6	182.3	2.1	10.5	257.8	12.1
94	5.5	324.7	1.9	9.3	294.8	16.1
95	4.8	323.5	1.1	10.6	258.0	44.6
96	7.3	149.5	3.1	14.1	269.0	16.5
97	9.9	162.9	3.8	11.7	241.6	13.3
98	8.9	165.4	3.9	13.5	282.6	11.0
99	12.3	167.4	5.2	12.6	239.1	6.7
100	5.8	144.5	2.0	13.2	268.9	43.9
101	7.9	146.2	2.1	10.9	241.2	46.9
102	7.2	177.2	2.9	12.9	282.3	21.3
103	6.5	180.6	1.7	12.0	283.5	65.6
104	8.7	183.0	4.2	14.7	268.4	8.7
105	5.1	323.8	1.3	9.0	290.1	44.5
106	5.4	322.7	2.0	10.6	288.3	15.0
107	4.8	323.9	1.1	12.2	257.6	45.2
108	5.5	223.3	2.0	11.2	268.9	14.1
109	6.8	144.7	2.0	12.0	248.1	45.7
110	5.7	288.5	2.9	13.1	284.5	20.2
111	5.9	324.2	1.9	13.5	272.6	48.0
112	10.9	162.5	4.6	13.0	246.7	8.0
113	9.4	180.0	3.3	11.7	247.3	17.6
114	7.4	183.9	4.4	14.4	272.4	8.1

Appendix C 10 year Wave bins

ID	Wind		Waves			Morfac
	Speed (m/s)	Direction (o)	Height (m)	Period (s)	Direction (o)	
115	8.2	251.4	4.3	14.3	284.8	8.4
116	5.4	324.2	1.8	12.0	284.2	61.1
117	6.6	182.0	3.0	14.1	272.3	17.8
118	4.5	324.2	1.0	11.7	254.7	51.2
119	5.2	324.2	1.3	8.6	295.8	43.2
120	5.4	290.4	2.2	10.0	295.1	14.3
121	5.4	216.4	2.4	11.4	265.3	10.1
122	5.4	252.6	2.9	12.8	285.3	20.3
123	4.3	217.2	1.8	13.9	269.5	46.6
124	4.9	252.9	3.0	13.7	269.6	17.1
125	8.7	253.1	5.3	13.4	235.8	5.6
126	6.5	252.9	4.0	14.1	282.3	9.3
127	5.2	288.4	2.0	10.3	236.3	50.9
128	6.9	254.4	3.4	11.9	240.8	15.3
129	5.0	324.2	1.8	11.4	287.1	60.9
130	6.0	241.7	4.3	14.9	270.3	7.9